Characterisation of *dstpk61* in *Drosophila* development and the role of *extramacrochaetae* in *Drosophila* oogenesis

Sofia Papadia

Thesis presented for the degree of Doctor of Philosophy
Institute of Cell Biology
The University of Edinburgh
2005

Declaration

I hereby declare that I alone am responsible for the composition of this thesis and the work presented in it, except where otherwise stated.

Sofia Papadia

September 2005

Abstract

Drosophila is an excellent model organism for studying cellular processes as many genes share similarity with those of higher multicellular organisms and it also benefits from a wide range of powerful genetic and molecular biology techniques which are available to study development. Oogenesis and spermatogenesis in *Drosophila* are processes involving the coordinated development of germ cells and somatic cells and are very good systems for studying differentiation and pattern formation and the role of signalling pathways in specifying patterns during development. Particularly in oogenesis, the oocyte is selected from a number of germline cells, positioned in the posterior of the egg chamber and polarised. The surrounding somatic follicle cells undergo differentiation to produce specialised subpopulations of cells with specific functions, receive and transmit signals to the oocyte beneath to co-ordinate the polarisation of the egg chamber, secrete the eggshell and form specialised structures such as the micropyle, operculum and dorsal appendages. Several genes and signalling pathways are involved in regulating all these processes. This investigation focused on two genes, *dstpk61* and *emc*; the former was identified in a screen for genes encoding sex-specific transcripts and I aimed at understanding its potential role in oogenesis and spermatogenesis, while the latter was identified in a screen for genes with interesting expression patterns in follicle cells and I aimed at elucidating its role in oogenesis, mainly in dorsal appendage formation and also in the early stages, during the potential oocyte determination or cyst envelopment by the follicle cells.

The serine/threonine kinase *dstpk61* is a key component of the insulin/IRS signalling pathway and is the *Drosophila* homologue of mammalian PDK1. It regulates cell growth and survival by phosphorylating a number of target kinases, most notably PKB/Akt, an anti-apoptotic protein kinase which is activated by combined PDK1 and possibly rictor-mTOR complex phosphorylation. The *dstpk61* locus produces several different transcripts and four predicted isoforms varying at the N'-terminus. Some transcripts were differentially expressed in male and female tissues and my work focused on investigating if different isoforms are responsible for different functions, particularly in reproductive development.

I demonstrate by RT-PCR and microarray analysis that transcript E51 which encodes the second longest *dstpk61* isoform is highly enriched in male testes and present in very low levels in other tissues, whereas transcripts for the other three isoforms are present in male and female gonads and carcasses, with E40 and E09 being slightly ovary-enriched. The levels of expression of these transcripts vary depending on the age, nutritional/hormonally induced stress and the mating status of the flies. *dstpk61* is expressed in follicle and germline cells in oogenesis, as shown by mRNA in situ hybridisation and antibody staining with an isoform-specific antibody I generated for E40. In spermatogenesis mRNA in situ hybridisation and RT-PCR show *dstpk61* E51 mRNA in testes rather than in accessory glands. I also made progress in generating constructs for the expression of each different Dstpk61 isoform for subsequent biochemical analysis.

The gene *extramacrochaetae* (*emc*) encodes a bHLH transcription factor which negatively regulates other HLH proteins by forming inactive heterodimers with them. Emc has regulatory roles in the developing eye and wing, in sex determination, sensory organ formation and embryonic development, among others, through the Notch and EGFR signalling pathways. *emc* has been recently linked with the regulation of follicle cell differentiation in oogenesis. We discovered a dynamic expression pattern of *emc* mRNA and protein in oogenesis, both in somatic and germline cells, that implies the existence of different roles for *emc* at different developmental stages. Ectopic expression and knock out of *emc*, as well as somatic *emc* clones in ovaries lead to eggs with abnormal appendages, shorter and closer together than wild-type and frequently with split ends. I demonstrate that *emc* mRNA expression is affected by mutations in *gurken, Egfr* and *fs(1)K10* and that mis-expression of *emc* alters the late pattern of Broad-Complex expression. Br-C expression is not inhibited by the absence of *emc* in follicle cell clones in oogenesis. Follicle cell *emc* clones allow development of egg chambers to proceed whereas homozygous mutations in the germline are lethal. We suggest that *emc* lies downstream of *grk, Egfr* and *fs(1)K10* in the GRK/EGFR signalling pathway in the late stages of oogenesis and has a role in dorsal appendage formation, possibly involving fine-tuning of the Br-C expression area in the follicle cells that will give rise to the dorsal appendages.

This research opens up the possibility of further study such as establishing the role of the *dstpk61* E51 transcript in testes. Once expressed *in vitro*, different Dstpk61 protein isoforms can be used to identify the substrates of each one, which may shed light on why transcripts E09 and E40 are enriched in ovaries and E51 in testes. For *emc*, its role in the germline can be investigated and the mechanism by which it regulates dorsal appendage formation, as well as its interactions with other genes that participate in the Grk/EGFR pathway investigated.

Acknowledgements

First I would like to thank my supervisor, Professor Mary Bownes, for her helpful advice, support and optimism during the years of my studies in her lab. Many thanks also to all members of the Bownes group I met while in Edinburgh for helping creating a friendly atmosphere and offering suggestions and help: George Tzolovsky, Jun Terashima, Tim Wood, Kathleen Rothwell, Hadas Millo, Leeanne McGurk, Shengyin Lin, Nataly Gruntenko, Marina Sokolova, Vasso Lazou, Jan Barfoot and to all the undergraduate students passing from the lab- Beth, Annika, Daniela, Sybille, Andrew, Neil, Caroline and Holly.

I am grateful to Professor Sir Kenneth Murray and the Darwin Trust of Edinburgh for financial support which allowed me to have this great experience of studying in Edinburgh.

Thanks to all the friends in the institute, dance societies and cavers, for helping me to have a lovely –and lively- time here. Many thanks also to Giles and all the people in the Vet School for their support and for making my time there enjoyable.

I would also like to thank my family for always being encouraging and supportive.

List of abbreviations

General Abbreviations:

♂	male
♀	female
~	approximately
3'-, 5'-	3-prime end, 5-prime end
[x]	concentration x
β	beta
γ	gamma
Δ	delta
λ	lambda
μ	micro- (1.10^{-6})
^{32}P	β-emitting isotope of phosphorus
aa	amino acid(s)
A_{xnm}	Absorption at X nm
bp	base pairs
c	Concentrated (for chemicals)
C-	Carboxy-terminal
cDNA	complementary DNA
cm	centimetre(s)
°C	degrees centigrade
e.g.	for example (*exempli gratia*)
g	gram(s)
g	G centrifugal force
i.e.	(*id est*) that is
IR	Infra-Red
kb	kilobase(s)
krpm	kilo (1000) revolutions per minute
l	litre
M	Molar
m	milli- (1.10^{-3})
ml	millilitre (1.10^{-3})

mM	millimolar (1.10^{-3})
min.	minutes
mol	-moles
n	nano- (1.10^{-9})
N-	Amino-terminal
nm	nanometres (1.10^{-9} m)
nt	nucleotide(s)
O/N (o/n)	overnight
OD_{xnm}	Optical Density at X nm
p	pico- (1.10^{-12})
PCR	Polymerase Chain Reaction
pers. comm.	personal communication
pH	-log10[hydrogen ion]
RT-PCR	Reverse Transcription PCR
U	Units (of enzyme activity)
UAS	Upstream Activation Sequence
UTR	Un-Translated Region
UV	Ultraviolet
v/v	volume to volume ratio
w/v	weight to volume ratio
w/w	weight to weight ratio

Chemicals:

Amp	Ampicillin
AP	Alkaline Phosphatase
$CaCl_2$	Calcium chloride
$CHCl_3$	Chloroform
dATP	2' deoxyadenosine-5'-triphosphate
dCTP	2' deoxycytosine-5'-triphosphate
ddH_2O	double distilled water
dGTP	2' deoxyguanosine-5'-triphosphate
DMF	N, N'-dimethylformamide
DMSO	Dimethylsulfoxide

DNA	Deoxyribonucleic acid
DNase	Deoxyribonuclease
dNTP	deoxynucleotide-5'-triphosphate
dTTP	2' deoxythymidine-5'-triphosphate
dUTP	2' deoxyuridine-5'-triphosphate
EtBr	Ethidium bromide
EtOH	Ethanol
HCl	Hydrochloric acid
HEPES	N-(2-hydroxyethyl)piperazine-N'-(2-ethanesulfonic acid)
Kan	Kanamycin
KCl	Potassium chloride
KH_2PO_4	Potassium dihydrogen phosphate
KOAc	Potassium Acetate
KOH	Potassium hydroxide
MeOH	Methanol
$MgCl_2$	Magnesium chloride
$MgSO_4$	Magnesium sulphate
$MnCl_2$	Manganese chloride
mRNA	messenger RNA
Na_2HPO_4	Disodium hydrogen phosphate
NaAc	Sodium acetate
NaCl	Sodium chloride
NaH_2PO_4	Sodium dihydrogen phosphate
NaOH	Sodium hydroxide
NH_4OAc	Ammonium acetate
PBS	Phosphate Buffered Saline
PIPES	Piperazine-N,N'-bis[2-ethanesulfonic acid]
RbCl	Rubidium chloride
RNA	Ribonucleic acid
rRNA	ribosomal RNA
SDS	Sodium Dodecyl Sulphate
Tris	Tris(hydroxymethyl)-amino-methane
Triton X-100	Octylphenoxypolyethoxyethanol

tRNA	transfer RNA
Tween-20	Polyoxyethylene sorbitan monolaurate

Single and triple letter amino acid code:

A	Alanine	Ala	L	Leucine	Leu
R	Arginine	Arg	K	Lysine	Lys
N	Asparagine	Asn	M	Methionine	Met
D	Aspartic acid	Asp	F	Phenylalanine	Phe
C	Cysteine	Cys	P	Proline	Pro
Q	Glutamine	Gln	S	Serine	Ser
E	Glutamic acid	Glu	T	Threonine	Thr
G	Glycine	Gly	W	Tryptophan	Trp
H	Histidine	His	Y	Tyrosine	Tyr
I	Isoleucine	Ile	V	Valine	Val

Table of contents

Chapter 1: Introduction

1.1 Investigating dstpk61 in Drosophila development

1.1.1 *dstpk61/PDK1* overview

A crucial function of multicellular organisms is the ability of their cells to communicate with one another in complex ways. Communication mechanisms depend on extracellular signalling molecules (ligands) which bind to specific receptors on the target cell; the receptors become activated and generate a cascade of intracellular signals that lead to a specific response (Alberts et al, 2002).

The *Drosophila* gene *dstpk61* (also known as *dPDK1*) encodes a novel serine/threonine protein kinase homologous to human phosphoinositide-dependent protein kinase (PDK1) which was identified at the same time (Alessi et al., 1997a). *dstpk61* was originally found in our laboratory as part of a screen for isolation of genes generating sex specific transcripts (MacDougall et al., 1999). The name *dstpk61* is short for "*Drosophila* serine-threonine protein kinase at position 61". Other research groups in subsequent publications (Cho et al, 2001; Rintelen et al, 2001; Radimerski et al, 2002) refer to it as *dPDK1* (*Drosophila PDK1*). In Flybase (http://flybase.bio.indiana.edu/) it is referred to as *Pk61C* (*Protein kinase 61C*).

PDK1 is a component of the insulin signal transduction pathway. Deregulation of this pathway is associated with human diseases like diabetes and cancer (Toker and Newton, 2000a, Mora et al, 2004). PI3K signalling through insulin stimulation influences both cell survival and death, as well as growth, motility, differentiation, longevity, reproduction and insulin metabolic action by activating multiple secondary signalling cascades (Toker and Newton, 2000a; Oldham and Hafen, 2003). In *Drosophila* the insulin receptor pathway seems to be the major regulator of growth (Johnston and Gallant, 2002), together with the TOR-S6K pathway (Oldham and Hafen, 2003).

Insulin signalling begins with the binding of either insulin or the insulin-like growth factors to their receptor, an action that triggers the recruitment and phosphorylation of insulin receptor substrate (IRS) to generate a docking site for phosphatidylinositol-

3-OH kinase (PI3K) at the membrane (Kozma and Thomas, 2002). Once docked to IRS, PI3K catalyses the phosphorylation of the lipid phosphatidylinositol 4,5-biphosphate (PIP2) to phosphatidylinositol 3,4,5-triphosphate (PIP3). PDK1 and protein kinase B (PKB, also known as Akt) interact through their pleckstrin homology (PH) domains with PIP3, they are translocated to the membrane and PDK1 transduces the signal from PI3K to PKB (Alessi et al, 1997a). For a schematic representation, including the main targets of PDK1 and PKB, see Figure 1.1.1.

Apart from PKB (Alessi et al, 1997a, 1997b; Stokoe et al 1997), considered as the principal substrate, PDK1 has multiple substrate kinases, activating them directly by phosphorylation at the activation loop or indirectly by "priming" them via phosphorylation for subsequent activation (Toker and Newton, 2000a). Substrates of PDK1 identified by *in vitro* studies and vertebrate cell culture systems include protein kinase C (PKC) isoforms (Dutil et al, 1998; LeGood et al, 1998; Chou et al, 1998, Dong et al, 1999), serum- and glucocorticoid-inducible kinase (SGK), p70 S6 kinase ($p70^{S6K}$) (Alessi et al, 1998; Pullen et al, 1998), PAK, RSK (Jensen et al, 1999; Frodin et al, 2000) and PRK/PKN (PKC-related kinase - Dong et al, 2000).

Homologues of PDK1 have been identified in *Mus musculus* (mPDK1- Dong et al., 1999), *Ovis aries* and *Rattus norvegicus* (Stephens et al., 1998), *Caenorhabditis elegans* (PDK1a and PDK1b splice variants- Paradis et al., 1999), *Arabidopsis thaliana* and *Oryza sativa* (Deak et al., 1999), *Saccharomyces cerevisiae* (two homologues, PKH1 and PKH2 - Casamayor et al., 1999b) and *Schizosaccharomyces pombe* (KSG1 - Niederberg and Schweingruber, 1999).

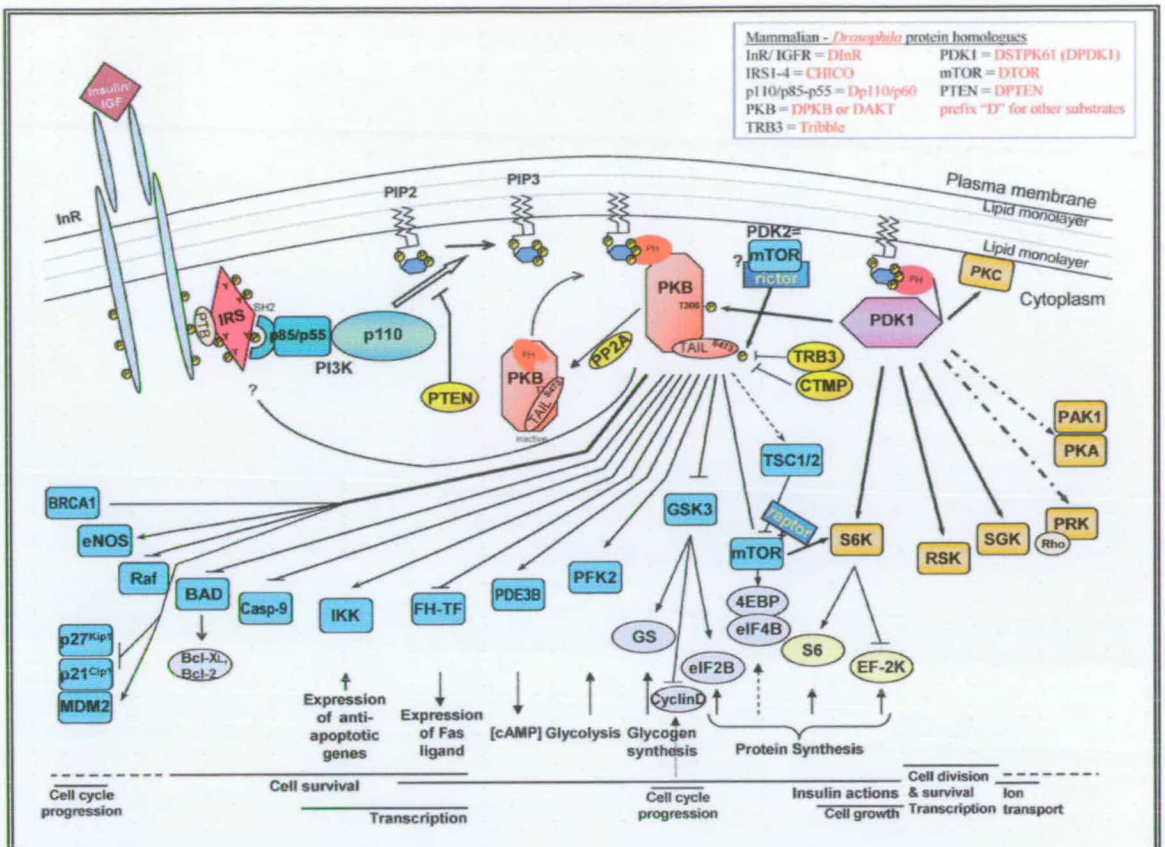

Figure 1.1.1 The insulin signal transduction pathway (IPS- PI3K branch), including substrates of PKB and PDK1
A horizontal bar indicates inhibition and an arrowhead indicates stimulation of the target protein by phosphorylation. Absence of such symbols indicates that the impact of PKB/PDK1 phosphorylation is unclear at the moment. A question mark (?) indicates relationships between pathway components for which a level of uncertainty exists. A dashed-dotted line indicates that this is a PDK1 substrate in mammals but not in *Drosophila*. In the case of PDK2, the most likely candidate for phosphorylating Serine 473 of PKB is shown. GS = glycogen synthase; eIF2B = eucaryotic initiation factor 2B; S6 = ribosomal S6 protein; IKKs = IκB kinases; FH-TF = Forkhead transcription factors, MDM2 = mouse double minute 2. For details on the pathway and further abbreviations, see text.

1.1.2 The insulin signal transduction pathway

1.1.2.1. Receptors - IRS

In vertebrates there are two related receptors, one for insulin, termed Inr and one for Insulin-like Growth Factor (IGF), termed IGF-1R. In *Drosophila* there is only one insulin-receptor, dInr (Johnston and Gallant, 2002). These receptors are tetramers, containing two extracellular chains with a cysteine-rich domain each, forming a

dimer that binds the ligand, and two transmembrane chains with intracellular tyrosine kinase domains. In vertebrates, signalling via Inr and IGF-1R is initiated by the binding of insulin and the insulin-like growth factors IGF-1 and IGF-2, respectively. Binding of the ligand to the receptor leads to a rearrangement of the transmembrane chains so that the two kinase domains come close together. The activated receptor first autophosphorylates its kinase domains at a number of tyrosine residues, some of which are recognised by the phosphotyrosine-binding (PTB) domain of specialised docking proteins, the Insulin Receptor Substrates (IRS) which are then recruited to the receptor at the cell membrane. The insulin receptor phosphorylates IRS molecules specifically on multiple tyrosine residues, therefore creating many more docking sites than could be accommodated on the receptor alone (Alberts et al., 2002; Lizcano and Alessi, 2002).

Four members of the IRS family have been identified in mammals, namely IRS-1, IRS-2, IRS-3 and IRS-4. IRS-1 and IRS-2 are widely distributed, IRS-3 is expressed in adipose tissue, fibroblasts and liver cells, whereas IRS-4 has so far been observed only in cultured cells from embryonic kidney. All IRS proteins have very similar N-terminal PH and PTB domains and they contain multiple potential tyrosine phosphorylation sites, most of which are in motifs favoured by the insulin receptor. The PH domain binds IRS to membrane phosphoinositides (PIP3- Razzini et al, 2000) and the PTB domain binds to a phosphotyrosine consensus motif on InR and IGFR. IRS-1 and IRS-2 functionally overlap to some degree, but are not functionally interchangeable for all cellular responses. IRS-1 is the main family member that binds PI3 Kinase in response to insulin stimulation, with IRS-3 being the preferable alternative. The interaction between PI3K and IRS-1 is specifically mediated by the Src-homology 2 (SH2) domain of the p85 regulatory subunit of PI3K [SH2 is a domain that escorts signalling proteins to tyrosine-phosphorylated growth factor receptors or adaptor proteins- in Fruman et al., 1999] . Binding of PI3K to IRS-1 directly stimulates the activity of IRS-1; another role of IRS in insulin signalling is by IRS-1 mediated targeting of PI3K to specific intracellular sites during insulin action, something that may contribute to the specific ability of insulin and IGF-1 to

stimulate responses such as translocation of the glucose transporter GLUT4 (Reviewed in Shepherd et al., 1998).

1.1.2.2 Phosphatidylinositol-3 kinase - Phosphoinositides

Inositol-containing lipids are a class of phospholipids consisting of a glycerol backbone with fatty acids (located within the inner lipid monolayer of the plasma membrane) attached at positions 1 and 2, and an inositol ring attached at position 3 via its phosphorylated 1'-OH. If this inositol ring carries no additional phosphates, this lipid is called phosphatidylinositol (PtdIns). In cells, all free -OH groups of the inositol ring of PtdIns, apart from those at the 2' and 6' positions, can be phosphorylated in different combinations. A phosphorylated derivative of PtdIns is called a phosphoinositide (PI). Phosphatidylinositol-3 Kinases phosphorylate the 3'-OH position of the inositol ring in inositol phospholipids, generating 3'-PIs. In the cells they produce three lipid products, PtdIns3*P*, PtdIns(3,4)P_2 and PtdIns(3,4,5)P_3 (Vanhaesebroeck and Waterfield, 1999; Vanhaesebroeck and Alessi, 2000).

Phosphatidylinositol-3 kinases (PI3Ks) exist as heterodimers which consist of an adaptor/ regulatory subunit associated with a catalytic subunit. There are multiple isoforms of PI3Ks that can be divided in three classes, I, II and III. The catalytic subunits of all classes contain a homologous region consisting of a catalytic core domain linked to the PIK (PI Kinase homology) domain with unknown function. Class I PI3Ks, the only class that has been shown to activate PKB in cells, prefer PtdIns(4,5)P_2 as a substrate in cells, catalysing its phosphorylation to PtdIns(3,4,5)P_3 [also termed PIP3] which can then give rise to PtdIns(3,4)P_2 via the action of 5'-inositol phosphatases. Class I PI3Ks are further subdivided into class I_A and I_B kinases which signal downstream of tyrosine kinases (such as the insulin receptor) and heterotrimeric G-protein-coupled receptors, respectively. All class I PI3Ks bind to the monomeric G-protein-coupled Ras. (Shepherd et al., 1998; Vanhaesebroeck and Waterfield, 1999; Vanhaesebroeck and Alessi, 2000).

Class I_A PI3Ks are made of a catalytic subunit (p110) with ~110 KDa molecular weight and an adaptor/regulatory subunit. I_A PI3Ks are a very diverse class in

mammals, having three catalytic p110 isoforms and seven adaptor proteins generated by alternative splicing of the three genes p85α, p85β or p55γ. In *Drosophila melanogaster* one type of I_A PI3K heterodimer exists (Dp110/p60); the nematode *Caenorhabditis elegans* also has only one heterodimer (AGE-1/AAP-1) while the slime mould *Dictyostelium discoideum* has three catalytic subunits (PI3K1-3). This class of PI3Ks has not been found in yeast, where there is absence of PtdIns(3,4)P2 and Ptd Ins(3,4,5)P3 as well, nor in plants, which lack PIP3. The catalytic subunit contains the kinase domain at the C-terminus and binding domains for p85 and Ras at the N-terminus. The regulatory subunits contain two SH2 domains and an inter-SH2 domain containing sequences that allow the interaction of the adaptor and catalytic subunits. The study for involvement of PI3Ks in a given biological system is greatly facilitated by the use of the specific PI3K inhibitors, wortmannin, which binds covalently to the PI3K catalytic subunits and LY294002 which is a competitive inhibitor of the ATP site (Vanhaesebroeck and Waterfield, 1999; Vanhaesebroeck and Alessi, 2000; Shepherd et al., 1998). The PI3K pathway can be activated by other growth factors (such as EGF and PDGF) apart from the insulin-like growth factor/insulin (Brazil et al, 2004).

Phosphoinositides in cells are specifically recognised by two structurally distinct lipid binding domains, the FYVE and PH domains. The FYVE domain consists of less than 80 amino acids and has two separate zinc coordination centres; it is less widespread than PH domain and its structure reveals that it selectively binds PtdIns(3)P (Fruman et al, 1999). PH (Pleckstrin homology) domains are globular protein domains of about 100 amino acids that can bind phospholipids, some of them with high affinity through specific motifs in their sequence. A subset of PH domains preferentially binds PtdIns(3,4)P_2 and PIP3 over other PIs. Certain PH domains may mediate protein-protein interactions (Vanhaesebroeck and Waterfield, 1999).

1.1.2.3 PKB, PDK1 and PDK2

PDK1 and PKB are key effectors of the PI3K insulin-stimulated pathway. They both contain PH domains, very important for the recruitment of these proteins to the cell membrane. PKB mediates many of the downstream events controlled by PI3K. There

are three PKB genes in mammalian cells [PKBα, PKBβ and PKBγ – the latter being highly enriched in the brain (Brazil et al, 2004)] and each is composed of an N-terminal PtdIns(3,4)P_2- and PIP3- binding PH domain, a C-terminal kinase catalytic domain and further towards the carboxy-terminal, a non-catalytic region known as the hydrophobic motif (HM). PKB belongs to the AGC subfamily of protein kinases, which includes protein kinase C (PKC) and the cyclic-AMP-dependent protein kinase (PKA) (Hanks classification, http://www.sdsc.edu/kinases/pkr/pk_catalytic/pk_hanks_class.html). Following PIP3 production through PI3K activation, inactive PKB is recruited from the cytosol to the plasma membrane where PIP3 is located. In this way PKB comes close to two kinases that phosphorylate PKB at residues Thr308 and Ser473. The phosphorylation of both of these sites results in maximal activation of PKBα (Alessi et al, 1996). Thr308 is located in the core of the catalytic kinase domain of PKB, in a region known as the activation loop or the T-loop, while Ser473 is in the hydrophobic motif (Alessi et al, 1997a; Lawlor and Alessi, 2001; Lizcano and Alessi, 2002). Following phosphorylation the activated PKB is drawn into the cellular interior and nucleus where it phosphorylates a variety of target proteins. Membrane binding of PKB acts simply to allow its co-localisation with the processing enzymes, the PDKs. Phosphorylation by these enzymes is thought to induce a conformational change that both reduces PKB affinity for 3'-phosphorylated lipids and opens up the catalytic cleft, allowing access to its substrates (reviewed in Stambolic et al, 1999).

Extensive biochemical studies have showed that the upstream kinase (Stokoe et al, 1997) responsible for the phosphorylation of the Threonine residue at position 308 of PKB is phosphoinositide-3 dependent protein kinase PDK1 (Alessi et al, 1997a). PtdIns(3,4)P_2 /PIP3 are essential for this phosphorylation. The identity of the protein kinase (or kinases) that phosphorylate Serine 473 of PKB is still under much debate, despite intensive research for several years (Dong and Liu, 2005). This elusive enzyme had been provisionally termed PDK2. Over time various theories had been proposed for the identity of PDK2: that it could be an integrin-linked kinase (ILK), a "modified" PDK1 (Balendran et al, 1999; Biondi et al, 2000) or PKB itself (Toker and Newton, 2000b). As discussed in Toker and Newton, 2000a, ILK is not the

elusive PDK2, as it increases Ser473 phosphorylation in transfected cells by an indirect mechanism (Lynch et al, 1999). PDK1 was proposed as PDK2 after observing that PDK1 interaction with PIF [PDK1-interacting fragment, a region of protein kinase C-related kinase-2 (PRK2)] or with a synthetic peptide encompassing the PDK2 consensus sequence of PIF, converted PDK1 from an enzyme that could phosphorylate only Thr308 of PKBα to one that phosphorylates both Thr308 and Ser473 of PKBα in a PIP3-dependent manner (Balendran et al, 1999). However, subsequent studies showed that the PIF- binding pocket of PDK1 interacts with S6K1 and SGK previously phosphorylated at their hydrophobic motif, to mediate their phosphorylation at the T-loop by PDK1, but it is not required for the phosphorylation of PKBα by PDK1 (Biondi et al, 2001). Toker and Newton (2000b) reported PKB autophosphorylation on the hydrophobic site *in vitro*, triggered by PDK1 phosphorylation of the activation loop of PKB. They proposed that PIF may render Ser473 more accessible to autophosphorylation by displacing PDK1 from the hydrophobic site of its target kinases, thus unblocking their autophosphorylation sites (Toker and Newton, 2000a). Furthermore, Hill et al (2002) identified a novel plasma membrane raft-associated PKB Ser473 kinase activity, that is distinct from ILK and PDK1 and is now shown to contain the catalytic subunit of the double-stranded DNA-dependent protein kinase (DNA-PKcs; Feng et al, 2004). Their model for activation of PKB by upstream kinases proposed that the insulin receptor and the constitutively active Ser473 kinase complex are sequestered in lipid rafts, whereas PKB and PDK1 are recruited to the membrane rafts by the increased levels of 3'-phosphoinositides following activation; on these rafts, PKB is phosphorylated on Ser473 and Thr308 by Ser473 kinase and PDK1, respectively; the activity of PDK1 is increased by its tyrosine phosphorylation by src family kinases, promoted by recruitment of PDK1 to rafts (Hill et al, 2002).

Several other proteins have also been proposed over time as the elusive PDK2, responsible for the phosphorylation of the HM site of ACG kinases, with data accumulating that support or contradict this claim (reviewed in Dong and Liu, 2005). These include the MAP kinase-activated protein kinase-2 (MK2 – Alessi et al, 1996), the p38 MAP kinase (Rane et al, 2001), PKC conventional isoforms α and βII

(Partovian and Simons, 2004; Kawakami et al, 2004), the NIMA (never in mitosis gene A)-related kinase 6 (NEK6- Belham et al, 2001), the ataxia telangiectasia mutated (ATM; Viniegra et al, 2005) and mTOR. A very recent and seemingly very plausible study (Sarbassov et al, 2005) using RNAi in *Drosophila* and mammalian cells suggests that the mTOR/GβL/rictor (rapamycin-insensitive companion of mTOR) protein complex is necessary for the Ser473 phosphorylation of PKB (and so, the PDK2) whereas the mTOR/ GβL/raptor (regulatory associated protein of mTOR) complex regulates cell growth partly by phosphorylating the HK motif of S6K1. This model explains several of the discrepancies concerning the role of mTOR as PDK2, most importantly the failure of rapamycin to block PKB activation, since the mTOR-rictor complex is rapamycin insensitive. However, it is still possible that there are multiple PDK2s, acting to phosphorylate different AGC family kinases at their HM site. Furthermore, this phosphorylation could be cell type, signalling pathway and substrate-specific (Dong and Liu, 2005).

The phosphorylation of PKB by PDK1 is regulated by the conformation of PKB. The PH domain of PKB masks the activation loop and its release by binding to PtdIns(3,4)P_2 /PIP3 is required for PDK1 phosphorylation (Toker and Newton, 2000a). However, it is still not known what drives the dissociation of activated PKB from PIP3 at the membrane to the cytoplasm and then to the nucleus (Lawlor and Alessi, 2001).

PDK1 itself seems to have a constitutive basal level of activity. Most probably, PDK1 function is primarily regulated by substrate conformation and by cellular relocalisation. Stimulated cells show a PH domain-dependent relocalisation of PDK1 from the cytosol to the plasma membrane (Anderson et al, 1998; Filippa et al, 2000) but another study using GFP-tagged PDK1 has shown constitutive association of PDK1 with the membrane in a wortmannin- and growth factor- independent manner in unstimulated cells, possibly due to the much higher affinity of PDK1 PH domain to PtdIns(3,4)P_2 / PIP3 rather than PKB PH domain. The interaction of PDK1 with PIP3 facilitates the rate at which it can activate PKB (Currie et al, 1999). However, other studies (Frodin et al, 2000; Biondi et al, 2000) show that PDK1 is also

activated, through the interaction of the Hydrophobic Motif (HM) of substrates with the PIF pocket of PDK1 (model described below), suggesting that PDK1 may not be active all the time.

1.1.2.4 PDK1 structure and other functions

PDK1 is a 556 amino-acid, 63 kDa Ser/Thr protein kinase with an amino-terminal catalytic domain of AGC protein kinase class, and a non-catalytic carboxy-terminal tail containing a PH domain (Alessi et al, 1997a). As a member of the AGC subfamily of protein kinases, it has to be phosphorylated at its T-loop (serine241 residue) in order to be active, like other members of this family. Ser241 is regulated by autophosphorylation and mutation of this site essentially abolishes kinase activity (Casamayor et al, 1999a). *In vitro* it phosphorylates other kinases apart from PKB, mostly AGC kinases like $p70^{S6K}$ (Alessi et al, 1998; Pullen et al, 1998), SGK (Lang and Cohen, 2001) and PKC isoforms (LeGood et al, 1998) ("atypical" -PKCλ/ι, PKCξ and "conventional"-PKCα,βI,βII and γ) (reviewed by Belham et al, 1999).

PDK1 phosphorylates p70 ribosomal S6 kinase (S6K) and the serum and glucocorticoid induced protein kinase (SGK) at their activation loop and another kinase (mTOR-raptor complex for S6K- Burnett et al, 1998-; an as yet uncharacterised kinase for SGK) phosphorylates their hydrophobic motif. S6K and SGK, unlike PKB, do not have a PH domain thus they cannot interact directly with PIP3. There is evidence indicating that PIP3 stimulates the phosphorylation of the hydrophobic motif of S6K and SGK either by activating the hydrophobic motif kinase or by inhibiting the phosphatase that dephosphorylates the hydrophobic motif. The phosphorylation of the hydrophobic motif generates a PDK1 docking site that allows PDK1 to interact with S6K and SGK, phosphorylate their activation loops and hence to activate them (Park et al, 1999; Kobayashi and Cohen, 1999; Lizcano and Alessi, 2002). Following recent crystallographic studies resolving the structure of PDK1, active and inactive PKB and a typical AGC kinase, PKA, the model for recruitment of substrates by PDK1 has been described in more detail (Biondi, 2004;

Mora et al, 2004). According to this, PDK1 acts as a sensor of protein conformation. The inactive AGC kinases (potential PDK1 substrates) have a C-terminal extension connecting the catalytic core to the hydrophobic motif that is absent from PDK1. They also have disrupted PIF pockets, so their phosphorylated HMs are available to interact with the PDK1 PIF pocket. This interaction promotes activation of PDK1, which then phosphorylates the activation loop of the substrate AGC kinase. Phosphorylation of the activation loop prompts binding of the HMs to their own PIF pockets and this stabilises the active conformation, which is no longer recognised by PDK1 (Biondi, 2004).

S6K has two physiological substrates so far, the ribosomal S6 protein (S6) and the elongation factor 2 kinase (EF-2K) through which it regulates translation. Phosphorylation of ribosomal S6 protein stimulates the translation of ribosomal protein mRNAs, thus enhancing the biosynthesis of ribosomes which are required during increased protein synthesis upon insulin stimulation. Phosphorylation of the elongation factor 2 kinase inhibits its activity resulting in dephosphorylation of elongation factor-2 (EF-2); dephosphorylated EF-2 stimulates the elongation stage of protein synthesis (Lizcano and Alessi, 2002).

RSK, the 90 KDa ribosomal S6 kinase, is another substrate of PDK1. RSK is a serine/ threonine kinase with two kinase domains, one amino- and one carboxy-terminal, named NTK (N- terminal kinase) and CTK (C- terminal kinase). CTK is activated by ERK-type MAP kinases and it autophosphorylates RSK at a Serine residue in the hydrophobic motif between the two kinase domains. This Serine acts as a docking site for PDK1 which is recruited to RSK, becomes activated by autophosphorylation and phosphorylates NTK which then phosphorylates the substrates of RSK (Frodin et al., 2000). RSK is important in the regulation of cell division and survival by controlling G_2-M phase progression in meiosis I, metaphase arrest in meiosis II and by inactivating BAD. It is probably also involved in transcriptional regulation through histone H3, CREB and estrogen receptor α phosphorylation (in Frodin et al., 2000).

PKC isoforms (α,β,γ,δ, ε and ι) are phosphorylated by PDK1 (studies in human and mouse; *in vitro* and in cell culture; Le Good et al, 1998; Dong et al, 1999) at threonine residues at the activation loop in a PIP3-dependent manner.

PRK1 and PRK2 (PKC Related Kinases) interact with Rho-GTP through their N-terminal Rho-binding domains and this results in a conformational change that enables PDK1 to interact with them and phosphorylate their T-loop (Flynn et al, 2000). In *Drosophila* though, *dPDK1* genetically does not interact with *dPKN* (*PRK*) (Rintelen et al, 2001).

PKA which was proposed to be a putative substrate of PDK1 by *in vitro* studies (Cheng et al, 1998) is not regulated by *Pdk1* in *Drosophila in vivo* (Cho et al, 2001) and it is activated normally in a PDK1-deficient line (Williams et al, 2000).

1.1.2.5 Targets downstream of PKB

PKB phosphorylates proteins at a specific motif that requires two arginine residues to be located 3 and 5 residues amino-terminal to the site of PKB phosphorylation (Lizcano and Alessi, 2002). Several potential targets of PKB have been identified that contain this consensus motif. Since in several of these studies PKB and/or its substrates have been overexpressed in cells, it is shown that PKB can phosphorylate these substrates but not that this also occurs under physiological conditions in cells.

PKB actions have usually been studied in the context of insulin signalling and the regulation of cell survival (reviewed by Vanhasebroeck and Waterfield, 1999).

a) Insulin signalling targets

Activated PKB directly mediates the phosphorylation and inactivation of GSK3 (Glycogen Synthase Kinase-3; Cross et al, 1995) as well as the Forkhead transcription factor (Kops et al, 1999) and in parallel it has been argued to mediate the activation of mTOR (the mammalian Target Of Rapamycin) by an unknown mechanism (Kozma and Thomas, 2002).

Glycogen synthase (GS) is a key GSK3 substrate which catalyses the final step in glycogen synthesis, the conversion of UDP-glucose into glycogen. Phosphorylation of glycogen synthase by GSK3 inhibits glycogen synthase. Therefore, inactivation of GSK3 via its phosphorylation by PKB results in dephosphorylation of glycogen synthase through the action of protein phosphatases, and in the activation of glycogen synthesis (Cross et al, 1995; Welsh et al, 1998). GSK3 also phosphorylates and inhibits a guanine nucleotide exchange factor, eIF2B, which controls the initiation stage of protein translation. Insulin induces the dephosphorylation of eIF2B at the site phosphorylated by GSK3, thereby stimulating the synthesis of protein from amino acids (Lizcano and Alessi, 2002).

In adipocytes, PKB mediates decrease of cellular concentrations of cyclic AMP by the phosphorylation and activation of a cAMP phosphodiesterase isoform, PDE3B, thus inhibiting lipid metabolism in fat cells (Kitamura et al, 1999). In the heart it phoshorylates and activates a cardiac-specific form of 6-phosphofructose 2-kinase (PFK2), a rate limiting enzyme of glycolysis, thus stimulating ATP production (Deprez et al, 1997). (Lizcano and Alessi, 2002). However, subsequent studies (Bertrand et al, 1999) using dominant negative (symbolised as KD) forms of PKB and PDK1 showed that the insulin-induced activation of PFK2 was prevented only by KD PDK1 and not by KD PKB, thus indicating that the insulin-induced activation of heart PFK2 is mediated by a PDK1 activated protein other than PKB and Mora et al (2003) also confirmed that PFK2 in the heart of mPDK1$^{-/-}$ mice is not stimulated. A kinase (WISK kinase) that phosphorylates and activates PFK2, probably located downstream of PDK1 in the insulin pathway, was partially purified from perfused rat hearts (Deprez et al, 2000).

The mammalian target of rapamycin (mTOR) is important in the positive regulation of protein translation and ribosome biogenesis; it also negatively controls autophagy, in a mitogen- and amino acid- dependent manner. It can be phosphorylated by PKB, although the impact of this phosphorylation on the activity of mTOR has not been firmly established (Nave et al, 1999) – the *Drosophila* homologue dTOR though does not have a functional PKB phosphorylation site. TOR proteins act in a nutrient-

sensing pathway to regulate growth either independently from the insulin/IGF pathway or the two pathways may be interwined, perhaps under specific circumstances; the relation of the TOR-S6K and the insulin/IGF pathway still needs to be clarified (Hennig and Neufeld, 2002; Oldham and Hafen, 2003).

b) Cell survival signals

Following the observation that overexpression of PKB delays cell death in many cellular model systems (Franke et al, 1997; Downward, 1998), a search began for PKB substrates among the components of the cell death machinery. This revealed two targets, BAD (Downward, 1999) and caspase-9 (Cardone et al, 1998).

BAD binds the antiapoptotic proteins Bcl-2 and Bcl-X_L and it prevents them from exerting their antiapoptotic function. When phosphorylated on Ser112 or Ser136, BAD no longer interacts with either Bcl-2 or Bcl-X_L, allowing them to inhibit apoptosis. PKB can phosphorylate BAD on Ser136. However, not all cell types express BAD and cell survival can be regulated independently of both PKB activation and BAD phosphorylation. PKA and MAP kinases (such as the 90 KDa ribosomal S6 kinase, RSK) are also important in BAD phosphorylation (Vanhaesebroeck and Waterfield, 1999).

Caspase-9 is a protease crucial for the initiation and possibly for later stages of apoptosis (Alnemri, 1999; Wolf and Green, 1999) which can be phosphorylated and inhibited by PKB (Cardone et al, 1998). However, the residue which PKB phosphorylates in human caspase-9 is not conserved in the mouse, rat and monkey homologues and mPDK1 is not phosphorylated by PKB *in vitro*. Furthermore, there is evidence that PKB promotes cell survival by intervening early on in the apoptosis cascade, before cytochrome c release from the mitochondria and caspase-9 activation, possibly by maintaining the integrity of the mitochondrial membrane (reviewed in Vanhaesebroeck and Alessi, 2000). There is a more recently identified substrate, the apoptosis signal-regulating kinase 1 (Ask1) which stimulates MAP kinase kinases that activate the JNK and p38 MAP kinases. Overexpression of activated PKB phosphorylates ASK1 at Ser83, resulting in inhibition of Ask-1

activity and reduced JNK activity (Kim et al, 2001). In some situations JNK can promote apoptosis; in this context, inactivation of ASK1 by PKB could promote cell survival (Lawlor and Alessi, 2001). Association of PKBα with JIP1 (JNK-interacting protein 1) in hippocampal neurons and PKBβ binding to POSH (Plenty of Src Homology domains) prevent the apoptotic role of JNK (reviewed in Brazil et al, 2004).

PKB also phosphorylates the Forkhead family of transcription factors (FKHR, FKHRL1, AFX) at 3 residues, generating strong interaction sites for the 14-3-3 family of scaffolding proteins. The binding of 14-3-3 to Forkhead proteins triggers their relocalisation from the nucleus to the cytoplasm, away from their nuclear targets. FH transcription factors have been implicated in expression of the Fas ligand which can induce cell death upon autocrine or paracrine production; PKB-mediated retention of FH transcription factors in the cytoplasm means the Fas ligand is not expressed allowing the cells to survive (Brunet et al, 1999) (Vanhaesebroeck and Waterfield, 1999; Lizcano and Alessi, 2002). YAP (Yes-associated protein) is another pro-apoptotic transcription factor inhibited by PKB, that was discovered recently (Basu et al, 2003).

PKB can associate with and activate I-κB kinases (IKKs) that regulate the activity of the NF-κB (nuclear factor κB) transcription factor. NF-κB is inactive as a transcription factor when bound to its cytosolic inhibitor I-κB. When IKKs phosphorylate I-κB it gets degraded, allowing NF-κB to move to the nucleus and activate the transcription of antiapoptotic proteins (Wang et al., 1999). The mechanism of PKB activation of IKKs is not clear, though.

Endothelial nitric oxide synthase (eNOS) is another enzyme that becomes activated upon phosphorylation by PKB (Fulton et al, 1999; Dimmeler et al, 1999). Sustained production of nitric oxide by endothelial cells has been implicated in many biological effects such as gene regulation and angiogenesis.

IRS-1 (involved in the insulin pathway), Raf protein kinase (also known as MAP-kinase-kinase-kinase) and BRCA1 are also proposed as PKB substrates (reviewed in

Vanhaesebroeck and Alessi, 2000) although the effect of the interaction is not always clear. For example, one study shows PKB to negatively regulate IRS-1 (Li et al, 1999), but another study proposes that PKB is a positive regulator of IRS-1 and that another PI3K-regulated kinase is responsible for the negative feedback regulation through IRS-1 (Paz et al, 1999).

c) Cell cycle regulation

PKB activity promotes cell cycle progression by facilitating the G1/S transition and initiation of the M phase. For the former, phosphorylation of FOXO transcription factors in the nucleus and degradation of p53 by PKB phosphorylation-dependent translocation of MDM2 (mouse double minute 2) to the nucleus, inhibits transcription of the cyclin-dependent kinase (CDK) inhibitor proteins $p27^{Kip}$ and $p21^{Cip}$, respectively. In addition, PKB can phosphorylate $p27^{Kip}$ and $p21^{Cip}$ proteins which leads to their accumulation in the cytoplasm. These interactions result in the relief of CDK2 activity inhibition and promote G1/S transition. Increase of Cyclin D mRNA translation by PKB-dependent inhibition of GSK3 by phosphorylation also contributes at this stage. PKB also inhibits CHFR (a checkpoint protein with FHA and ring-finger domains) and Myt1 (another protein kinase) and thus helps in the cell cycle progression to M phase (reviewed in Brazil et al, 2004).

1.1.2.6 Negative regulators of the pathway

The phospholipid phosphatase PTEN is a negative effector of PI3K pathway. PTEN encodes a 3'-phosphatase that converts PtdIns(3,4)P_2 into PtdIns4P and PtdIns(3,4,5)P_3 to PtdIns(4,5)P_2 (Myers et al, 1997). In *Drosophila* the Tuberous Sclerosis Complex gene products dTSC1 and dTSC2 (homologues of hamartin and tuberin, respectively) inhibit the insulin signalling pathway downstream of PKB (Gao and Pan, 2001; Potter et al, 2001; Tapon et al, 2001). Negative effectors of the pathway are also the inhibitor of initiation factor 4E (4E-BP1-3; (Pause et al, 1994) and a negative feedback loop that is mediated by mTOR at the level of IRS phosphorylation to suppress downstream signalling (Ozes et al, 2001). Novel negative regulators of PKB include TRB3, a homologue of *Drosophila* Tribbles,

which blocks PKB activation in hepatocytes (Du et al, 2003) and CTMP (Carboxyl-terminal modulator protein) which blocks HM phosphorylation and activation of PKB by binding to its C-terminus (Maira et al, 2001). [Summarized in Kozma and Thomas, 2002; Brazil et al, 2004].

1.1.3. Role of the PI3K pathway

It is evident from the roles of their substrates that PDK1 and PKB mediate many of the metabolic actions of insulin. The PI3K pathway is being studied in detail under the perspective of generating drugs that can activate PKB and which could be used potentially to trigger insulin-dependent processes for the treatment of diabetes (Lawlor and Alessi, 2001). Type II diabetes, which affects approximately 90% of diabetics, is caused when target tissues of insulin (skeletal muscle, adipose tissue and liver) become resistant to the effects of insulin, presumably because the insulin signalling pathway is impaired (Lizcano and Alessi, 2002). Consistent with this, over-expression of dominant negative PI3-kinase mutants and use of inhibitors of PI3K block many of the physiological responses of a cell to insulin (Bevan, 2001). There is increasing evidence for a deregulation of PI3K action in diabetes, including findings that mice deficient in PKBβ display many of the typical features of type II diabetes in humans and data that establish PKBβ as an essential gene for the maintenance of normal glucose homeostasis (in Lawlor and Alessi, 2001; Kandel and Hay, 1999).

The pathway has also been implicated in tumorigenesis and cancer. Positive regulators of the PI3K signal transduction pathway are mutated or overexpressed in certain cancers. The inactivation of PTEN, an important tumor suppressor, results in increased levels of 3'-PIs, leading to elevated PKB activity (Stambolic et al., 1998). Indeed, PKB was found overexpressed in a significant number of different types of cancer (Kandel and Hay, 1999), including ovarian, breast and pancreatic (Lawlor and Alessi, 2001). Activation of PKB probably contributes to the genesis of cancer by promoting cell survival through its anti-apoptotic signals and by promoting

proliferation. These responses have been demonstrated by over-expression of constitutively activated PKB mutants in many cell types (Lawlor and Alessi, 2001). Consequently, PKB is an attractive therapeutic target for cancer treatment, via the design of PKB inhibitors.

Therefore, the PI3K pathway plays a role in the regulation of overall growth by controlling metabolism, cell size and cell number (Bohni et al., 1999), in vertebrates and *C. elegans* as well as in *Drosophila.* In hypomorphic PDK1 mutant mice though the reduction in animal and organ size observed is due to smaller cells rather than a reduction in cell number (Lawlor et al, 2002). The effects of the pathway in growth regulation are more pronounced in *Drosophila* than in mammals, since *Drosophila* has a single insulin-like receptor for both insulin and IGFs (which regulates postembryonic growth, reproduction and aging) while in mammals the primary role of insulin and InR is energy homeostasis by the regulation of blood glucose levels and the IGF-1 receptor mediates the primary growth regulatory function (Ikeya et al., 2002).

1.1.4. Insulin signal transduction in *Drosophila melanogaster*

The insulin signalling pathway is conserved in *Drosophila* and homologues exist for all the mammalian components. Thus dInr, chico, Dp110/p60, dPTEN, DSTPK61, dPKB (or dAkt), dTSC1/dTSC2, dTOR, dS6K, dRSK, dSGK are the homologues of the insulin/IGF-1 receptor, IRS1-4, PI3K catalytic/adaptor subunit, PTEN, PDK1, PKB, TSC1/TSC2, mTOR, S6K, RSK, SGK respectively.

Studies using *dPDK1* mutants suggest that *dPDK1* genetically interacts with *dRSK* but not with *dPKN* (the PRK *Drosophila* homologue) (Rintelen et al, 2001). In *Drosophila* genetic studies have confirmed dPDK1 as a key regulator of dPKB and dS6K activation (thus regulating the control of growth and cell size) (Rintelen et al, 2001) and have provided further evidence that dPDK1 is a vital downstream effector of PI3K in cell and compartment size control (Cho et al, 2001).

The PI3K pathway is very important in the control of cell growth. This was first demonstrated by experiments in *Drosophila*, where over-expression of a dominant negative (interfering) allele of PI3K in the wing reduced cell size, whereas over-expression of the activated allele increased cell size (Leevers et al, 1996), and is also supported by studies in PKBβ- and S6K1- deficient mice (in Kozma and Thomas, 2002). Subsequent studies in *Drosophila melanogaster* showed that mutations in the pathway components *dInr* (Brogiolo et al., 2001), *Chico* (Bohni et al, 1999), *dPTEN* (Huang et al, 1999; Goberdhan et al, 1999), *dPKB* (Scanga et al., 2000), *dTSC1/dTSC2*, *dTOR*, *d4E-BP* and *dS6K* have a striking effect on cell size and cell number, with the exception of *dS6K* (Montagne et al, 1999) where mutations affect only cell size, and *d4E-BP* (Miron et al, 2001), where loss-of-function mutations do not have any apparent effect on cell growth, although over-expression of d4E-BP variants modified to bind dIF4E more strongly have pronounced effects on cell growth. For more details on the *Drosophila* insulin signalling pathway (ISP) genes and the phenotypes of mutants and over-expression, see Tables 1.1.1 and 1.1.2.

Genetic studies with loss- and gain- of function mutations of all the components of the PI3K pathway in *Drosophila* over the last few years have provided a significant amount of information about the interactions between the effectors of the pathway *in vivo* and their functions and therefore they allow new models to be proposed. Kozma and Thomas (2002) proposed a model for the PI3K signalling pathway, where PKB and S6K reside on parallel rather than equivalent signalling pathways (see figure 1.1.2). Radimerski et al (2002) provide biochemical, pharmacological and genetical evidence to support this model; moreover they show that dS6K resides on an insulin signalling pathway distinct, not only from that of dPKB, but also from that of dPI3K, but despite dPI3K/dPKB independence, dS6K activity is dependent on dPDK1 (DSTPK61). Thus they suggest that dPDK1- and dTOR-mediated dS6K activation is PIP3 independent. For *dPDK1* to access the S6K1 activation loop site, it only requires phosphorylation of key residues at the carboxy-tail of S6K1 by mTOR.

***Drosophila* gene**	**Mutation**	**Phenotype**	**References**
dInr	Point mutations causing loss of function of varying levels in homozygous flies (partial to almost null) There are 5 alleles. Mosaic animals with homozygous mutant head and heterozygous body:	-delay in development -body size is severely but proportionately reduced, by reduction in cell size and cell number -half body weight compared to heterozygotes -female sterility -2-fold increase in lipid content -flies with smaller heads (pin heads) compared to wild type	Brogiolo et al, 2001 Chen et al, 1996
chico	*chico*^{1}- null mutation, P element-induced *chico*^{2} – synthetic chico deletion Mosaic animals with heads largely homozygous for *chico*:	-semilethality -developmental delay -weight reduction -cell autonomous reduction in cell size and cell number (smaller flies) -increased lipid levels in males -no increase in cell death -eyes and head are reduced in size whereas proboscis and body are of wild-type size	Bohni et al., 1999
Dp110/p60	Null mutations by small deletions Mosaic animals for Dp110- and Dp60- eye clones.	-reduced growth rate and cell size in a similar way to *chico* -decrease in cell size and number -no increase in programmed cell death -third instar larval lethal But: ectopic expression of a dominant negative Dp110 mutant can induce apoptosis contain ommatidia reduced in size	Leevers et al., 1996 Weinkove et al., 1999 Scanga et al., 2000
dPKB	Mutations by genetic recombination: -Partial loss of function -Null allele (loss of function) in germline clones -Null allele	-reduction in body and cell size, cell autonomous -embryonic lethality and increased apoptosis -decrease in cell size in wing; not cell number. But it affects cell number since it rescues Dp110 null mutants	Verdu et al., 1999 Stocker et al, 2000 Staveley et al, 1998 Scanga et al., 2000
dPDK1	EP line PDK1-deficient line by imprecise excision of the P element in another EP line Loss of function alleles by EMS mutagenesis (point mutations in the kinase domain)	-embryonic lethal -apoptosis is induced in homozygous embryos -mutants of varying strengths by different allelic combinations: a) second instar larval lethal b) viable mutants with developmental delay, smaller than heterozygous, with reduced body weight – caused by decreased cell size. Almost complete male sterility Cell autonomous effects	Cho et al, 2001 Rintelen et al., 2001

***Drosophila* gene**	**Mutation**	**Phenotype**	**References**
dPTEN	Loss of function mutations of varying strength	-increased cell size -increased proliferation -2-fold increase in PIP3 levels -pupal lethal heteroallelic combination; viable escapers have increased body and organ size due to an increase in both cell size and cell number. -decrease in lipid and glycogen levels -2-fold increase in the level of mortality under dietary restriction	Goberdhan et al., 1999 Huang et al., 1999 Oldham et al, 2002
	Mosaic animals with homozygous mutant head and heterozygous body	-disproportionately larger head with more and larger cells	
dTSC1/dTSC 2	*gigas* mutation (*dTSC2*)	-homozygous early 3rd instar larval lethal -increased cell size, abnormal cell cycle progression	Ito et al., 1999 Tapon et al., 2001 Potter et al., 2001
	Point mutation for *dTSC1*	-dramatic increase in cell size	
dS6K	Mutant with P element insertion Loss of function alleles by imprecise excision	-female sterility -strong developmental delay -reduced body size due to cell size, not cell number, in a cell autonomous manner -lethality (often)	Montagne et al., 1999
dTOR	P element insertions Further loss of function mutants by deletions due to imprecise excisions	-homozygous lethal -developmental delay -severe reduction in total body mass -extended life-span as larvae; die without pupating -cell autonomous reduction in the size of proliferating and post-mitotic cells and their number -nucleolar size reduction, lipid vesicle aggregation, endoreplicative cell cycle arrest, as in starvation conditions.	Zhang et al., 2000 Oldham et al., 2000
d4E-BP	Mutants that bind the substrate deIF4E more strongly than wild type, of variant strength	-reduction in cell size; cell number is reduced only in the strongest mutants -higher proliferation in mitotically inactive tissues -viable null mutants, no increased growth	Miron et al., 2001

Table 1.1.1: Mutant phenotypes for *Drosophila* ISP components

***Drosophila* gene**	**Over-expression**	**Phenotype**	**References**
dInr	-in the eye	-outgrowth in adult eye because of increased number of ommatidia	Brogiolo et al, 2001
dilp2 (potential dInr ligand)	-in eye, wing	-bigger flies due to increase in cell size and cell number	
Dp110/p60	-of *Dp110* in imaginal discs	-enlarged adult organs	Leevers et al., 1996
	-of a dominant- negative form of Dp110	-cell size reduction	
	-of the activated allele of Dp110	-cell size increase	
dPDK1	-in eye, wings	-increase in cell size; cell autonomous	Cho et al, 2001
	-co-overexpression with *dPKB*	-increase in cell size, cell autonomous	Rintelen et al., 2001
dS6K	-in the wing	-cell size increase	Montagne et al., 1999
	-constitutive overexpression	-partially rescues *dTOR* mutant flies to viability	Zhang et al., 2000
dTSC1/dTSC 2	co-overexpression of *dTSC1* and *dTSC2*	-decrease in cell size, cell number and organ size	Potter et al., 2001 Tapon et al., 2001
dTOR		growth inhibition, cell size reduction	Zhang et al., 2000
	-overexpression (UAS system)	reduction in cell size and proliferation rate -decrease in growth, as in dTOR loss of function mutations	Hennig and Neufeld, 2002
d4E-BP	-overexpression	-no phenotype	Miron et al, 2001
	-co-overexpression with *dPKB* or *Dp110*	-supresses growth enhancement caused by expression of these kinases	

Table 1.1.2: Overexpression phenotypes for *Drosophila* ISP components

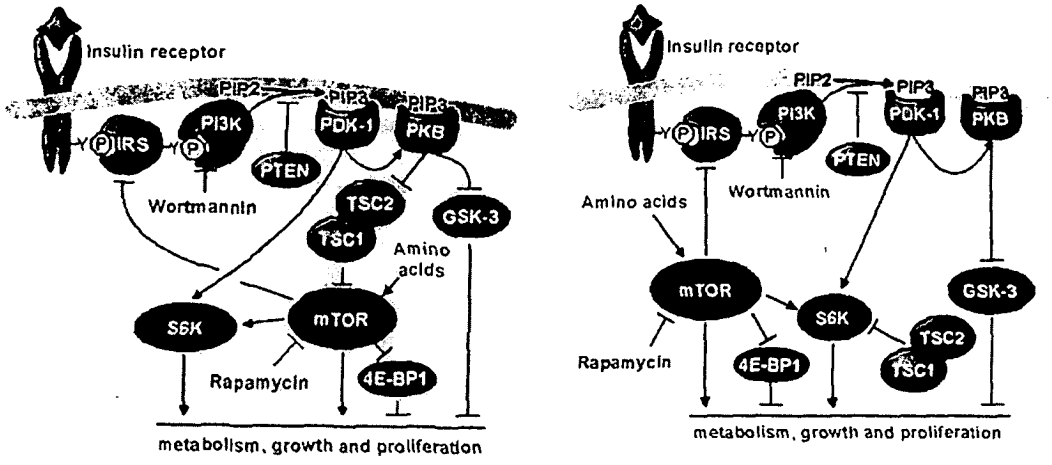

Figure 1.1.2 Models for the relation of S6K and the PI3K pathway (from Kozma and Thomas, 2002)
Proposed model (on the right) for PI3K signalling pathway, dissociating S6K from the PI3K-PKB pathway, compared with a general model of the PI3K pathway, on the left. This proposed model places S6K on a parallel insulin signalling pathway distinct from that of PKB, after taking into account studies that show dS6K is activated independently of dPKB and results in *Drosophila* showing that loss of function mutations in dPTEN and dTSC1/dTSC2 are additive for cell growth, thus indicating that PKB and dTSC1/dTSC2 probably lie on parallel pathways (reviewed in Kozma and Thomas, 2002).

Utilizing the Gal4/UAS system, Cho et al. (2001) showed that over-expression of DSTPK61 increased cell and organ size in a dPI3K-dependent manner. *Drosophila* flies deficient in the *dstpk61* gene were embryonic lethal exhibiting an apoptotic phenotype. Thus their evidence suggests that *dstpk61* regulates cell growth and apoptosis during *Drosophila* development via the PI3K-dependent signalling pathway (Cho et al, 2001).

Oldham et al., (2002) provide genetic evidence that the insulin/IGF signalling controls growth and size during development via the PI3K pathway, whereas the Ras pathway plays little or no role in the InR-mediated control of cell growth. They also show that increased levels of PIP3 (through loss of *dPTEN*) are sufficient to compensate for the complete loss of the Inr/IGF1 receptor function and that reduction of PTEN activity is sufficient to vastly increase organism size.

Apart from affecting cell size and number in a cell autonomous way, effectors of the InR-PI3K pathway seem to have independently an effect on life span. The mutation in *chico* (*chico*^{1}) that results in reduction of cell size and number (Bohni et al., 1999) was found to increase life-span (Clancy et al., 2001), indicating that the wild type *chico* gene acts to accelerate aging. This is consistent with data from *Caenorhabditis elegans*, where inactivation of InR, PI3K, PDK1 and PKB homologues increases longevity by extending the dauer stage, which is a stage characterised by metabolism retardation, storage of fat and dormancy. *C. elegans* usually enters a dauer stage in response to stress conditions like food shortage or overcrowding (reviewed in Stambolic et al., 1999).

It was shown that reduced Ins/IGF signalling (*chico*^{1} mutation) and dietary restriction act through overlapping mechanisms towards slowing aging (Clancy et al., 2002). Further analysis is required in order to investigate the nature of the mechanisms by which reduced insulin/IGF signalling acts like dietary restriction; possibly they both alter some common downstream process. More recently, induced expression of dFOXO in the female adult fly fat body was shown to increase life-span and reduce fecundity, without having an effect on life-span in males (Giannakou et al, 2004). FOXO is a forkhead transcription factor inactivated by insulin/insulin-like factor signalling (by PKB phosphorylation), thus its over-expression reflects lowered Ins/IGF signalling. This study, apart from identifying FOXO expression during adulthood as sufficient to increase longevity and reduce fertility, also demonstrated the importance of adipose tissue (the fat body in *Drosophila*) in mediating extension of life-span in the fruit fly, consistent with findings in the mouse and worm (Giannakou et al, 2004).

1.1.5. Project Background - Aims

dstpk61 identified in our lab was found to be structurally and functionally homologous to human PDK1 and it phosphorylated PKBα *in vitro* (Alessi et al, 1997b). DSTPK61 has 54% identical amino acid sequence in the catalytic domain

with PDK1 and 61% identical (79% similar) on the PH domain. The importance of *dstpk61* in the insulin signalling pathway has since been demonstrated beyond any doubt (Cho et al, 2001; Rintelen et al, 2001; Radimerski et al, 2002).

The *Drosophila dstpk61* gene is a complex locus that produces multiple transcripts by utilising alternative promoters, alternative splicing and alternative polyadenylation sites. A male-testis specific, an ovary-specific, a non-specific and a female carcass-specific transcript were detected by Northern blot analysis (MacDougall et al, 1999). *In situ* hybridisation with a DIG-DNA probe (common to all *dstpk61* transcripts) showed that there is mRNA expression in male but not in female gonads and that this transcript does not belong to transcript groups 1 and 2 (groups shown in Figure 1.1.3) (Clyde, 1999). Twenty-one Expressed Sequence Tags (ESTs) have been previously reported (currently 48 have been identified in the EST database) and there are at least seven different transcripts (the 3rd release -August 2002- of *Drosophila* genomic annotation gives eight) (Clyde and Bownes, 2000). However, these transcripts encode to date only four different DSTPK61 protein isoforms with variant N-termini (see figure 1.1.4). Many of the transcripts vary in their 5' and 3' untranslated regions (UTRs), hence the number of protein isoforms is smaller than that of transcripts.

The available ESTs were grouped according to their 5' sequence in three groups (figure 1.1.3 – the EST information available at the beginning of this study). Group 1 transcripts have exon 1a spliced to exon 2, Group 2 transcripts include exon 1b spliced directly to exon 2 and Group 3 includes EST51 (GH15751/ AT02760 etc.) which has a novel first exon, 1c, only 76 bp long, and other ESTs with 5' sequence different to that observed in the EST's from either Group1 or Group 2 (Clyde, 1999). 3 cDNAs from each Group 1 and Group 2 were fully sequenced, as well as EST51. Some of the ESTs of Group 3 are likely to belong to one of the other groups, since they quite probably do not contain the 5' end of the transcript and the translation may start upstream of the site indicated here.

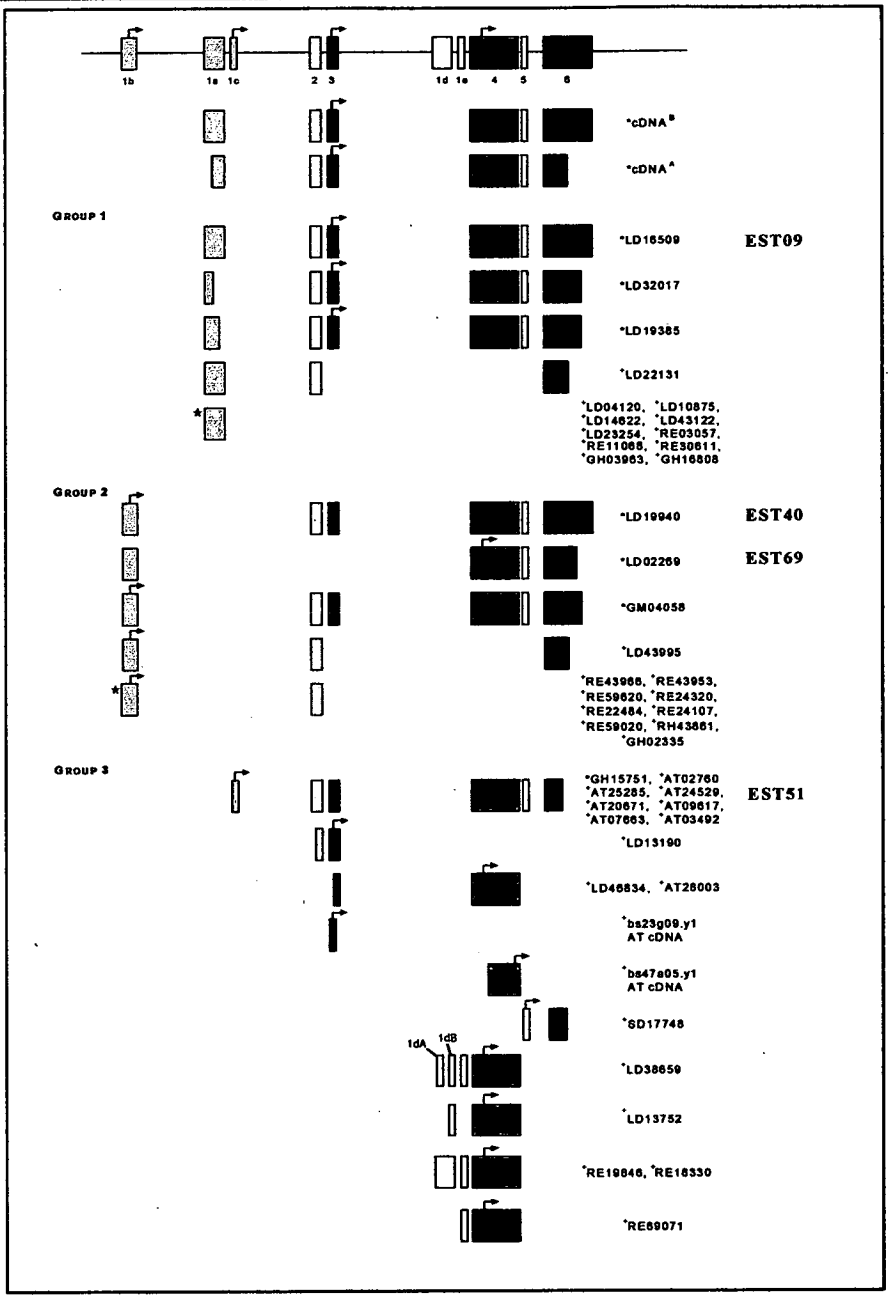

Figure 1.1.3: The exon structure of the three groups of *Dstpk61* transcripts and of the *Dstpk61* gene locus

cDNAs marked * have been fully sequenced while the sequence of those marked + has been taken from the EST database The bent arrow (↱) indicates potential translational start sites. LD, RE = embryonic libraries, GH, RH = adult head libraries, GM = ovary library, AT = adult testes library. A red asterisk indicates that each of the different ESTs has an exon with slightly different 5' and 3' ends. On the right of the figure there are the names of the transcripts that encode different protein isoforms. (updated from Clyde and Bownes, 2000)

RT-PCR with different sets of primers that correspond to different exons was used to demonstrate that EST40 (LD19940) and EST09 (LD16509) represent real transcripts. RT-PCR results indicate that EST40 represents the 4.5kb female-specific transcript, and EST69 (LD02269) is present in almost equal amounts in both male and female carcasses (MacDougall et al, 1999). EST09 was found in male and female somatic tissues, as well as in ovaries. In situ hybridisation with DIG-DNA probes specific for group 1, group 2 transcripts and the core region showed that mRNA transcripts are predominantly located in the cytoplasm of the nurse cells and the cytoplasm of the oocyte (C. Mayor, 4-month project, 2001), but these results have to be verified. It is worth mentioning that even though E51 was initially identified as a cDNA from an adult head library, there are now several ESTs from an adult testis library that share the same sequence (Figure 1.1.3). Thus E51 seems to be a testis-enriched transcript; this speculation will need to be investigated by RT-PCR though.

The four protein isoforms contain all or some of the following domains and motifs: a kinase domain, essential for the role of DSTPK61 as a signalling molecule; a pleckstrin homology domain which is involved in membrane and protein:protein interactions; an OPA repeat/DNA binding domain- OPA repeat domains in *Drosophila* are mainly found in proteins with developmentally restricted expression patterns; nuclear localisation signals; a mitochondrial intermembrane space targeting sequence (Figure 1.1.4- Clyde and Bownes, 2000).

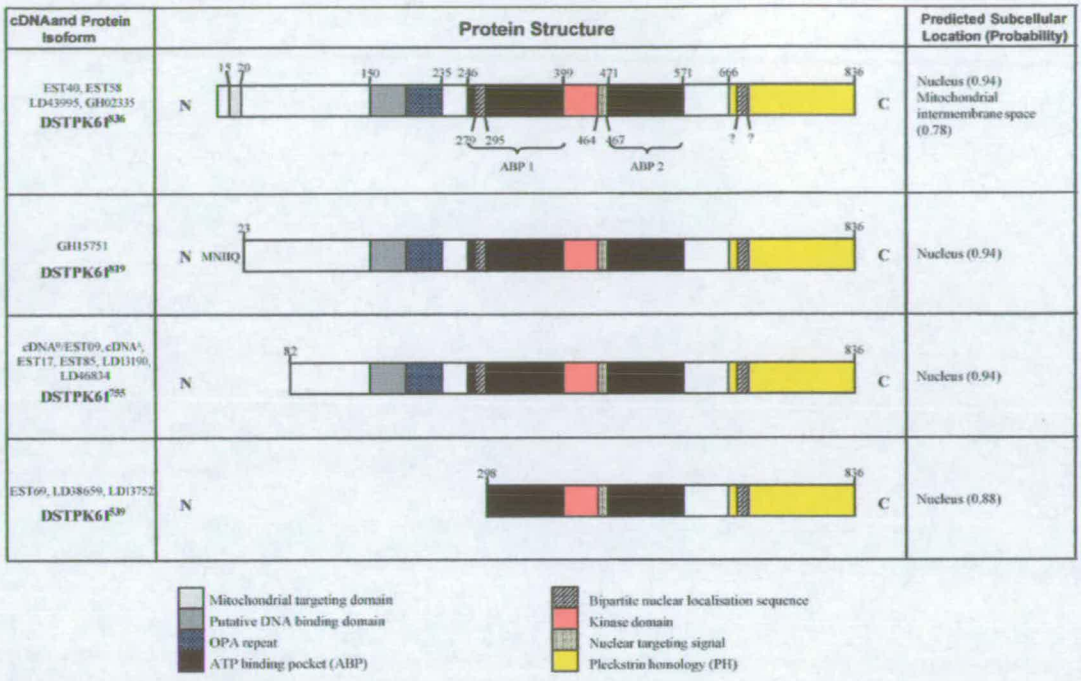

Figure 1.1.4 Structure of the four predicted DSTPK61 isoforms encoded by *Dstpk61* EST cDNAs
The motifs and domains are coded according to the key above (From Clyde and Bownes, 2000).

My project aims included the detailed study of the different DSTPK61 protein isoforms in an attempt to elucidate the function of each isoform. In particular I wanted to investigate the role of *Dstpk61* in developmental processes, given that some of the gene products appeared to be sex-specific and others tissue-specific or tissue-enriched. My working hypothesis was that different isoforms are necessary for different events, some isoforms being specific for a particular function while others have a more general function. Given that the isoforms are predicted to contain variant localisation signals (DSTPK61^{836} has a mitochondrial targetting sequence in addition to the nuclear localisation signal common to all isoforms), it is possible that locating the protein to different subcellular compartments might ensure that it interacts in one signalling pathway rather than another. Another hypothesis was that low levels of kinase activity could be needed for cell growth and higher levels for tissue-specific events.

1.2 Gametogenesis in Drosophila melanogaster

1.2.1 Oogenesis

1.2.1.1 Overview of oogenesis

The *Drosophila* ovary consists of about sixteen ovarioles which are independent egg assembly lines. There is a pair of ovaries connected to the uterus via a common oviduct in adult *Drosophila* females (King, 1970) (Figure 1.2.1.1). Each ovariole contains increasingly mature egg chambers that will develop into mature eggs which will travel to the uterus and become fertilised by sperm stored in the spermathecae and seminal receptacle before being laid. Morphologically the ovariole comprises of the germarium at the anterior (towards the tip of the ovary), where new egg chambers are generated and of the vitellarium at the posterior (towards the oviduct), which contains the progressively developing egg chambers (Figure 1.2.1.2A). There are usually up to seven egg chambers in the vitellarium of each ovariole. Each egg chamber contains both somatic and germline cells and egg chambers are separated from each other in an ovariole by stalk cells. The outer peritoneal sheath and the inner epithelial sheath cover the ovaries and assist with the progression of developing egg chambers. *Drosophila* oogenesis is divided in 14 stages which represent morphologically distinct periods. (King, 1970; Ashburner, 1989; Spradling, 1993)

Oogenesis starts in the germarium (Fig. 1.2.1.2B), where a germline stem cell divides asymmetrically to give a daughter stem cell and a differentiated cystoblast which undergoes four mitotic divisions with incomplete cytokinesis (in the germarium region 1). This results in the formation of a sixteen-cell germline cyst within which the cystocytes (germline cells) are interconnected by cytoplasmic bridges called ring canals (Robinson et al, 1994). The two cystocytes possessing four ring canals become pro-oocytes and enter meiotic prophase I in region 2a. The germline cyst becomes enveloped by follicle cells in region 2b, while within the cyst one of the two pro-oocytes (cystocytes with four ring canals) differentiates into the oocyte and the other germline cells become nurse cells as the cyst moves through germarium region 2. In germarium region 3 the sixteen germline cells enveloped by a cuboidal

epithelium of follicle cells are a stage 1 egg chamber (follicle) (Fig. 1.2.1.2A, B, J). (King, 1970; Spradling, 1993)

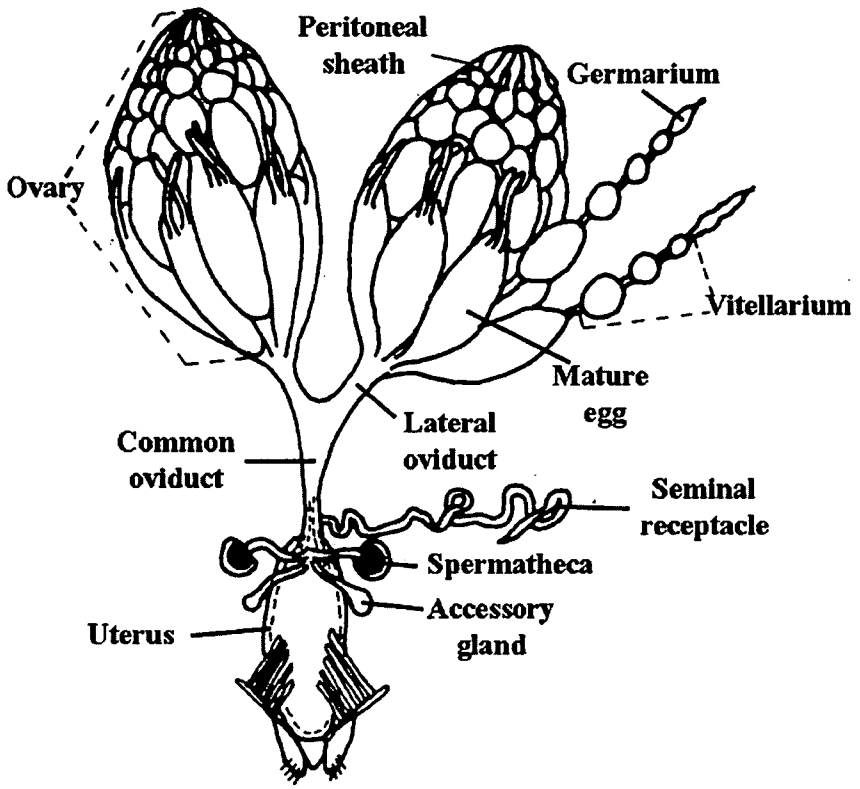

Figure 1.2.1.1 The *Drosophila melanogaster* female reproductive system
An adult female fly has two ovaries, each consisting of 16-20 ovarioles with progressively maturing egg chambers. At the distal tip of each ovariole there is the germarium, a region where oogenesis begins. The part of the ovary containing the developing egg chambers is called vitellarium, at the proximal tip of the ovary. The ovaries are connected to the uterus via a common oviduct. The mature eggs are fertilised in the uterus by sperm stored in the seminal receptacle and spermathecae. Drawing reproduced from *Drosophila* Protocols (ed. Sullivan et al, 2000), originally from Miller, 1950.

At stage 2 the egg chamber has left the germarium. Some (5-8) follicle cells become stalk cells, which separate adjacent egg chambers. Stage 2-6 egg chambers increase in size and their shape changes from spherical to ovoid. During these stages the oocyte has approximately the same size as a nurse cell. The oocyte grows faster than the nurse cells during stages 7-10A, resulting in the posterior half of a stage 10 egg chamber being occupied by the oocyte and the anterior half by the 15 nurse cells (Mahajan-Miklos and Cooley, 1994; Spradling, 1993). The rapid increase of the oocyte size at these stages is a consequence of the uptake of yolk proteins. Yolk

proteins are synthesized in the fat body and the follicle cells (Bownes and Hames, 1978; Brennan et al, 1982). The yolk proteins synthesized by the fat body are initially secreted into the haemolymph and then selectively endocytosed into the oocyte. The yolk proteins from the (columnar) follicle cells are transported directly to the oocyte surface. Yolk protein uptake by the oocyte occurs during stages 8-10B/11 of oogenesis and ceases when the eggshell is assembled. The yolk supplies nutrients to the embryo and acts as a carrier for other molecules (reviewed in Bownes, 1994).

The somatic follicle cells remain as a single cell layer surrounding the germline cells up to stage 8, proliferating up to stage 6 (King, 1970). Within the follicle cell epithelium the polar cells are visibly differentiated during stages 6-8 (Dobens and Raftery, 2000) and participate in subsequent patterning of the terminal follicle cells (Gonzalez-Reyes and St Johnston, 1998). At stage 9 several follicle cell migrations start taking place and three subtypes of follicle cells can be observed. The majority of follicle cells migrate posteriorly to form a thick columnar epithelium over the oocyte. The remaining 5% of follicle cells at the anterior are stretched and flattened to form a thin layer covering the nurse cells (nurse cell associated follicle cells or squamous epithelium). The border cells (a cluster of 6-10 anterior follicle cells recruited by the anterior polar cells) start migrating through the nurse cells towards the anterior tip of the oocyte (Montell et al, 1992, Fig. 1.2.1.2K) where they arrive by stage 10. They participate in the formation of the micropyle from stage 11. At stage 10B the centripetal migration takes place: the anterior columnar follicle cells move centripetally towards the border cells to cover the anterior end of the oocyte (Keyes and Spradling, 1997; Dobens and Raftery, 2000).

The nurse cells transfer their cytoplasm to the oocyte during stages 10B-12 through the ring canals and the oocyte expands to gradually fill the whole egg chamber. The vitelline membrane is secreted by the follicle cells during stages 9-10B (Burke et al, 1987). Oocyte maturation is completed in stages 12-14 with the full resorbtion of the nurse cells and the formation of the endo- and exo-chorion layers by the follicle cells before they undergo apoptosis. (Theurkauf, 1994; Mahajan-Miklos and Cooley,

1994; Margaritis and Mazzini, 1998). The eggshell is composed of the vitelline membrane and the chorion; between those there is a thin wax layer and the innermost chorionic layer (ICL) which contribute to the water resistance of the oocyte to prevent water loss from the developing embryo. The endochorion protects the mature egg and embryo and the exochorion helps in the attachment of the laid egg to the substrate. Specialised structures of the eggshell include: i) anteriorly the operculum and collar [at the base of the micropyle and the dorsal appendages] which facilitate larval exit; ii) the micropyle , necessary for sperm entry and iii) the dorsal (respiratory) appendages which are required for gas exchange of the developing egg through the eggshell (Margaritis, 1986, Mouzaki, 1991). The dorsal appendages are specified by two groups of dorsal anterior columnar follicle cells (Fig, 1.2.1.2L) which start migrating anteriorly at stage 11 (Deng and Bownes, 1997).

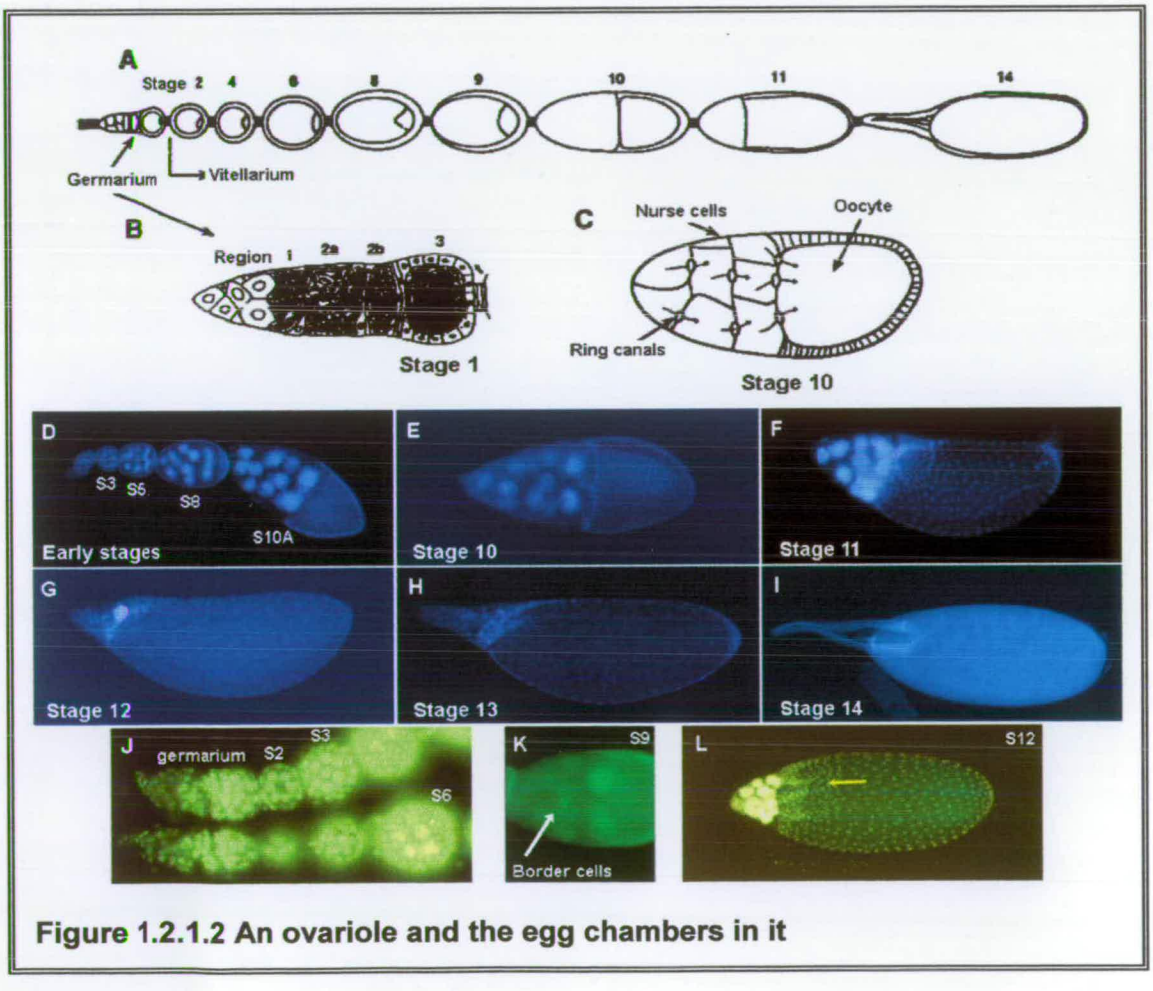

Figure 1.2.1.2 An ovariole and the egg chambers in it

Figure 1.2.1.2 An ovariole and the egg chambers in it
(A) An ovariole with the germarium at the anterior end and the vitellarium containing increasingly mature egg chambers. The stage of the egg chambers drawn here are written on top of each egg chamber. The oocyte is located at the posterior of each egg chamber. (B) The germarium is divided in 4 regions, 1, 2a, 2b and 3. Region 1 contains germline stem cells, the dividing cystoblast and cap cells. Region 2a contains the newly formed 16-cell cysts whereas in region 2b individual cysts become lens-shaped and span the whole width of the germarium. Somatic stem cells located at the border between regions 2a/2b divide to produce profollicle cells and in region 2b inwardly migrating follicle cells separate off individual cysts. As the cyst moves to the posterior, one of the cystocytes becomes the oocyte and the remaining 15 become nurse cells. In region 3 the 16-cell cyst has acquired a monolayer of follicle cells and this cell complex is referred to as a stage 1 egg chamber. (C) A stage 10 egg chamber where the oocyte occupies the posterior half of the egg chamber, surrounded by the follicle cells. At the anterior lie the 15 nurse cells and the arrows indicate the flow of cytoplasm from the nurse cells to the oocyte through the ring canals.
(D-I) Egg chambers in various stages of oogenesis. The germarium is at the left in (D) and egg chambers increase in size as they progress in the vitellarium. At stage 8 yolk is visible in the oocyte (posterior of the egg chamber) (D). At stage 9 the oocyte with its nucleus occupies the posterior 1/3 of the egg chambers, the nurse cells are in the anterior and three subpopulations of follicle cells can be recognised. The columnar follicle cells start migrating over the oocyte, the nurse cell associated follicle cells remain to cover the the nurse cells and are stretched, and the border cells (see K) start migrating between the nurse cells towards the anterior of the oocyte. At stage 10B the nurse cells start dumping their cytoplasm to the oocyte and the columnar follicle cells covering the oocyte flatten to cover the expanding oocyte; migration of the centripetal follicle cells to cover the anterior of the oocyte is also in progress and is completed by stage 11 (F) while the nurse cells continue to dump material to the oocyte (up to stage 12-G). Two groups of follicle cells migrate anteriorly to produce the dorsal appendages. The follicle cells start depositing the chorion (eggshell).
At stage 13 (H) the dorsal filaments are visible at the anterior end and the nurse cell nuclei degenerate. At stage 14 (I) the mature egg is covered with an eggshell that has several differentiated regions. The dorsal appendages at the anterior are used for gas exchange (respiration). The operculum is the base of the dorsal appendages and the micropyle and is the larval exit. The micropyle (seen in I as the protrusion below and between the dorsal appendages) facilitates sperm entry and at the posterior pole of the egg the aeropyle is a specialised chorion structure with respiratory functions in some *Drosophila* species. The corresponding stage is either written under the picture or indicated by an "S" and a number. The egg chambers (J-L) show in more detail the germarium and early stage egg chambers (J), the migrating border cells in a stage 9 egg chamber (K, arrow) and the follicle cells of a stage 12 egg chamber where two subpopulations of follicle cells either side of the dorsal midline will form the dorsal appendages (L, dorsal midline indicated by yellow arrow). A-C are from Mahajan-Miklos and Cooley, 1994). D-I and K-L are with the same magnification whereas J is magnified 4x in comparison. DNA in egg chambers is stained with Hoechst 33258 (blue) in D-I, nuclear yellow in J and L and fluorescein (green) in K. Anterior is to the left and dorsal (F-H) or dorso-lateral (I, L) to the top.

1.2.1.2 Germline differentiation and the origin of polarity (oocyte selection)

The transition from a syncytium of 16 germline cells to a mature egg requires highly regulated cell differentiation and polarisation of the egg chamber. During mid-oogenesis first the Anterior-Posterior (A/P) polarity and then the Dorso-Ventral (D/V) polarity are established through critical interactions between germline cells and somatic follicle cells (Spradling, 1993; Deng and Bownes, 1998). However, the origin of polarity can be traced much earlier in oogenesis, in the germarium, with the determination of an oocyte in the cystoblast and the polarisation of this oocyte to the posterior of the cyst, observed as early as during the move between germarium regions 2b-3 (Gonzalez-Reyes and St Johnston, 1998). The microtubule and actin cytoskeletons and centriole segregation have central roles in establishing and maintaining egg polarity (Theurkauf, 1994; Knowles and Cooley, 1994).

Theurkauf et al. (1993) observed preferential accumulation of specific mRNAs (*Bic-D, orb, cyclin B, oskar, 65F, hts*) and the possession of a microtubule organising centre (MTOC) within the oocyte in region 2b. The MTOC represents the minus-ends of microtubules and the microtubule network extends to the nurse cells (plus-ends) through the ring canals (Cooley and Theurkauf, 1994). In germarium region 3 the cyst is a complete egg chamber, containing an oocyte and fifteen nurse cells enveloped by a monolayer of follicle cells. The mechanism of oocyte determination is still not clear, although recently it has been shown that multiple processes (such as proteins and mRNA localisation, microtubule polarisation, centriole migration and control of entry into meiosis) function in parallel to restrict different aspects of oocyte identity to one of the two pro-oocytes (reviewed in Huynh and St Johnston, 2004). Two main models for oocyte determination have been proposed. The currently favoured model suggests that the oocyte is specified as early as the first cyst division, through the asymmetric inheritance of the fusome (de Cuevas and Spradling, 1998) and is supported by recent evidence showing that the oldest cystocyte which possesses more fusome material than the other cells is more likely to become the future oocyte since it accumulates the centrosomes and *osk* and *orb* mRNAs (Grieder et al., 2000; Cox and Spradling, 2003). The second model proposes that the two pro-oocytes have initially the same probability of becoming the oocyte

and they compete so that whichever pro-oocyte advances into meiosis the fastest would become the oocyte and the other pro-oocyte would revert to the nurse cell fate (Carpenter, 1994). The accumulation of evidence supporting the other model does not rule out the possibility that both pro-oocytes can become the oocyte but shows that if there is a competition, it is strongly biased (Huynh and St Johnston, 2004).

The fusome is a vesicular cytoplasmic structure present in developing germline cysts and contains components of the sub-membrane cytoskeleton such as α- and β-spectrin, dynein, Hu-li tai shao (Hts, a *Drosophila* homologue of mammalian adducin) and Cyclin A (Yue and Spradling, 1992; Lin et al, 1994). It originates from the spectrosome, a small spherical structure in the germline stem cell (GSC) and cystoblasts (Deng and Lin, 1997) which is asymmetrically inherited by the daughter cells and interacts with one of the centrosomes. During each cell division the inherited fusome (spectrosome) anchors one pole of the mitotic spindle and a new fusome plug forms in each ring canal. Then the ring canals move so that the fusome plugs fuse with the original fusome. This results in one cystocyte having more fusome material than the others and containing the same (original) centrosome (Spradling et al, 1997; Huynh and St Johnston, 2004). Genes critical for MTOC polarisation are *egalitarian* (*egl*), *Bicaudal-D* (*Bic-D*) and *stonewall* (*stwl*) (Theurkauf, 1993; Clark and McKearin, 1996), mutations which result in egg chambers with 16 nurse cells and no oocyte (Schüpbach and Wieschaus, 1991).

The oocyte fate needs to be maintained (through the function of genes regulating cell cycle state, such as *encore*, *da capo, string/cdc25*) (reviewed in Huynh and St Johnston, 2004). The oocyte positioning at the posterior of the stage 1 egg chamber is driven by Cadherin-dependent adhesion and requires upregulation of DE-cadherin adhesion complex components (DE-Cadherin, encoded by *shotgun*, Armadillo = β-catenin, α-catenin) in both the oocyte and the follicle cells surrounding the posterior of the cyst (Gonzalez-Reyes and St Johnston, 1998; Godt and Tepass, 1998). The oocyte movement also requires the products of the five *spindle* genes (*spnA-E*) (Morris and Lehmann, 1999), *okra, aubergine, vasa, maelstrom* and *dicephalic* (Gonzalez-Reyes and St Johnston, 1994; Gonzalez-Reyes et al, 1997; Ghabrial et al,

1998; Findley et al, 2003). The PAR proteins (Baz/PAR-6/aPKC, PAR-1/14-3-3), probably targeting the microtubule cytoskeleton in the oocyte, are also needed for the transport of the oocyte-specific proteins and mRNAs, centrosomes and mitochondria that are associated with the fusome remnants at the oocyte anterior to the posterior of the oocyte (Huynh and St Johnston, 2004).

The follicle cells form a symmetrical pattern along the A/P axis, with polar cells at the anterior and posterior ends differentiating from the rest of the follicle cells (Margolis and Spradling, 1995). Hedgehog (Hh) signalling regulates proliferation and differentiation of the stalk and polar cell precursors (Forbes et al, 1996). The *Notch/Delta* signalling pathway is also involved in cyst encapsulation and follicle cell differentiation. Delta is a transmembrane protein acting as a ligand for Notch, which regulates stalk cell subdivision in a concentration-dependent manner: Some mutations of *Notch* lead to fused egg chambers due to encapsulation of two or more germline cysts (Goode et al, 1996). Reduced Notch signal levels cause loss of stalk cell marker expression (Ruohola et al, 1991) but other mutations causing low levels of activated Notch induce extended stalk structures early in oogenesis and later result in the loss of polar cells (Larkin et al, 1996). The way by which the posterior (and not the anterior) polar cells up-regulate Cadherin and thus pull the oocyte towards them has been recently resolved (Torres et al, 2003). The anterior polar cells differentiate much earlier than the posterior ones in an egg chamber upon Delta signalling. These cells then start expressing Unpaired, the JAK/STAT pathway ligand, which induces the anterior polar stalk cell precursors to differentiate into stalk cells. These cells are believed to up-regulate Cadherin to adhere to the oocyte of the adjacent (younger) egg chamber.

1.2.1.3 Anterior-Posterior axis determination

The Grk/EGFR signalling pathway establishes and regulates axis polarity (Neuman-Silberberg and Schüpbach, 1993; Queenan et al., 1997), initially along the A/P and later the D/V axis through interactions between the germline cells and somatic follicle cells (Gonzalez-Reyes et al, 1995; Roth et al, 1995). The transforming growth factor alpha (TGF-α) homologue *gurken* (*grk*) transcript is localised to the

posterior pole of the oocyte during stages 1-7 of oogenesis. Grk protein, the ligand for the Epidermal Growth Factor Receptor (EGFR/Torpedo- a tyrosine kinase) is synthesized there and is internalised by the adjacent posterior polar and main body follicle cells (Figure 1.2.1.3). The product of the *cornichon* gene is required for signal transmission and EGFR in the follicle cells is essential to receive the signal. Only the previously differentiated polar follicle cells (see above) respond to the Grk signal, through a signal transduction pathway involving *Ras, D-raf* and *Dsor1*, and adopt a posterior fate [anterior is the default state]. These follicle cells signal back to the oocyte with a so far unknown signal that directs reorganisation of microtubules within the oocyte. Protein kinase A (PKA) participates in the transduction of this signal in the oocyte (Lane and Kalderon, 1994). Another gene required for proper microtubule reorganisation is *mago nashi* (*mago*) (Micklem et al, 1997).

Microtubule reorganisation involves the gradual disappearance of the posterior MTOC during stages 7-10 and its replacement with an anteriorly localised MTOC in the oocyte. The MTOC repolarisation results in the localisation of the maternal mRNAs *bicoid* and *oskar* to the anterior and posterior poles of the oocyte, respectively. In addition, the oocyte nucleus begins to move from the posterior to an anterior-dorsal position; *grk* mRNA and protein are also redistributed to the anterior-dorsal position from which they will later participate in the D/V axis patterning of the eggshell (Fig. 1.2.1.3). Bic-D, Egl and DLis-1 (*Drosophila* Lissencephaly-1) are involved in the migration and localisation of the nucleus (Swan and Suter, 1996; Mach and Lehmann, 1999; Swan et al, 1999).

Posteriorly localised *oskar* transcripts synthesize Osk protein which plays a key role in pole plasm formation (confers germ line fate to posterior cells in the embryo) and localisation of other transcripts (Ephrussi et al, 1991; Kim-Ha et al, 1991; Ephrussi and Lehmann, 1992). The products of genes *orb, vasa, mago, staufen, TmII* and *Bru* participate in *osk* localisation and translational regulation (reviewed in Cooperstock and Lipshitz, 2001). The anterior determinant *bicoid* (*bcd*) is translated after fertilisation of the egg to produce an anterior to posterior gradient in the embryo (St Johnston et al, 1989). The genes *exuperantia* (*exu*), *swallow* and *staufen* (Wang and

Hazelrigg, 1994; Stephenson et al, 1988; St Johnston et al, 1991) are involved in *bcd* RNA positioning.

1.2.1.4 Dorsal-Ventral axis determination – dorsal appendage formation in *Drosophila* egg chambers

The oocyte nucleus moves from the posterior to the anterior of the oocyte during stages 7- 8 of oogenesis in a microtubule-dependent manner and as a result *gurken* (*grk*) mRNA and protein are expressed at the presumptive dorsal-anterior region of the oocyte from stage 9. Gurken signals to the Epidermal Growth Factor Receptor (EGFR) on the surface of the adjacent follicle cells which adopt a dorsal fate. Through an elaborate regulation involving several genes that include *rhomboid, pointed, argos, spitz, kekkon-1, mirror* and *Broad-Complex* (*Br-C*), EGFR signalling results in two subsets of dorsal anterior follicle cells either side of the dorsal midline to become determined to migrate anteriorly and secrete the dorsal appendages and the operculum (Fig. 1.2.1.3). (Deng and Bownes, 1998; Van Buskirk and Schüpbach, 1999; Wassermann and Freeman, 1998; Deng and Bownes, 1997; Zhao and Bownes, 1999; Ruohola-Baker et al, 1993; Morimoto et al, 1996; Cooperstock and Lipshitz, 2001).

Specifically, *grk* transcript is synthesized in the oocyte nucleus in mid-oogenesis (Saunders and Cohen, 1999) and in stages 9-12 *grk* RNA is concentrated in a cap overlying the oocyte nucleus at the dorso-anterior corner of the oocyte (Neuman-Silberberg and Schüpbach, 1993). The gene *fs(1)K10* is required for the localisation of *grk* RNA to the anterior dorsal region (Schüpbach, 1987) and encodes a helix-loop-helix DNA binding protein. The *k10* mRNA localises to the oocyte nucleus as a result of *cappuccino* and *spire* activity and K10 is necessary to retain SquidS (SqdS) (Norvell et al, 1999), a protein that binds to *grk* 3'-UTR. The *squid* locus encodes three Sqd protein isoforms related to hnRNP proteins that transfer RNA from the nucleus to the cytoplasm (Kelley, 1993; Norvell et al, 1999). *Grk* RNA bound to SqdS is exported from the nucleus and SqdS is replaced in the cytoplasm by SquidA. Bruno (Bru), a cytoplasmic translational suppressor is also bound to *grk* 3'-UTR (Kim-Ha et al, 1995), being recruited by SqdS, and represses translation of the *grk*

transcripts in the dorsal anterior. Orb (Christerson and McKearin, 1994; Lantz et al, 1994) and Spn-E/Hls are necessary for *grk* RNA localisation to the dorsal anterior corner, where activated Vasa (post-translationally modified by Okra, SpnB and SpnC- Ghabrial, 1998; Gonzalez-Reyes et al, 1997) (Tinker et al, 1998) and Orb remove Bru suppression and the *grk* RNA can be translated in the Grk protein. [Model based on Ghabrial and Schüpbach, 1999; Norvell et al, 1999].

Transfer of the Grk signal from the oocyte to the adjacent follicle cells requires the function of *cornichon* and *brainiac* (*brn*) genes. Cornichon is a small protein with a characteristic large hydrophobic domain, controlling the transport of Grk to the oocyte plasma membrane (Roth et al, 1995, Peri and Roth, 2000). *brn*, a neurogenic gene, is required for the maintenance of the follicular epithelium in the egg chamber and for regulation of Grk/EGFR interactions.

The relation between A/P and D/V axes lies with overlapping concentration gradients and spatially specific gene activation/inhibition. Decapentaplegic (Dpp) is a TGF-β homologue required for patterning of anterior eggshell structures (Twombly et al, 1996). It is a morphogen expressed in the centripetal cells and the nurse cell associated follicle cells at stage 10. Changes in the expression levels of Dpp shift the antero-posterior position of the dorsal appendages (Twombly et al, 1996), most probably through modifying the position of Broad-Complex-expressing cells, since Br-C expression along the A/P axis is regulated by Dpp (Deng and Bownes, 1997). The second Grk-induced activation of the EGFR pathway in the dorsal follicle cells restricts *pipe* (Jordan and Ruohola-Baker, 2000) expression to the ventral follicle cells.

Several genes function downstream of Grk/EGFR to lead the initial EGFR activation by Grk binding into a two-peak signal essential for dorsal appendage formation (Wassermann and Freeman, 1998) (Fig. 1.2.1.3). The Ras/Raf and Dsor1 pathway (MAPKinase cascade) is activated by binding of a ligand to EGFR (Brand and Perrimon, 1994; Schnorr and Berg, 1996). According to Wassermann and Freeman (1998), first there is initiation of EGFR activity in the follicle cells directly above the Grk expression area (paracrine signal). In response to this EGFR activity the

rhomboid (*rho*) and *vein* genes are transcribed in these follicle cells. Rhomboid (Ruohola-Baker et al, 1993) is a transmembrane protein that regulates the cleavage, and thus activation, of Spitz, another EGFR ligand. The initial EGFR activation leads to the loss of the transcriptional repressor CF2 (which is active in the ventral cells) and subsequently to the de-repression of *rho* expression. So the second step in Grk/EGFR- D/V signalling (stage 10) is the autocrine amplification of the EGFR signal from the initial Grk-receiving follicle cells to their adjacent ones by Spitz and Vein (a third EGFR ligand) diffusion. This method of signal amplification is particularly useful since the formation of the vitelline membrane between the follicle cells and the oocyte would prohibit any further signalling from the oocyte to the follicle cells after stage 10-11. The third response to EGFR activity is the expression of *argos* (*aos*), which encodes a secreted EGFR inhibitor (Freeman et al, 1992; Zhao and Bownes, 1999), in the middle (dorsal midline) follicle cells, those which would have the peak of EGFR signalling and therefore exceed an EGFR concentration that acts as a threshold for *argos* activation. Together with the expression of *kekkon 1* (Musacchio et al, 1996; Ghiglione et al, 1999), another EGFR inhibitor in the dorsal midline, Argos eventually inhibits the EGFR pathway in the dorsal midline and allows its expression in the two dorsal anterior areas either side of the dorsal midline, that will subsequently form the two dorsal appendages. The DPP gradient participates through an unknown mechanism to the refinement of the exact positions of the dorsal appendages together with the EGFR gradient.

Broad-Complex (*Br-C*) is a gene encoding a family of zinc-finger transcription factors that is expressed in a dynamic pattern in oogenesis and acts downstream of Dpp and Grk/EGFR pathways (Deng and Bownes, 1997; Tzolovsky et al, 1999). At stages 12 and 13 of oogenesis Br-C is expressed in two groups of dorsal anterior follicle cells that will give rise to the dorsal appendages. Specifically the Br-C expressing cells produce the roof of the dorsal appendages whereas Rho-expressing cells that migrate underneath them produce the floor (Dorman et al, 2004; Berg, 2005). The gene *pointed* (*pnt*) (Morimoto et al, 1996) is expressed in the dorsal midline follicle cells with the highest EGFR concentration and represses *Br-C* expression there.

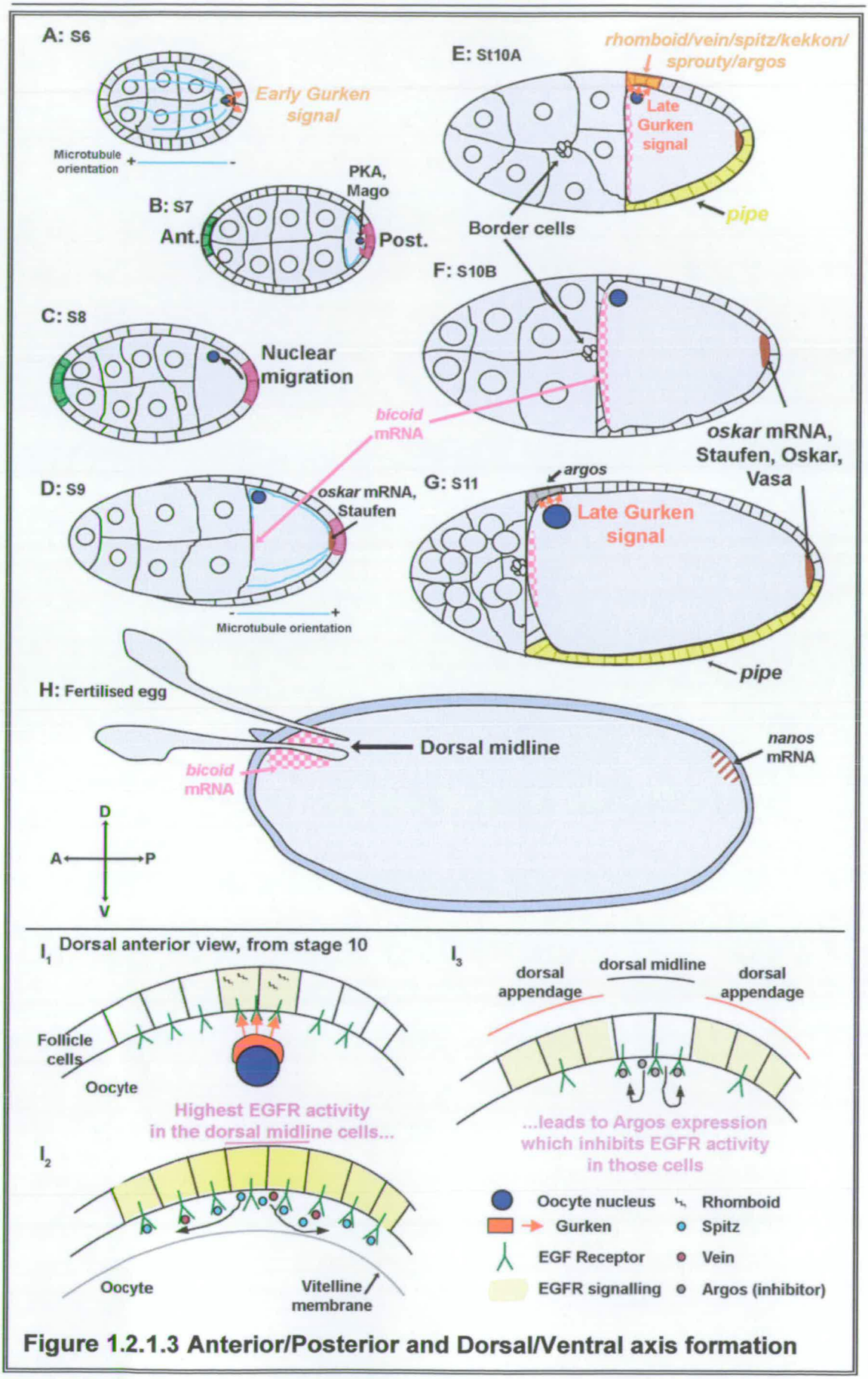

Figure 1.2.1.3 Anterior/Posterior and Dorsal/Ventral axis formation

Figure 1.2.1.3 Anterior/Posterior and Dorsal/Ventral axis formation
A: The oocyte contains a microtubule organising centre (MTOC) during stages -1-6 that extends to the nurse cells and polarises the egg chambers (microtubules labelled in light blue). At stage 6 the oocyte nucleus (blue) and the Gurken signal (red) produced by it are localised to the posterior of the oocyte. Grk signals to the adjacent follicle cells (red arrows) and induces them to adopt a posterior fate (labelled in purple from B). The follicle cells at the anterior of the egg chamber acquire the anterior fate (green from B).
B: At stage 6-7 the posterior follicle cells send an unknown signal back to the oocyte (purple arrows). This leads to reorganisation of the microtubule cytoskeleton. Protein Kinase A (PKA) and Mago nashi (Mago) are required in the oocyte to relay the signal.
C: The posterior MTOC disappears and a new MTOC is nucleated at the anterior. The oocyte nucleus migrates in a microtubule-dependent manner from the posterior to an anterior position, which will later define the dorsal side.
D: The rearranged microtubule cytoskeleton is required at stage 9 to localise *bicoid* mRNA (pink checked) to the anterior and *oskar* mRNA and Staufen protein (dark red-brown) to the posterior of the oocyte.
E: The late Gurken signal (red arrows) is necessary to activate the EGFR pathway in the adjacent follicle cells which will adopt a dorsal fate (orange) as a result of the activation of several genes (see also Fig.1.2.1.3I). The EGFR pathway activation and assignment of dorsal fate restricts *pipe* expression (yellow) to the ventral follicle cells.
F: The Oskar protein at stage 10B is required to anchor its own *osk* mRNA to the posterior and to recruit Vasa and other future pole plasm components there.
G: Activation of EGFR by Grk, Spitz and Vein causes the expression of EGFR inhibitor Argos (grey) in the dorsal anterior cells above the oocyte nucleus. Argos represses the EGFR signal in these cells, so the signal is split in two dorso-lateral peaks (also in I_3).
H: *bicoid* mRNA is translated in the fertilised egg to produce a gradient of the anterior morphogen. *nanos* mRNA (brown lines), which localises to the posterior from stage 12, is also translated to allow abdomen formation, via inhibition of translation of *hunchback* mRNA at the posterior by the Nanos protein (Gilbert, 2003).
I: How the initially uniform dorsal signal results in the formation of two dorsal appendages.
I_1: At stage 10 Gurken (red shape and arrows) synthesized at the anterior corner where the oocyte nucleus (blue) is (see text for more details), is secreted towards the adjacent follicle cells and activates EGFR signalling (yellow shade) by binding to EGFR (green). Rhomboid (black lines) expression is induced by EGFR activation and activates another EGFR ligand, Spitz.
I_2: Spitz (light blue) and Vein (purple), an EGFR ligand the expression of which was also induced by EGFR dorsal activation, amplify the dorsal signal by binding to EGFR receptors in neighbouring follicle cells and activating the EGFR signalling. EGFR activity is higher in the cells that received the original Grk signal, though.
I_3: The high EGFR activity (above a certain threshold) induces expression of Argos (grey), an EGFR inhibitory ligand in the central dorsal cells. Argos, together with Kekkon and Sprouty, two other EGFR pathway inhibitors induced by dorsal EGFR activity, represses signalling in the central dorsal follicle cells (dorsal midline). Therefore the single peak of EGFR activation is split in two dorso-lateral peaks either side of the dorsal midline. These peaks specify the positions of the dorsal appendages.
A-H are adapted from Van Eeden and St Johnston, 1999 and Cooperstock and Lipshitz, 2001. I_{1-3} are based on Wasserman and Freeman, 1998.

Many more genes participate in the establishment of the Dorso-ventral axis. The gene *mirror* (*mirr*) acts downstream of the Grk/EGFR signalling cascade and is expressed in the dorsal anterior side in mid-oogenesis (Zhao et al, 2000a), repressing the expression of *fringe* (Zhao et al, 2000b), *wind* and *pipe* in these cells and allowing them only to be expressed or their products activated in the ventral side.

Downregulation of EGFR signalling results in a reduction of the number of cells exhibiting a dorsal fate leading to a reduction in the distance between the dorsal appendages whereas EGFR overexpression results in dorsalised eggs and embryos by increasing the distance between dorsal appendages (Neuman-Silberberg and Schüpbach, 1993; 1994; Queenan et al, 1997). In the absence of a dorsal signal (Grk/EGFR signalling) the follicle cells exhibit the default ventral fate.

1.2.2 Spermatogenesis

The male reproductive system of *Drosophila melanogaster* consists of a pair of testes connected via the testicular ducts to seminal vesicles. The seminal vesicles and a pair of accessory glands are connected to the ejaculatory duct, through which the seminal fluid is transferred to the female during copulation (Figure 1.2.2.1). The *Drosophila* testes are long tubes with a straight apical and a coiled basal end. The characteristic yellow colour of adult *D. melanogaster* testes and seminal vesicles is due to the pigment cells of the outer layer of the testis sheath; the inner layer of this sheath is composed of muscle cells. Secretions of the male accessory glands and ejaculatory duct which are passed together with the sperm to the female greatly enhance male fertility. The 36-amino acid sex peptide, produced by the accessory glands, is one of the seminal fluid components transferred across to the female. It controls female mating and reproduction by suppressing sexual receptivity (to other males) and inducing oviposition (Chen et al, 1988; Ashburner, 1989; Fuller, 1993).

At the apical tip of the testis is the germinal proliferation centre. A compact group of somatic specialised cells is known as the hub and is located at the apical tip of the

testis (Figure 1.2.2.2). A rosette of male germline stem cells (GSCs, there are 5-9 in adults) flanks the hub. Each GSC in turn is flanked by a pair of cyst progenitor cells (CP) which are somatic stem cells that are also in contact with the hub (Fuller, 1993; 1998). Male GSCs are maintained by signals produced by the hub. Specifically, hub cells express *unpaired* (Upd) which activates the JAK-STAT pathway in the adjacent GSC and induces it to maintain male GSC identity (Kiger et al, 2001; Yamashita et al, 2003).

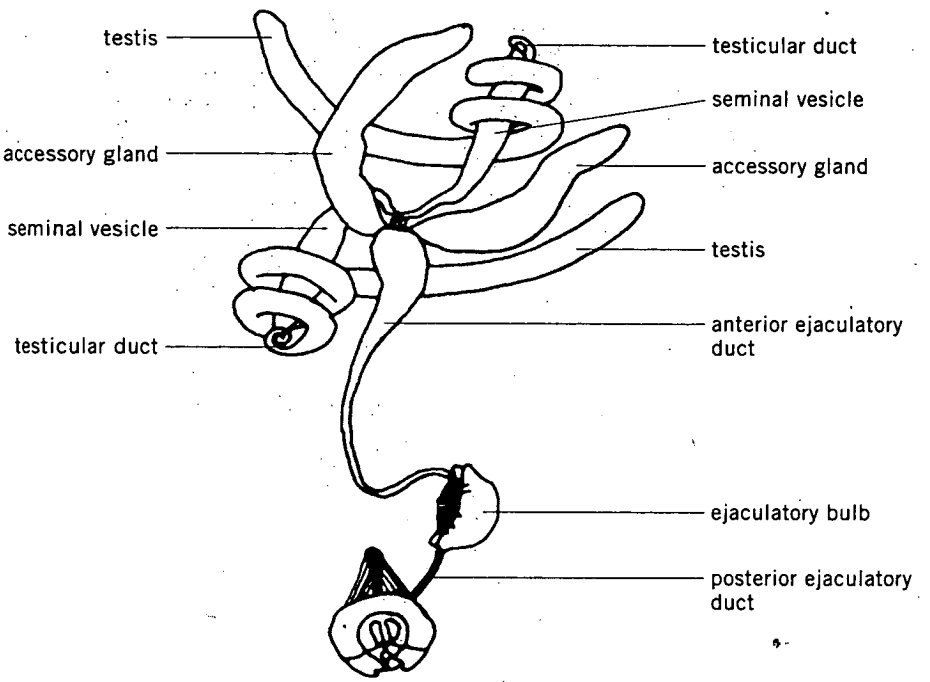

Figure 1.2.2.1 Adult male reproductive system
Male germline and somatic stem cells are positioned at the anterior (apical) tip of the testis and through a series of mitotic and meiotic divisions and differentiation, produce cysts with 64 spermatids. Increasingly mature cysts move away from the apical tip of the testis towards the coil and the elongating spermatids occupy the testis lumen. The individualised sperm coils to the base of the testis and is released into the seminal vesicle. Accessory glands and the ejaculatory duct produce components of the seminal fluid. Drawing reproduced from *Drosophila* Protocols (ed. Sullivan et al, 2000), originally from Miller, 1950.

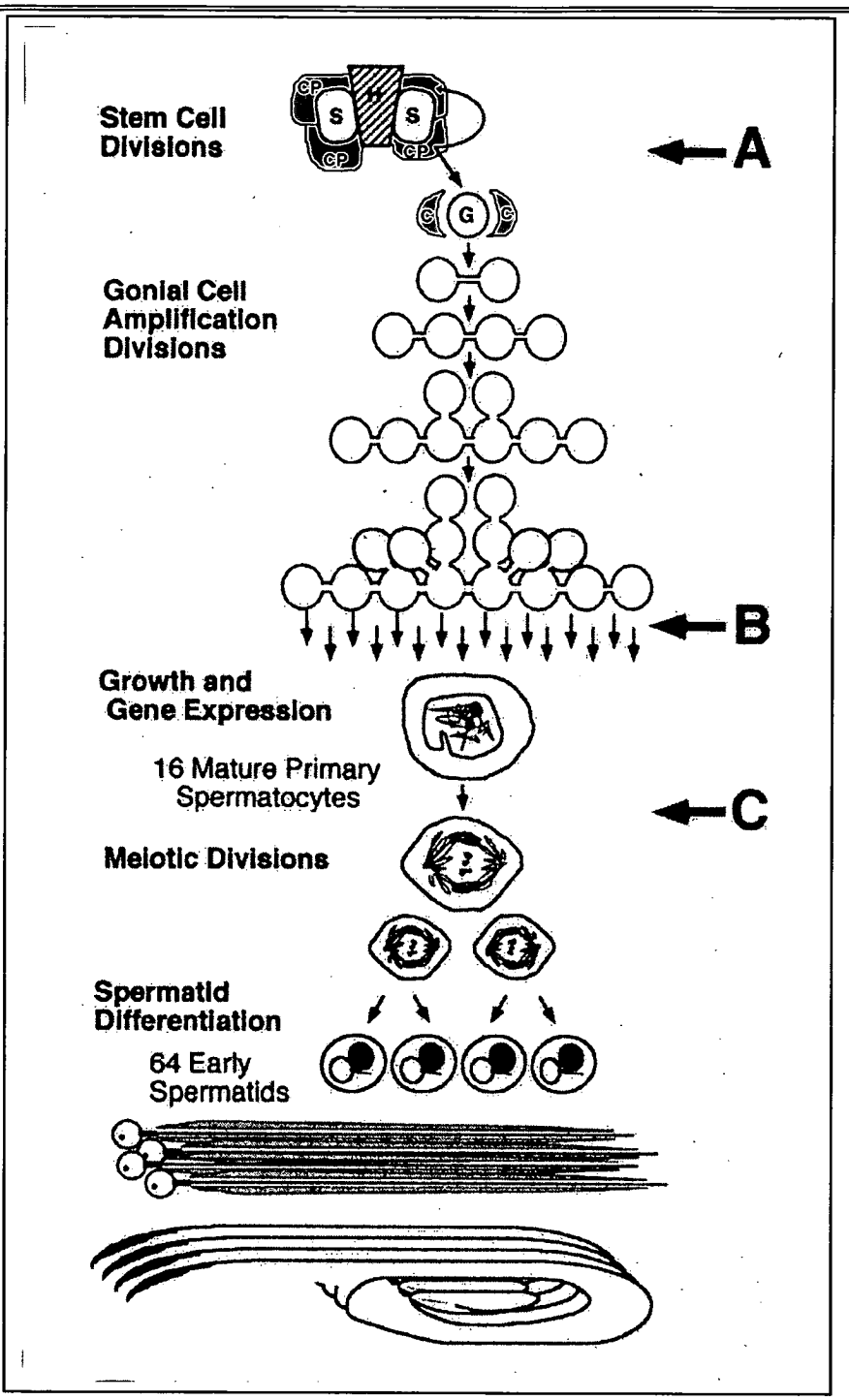

Figure 1.2.2.2 Overview of spermatogenesis in *D. melanogaster*
A, B and C indicate the three major cell fate transitions occurring in spermatogenesis, which are stem cell divisions, primary spermatocyte growth and gene expression period, and completion of meiosis and onset of spermatid differentiation, respectively (Fuller, 1998).

Figure 1.2.2.2 Overview of spermatogenesis in *D. melanogaster* (continued)
Male germline cells (S) lie next to the hub (H) at the apical tip of the testis and are flanked by somatic stem cells, the cyst progenitor cells (CP). Spermatogenesis begins with a male germline cell dividing asymmetrically to produce a daughter stem cell and a gonialblast (G). Similarly two cyst progenitor stem cells divide to produce new cyst progenitor cells and cyst cells (C). Two cyst cells enclose each gonialblast and accompany it through all its mitotic and meiotic divisions and differentiation, but they do not divide again (Cyst cells here shown only around the gonialblast for simplicity). The gonialblast undergoes four rounds of mitotic divisions with incomplete cytokinesis. This results in a cyst of 16 interconnected spermatogonia.
The germline cells of the cyst switch from spermatogonial mitotic divisions to the meiotic program and a period of growth and gene expression during which they are called primary spermatocytes. Only one spermatocyte of the 16 is shown for simplicity.
The spermatocytes exit the cell growth and transcription programme and enter the first meiotic division. They all undergo two meiotic division, resulting in a cyst of 64 interconnected haploid spermatids (also called onion stage). During this stage the mitochondria are assembled into a large mitochondrial derivative (black sphere in the drawing) the same size as the nucleus (white sphere).
The haploid spermatids undergo dramatic differentiation (spermiogenesis) in synchrony and they are fully elongated while still interconnected. Finally after individualisation, the 64 sperm coil to the base of the testis and are transferred to the seminal vesicle.
Drawing reproduced from Fuller, 1998 with some additions (cyst progenitor cells, cyst cells) based on Schulz et al, 2004.

A male germline stem cell divides asymmetrically to produce a daughter stem cell (invariably the daughter cell which maintains contact with the hub and thus receives Upd) and a gonialblast (a founder gonial cell, committed to differentiation). The somatic stem cells (progenitor cyst cells) also divide asymmetrically and produce a daughter somatic stem cell and a cyst cell. Each gonialblast is enclosed by a pair of cyst cells (Fig. 1.2.2.2). The two cyst cells do not divide again and differentiate together with the gonialblast and its progeny throughout spermatogenesis. The assembly of two cyst cells and the progeny of a single gonialblast is called a cyst.

The gonialblast undergoes a series of four synchronous mitotic amplification divisions, resulting in a cyst of sixteen (16) spermatogonia in *D. melanogaster* (in other *Drosophila* species the number of mitotic divisions can vary). Cytokinesis is incomplete during these divisions and the cells are interconnected with cytoplasmic bridges called ring canals, which have a different structure and biogenesis to the ring canals in the ovarian germline. A spectrin-rich fusome is extended through the ring canals into each germ cell of the cyst.

After the fourth mitotic division the cells cease mitosis and enter the meiotic prophase as primary spermatocytes. At this point they enter a programme of extensive growth and gene expression. In the approximately 3.5 days this stage lasts, the primary spermatocytes grow 25 times in size and express genes, many of which are required only for spermatogenesis or are encoding male germline-specific isoforms of proteins found also elsewhere. Most transcription is shut down at the end of the primary spermatocyte growth. The meiotic divisions I and II that follow lead to the formation of a cyst of 64 interconnected haploid spermatids (Fig.1.2.2.2).

The process of differentiation of the haploid spermatids is called spermiogenesis and involves dramatic morphological changes with remodelling of subcellular components. The early round haploid spermatids are also described as "onion stage", because the mitochondrial membranes in them are arranged in concentric layers and this structure resembles an onion slice in cross sections. The mitochondria are separated equally among the daughter cells during the meiotic divisions. After meiosis ceases, all the mitochondria in each early haploid spermatid fuse into two giant mitochondria (aided by the expression of the *fuzzy onions* (*fzo*) gene product) which wrap around each other to form a spherical structure called the Nebenkern or mitochondrial derivative. This structure appears dark in phase-contrast microscopy and lies next to the phase-light spherical nucleus of the spermatid which has the same size as the mitochondrial derivative (Fig. 1.2.2.2). The onion stage spermatids are located near the testis wall at the beginning of the testis coil and are easily identified by the paired black and white spheres in them.

During the elongation stages that follow, each spermatid assembles a microtubule-based flagellar axoneme, along which the two giant mitochondria elongate after the mitochondrial derivative is unwrapped. The ring canals and fusome are concentrated at the elongating end of the bundle of flagellae, opposite the nuclei. One of the surrounding cyst cells, the head cyst cell, together with the spermatid nuclei insert into the specialised terminal epithelium at the base of the testis and are held by it. The other cyst cell (tail cyst cell) elongates to cover fully the bundle of maturing spermatid flagella, which stretch along the testis lumen, almost to its entire length.

The mature, fully elongated spermatids are individualised by an actin-based structure called the individualisation complex (Fuller, 1998). Myosin VI was also shown to participate in this structure (Hicks et al, 1999; H. Millo, unpublished observations). The individualisation complex starts at the head of the spermatid cyst (in the base of the testis) and travels down the spermatid bundle. As it passes, it pushes almost all of the spermatid cytoplasm into a growing waste bag and leaves 64 individual sperm, each tightly invested in its own plasma membrane. After individualisation is completed, the sperm bundle coils and is withdrawn into the base of the testis. Subsequently the mature sperm are released into the testis lumen and are then passed to the seminal vesicle.

(Ashburner, 1989; Fuller, 1993; Wellington and Lehmann, 1996; Fuller, 1998; Schulz et al, 2004)

A great deal is known about the genetics of spermatogenesis, with current research shedding light on an increasing number of mechanisms. There is insufficient space in this thesis to cover this topic in depth and most of the experiments done during my PhD work relate to the genetics of oogenesis; for *dstpk61*, my work on spermatogenesis included some general experiments and time limitations did not allow for a thorough analysis of the genetics of spermatogenesis.

1.3 Investigating the role of extramacrochaetae in Drosophila oogenesis

This project was started initially in parallel to my work on the *dstpk61* gene, as a secondary project, for two main reasons: To allow me to study oogenesis (and familiarise myself with it) more in depth than the *dstpk61* project was leading to and as an opportunity to gain experience in different techniques, such as genetic crosses and generation of mosaic flies, as well as studying events in an intriguing pathway, namely the Grk/EGFR signalling events that lead to the dorso-ventral axis determination and the formation of the dorsal appendages. Additionally, it enabled me to have an extra project since my original aims of expressing protein isoforms and studying their potentially different enzymatic activity in the *dstpk61* project were proving quite problematic and progress was quite slow. Eventually, due to the demands of the extended experimental work and the prioritisation of the *emc* work as closer to publication, the *emc* project became my full-time work for the last third of my PhD, and did result in a publication (Appendix A).

1.3.1 The gene *extramacrochaetae* (*emc*)

The gene *extramacrochaetae* (*emc*) encodes a transcription factor and is involved in many diverse processes at various stages of *Drosophila* development (Campuzano, 2001 for a review). It was named after the first phenotypic observations in *emc* loss-of-function mutants, where extra macrochaetae were observed on the fly notum (Moscoso del Prado and Garcia-Bellido, 1984). It negatively regulates the *achaete-scute* Complex (AS-C) (Botas et al, 1982) and encodes a Helix-Loop-Helix (HLH) protein (Ellis et al, 1990; Garrell and Modolell, 1990).

The helix-loop-helix family of transcriptional regulatory proteins has over 240 members in various organisms (Massari and Murre, 2000), all sharing the HLH motif. This motif consists of two amphipathic alpha helices separated by a loop (Murre et al, 1989) and functions as a dimerisation domain. Most proteins of the

family also have a "basic region" towards the amino-terminus, which, together with residues in the loop and helix 2, is responsible for DNA binding to a consensus hexanucleotide E-box (Murre et al, 1989; Ellenberger et al, 1994; Voronova and Baltimore, 1990); these are referred to as bHLH proteins (basic HLH). Emc belongs to class V of HLH proteins (Massari and Murre, 2000), or, according to a different classification, to Group D of HLH proteins (Atchley and Fitch, 1997), together with the Id proteins (Inhibitor of differentiation) in mammals (Benezra et al, 1990). Proteins of this class lack the basic region, thus are unable to bind DNA (Davis et al, 1990) and are negative regulators of class I and class II HLH proteins by forming inactive heterodimers with them. Class I proteins, which include Daughterless, are expressed in many tissues and can form homo- or hetero-dimers (Murre et al, 1989b). Class II HLH proteins include the Achaete-Scute complex, MyoD and Atonal; their expression is tissue-restricted, they are generally unable to form homodimers and they heterodimerise preferentially with Class I HLH proteins (Massari and Murre, 2000) (Class I and II are also referred to as A and B, respectively – Carmeliet, 1999).

1.3.2 Roles of *emc* in *Drosophila*

Emc regulates Sensory Organ (bristle - SO) formation in a concentration dependent manner by forming heterodimers with Daughterless and the AS-C proteins (Van Doren et al, 1991; Cabrera et al, 1994). It therefore limits the amount of Daughterless (Da) and Scute (Sc) available to form active heterodimers that promote Sensory Mother Cell (SMC, the precursor cell of SOs) formation. Thus only cells with sufficiently high levels of Da, Ac and Sc to titrate Emc and to activate the downstream genes of the neural differentiation pathway are able to become SMCs (Campuzano, 2001). Emc function is also required in early embryogenesis for sex determination. The interaction between X-linked "numerator" bHLH proteins (encoded by *sisterless*-a, *scute* and *sis-c*) and autosomal "denominators" such as Emc, Daughterless and Deadpan regulates the X:A ratio which, in turn, determines whether *Sex-lethal* will be transcribed or not, thus regulating sexual fate (Younger-Shepherd et al., 1992). Only in females, with twice the concentration of Sc compared

to males, are there sufficient active Sc/Da heterodimers to overcome the inhibitory effects of Emc and other putative autosomal-linked negative regulators and to activate Sxl (Campuzano, 2001). Later in embryogenesis *emc* is required for a number of processes, including Malpighian tubule formation, tracheal and muscle development and visceral mesoderm migration, by interacting with EGFR, Achaete, Breathless and Trachealess, Da and Twist (Cubas et al, 1994; Ellis, 1994).

In the developing eye Emc and Hairy negatively regulate the expression of *atonal*, a bHLH gene which, together with Da, is necessary for the specification of R8, the first photoreceptor in an ommatidium. Downregulation of *emc* and *hairy* at specific locations by the Notch signalling pathway is essential for the initiation of eye development (Baonza and Freeman, 2001).

In the wing Emc is involved in vein differentiation (de Celis, 1998, review). *emc* is expressed in the intervein cells flanking the veins where *Notch* and *E(spl)mβ* are expressed (Baonza et al, 2000). Very recently, Adam and Montell (2004) in a screen for genes involved in cell fate decisions in the ovary, showed that Emc has a role in follicle cell differentiation by inducing or maintaining EYA (Eyes Absent, a negative regulator of polar/stalk cell fate) in the epithelial follicle cells upon signalling from Notch, during early oogenesis.

1.3.3 Project aims

It had been observed previously in our laboratory that *emc* is expressed dynamically throughout oogenesis. At that time there was only an early report of the presence of *emc* RNA in ovaries (Ellis et al., 1990) but no detailed study had been made and no role had been reported for *emc* in oogenesis. Mis-expression of *emc* was made possible by the generation of heatshock-inducible fly lines by P-element transformation (Spradling, 1986); these lines can express sense or antisense *emc*- the corresponding RNA interferes with the endogenous *emc* RNA and leads to ectopic expression or knock-out, respectively. Eggs laid by heatshocked sense and antisense *emc* fly lines were generally smaller than wild-type and ventralised and had

abnormal dorsal appendage phenotypes (thicker, shorter appendages than wild-type, with malformed – occasionally split- ends). Therefore it was hypothesized that *emc* has a role in dorsal appendage formation. Observations of early stage egg chambers with two or no oocytes (by in situ hybridisation with *oskar* that marks the oocyte) in emc mis-expression fly lines led to the suggestion that *emc* also has a role early in oogenesis, in oocyte determination, in the procedure of selecting one of the two pro-oocytes to become the oocyte.

My aims were to study the effect of *emc* mutations in oogenesis, in germline and somatic tissues and to establish a link between *emc* and the signalling pathways regulating the Dorso-Ventral (D-V) axis formation. For the former, clones of *emc* mutant cells in the follicle cells and the germline during oogenesis were generated and for the latter a series of in situ hybridisation experiments for *emc* expression on fly lines mutant for or mis-expressing genes involved in the D-V axis determination were undertaken.

The background work on the *emc* project in our laboratory and the aims of the current work are discussed in more detail in Chapter 7.1.

Chapter 2: Materials and methods

2.1 Materials

2.1.1 Chemicals, reagents and radioactive isotopes

General purpose chemicals were obtained from BDH, Fisher Scientific, Fluka and Sigma Aldrich, unless otherwise stated in the text.

Radioactive isotopes ([^{32}P]dCTP) were obtained from Amersham Biosciences.

Digoxygenin labelling and detection reagents were from Roche Molecular Biochemicals.

2.1.2 Restriction endonucleases and modifying enzymes

Restriction endonucleases were purchased from New England Biolabs and Promega.

Taq polymerase and the relevant buffers were obtained from Qiagen and *Pfu* Turbo high-fidelity thermostable polymerase and accompanying buffer were supplied by Stratagene.

T4 DNA ligase was supplied by Promega and New England Biolabs (NEB).

T3, T7 and SP6 RNA polymerases were obtained from Ambion.

Reverse Transcriptase (Superscript II^{TM}) was obtained from Invitrogen Life Technologies.

2.1.3 Buffers and solutions

Double distilled water (ddH_2O) was used to make all buffers and solutions. Sterilisation was achieved by autoclaving for 30 minutes at 15 psi or by filtering through a .22μm filter (Sartorius). All solutions were stored at room temperature (~ 25°C) unless otherwise stated. A list of all general solutions and buffers is presented in Table 2.1.3.1, electrophoresis buffers in Table 2.1.3.2, staining solutions and detection reagents in Table 2.1.3.3 and mounting media for microscopy in Table 2.1.3.4.

Solution/Buffer	Components/Preparation	Final concentration
$CaCl_2$	73.5g $CaCl_2.2H_2O$ (Mw: 147.0) Adjust the volume to 100ml with ddH_2O	5M
Denhardt's (100x)	1g BSA (bovine serum albumin) 1g Ficoll (Wt: 400,000) 1g Polyvinylpyrolidone (Wt: 360,000) Adjust the volume to 50ml with ddH_2O	2% 2% 2%
DNA Hybrix (for in situ)	25ml deionised formamide (Mw: 45.04) 12.5ml 20x SSC 250μl sssDNA [10mg/ml] 50μl [50mg/ml] Heparin 500μl 10% Tween-20 11.5ml ddH_2O Store at -20°C	50% 5x 50μg/ml 50μg/ml 0.1%
dNTP mix (10mM each dNTP)	10μl 100mM dATP 10μl 100mM dCTP 10μl 100mM dGTP 10μl 100mM dTTP 60μl ddH_2O Store at -20°C	10mM 10mM 10mM 10mM
EBR (Ephruzzi Beadle Ringer)	7.5g NaCl (Mw: 58.44) 0.35g KCl (Mw: 74.55) Adjust the volume to 1L with ddH_2O	0.75% 0.035%
EDTA, pH 8.0	93g $Na_2EDTA.2H_2O$ (Mw: 372.24) Adjust the pH to 8.0 with ~20g NaOH Adjust the volume to 500ml with ddH_2O	0.5M
EGTA, pH 8.0	1.9g EGTA (Mw: 380.4) Adjust the pH to 8.0 with 10N NaOH Adjust the volume to 10ml with ddH_2O	0.5M
Fix (for testes in situ)	2g para-formaldehyde Dissolve in ~40ml ddH_2O at 65°C. Add: 5ml 1M HEPES pH 6.9 100μl 0.5M EGTA pH 8.0 100μl 1M $MgSO_4$ Adjust volume to 50ml with ddH_2O. Store at -20°C	4% 100mM 1mM 2mM
FBS	2g paraformaldehyde 5ml 10xBPS (what is BPS?) 45ml ddH_2O	4% 1x

	Dissolve at 65°C. Sterilise through a 22μ filter	
Glycine	100mg Glycine (Mw: 75.07) in 1ml ddH_2O Store at -20°C	100mg/ml
Glycine	6g Glycine in 30ml ddH_2O. Store at RT	200mg/ml
HB **(Hybridisation buffer for testes RNA in situ)**	25ml deionised formamide 12.5ml 20x SSC 500μl sssDNA (10mg/ml) 50μl Heparin (50mg/ml) 500μl 10% Tween-20 Adjust pH to 4.5 with citric acid 0.1M Adjust volume to 50ml with ddH_2O Store at -20°C	50% 5x 100μg/ml 50μg/ml 0.1%
HCl	8.6ml concentrated HCl Adjust the volume to 50ml with ddH_2O	2N
Heparin	50mg Heparin 800μl ddH_2O 200μl 20xSSC Store at -20°C	50mg/ml 4x
HEPES	23.83g Hepes (Mw: 238.3) Adjust the volume to 100ml with ddH_2O	1M
HEPES pH 6.9	11.91g HEPES (Mw: 238.3) Adjust pH to 6.9 with 10N NaOH and 2N NaOH. Adjust volume to 50ml with ddH_2O	1M
HP Buffer **(High pH buffer for testes RNA in situ)**	300μl 5M NaCl 1.5ml 1M Tris-HCl pH 9.5 750μl 1M $MgCl_2$ – add last 150μl 10% Tween-20 12.3ml ddH_2O	100mM 100mM 50mM 0.1%
K Acetate	78.59g CH_3COOK (Mw: 98.14) Adjust the volume to 100ml with ddH_2O	8M
K Ferricyanide	1.65g $K_3[Fe(CN)_6]$ (Wt: 329.25) (red) 50ml ddH_2O	0.1M
K Ferrocyanide	2.11g $K_4[Fe(CN)_6].3H_2O$ (Wt: 422.4) (yellow) 50ml ddH_2O	0.1M
K_2HPO4	17.42g K_2HPO_4 (Mw: 174.18) Adjust volume to 100ml with ddH_2O	1M

KCl	7.46g KCl (Mw: 74.55) in 100ml ddH_2O	1M
K_2HPO_4	13.61g K_2HPO_4 (Mw: 136.09) in 100ml ddH_2O	1M
KOH	28.06g KOH (Mw: 56.11) in 100ml ddH_2O	5M
Levamisole	0.24g Levamisole (Mw:240.8) 500μl H_2O 500μl Glycerol Adjust the volume to 1ml with ddH_2O	1M 50%
Lysozyme	50mg Lysozyme 1ml ddH_2O	50mg/ml
$MgCl_2$	9.5g $MgCl_2$ (Mw:95.21) Adjust the volume to 100ml with ddH_2O	1M
$MgSO_4$	24.6g $MgSO_4.7H_2O$ (Mw:246.5) Adjust the volume to 100ml with ddH_2O	1M
$MnCl_2$	39.58g $MnCl_2.4H_2O$ (Mw: 197.9) Adjust the volume to 100ml with ddH_2O	2M
MOPS pH 6.8	20.9g MOPS (Mw:209.3) Adjust the pH to 6.8 with NaOH pellets. Adjust the volume to 100ml with ddH_2O Sterilise by filtration through a 0.22μm filter	1M
NaAc (Na acetate) pH 4.0	13.6g $CH_3COONa.3H_2O$ (Mw:136.08) Adjust the pH to 4.0 with glacial Acetic Acid Adjust the volume to 50ml with ddH_2O	2M
NaAc pH 5.2	40.8g $CH_3COONa.3H_2O$ (Mw:136.08) Adjust the pH to 5.2 with glacial Acetic Acid Adjust the volume to 100ml with ddH_2O	3M 5M Acetate
Na Citrate pH 7.5	14.7g $Na_3C_6H_5O_7.2H_2O$ (Mw:294.1) Adjust the pH to 7.5 with Citric Acid Adjust the volume to 50ml with ddH_2O	1M
NaCl	146.1g NaCl (Mw:58.44) in 500ml ddH_2O	5M
NaOH	80g NaOH (Mw:40.0) Adjust the volume to 20ml with ddH_2O	10N
NaOH	16g NaOH (Mw:40.0) Adjust the volume to 1000ml with ddH_2O	0.4N
PBS (10x) pH 7.5	40g NaCl (Mw:58.44) 5.7g Na_2HPO_4 (Mw:142.0) 1.2g NaH_2PO_4 (Mw:120.0) Adjust the pH to 7.4 with 10N NaOH	1.37M 80mM 20mM

	Adjust the volume to 500ml with ddH_2O	
PBT (1x)	50ml 10xPBS 450ml ddH_2O 500μl Tween-20	1x 0.1%
Phenol/Chloroform (For DNA deproteinisation)	50ml Phenol (saturated with TE buffer, pH-8.0) 50ml Chloroform	
Phosphate buffer pH 6.8	8.66g K_2HPO_4 (Mw:174.18) 6.8g KH_2PO_4 (Mw:136.09) Dissolve in 100ml ddH_2O	1M
PIPES	15.12g PIPES (Mw:302.37) in 100 ml ddH_2O. Adjust pH to 6.95 and filter sterilize.	0.5M
PMS	2g p-Formaldehyde 40ml H_2O 30μl 10M NaOH Dissolve at 65°C. Add: 5ml 0.5M PIPES, pH-7.0 100μl 0.5M EGTA, pH-8.0 100μl 1M $MgSO_4$ Adjust pH to 6.8 with 1N HCl. Adjust the volume to 50ml with ddH_2O.	4% 50mM 1mM 2mM
Proteinase K	20mg Proteinase K 10μl 1M Tris-HCl, pH 7.5 590μl ddH_2O 400μl Glycerol	20mg/ml 10mM
RbCl	12.09g RbCl (Mw:120.9) in 100ml ddH_2O	1M
Ringer's saline for *Drosophila* pH 7.2	6.8g KCl (Mw:74.55) 1.35g NaCl (Mw: 58.44) 0.17g $CaCl_2.2H_2O$ (Mw: 147.0) 0.6g Tris Base (Mw:121.14) Adjust pH to 7.2 with 1N HCl. Adjust the volume to 500ml with ddH_2O. Sterilise though a 0.22μm filter.	180mM 45mM 2.3mM 10mM
RNA Hybridisation buffer (for Northern blots)	125ml Formamide (Mw:45.04) 62.5ml 20x SSC 5ml 1M Na-Phosphate buffer, pH 6.8 25ml10% SDS 12.5ml 100x Denhardt's 2mg total yeast RNA or sssDNA	50% 5x 20mM 1% 5x 8μg/ml

	(denatured) Adjust the volume to 500ml with ddH_2O	
RNA Hybrix (for in situ)	25ml Deionised Formamide (Mw:45.04) 12.5ml 20x SSC 100μl RNase-free tRNA (50mg/ml) 50μl Heparin (50mg/ml) 500μl 10% Tween-20 12ml ddH_2O Adjust the pH to 6.5 with HCl. Store at -20°C	50% 5x 100μg/ml 50μg/ml 0.1%
RNase **(Dnase-free)**	Dissolve 10mg RNase in 1ml RNase-free H_2O. Aliquot into 4 eppendorf tubes. Heat to 110°C for 20min. at the heating block. Leave in the block to cool down gradually to RT. Store at -20°C.	10mg/ml
SBE buffer	20g $NaHCO_3$ (Mw:84.01) 2ml 0.5M EDTA, pH 8.0 Adjust the volume to 1L with ddH_2O	2% 1mM
SDS	50g SDS (Mw:288.38) Adjust the volume to 500ml with ddH_2O	10%
SSC (20x) **pH 7.0**	87.65g NaCl (Mw:58.44) 44.1g $Na_3C_6H_5O_7.2H_2O$ (Mw:294.1) Adjust the pH to 7.0 with 10N NaOH Adjust the volume to 500ml with ddH_2O	3M 300mM
SSPE **pH 7.4**	87.65g NaCl (Mw:58.44) 15.6g NaH_2PO_4 (Mw:156.01) 4.7g $Na_2EDTA.2H_2O$ (Mw:372.24) Adjust the pH to 7.4 with ~3ml 10N NaOH Adjust the volume to 500ml with ddH_2O	3M 200mM 25mM
sssDNA	10mg sonicated salmon sperm DNA 1ml ddH_2O	10mg/ml
Sucrose	8.56g Sucrose (Mw:342.3) in 100ml ddH_2O	250mM
TFB1 Buffer	1.88ml 8M KAc 1ml 5M $CaCl_2$ 12.5ml 2M $MnCl_2$ 50ml 1M RbCl 75ml Glycerol Adjust the pH to 5.8 with 1M Acetic Acid Adjust the volume to 500ml with ddH_2O Filter sterilise and store at 4°C	30mM 10mM 50mM 100mM 15%

TFB2 solution	0.3g PIPES (Mw:302.4) 1.5ml 5M $CaCl_2$ 1ml 1M RbCl 15ml Glycerol Adjust the pH to 6.5 with 1N KOH (essential for PIPES to dissolve) Adjust the volume to 100ml with ddH_2O. Filter sterilise and store at 4°C	10mM 75mM 10mM 15%
TBS (10x)	12.1g Tris Base (Mw:121.14) 40g NaCl (Mw:58.44) Adjust the pH to 7.6 with cHCl Adjust the volume to 500ml with ddH_2O	200mM 1.37M
TBS-T (1x)	50ml TBS 10x 450ml ddH_2O 500µl Tween-20 of 5ml 10% Tween-20	1x 0.1%
TE **pH 8.0**	1ml 1M Tris, pH 8.0 200µl 0.5M EDTA, pH 8.0 Adjust volume to 100ml with ddH_2O	10mM 1mM
Tris-HCl **pH 7.4** **pH 7.6** **pH 8.0**	60.55g Tris Base (Mw:121.14) For pH 7.4 add ~ 35ml cHCl For pH 7.6 add ~ 30ml cHCl For pH 8.0 add ~ 20ml cHCl Adjust the volume to 500ml with ddH_2O	1M
Triton X-100	0.5ml Triton X-100 Adjust the volume to 500ml with ddH_2O	0.1%
Triton X-100	5ml Triton X-100 Adjust the volume to 50ml with ddH_2O	10%
tRNA (RNase-free)	50mg tRNA in 1ml ddH_2O	50mg/ml
Tween 20	5ml Tween-20 Adjust the volume to 50ml with ddH_2O	10%

Table 2.1.3.1 General solutions and buffers

Buffer	Components/Preparation	Final concentration
DNA sample buffer (6x)	3ml 0.1% Bromophenol Blue 3ml Glycerol 4ml ddH_2O	0.03% 30%
MOPS buffer (10x), pH 7.0	20.9g MOPS (Mw:209.3) 5.44g CH_3COONa (Mw:136.08) 10ml 0.5M EDTA, pH 8.0 Adjust the pH to 7.0 with 2N NaOH Adjust the volume to 500ml with ddH_2O Sterilise through a 0.22μm filter	200mM 80mM 10mM
PIPES, pH 6.5 and pH 7.0	As before (Table 2.1.3.1) Adjust the pH to 6.5 or 7.0 with cHCl.	1M
Protein Sample buffer (2x) (Laemmli)	1.25ml 1M Tris-HCl, pH 6.8 2ml Glycerol 4ml 10% SDS 1ml 14.4M β-Mercaptoethanol (Mw:78.01) 1ml 0.1% Bromophenol Blue 0.75ml ddH_2O	125mM 10% 4% 1.44M 0.01%
RNA sample buffer (1.5x)	500μl Deionised Formamide (Mw:45.04) 100μl 10x MOPS 270μl 37% formaldehyde 100μl Glycerol 30μl 0.1% Bromophenol Blue 2μl 10mg/ml EtBr	50% 1x 10% 10% 0.003% 20μg/ml
TAE (50x)	121g Tris Base (Mw:121.14) 28.55ml Glacial Acetic Acid 50ml 0.5M EDTA, pH 8.0 Adjust the volume to 500ml with ddH_2O	2M 50mM
PAGE Running buffer (10x)	15.15g Tris Base (Mw:121.14) 72g Glycine (Mw:75.07) 5g SDS (Mw:288.38) Adjust the volume to 500ml with ddH_2O	250mM 1.92M 1%

Table 2.1.3.2 Loading buffers and running buffers for gel electrophoresis

Name	Components/Preparation	Final concentration
Coomassie gel destain	100ml Methanol 100ml Glacial acetic Acid 800ml ddH_2O	10% 10%
Coomassie gel stain	1g Coomassie Blue R-250 450ml Methanol 450ml ddH_2O 100ml Glacial Acetic Acid	0.1% 45% 10%
Galactosidase staining buffer	500µl 1M Phosphate buffer, pH 7.0 3ml 0.1M $K_3[Fe(CN)_6]$ (or 99mg) 3ml 0.1M $K_4[Fe(CN)_6]$ (or 127mg) 1.5ml 5M NaCl 50µl 1M $MgCl_2$ Adjust the volume to 50ml with ddH_2O	10mM 8mM 8mM 150mM 1mM
Hoechst (1000x)	1mg Hoechst 33258 1ml 1x PBS	1mg/ml
Nuclear Yellow (1000x)	1mg Hoechst 33342 1ml DMF (N, N'-Dimethylformamide) (Mw:73.09)	1mg/ml
Propidium Iodide	2.5µl of 1mg/ml Propidium Iodide stock in 1ml PBT (1xPBS + 0.1% Triton X-100)	2.5µg/ml
Sytox Green	10µl original 5mM stock in DMSO 990µl ddH_2O	50µM
TO-PRO	250µl original 1mM stock in DMSO 750µl ddH_2O	250µM
IPTG	120mg Isopropyl β-D-thiogalactoside (Mw:238.3) Adjust the volume to 1ml with ddH_2O	0.5M
NBT	75mg 4-Nitro blue tetrazolium chloride 700µl DMF (Mw:73.09) 300µl ddH_2O	75mg/ml 70%
Ponceau-S	2g Ponceau S 30g Trichloroacetic acid (Mw:163.39) 30g 5-Sulfosalicylic acid dihydrate (Mw:254.22) Adjust the volume to 100ml with ddH_2O	2% 30% 30%
p-Coumaric Acid Stock	0.15g p-Coumaric Acid (Mw:164.2) 10ml DMSO	90mM

Luminol Stock	0.44g Luminol (Mw:177.2) 10ml DMSO	250mM
ECL reagent	250μl Luminol stock 110μl p-Coumaric acid Stock 5ml 1M Tris-HCl, pH 8.5 Adjust the volume to 50ml with ddH_2O	1.25mM 0.2mM 100mM
Staining solution (for in situ)	5ml 1M Tris-HCl pH 9.5 1ml 5M NaCl 2.5ml 1M $MgCl_2$ 500μl 10% Tween-20 41ml ddH_2O	100mM 100mM 50mM 0.1%
X-Gal	80mg X-Gal (Mw:408.64) 1ml DMF (Mw:73.09)	8%
X-Phosphate (BCIP)	50mg X-Phosphate (5-Bromo-4-chloro-3-indolyl phosphate p-toluidine salt) 1ml DMF (Mw:73.09)	50mg/ml
Bradford Stock Solution	50ml 95%(v/v) ethanol 100ml 88% (v/v) phosphoric acid 175mg Coomassie Brilliant Blue G-250 Store in the dark at RT	31.67% 58.67% 0.11%
Bradford Working Solution	7.5ml 95% (v/v) ethanol 15ml 88% (v/v) phosphoric acid 15ml Bradford stock solution 212.5ml ddH_2O Filter through Whattman no.1 fliter paper Store at RT in the dark	2.85% 5.28% 6%

Table 2.1.3.3 Staining solutions and detection reagents

Media	Components/Preparation	Final concentration
FISH medium	5ml 1M Tris-HCl, pH 8.5 1.25g DABCO (Mw:112.2) 45ml Glycerol	100mM 2.5% 90%
Glycerol/PBS, pH-7.4	5ml 10x PBS,pH 7.4 40ml Glycerol 5ml ddH_2O	1x 80%
Hoyer's medium	6g Arabic gum in 10ml ddH_2O Dissolve completely O/N. Then add: 4g Glycerol 40g Chloral Hydrate (Mw:165.4) Centrifuge for 2hr at maximum speed and collect the cleared supernatant	15% 10% 100%
Hoyer's mount medium	20ml Hoyer's medium 20ml concentrated Lactic Acid	50% 50%
GMM	4:1 liquid Canada balsam: methylsalicylate	

Table 2.1.3.4 Mounting media for fluorescent and conventional microscopy

2.1.4 Growth media

All media (Table 2.1.4) were prepared by Institute media staff and were sterilised by autoclaving (15 minutes at 15 psi). The media were then stored at room temperature. Agar-containing media were heated to liquefy prior to pouring into plates.

Media type	Components/Preparation	Final concentration
LB (Luria Broth)	10g NaCl 10g Bacto-tryptone 5g Yeast extract Adjust the volume to 1L with ddH_2O	1% 1% 0.5%
LB agar	10g NaCl 10g Bacto-tryptone 5g Yeast extract 15g Difco agar	1% 1% 0.5% 1.5%

	Adjust the volume to 1L with ddH_2O	
SOC medium	Provided with DH5A competent cells from Invitrogen	

Table 2.1.4 Media list

2.1.5 Antibiotics

Stock solutions from all antibiotics were prepared (as in Table 2.1.5) and stored at -20°C.

Antibiotic	Stock solution concentration	Working concentration
Ampicillin (Amp)	50mg/ml in water	50μg/ml
Chloramphenicol (Chl)	68mg/ml	50μg/ml
Kanamycin (Kan)	25mg/ml	50μg/ml
Tetracycline (Tet)	5mg/ml in ethanol	50μg/ml

2.2 Bacterial strains and plasmids

The bacterial strains and the plasmid constructs used are summarised in Tables 2.2.1 and 2.2.2.

Host strain	Genotype
BL21 (DE3) pLysS (Stratagene)	*F ompT hsd*S_B (r_B m_B) *gal dcm* λ (DE3) (pLys *Cam*^{r})
Top 10 (Invitrogen)	*F mcr*A Δ(*mrr-hsd*RMS-*mcr*BC) Φ80 *lacZ*ΔM15 Δ*lacX*74 *deo*R *rec*A1 *ara*D139 Δ(*ara-leu*)7697 *gal*U *gal*K *rps*L (*Str*^{R}) *end*A1 *nup*G
XL1Blue (Stratagene)	*rec*A1 *end*A1 *gyr*A96 *thi*-1 *hsd*R17 *sup*E44 *rel*A1 *lac*[F' *pro*AB *lacI*^{q}ZΔM15 *Tn*10 (*Tet*^{R})]

Table 2.2.1 List of bacterial strains used

Construct name	Insert	Vector	Cloning enzymes	Selection	Strain
E09	DSTPK61 cDNA[A] clone - GST	pGEX-3X (Pharmacia Biotech)	EcoRI + BamHI	Amp^R	XL1Blue
E40	DSTPK61 E40 coding sequence - GST	pGEX-3X (Pharmacia Biotech)	EcoRI + BamHI	Amp^R	XL1Blue
E40pfu	DSTPK61 E40 coding sequence- GST	pGEX-3X (Pharmacia Biotech)	EcoRI + BamHI	Amp^R	XL1Blue BL21(DE3)Lys
E40/pRSET	DSTPK61 E40 coding sequence- 6xHis	pRSET-C (Invitrogen)	EcoRI + BamHI	Amp^R	BL21(DE3)Lys
E51	DSTPK61 E51 coding sequence- GST	pGEX-3X (Pharmacia Biotech)	EcoRI + BamHI	Amp^R	XL1Blue BL21(DE3)Lys
E51pfu	DSTPK61 E51 coding sequence- GST	pGEX-3X (Pharmacia Biotech)	EcoRI + BamHI	Amp^R	XL1Blue BL21(DE3)Lys
E69	DSTPK61 E69 coding sequence- GST	pGEX-3X (Pharmacia Biotech)	EcoRI + BamHI	Amp^R	XL1Blue BL21(DE3)Lys
pN2	EGFP	pUASP (Rorth 1998)	KpnI + BamHI	Amp^R	XL1Blue
pUASP	n/a	pUASP (Rorth 1998)	n/a	Amp^R	XL1Blue
CNF/NR	EGFP-core DSTPK61 domain	pUASP (Rorth 1998)	KpnI + BamHI	Amp^R	XL1Blue
TOPO	n/a	pCR-II-TOPO (Invitrogen)	n/a	Kan^R	Top 10

Table 2.2.2 List of plasmids

2.2.1 Growing bacteria on agar plates

Bacterial cells were streaked on an agar plate containing the appropriate antibiotic, to obtain a single colony. The cells are obtained from another plate, a stab or from a frozen glycerol stock.

A flame-sterile inoculating loop was used to streak the bacteria onto the plate in a sequential manner to obtain the required density (up to single cells). A flamed glass spreader was used when larger volumes of cells, such as transformed competent cells, needed to be plated. Plates were grown at 37°C O/N.

2.2.2 Growing bacteria in liquid cultures

For small-scale bacterial cultures, 5ml of LB in a bijou bottle were inoculated with a single bacterial colony (using a sterile toothpick). The appropriate antibiotic was added and the cultures were grown O/N at 37°C with shaking (150rpm).

For larger scale cultures, a small-scale O/N culture was used to inoculate 50-500ml fresh LB containing the appropriate antibiotic. The cultures were grown at 37°C with shaking (250rpm) until the required cell density (measured by OD_{600}) was obtained.

2.2.3 Bacterial culture storage

Short-term storage (up to one month) can be done by streaking a single colony on an LB agar plate containing the appropriate antibiotic, growing the curture overnight at 37°C and storing it at 4°C.

For long-term storage bacterial stabs were prepared. A single colony from a plate was picked up with a sterile toothpick and stabbed into a vial containing LB broth supplemented with 0.6% agar. The stabs were incubated for 6hr at 37°C and stores at RT in the dark, for up to 5 years.

Glycerol stocks were prepared by adding 800μl of an O/N culture to 200μl sterile glycerol in a sterile 2ml screw-top tube. The mixture was homogenised by vortexing and stored at -80°C (for indefinite storage).

2.3 Drosophila methods

2.3.1 Maintenance of *Drosophila* stocks

Fly stocks were kept at 18°C in vials or bottles with Staffan food (Table 2.3.1). Stocks with reduced viability and stocks used in ongoing experiments were kept at 25°C. Filter paper strips pre-soaked in 3% (v/v) Benzyl Benzoate in ethanol and then dried were added to each vial/bottle to prevent mite infections. Baker's yeast was sprinkled on the surface of the fly food, or made into a paste and spread on top of food plates, to improve egg laying. Fly food (Staffan, Adh, red wine agar plates) was made by media staff for the Institute.

The genotypes of some of the stocks used are given in Table 2.3.2. Other stocks used for crosses and the *emc*-related experiments are mentioned in the relevant chapters (3 and 7). Stocks were obtained from Bloomington Stock Centre (flystocks.bio.indiana.edu/), unless otherwise stated.

Food name	Components/Preparation	Final concentration
Staffan food	10g agar	1%
	50g sugar	5%
	25g cornflour	2.5%
	17.5g live yeast	1.75%
	10g polenta	1%
	15ml Nipagin	1.5%
	1ml Ampicillin	0.1%
	Porage oats	
	dH_2O to 1L	
	Agar and water were boiled for 10'. Polenta and cornflour were mixed with warm water individually in beakers. Yeast was mixed with cold water in a beaker. Cornflour and polenta were added to the boiling agar and brought back to the boil; yeast was added while stirring constantly. After turning the heat off sugar and nipagin were added. Volume was adjusted by adding dH_2O. Each bottle and vial was sprinkled with dry porage oats before filling with the warm food mixture.	
Adh food	100g Dried flake yeast	10%
	100g Sugar	10%
	16g Agar	1.6%
	30ml Nipagin	3%
	dH_2O to 1L	
	Dried yeast and agar were boiled in water for 10 min., then nipagin and sugar were added. The food was stored in bottles, at 50°C. While dispensing into	

	bottles and vials the mixture was stirred constantly, to avoid separation.	
Apple/grape juice plates	5g agar 5g sucrose 150ml ddH_2O, boil. Then add: 50ml apple juiced or red grape juice 0.2ml 10% Nipagin in 95% ethanol	2.5% 2.5% 25% 0.01%
Red wine agar plates	22.5g agar 25g sucrose 1.5g Nipagin 875ml H_2O 125g red wine concentrate Agar and sucrose were melted in dH_2O and brought to the boil. After mixing, Nipagin and red wine concentrate were added.	2.25% 2.5% 0.15% 12.5%

Table 2.3.1 Fly food and related media

Stock/Synonym	Genotype/comment	Comments/Donor
Oregon R (*OrR*)	Wild-type	Red eyed wild type
EP(3)3091/dPDK[1]	EP insertion in the 4th intron of *dstpk61*	Szeged Stock Centre (Deak et al, 1997; Cho et al, 2001)
261/31	*lacZ* mimics *emc* expression pattern	(Deak et al, 1997)
***grk*^{22J}**	Has4 copies of *grk*	(Neuman-Silberberg and Schüpbach, 1994)
***grk*^{ED11}**	*grk*^{ED11}	(Neuman-Silberberg and Schüpbach, 1993)
***top*^{QY1}**	*pr cn top*^{QY1} *bw/CyO*	(Schüpbach, 1987)

Table 2.3.2 Fly stocks

2.3.2 *Drosophila* egg preparation for dark-field microscopy

Flies were left to lay eggs on apple or grape juice plates for 6-20 hr. The plate was observed under a dissecting microscope to score eggs with abnormal dorsal appendage phenotypes. Eggs were then picked up from the plate and placed into a drop of Hoyer's mounting medium on a microscope slide and covered with a coverslip. The slides were incubated O/N at 65°C and stored at RT.

2.3.3. Collection of virgin flies and crosses

Virgin flies (male and female) were collected by emptying the fly bottles from any eclosed flies and then collecting the newly eclosed flies every 5-6hr (at 25°C). These flies were sexed and flies from the same sex were transferred together in vials with fresh fly food. Males and females are distinguished by the sexual dimorphism characteristics, including body shape and size, abdomen pigmentation and the presence of sex combs in the first pair of legs in males.

An alternative approach for collection of virgin flies was to pick up dark pupae with a wet paintbrush and place them individually into vials with fresh fly food. The newly eclosed flies were anesthetised with CO_2, sexed and flies from the same sex were kept together.

Fly crosses were generally carried out by transferring a minimum of 2-4 virgin females and 3-5 male flies into the same vial containing fresh fly food with yeast paste. Larger scale crosses were set in cages, with Adh fly food supplemented with yeast paste. The flies were incubated at 25°C or 18°C for up to 4 days and then transferred to another vial. For cage crosses, the plate containing food and laid eggs was changed every day and the plates were kept separately in a box at 25°C for the progeny of the cross to be selected, put to fresh vials and hatch.

2.4 Nucleic acids methods

2.4.1 Techniques for DNA and RNA purification

2.4.1.1 Phenol/Chloroform extraction

Phenol/chloroform extraction was used to remove protein impurities from nucleic acid preparations. For DNA the phenol solution must be equilibrated to pH 8.0, whereas for RNA the phenol solution must have pH 4.3. An equal volume of phenol/chloroform was added to the DNA or RNA solution and the sample was mixed thoroughly by inverting the tube gently for 5 minutes. The suspension was centrifuged at 14000g for 5 min. and the top aqueous phase was transferred to a clean tube. This step was repeated until the interphase between the phases was clear. The

complete removal of phenol was achieved by a final extraction with an equal volume of chloroform.

2.4.1.2 Ethanol/Isopropanol precipitation of nucleic acids

DNA or RNA was precipitated from solution by adding 0.1 volumes of 3M NaAc (pH 5.2) to the sample and 2.5 volumes 99.7% EtOH. Ethanol could be replaced by 0.6 volumes ice-cold isopropanol. Typically the nucleic acid was precipitated for 1hr at -20°C (for ethanol; no freezing was necessary when isopropanol was used) and centrifuged at 15000rpm for 15 min. at 4°C. The resulting pellet was washed once with 75% EtOH and centrifuged at 15000 rpm for 5 min. at 4°C. The pellet was air-dried and was resuspended in an appropriate volume of 10mM Tris-HCl pH 8.0 for DNA or in RNase-free water for RNA.

2.4.1.3 Estimation of nucleic acid concentration by UV spectrometry

The nucleic acid concentration and purity was determined by UV spectrophotometry, measuring the absorbance of DNA/RNA at 260nm and 280nm in a Hitachi two-beam spectrometer or a Cecil single-beam spectrometer. The OD_{260} measurement was used to calculate the nucleic acid concentration of the sample by the following formula:

$$\text{DNA/RNA concentration in } \mu g/ml = \frac{OD_{260} \times DF \times Sc}{1000}$$

Where DF: Dilution factor and Sc: Spectrophotometric conversion (specific DNA/RNA absorption value) which equals 50 for double stranded DNA and 40 for RNA or single stranded DNA.

The ratioA_{260}/A_{280} was used to estimate the purity of the nucleic acid. DNA was considered to be sufficiently free of protein at ratios greater than 1.8; for RNA, at ratios greater than 2.0.

2.4.2 Isolation of genomic DNA

Around 130mg of flies were ground in 250μl Fly buffer (Table 2.4.1) using a plastic pestle and tip. 750μl more Fly buffer was added, followed by addition of 8μl RNase 10mg/ml and incubation for 1hr at 37°C. 30μl Proteinase K (10mg/ml) was added and the sample was incubated for 1hr at 50°C. After centrifugation for 15 min. at 15000rpm at 4°C, the supernatant was transferred to a new tube and phenol/chloroform extraction followed. Genomic DNA was stored at 4°C.

Solution	Composition/Preparation	Final concentration
Fly Buffer	5ml 1M Tris-HCl pH 8.5	100mM
	800μl 5M NaCl	80mM
	2.5g Sucrose	5%
	2.5ml 10% SDS	0.5%
	5ml 0.5M EDTA pH 8.0	50mM
	Adjust the volume to 50ml with ddH_2O	

Table 2.4.1 Solutions for genomic DNA isolation

2.4.3 Plasmid DNA isolation

2.4.3.1 General purpose DNA miniprep

A 5ml O/N culture was centrifuged for 5 min, 5000rpm to pellet the bacterial cells. The pellet was resuspended in 250μl Resuspension buffer (Table 2.4.2) and transferred to eppendorf tubes. 350μl Lysis solution was added and mixed by inverting gently several times. After 5 min. incubation at RT 350μl Neutralising solution was added, mixing was achieved by inversion, and the sample was centrifuged at 15krpm for 15 min. at 4°C. The supernatant was transferred to a clean eppendorf tube and the plasmid DNA was recovered by isopropanol precipitation and stored at -20°C.

Solution	Composition/Preparation	Final concentration
Resuspension buffer	500μl 1M Tris-HCl pH 7.6	50mM
	200μl 0.5M EDTA pH 8.0	10mM
	100μl 10mg/ml RNase (DNase-free)	100μg/ml
	Adjust the volume to 10ml with ddH_2O	

Lysis solution	2ml 10N NaOH 10ml 10% SDS Adjust the volume to 100ml with ddH_2O	0.2M 1%
Neutralising buffer	3.24g CH_3COOK (Mw: 98.14) Adjust the pH to 4.8 with Glacial Acetic Acid (~ 2ml) Adjust the volume to 25ml with ddH_2O	1.32M

Table 2.4.2 Solutions for plasmid DNA preparation

2.4.3.2 DNA mini- and midi-prep using commercial kits

For sequencing and cloning experiments the QIAprep Spin Miniprep kit (Qiagen) and the GenElute HP Plasmid Midiprep kit (Sigma) were used according to the manufacturer's instructions.

2.4.4 DNA agarose gel electrophoresis

To separate DNA molecules according to their size, agarose gels of different agarose concentration were used, depending on the requirements. 1% gels were generally used for separation of DNA molecules up to 8kb, whereas 1.5-3% gels were used for visualisation of bands as small as 70bp. EtBr was added to the gel to a final concentration of 0.2mg/ml. The samples were mixed with loading buffer (Table 2.1.3.2) to a final concentration of 1x before loading on the 1xTAE gel. The gels were electrophoresed at 4-7V/cm in 1x TAE buffer until the required degree of separation was obtained.

The nucleic acids stained with EtBr were visualised on a UV transilluminator and pictures of the gel pattern were taken with a video imager and printed on thermal paper.

Molecular markers used to determine the size of DNA fragments on the gel were the 1Kb ladder (Invitrogen), used at ~0.5μg/gel and the HyperLadder I (Bioline) which was used also for estimating the amount of DNA in unknown bands. 5μl of this ladder ran on a 1% agarose gel would produce a set of bands with a known amount

of DNA/band. The intensity of these bands was then compared with the unknown DNA fragments in question.

2.4.5 Extraction of DNA fragments from agarose gels

The QIAEX II Gel Extraction Kit (Qiagen) was used to recover DNA fragments (up to 15kb) from agarose gels. The manufacturer's protocol was used with the following modifications: the excised band was weighed and dissolved in 3 volumes buffer QXI, by 10 min. incubation at 65°C. Then 10μl 3M NaAc pH 5.0 and 10μl QIAEX II resin were added. The sample was incubated for 10 min. at RT with agitation, centrifuged at 13krpm at RT for 1 min. and the pellet was washed once with QX buffer and twice with PE buffer. The pellet was dried in a 65°C incubator with open door and the bound DNA was eluted by adding 15μl Tris-HCl 10mM pH 8.0 to the pellet, incubating for 5 min. at 65°C and centrifuging for 1 min. at 13krpm. The cleared eluate was transferred to a new tube and the elution procedure was repeated and the eluates combined.

2.4.6 DNA sequencing and sequence analysis

Sequencing reactions contained 8μl labelling Mix (BigDye Terminator for Cycle Sequencing, ABI PRISM, Applied Biosystems), 3.2pmol of the appropriate primer, high quality DNA template (50-200ng PCR product or 400ng plasmid DNA) and water to a final volume of 20μl. The thermal cycling programme was: 25 cycles of 95°C for 30 sec., 50°C for 20 sec. and 4 minutes extension at 60°C. The unincorporated dye terminators were removed by passing the sequencing reaction through a purification column. This and the sequence analysis on an ABI PRISM 377 DNA sequencer were done by Jill Lovell (ICAPB- Edinburgh University) or at the ICMB Sequencing facility of Edinburgh University.

Sequence analysis was done using the Chromas software (for PC) or the Factura and GeneJockey programmes (for Macintosh).

2.4.7 Enzymatic reactions

2.4.7.1 Endonuclease restriction of DNA

A typical reaction was in a 20μl volume, containing 0.2-1.0μg DNA sample, the appropriate restriction buffer for the enzymes used and 10U of the restriction enzyme. The samples were incubated at the recommended temperature for the enzymes used (typically 37°C) for 2-6hr and the reaction was stopped by heat inactivation of the enzyme (20 min. at 65°C) where applicable. A fraction of the digest was ran on an agarose gel to monitor the results of the restriction reaction.

2.4.7.2 DNA ligation

DNA ligation was performed by incubating DNA fragments with the appropriate linearised cloning vector in a solution containing 1x buffer and 400U T4 DNA ligase (NEB or Promega) in a 20μl final volume. The reaction was incubated o/n at 4°C for joining dsDNA with sticky ends or at 18°C for DNA molecules with blunt ends. The T4 DNA ligase was heat-inactivated by 20 min. incubation at 65°C and 1-2μl of the reaction was used to transform competent cells.

2.4.8 DNA transformation of chemically competent cells

2.4.8.1 Preparation of competent cells

A 5ml O/N culture (XL1Blue or BL21Lys cells) without antibiotic added was used to inoculate 100ml pre-warmed LB medium in a 500ml flask. 2ml 1M $MgSO_4$ (20mM end concentration) was added and the culture was grown at 37°C, 250rpm until the OD_{550} reached 0.4-0.6. The cells were pelleted at 4500g for 10 min. at 4°C, in two 50ml tubes. All the remaining steps were done on ice or at 4°C with pre-cooled materials. The cells in each tube were gently resuspended with 2ml ice-cold TFB1, then 18ml more TFB1 was added and the cells were combined in one tube. After incubating on ice for 5 min. the cells were pelleted at 4500g for 5 min. at 4°C and gently resuspended in 4ml ice-cold TFB2. Then the cells were incubated on ice for

15-60 min. and aliquots of 100μl cells per tube were made in pre-cooled tubes. The aliquots were frozen immediately and stored at -80°C.

2.4.8.2 Transformation

A 100μl aliquot of competent cells was thawed on ice for 5-10 minutes. 10-50μg of plasmid DNA was added (maximum volume of 10μl) and mixed briefly with the pipette tip. The cells-DNA mixture was incubated on ice for 30 min. and then placed in a waterbath at 42°C for 60-90 seconds and immediately on ice for 2 min. to cool. 1ml LB liquid medium was added and the cells were incubated for 45 min. at 37°C, 250rpm with shaking, to express the antibiotic resistance phenotype. 100-200μl of this were streaked onto LB agar plates with the appropriate antibiotic and the plates were incubated O/N at 37°C.

2.4.9 Polymerase Chain Reaction (PCR)

A list of all primers used is presented in Table 2.4.3.

2.4.9.1 Conventional PCR

The standard polymerase reaction contained the following: 50pmol of the forward and reverse primers (1μl of 50mM stock), 0.2mM of each dNTP (dATP, dCTP, dGTP, dTTP) (by Amersham Biosciences or Roche, 1 x Taq Polymerase Buffer (Qiagen), 1x Q Solution (Qiagen), 3U Taq Polymerase (Qiagen), ~50-100ng DNA template and nuclease-free water to a final volume of 50μl. [PCR using the Pfu Turbo polymerase (Stratagene) were done according to the manufacturer's protocol]. The PCR reaction was carried out as follows: 2 min. at 94°C for initial denaturation; 20-40 cycles of 3 steps- step 1 at 94°C for 40 sec. (denaturation), step 2 at 50-60°C for 40 sec. (annealing-depending on the melting temperature of the primers used), step 3 at 72°C for 1-15min (extension- depending on the length of the produced fragment, typically 1 min./kb); a final elongation step of 10 min. at 72°C. A Touchdown Thermal Cycler (Hybaid) or a Hybaid PCR Express Cycler, allowing for

gradient PCRs, were used. 5-10μl of the reaction product was run on agarose gels to visualise the PCR products.

2.4.9.2 Quantitative PCR (real-time- or qPCR)

An iCycler (Biorad) was used for the quantitative PCR experiments. The reactions were set in 96-well plates and consisted of the following: 1μl cDNA template (1/20th RT reaction), 10μl SYBR Green mix (ABgene AB1220), 0.5μl each primer 10μM (Forward and Reverse), 8μl H_2O. The programme used consisted of one cycle at 95°C for 10 min.; 40 cycles of 94°C for 1 min., 60°C for 1 min., 72°C for 1 min. (this step with real-time measurement); 1 cycle at 95°C for 1 min.; 1 cycle of 1 min. at 55°C and 80 cycles of 10 sec. at a temperature starting from 55°C and increasing by 0.5°C per cycle, for the melting curve. Assessment of the success of the reaction and data analysis (Amplification plot, Threshold Cycle calculation, Melting curve plot) were done using the MyiQ^{TM} Single-Color Real –Time PCR detection system software according to the manufacturer's instructions. Samples were loaded in triplicate and standard curves were made from samples at 1x, 0.1x, 0.01x and 0.001x cDNA. A test reaction using several different primer combinations for *dstpk61* E51 and for control genes was ran first, to select the primer pair that would not produce primer dimers (SYBR Green fluoresces when bound to double-stranded DNA so one should ensure the PCR product is the only double stranded DNA molecule produced). We used primers 51F2/ex2R1 (for E51) and rpL32 5'/rpL32 3' (for *rp49*) – Table 2.4.3 for all primers used.

2.4.10 Reverse Transcription and PCR (RT-PCR)

Reverse transcription was carried out in a 20μl reaction volume using typically 2μg total RNA (maximum volume 10μl), 2μl 50mM poly-T-EcoRI primer (G7020), 10mM DTT, 1x RT buffer, 0.5mM each dNTP and 200U Superscript II (Invitrogen) reverse transcriptase. The RNA and primer (with dH_2O up to a volume of 12μl) were pre-mixed, heated at 70°C for 5 min. and cooled on ice for 3 min. Then the remaining components were added and the mix was incubated at 42°C for 1 hr and

the reaction was stopped by heat inactivation of the enzyme at 70°C for 15 minutes. 2μl, 1μl or 1:10 and 1:50 dilutions of the RT reaction were used as template for subsequent PCR amplification, using conditions as described above (2.4.9).

2.4.11 Inverse PCR (iPCR)

Genomic DNA was prepared from flies containing P-element insertions and approximately 8μg of this DNA was digested with *Sau*IIIA for 6 hr at 37°C. The reaction was stopped by heating the mix at 65°C for 20 min. The digest was used directly in a 200μl ligation reaction with 800U T4 DNA ligase, with O/N incubation at 4°C. The DNA was recovered by ethanol precipitation the following day and resuspended in 150μl 10mM Tris-HCl pH 8.0. 5μl of the re-ligated genomic DNA were used as a template for PCR amplification with P-element-specific primers (Pry1 and Pry4), using standard PCR conditions.

Primer name	Sequence (5'>3')	Length nt	Tm (°C)	Use
T3PR	AAT TAA CCC TCA CTA AAG GG	20	56	vector-sequencing
T7-20	TAA TAC GAC TCA CTA TAG GG	20	56	vector-sequencing
T7-LN	GTA ATA CGA CTC ACT ATA GGG	21	60	vector-sequencing
M13	GTA AAA CGA CGG CCA GT	17	52	vector-sequencing
M13rev	GGA AAC AGC TAT GAC CAT G	19	56	vector-sequencing
G7020	GGA ATT CTT TTT TTT TTT TTT TTT	24	37	RT reaction
Rp49-1	AAG CCC AAG GGT ATC GAC AAC	21	62	rp49 PCR
Rp49-2	ATT GAA CTC GGC ACT GGC ACA	21	62	rp49 PCR
Pry 1 (3'PZ)	CCT TAG CAT GTC CGT GGG GTT TGA AT	26	65	Inverse PCR
Pry 4 (3'PZ)	CAA TCA TAT CGC TGT CTC ACT CA	24	62	Inverse PCR
PGEXF	CAA TGT GCC TGG ATG CGT TC	20	62	pGEX-3X –sequenc.
PGEXR	GTG ACT GGG TCA TGG CTG C	19	62	pGEX-3X –sequenc.
RSETR	TAG TTA TTG CTC AGC GGT GG	20	60	pRSETC sequencing
51FOR	CGG GAT CCT CAT GAA CAT AAT TCA GAT CAA CG	32	60 (75)	E51 subcloning to expression vectors
51RT	AAG TCG AGA TTA ACA CAA GTT C	22	60	E51For (exon 1c)-RT-PCR, in situ, qPCR

51R2	GCT GTG TAC CGT TGA TCT GAA	21	62	E51Rev (exon 1c)-qPCR
51F2	ATG AAC ATA ATT CAG ATC AAC G	22	58	E51For (exon 1c)-qPCR
Ex2R2	GTT TTC GCC GCA ATC CGA TG	20	62	Dstpk61 exon 2-qPCR
Ex2R1	TGC TTT CTC CTT GGC CAT AG	20	60	Dstpk61 exon 2-qPCR
13R	CAG GAC ACT GCA GAT GTG G	19	60	Dstpk61 exon 6-sequencing
14R	CTT CTC GGC ATC GTT CAG G	19	60	Dstpk61 exon 5-sequencing
HF	GAA GCA GGA CTA CAT CAA GC	20	60	Dstpk61 exon 4-sequencing
JF	AGT ATG CGA GAA GCG GCT G	19	60	Dstpk61 exon 4-sequencing
15R	TGT GGA TGA CAC AGT ACC TG	20	60	Dstpk61 exon 1c and intron- PCR/ in situ
16R	GAC ACA GTA CCT GAA TTA TGT TC	23	64	Dstpk61 exon 1c and intron- PCR/ in situ
C	CGT AAT GTG GTG CAC CG	17	54	Dstpk61 exon 4-sequencing
61Rev	CGG AAT TCA CTT AGA CGC CGT CTT CTT G	28	64	Dstpk61 subcloning (3'end)
40FOR	CGG GAT CCT CAT GAA ATG TAA AAG CTG GTC CAA C	34	76	E40 subcloning
09FOR	CGG GAT CCT GAT GCA CCA GAT GAC CAA CGT TCC C	34	80	E09 subcloning
3R	GCT TTC TCC TTG GCC ATA GC	20	62	Dstpk61 exon 2-sequencing
9	TCT GCT GCC TTA TGT CAT TC	20	58	Dstpk61 exon 3-sequencing
10	AAC TAT ACA TCC CAG TGC CC	20	60	Dstpk61 exon 4-sequencing
LF	GTT GCT AGC AAC AGT TCG TC	20	60	Dstpk61 exon 3-sequencing, in situ
MF	GAC ATG TTG CCA TAC ATC AAC	21	60	Dstpk61 exon 4-sequencing, in situ
1bF	CCG AGT CTT CGT GTA TAC GT	20	60	E40 RT-PCR, in situ
1aF	GTT CGT GTG ATG TAG TGC TG	20	60	E09 RT-PCR, in situ
4R	AGG ATG TTC TCG GGC TTG AG	20	62	Dstpk61 RT-PCR
1R	CGT ATT GTG CTT CCC TTG A	19	56	Dstpk61 exon 1a- in situ, PCR
ex4R	ATC GTC TTC ATC GGA GTT GC	20	60	Exon 4 dstpk61- in situ
40NF	GCT GGT ACC ATG AAA TGT AAA AGC TGG TCC AAC	33	56	E40 subcloning-GFP

40NR	CTG GAT CCA ACT TAG ACG CCG TCT TCT TG	29	62	E40 subcloning-GFP
40CNF	GCT GGT ACC ATG AGC AAG TAT CTG ACA AAC GG	32	56	Core dstpk61 subcloning-GFP
40KNF	GCT GGT ACC ATG AGG TCT CCG AAT GAT TTC A	31	52	Kinase domain subcloning-GFP
40KNR	CTG GAT CCC GGA GCG TCT GCC AGT CAA TG	29	68	Kinase domain subcloning-GFP
tweF1	CAG CAC CAC CGT TCT GTC	18	58	twine-in situ
tweF2	CAG TTT CAG TAG CTC CTG CT	20	60	twine-in situ
tweR	CAC GAT GTC TAA TGC CTG TG	20	60	twine-in situ
CycBF	CAA GGA TCT CAA GCT CAC A	19	56	CyclinB-in situ
CycBR	TCG TAG TGA CTG CAC TGT TG	20	60	CyclinB-in situ
EMST2	TTC GTT GTC TGA CCG CTC G	19	60	emcF –in situ
EMC4F	GTC TGC CAG ACA GGT GCC	18	60	emc –in situ, PCR
EMC5R	GTT GCT AAA CTG TTG GAC AGT	21	60	emc –in situ, PCR
EMC6R	ATG ACG TGC TGG ATG ATC TC	20	60	emc

Table 2.4.3 Primers used

2.4.12 RNA preparation and electrophoresis

2.4.12.1 Total RNA isolation

Isolation of total RNA was done either by using the RNeasy mini kit (Qiagen) (for the testes versus accessory glands experiment) according to the manufacturer's instructions or by using the TRIzol reagent (Invitrogen) for all other isolations. For the TRIzol method, ~50mg of fly tissue was homogenised in 300μl TRIzol for 1.5 minutes. 700μl more TRIzol reagent was added and the sample was mixed by inverting. Then it was incubated at RT for 5 min. followed by the addition of 200μl chloroform and mixing by vigorous shaking. The mixture was incubated at RT for 2 min. and the phases were separated by centrifugation at 4°C for 15 min. at 15000rpm. The top aqueous phase containing the RNA (~500μl) was carefully transferred to a new tube, ensuring the interphase was not disturbed. 500μl ice-cold isopropanol was added to the top phase, mixed by inverting and the sample was incubated for 10 min. at RT. Centrifugation at 4°C, 15000rpm, for 10min. followed to pellet the RNA. The pellet was washed once with 1ml 75% EtOH and air-dried for 15-20 min. at RT. The RNA was resuspended in 70μl RNase-free water for 10 min. at 65°C and, if a pellet

was still visible, the sample was centrifuged for 5 min. at 15krpm and the cleared supernatant, containing the resuspended RNA, was transferred to a new tube and stored at -80°C.

2.4.12.2 RNA gel electrophoresis

A 1.2% agarose gel was prepared with DEPC-treated water and cooled down to 60°C. Then 20x MOPS and 37% formaldehyde were added (1x and 1.8% final concentrations, respectively) and the gel was poured in a tray and allowed to solidify for 1 hr.

RNA samples were pre-mixed with RNA sample buffer (Table 2.1.3.2) in a 1:3 ratio. The samples were incubated for 5 min. at 65°C to remove any secondary structures from the RNA and cooled on ice. Gels were run in 1x MOPS buffer at 7 V/cm for 1-2 hr (to check RNA presence) or O/N at 2-3 V/cm (for Northern blots).

2.4.13 Northern blot hybridisation

2.4.13.1 Northern Blot

The RNA gel was pre-soaked for 2x 20 min. in 10x SSC at RT and the nylon membrane (Hybond-N^+ from Amersham Biosciences or Schleicher and Schuell nylon membrane) was pre-soaked for 5 min. The transfer sandwich was assembled according to the manufacturer's instructions and the transfer was allowed to proceed O/N in 10x SSC. The membrane was exposed to UV for 5 min. to fix the RNA to the membrane.

2.4.13.2 Radio-labelling of probes

DNA probes were labelled with [^{32}P]dCTP (Amersham Biosciences) using Ready-To-Go DNA Labelling Beads (-dCTP) from Amercham Biosciences following the manufacturer's instructions. About 100ng DNA was used per labelling and unicorporated nucleotides were removed by passing the probe through NICK Columns (Pharmacia Biotech) which are pre-loaded with G-50 Sephadex for gel filtration. The high MW DNA passes faster through the column than the

unincorporated nucleotides and is collected in a new tube. The radio-labelled probes were denatured for 5 min. in boiling water and snap cooled on ice.

2.4.13.3 Hybridisation with [^{32}P]dCTP radio-labelled probes

The membrane was prehybridised for 6hr-overnight in hybridisation buffer without the probe, at 45°C in a glass tube in a Hybaid rotating oven. The denatured radio-labelled probe was added to the hybridisation buffer and the membrane was hybridised O/N at 45°C. The next day the membrane was washed twice for 20 min. in 1xSSC, 0.1% SDS at 45°C (medium stringency wash) and then twice for 20 min. in 0.1x SSC, 0.1% SDS at 45°C (high stringency wash). The membrane was then sealed in a polythene bag and placed in an autoradiography cassette with intensifying screens and exposed to X-ray film (Kodak) for 1-10 days at -70°C before the film was developed or placed in a phosphorimager cassette for O/N – 3 days and then the cassette was scanned in a STORM Phosphorimager (COIL, ICB).

2.4.14 In situ hybridisation to mRNA

2.4.14.1 Preparation of digoxygenin-labelled probes

The PCR DIG labelling mix (Roche) was used to generate single-stranded digoxygenin-labelled DNA probes, using a PCR fragment from cloned DNA as a template and a specific primer to generate ssDNA (antisense for the probe and sense for a negative control). 5μl of the probe was checked on an agarose gel. The digoxygenin-labelled probe was boiled for 15 minutes to remove any secondary structures and break down the DNA to short fragments and then chilled on ice.

For single-stranded digoxygenin-labelled RNA probes templates were transcribed with either T7 or T3 polymerases (Ambion) using the DIG RNA labelling kit (Roche) according to the manufacturer's instructions.

2.4.14.2 In situ hybridisation to whole-mount ovaries using DNA probes

The protocol is based on a procedure previously described (Tautz and Pfeifle, 1989) with minor modifications. The ovaries were collected in Ringer's saline, fixed for 20 min. in PMS at RT and washed 3x 5 min. in PBT. Then they were digested in 10μg/ml Proteinase K for 10-15 min. at RT without rotating. Digestion was stopped by washing in PBT containing 2mg/ml Glycine. After 3 more washes of 5 minutes each in PBT at RT (with rotating), the ovaries were post-fixed in PMS for 10 min., washed 3x20 min. at RT and equilibrated for 10 min. in PBT: Hybrix 1:1 at RT. Then they were pre-hybridised in DNA Hybrix (without the probe) for 1 hr at 45°C (in the heated block or oven) and hybridised overnight in DNA Hybrix containing the digoxygenin-labelled probe (1:10-1:20 dilution). The probe can be re-used up to three times.

The next day the ovaries were washed with preheated DNA Hybrix for 20 min. at 45°C, in PBT:Hybrix 1:1 for 20 min. at 45°C and in PBT at 45°C for 20 min. Then they were left at RT to cool down and subsequently washed 5 times for 5 min. each in PBT at RT with rotating. The ovaries were incubated for 1 hr with the antibody (anti-DIG Alkaline Phosphatase-AP, preabsorbed with wild-type ovaries O/N) at 1:600- 1:1000 dilution. Staining solution containing 5mM Levamisole, 4.5μl/ml NBT and 3.5μl/ml x-Phosphate was added to the ovaries and the tubes were kept in the dark until the colour developed (monitored under the dissecting microscope- takes 30 min – several hours). The colour reaction was stopped by washing the ovaries in PBS; the ovaries were then mounted in Glycerol:PBT 4:1, the ovarioles were separated on a microscope slide and the staining pattern was analysed in a microscope with Nomarski optics.

2.4.14.3 In situ hybridisation to whole-mount ovaries using RNA probes

The protocol is based on the Tautz and Pfeifle (1989) procedure with the following modifications. Ovaries were collected and fixed in PMS, washed for 3x10 minutes in PBT, equilibrated for 10 minutes in RNA Hybrix/PBT (1:1) and then prehybridised for 1 hour at 65°C in RNA Hybrix (50% deionised formamide, 5x SSC, 100 μg/ml

tRNA (RNase free), 50 µg/ml Heparin, 0.1% Tween 20). The ovaries were hybridised overnight at 65°C in RNA Hybrix containing digoxigenin-labelled RNA probe. Detection was carried out with 1:80 dilution of anti-DIG HRP antibody (DakoCytomation, #D5101) for 1 hour at room temperature (RT). For visualisation TSA-Cy3 reagent (PerkinElmer, #SAT704A) was used according to manufacturer's instructions. Ovaries were mounted in Vectashield (Vector Laboratories, #H1000) for observation.

2.4.14.4 In situ hybridisation to whole-mount testes

A protocol from Dr. H. White-Cooper was used with RNA-DIG labelled probes with minor modifications. Testes from 0-1.5 day old males were dissected in Ringer's saline and transferred to the lid of an eppendorf tube in a drop of Ringer's. 600µl Fix was added to the tube, the lid was closed and the tube was inverted a few times to mix the testes with the Fix. 400µl more Fix was added and the tube was left on its side for 20 min.-1hr to fix the tissue. The testes were washed 3x 5 min. each in PBT at RT, followed by an incubation with 50µg/ml Proteinase K for 5-7 min. The reaction was stopped with 2mg/ml Glycine in PBT and then the testes were washed 2x 5 min. in PBT and fixed again for 20 minutes in Fix. After a 10 min wash in 1:1 PBT:HB (Hybridisation buffer) and a 10 min. wash in HB, the testes were carefully transferred into tissue culture inserts (BD Biosciences, #353097) that were pre-washed in PBT, in a 24-well tissue plate. For all subsequent steps the wash was added into the inserts and removed by lifting up the insert and aspirating solution from the well. To facilitate solution passing through the mesh, the plate with the inserts was rotated very gently on a "belly dancer" shaker.

The testes were pre-hybridised in HB at 65°C for at least 1 hr. Meanwhile the probes were diluted in HB buffer (500µl of 1:300 dilution), heat-denatured at 80°C for 10 min. and chilled on ice. The testes were hybridised at 65°C O/N in the oven. Next day there was a series of washes, as follows: at least 6x 30 min. in pre-heated HB at 65°C, 15 min. in 4:1 HB:PBT at RT, 15 min. in 3:2 HB:PBT at RT, 15min. in 2:3 HB:PBT at RT, 15 min. in 1:4 HB:PBT at RT and 2x 15 min. in PBT. The testes were incubated O/N in 1:700 AP-conjugated anti-Digoxygenin antibody (pre-

absorbed O/N with embryos) in PBT. Then they were washed 4x 20 min. at RT in PBT and 3x 5 minutes in freshly made buffer HP. Meanwhile the staining solution was made in HP buffer by adding 4.5μl NBT and 3.5μl X-Phosphate per ml . The colour reaction solution was added to the testes and the plate was left in the dark at RT for the colour to develop. The signal takes 10 min.- several hours [20-25min for the E51 experiment]. The reaction was stopped by washing 3x 5 min. in PBT and the tissue was dehydrated through an ethanol series [10 min. in each of 30%, 50%,70%, 90%, 100%, 100% ethanol]. The testes were transferred with a thin needle into a glass staining block where they were incubated for 15 min. in 1:1 ethanol: methyl salicylate and then in 100% methyl salicylate. Finally they were mounted in GMM, transferred to microscope slides and observed with Nomarski optics.

2.4.15 Nuclear staining

For multicolour imaging DNA was counterstained with the appropriate nuclear stain. For blue colour DNA was stained with Hoechst 33258 (1μg/ml) for 5 minutes in PBT. Nuclear yellow (Sigma, #N2137) was also used in 1μg/ml concentration. For green colour we used Sytox Green (Molecular Probes, Invitrogen) at 150nM concentration whereas TO-PRO-3 (Molecular Probes, Invitrogen), which can be detected in the infrared channel, was used at 250nM concentration. No RNase digest was necessary when staining with Hoechst or Nuclear Yellow. Sytox Green and TO-PRO-3 can stain DNA as well as RNA, therefore samples were pre-digested in 250μg/ml RNase-A for 5-10 minutes. Stained samples were examined and captured digitally either on a Zeiss Axiophot fluorescent microscope or a Leica TCS SP confocal microscope.

2.5 Protein methods

2.5.1 Preparation of protein samples

2.5.1.1 Protein preparation from *Drosophila* tissues

Tissues were dissected in *Drosophila* Ringer's and homogenised in the required volume of Protein Sample buffer (Laemmli). Samples were boiled for 5 minutes and cooled on ice. The cell debris was discarded after centrifugation at 15krpm, RT for 5 min. and the supernatant was transferred to a clean tube. The samples were stored at -20°C but ran immediately on a protein gel whenever possible.

2.5.1.2 Protein preparation from cell extracts

Protein samples were prepared from bacterial cultures by centrifuging 1ml of overnight culture (OD_{600}= 1.5-2.0) at 6krpm for 1 minute. The pellet (which could be frozen and used later) was resuspended in 100μl Protein Sample buffer, vortexed and boiled for 5 minutes. The sample was centrifuged at 13krpm for 5 minutes to remove the cell debris and the supernatant was transferred to a new tube.

2.5.2 Bradford assay

The Bradford assay, based on the proportional binding of the dye Coomassie to proteins, was used for determination of protein concentration of samples. The more protein there is in a sample the darker the colour becomes. The protein concentration is determined by comparison to the readings of known amounts of protein (typically BSA) which are used to make a standard curve. A stock solution of BSA (1mg/ml) was used to make samples containing 1, 5, 10, 15 and 20μg BSA (in 20μl volumes, made up with ddH_2O) in duplicates or triplicates. Appropriate dilutions of the unknown sample were made, to a final volume of 20μl. 1ml working Bradford Solution was added to each tube of standards and unknowns and the tubes were incubated in the dark at RT for 10 min. The absorbance of each sample at 595nm was measured in a spectrometer and the standard curve was created. The readings from the sample dilution falling into the linear phase of the graph were used to determine the sample concentration.

2.5.3 SDS-Polyacrylamide gel electrophoresis (PAGE)

The glass plates for PAGE were assembled and sealed according to the manufacturer's instructions. About 20ml Separation mix (Table 2.5.1) was poured between the plates and a little dH_2O was gently added on top to even the surface. The gel was allowed to set for 30-60 min. at RT. Then the water was removed and 5ml of Stacking Mix was poured on the top of the set separation mix and the appropriate gel comb was inserted. After polymerisation the gel assembly was placed in the electrophoresis tank and 1x PAGE running buffer was added. Protein samples were loaded and the gel was run at 40V O/N.

2.5.4 Coomassie Blue polyacrylamide gel staining

If the gel was not used for a Western blot, the proteins were visualised after staining with a Coomassie Blue containing solution. The gel cassette was dissembled and the gel, after cutting the stacking mix was transferred to a plastic tray and was incubated with Coomassie gel staining solution for 15 minutes at RT with agitation. Instead of 15 min. incubation the gel could be microwaved for 5-15 seconds at full power, with a lid on the tray- once condensation starts appearing on the lid (or steam appears) the tray should be removed from the oven. The excess Coomassie solution was recycled and the gel was washed with dH_2O in the tray and then in destaining solution (50ml glacial acetic acid, 50ml MeOH and 400ml H_2O). The gel was heated in the microwave for 1 min. at medium power (power 6) with the destaining solution. Then the gel was incubated at RT for 1hr in the destaining solution with agitation (40rpm). After 1 hr the destaining solution was replaced and the gel was agitated O/N or microwaved again for 1 min at power 6 and agitated for 1 hr at RT. The gel was scanned between two plastic sheets in a Hewlett-Packard flatbed scanner and the picture saved in JPEG format.

Protein bands from gels for sending to the MALDI-TOF facility needed to be stained with a special staining solution, GelCode Blue Stain (Pierce) to visualise the proteins. The desired band was then excised from the gel, cut in small pieces and placed in a sterile eppendorf tube- at this step it could be stored at -20°C. The sample was sent to

the facility (ICMB, University of Edinburgh) where the protein was trypsin digested and processed before being analysed by MALDI-TOF.

2.5.5 Western Blot and Immunodetection

2.5.5.1 Semi-dry transfer

Proteins were transferred from the gel to a Hybond-C Super nitrocellulose membrane (Amersham Biosciences) by semi-dry transfer, according to the manufacturer's instructions. The assembly consisted of 3 Whatmann filter papers (pre-soaked in Running buffer) adjacent to the anode (+), the membrane (also pre-soaked) on top of them, followed by the gel (after cutting the stacking part), three more filter papers and the cathode (-). The membrane and papers were cut to the same size as the gel. The proteins were transferred at 15V (400mA) for 2 hours.

Alternatively a PVDF membrane was used (Hybond P, Amersham Biosciences) according to the accompanying instructions. The main differences was that the PVDF membrane needed to be rehydrated in 100% Methanol for 1 min., washed in ddH_2O for 5 min. and then soaked in transfer buffer containing 20% methanol.

2.5.5.2 Ponceau-S staining

The efficiency of the transfer was monitored by staining the nitrocellulose membrane with Ponceau S for 10 min., rinsing off excess stain with water and taking a picture. Ponceau S staining was sometimes successful when using the PVDF membrane but is not always reliable; it is generally not recommended for this type of membrane.

2.5.5.3 ECL immunodetection

The membrane was incubated in 50ml Blocking buffer (Table 2.5.1) at 4°C O/N or for 1 hr at RT with shaking (40rpm). The membrane was then transferred to a nylon bag with 16ml 1x TBS containing the primary antibody at the appropriate dilution (1:500-1:1000 for serum –anti-E40, anti-DSTPK61 and ~1:10000-1:20000 for affinity-purified antibodies such as anti-GST and anti-GFP) and was incubated O/N at 4°C with shaking. After the O/N incubation the membrane was washed 3x 10 min. in TBS-T with shaking at 40rpm. Then it was blocked for 20 min. at RT in 0.4%

normal serum from the animal species in which the secondary antibody was raised in. Following that the membrane was sealed in a nylon bag with 16ml 1x TBS containing the secondary antibody and was incubated for 1hr at RT with shaking (60rpm). Subsequently it was washed 3x 10 minutes in TBS-T and immersed in 20ml ECL reagent with 8µl 30% H_2O_2 (freshly added) for 1 minute. The membrane was then sealed in a nylon bag avoiding the formation of air bubbles, placed in an autoradiography cassette with intensifying screens and exposed to X-ray film (Kodak X-OMAT) for 15 seconds – 30 minutes at RT.

Quantification of band intensity, where applicable, was done with ImageJ software (http://rsb.info.nih.gov/ij/). A list of antibodies is shown in Table 2.5.2.

Dot-Blots were done in a Schleicher and Schuell Minifold II slot-blotter, according to the manufacturer's instructions. The ECL detection was as before.

Solution	Components/Preparation
Separating mix	For 20ml 10% acrylamide (for 21-100kDa proteins) 7.9ml ddH_2O 5ml 1.5M Tris-HCl pH 8.8 200µl 10% SDS 6.7ml 30% Protogel (30% Acrylamide/0.8% Bis-acrylamide- 37.5:1) 200µl 10% (w/v) $(NH_4)_2S_2O_8$ (APS) 20µl TEMED
Stacking mix	3.44ml ddH_2O 630µl 1M Tris-HCl pH 6.8 50µl 10% SDS 830µl 30% Protogel (30% Acrylamide/0.8% Bis-acrylamide- 37.5:1) 50µl 10% (w/v) $(NH_4)_2S_2O_8$ (APS) 10µl TEMED
Blocking Buffer (5% Casein)	15g Casein 15ml Ethanol Add 50ml 1xTBS and mix well (vortex). Add 100ml more 1xTBS and make sure the casein is completely dissolved. Add 135ml 1x TBS. Store at 4°C.
Stripping Buffer	3.47ml 14.4M β-Mercaptoethanol 100ml 10% SDS 31.25ml 1M Tris-HCl pH 6.7

Table 2.5.1 Solutions for SDS-PAGE and Western blot

2.5.5.4 Membrane stripping

The membrane was sealed in a bag with 50ml stripping buffer (Table 2.5.1) and incubated at 50°C or 70°C (for higher stringency) for 30 minutes.

Antigen		Host animal	Working concentration		Source/ product number
			Immuno-histochemistry	Western detection	
DSTPK61		Sheep	n/a	1:1000-1:3000	Raised in our laboratory
E40 isoform		Rabbit	1:100-1:200	1:1000-1:2000	Raised in our laboratory
Emc		Rabbit	1:600	1:6000	Gift from L.Y. Jan and Y.N. Jan, University of California, San Francisco
Br-C core		Mouse	1:60	n/a	Gift from G. Guild, University of Pennsylvania
GFP		Rabbit	1:200	n/a	Molecular Probes A11122
GST		Rabbit	n/a	1:20000	Sigma G7781
His-Tag		Mouse	n/a	1:1000	Cell Signaling #2366
Digoxygenin -AP		Sheep	1:700-1:1000	n/a	Roche No:1 093 274
Yolk protein		Rabbit	n/a	1:2000	Raised in our laboratory
Secondary Antibodies	**Labelling**	**Host animal**	**Immuno-histochemistry**	**Western detection**	**Source/ product number**
Rabbit IgG	**HRP**	Goat	n/a	1:4000	Sigma A 8275
Sheep IgG	**HRP**	Donkey	n/a	1:4000	Sigma A3415
Rabbit IgG	**FITC**	Goat	1:100	n/a	Sigma F9887
Rabbit IgG	**Alexa 568**	Goat	1:400	n/a	Molecular Probes A-11011
Mouse IgG	**Alexa 568**	Goat	1:400	n/a	Molecular Probes A-11004
Mouse IgG	**Alexa 488**	Goat	1:400	n/a	Molecular Probes A11017

Table 2.5.2 Primary and secondary antibodies used

2.5.6 Immunohistochemical detection in whole-mount ovaries

Ovaries were dissected in Ringer's and fixed for 20 minutes in PMS, washed 3x 10 min. with PBTW (PBS containing 0.5% Triton X-100) and incubated with 5% NGS (Normal Goat Serum) in PBTW for 1 hour at RT [The blocking agent is the normal serum from the animal species in which the secondary antibody was generated]. Primary antibody was added at the appropriate dilution and the ovaries were incubated O/N at 4°C while rotating. Next day the antibody was removed and the ovaries were washed three times for 30 min. each, in PBTW. Then they were blocked for 30 min. in 5% NGS in PBTW and the secondary antibody was added (at the appropriate dilution in PBTW); the ovaries were incubated with it for 1hr at RT. Subsequently there were 3 30-minute washes in PBTW and fluorescently stained ovaries were mounted in DABCO or Vectashield and analysed and photographed on a fluorescent microscope (Axiophot) fitted with a digital camera or on a Leica SP confocal microscope.

2.5.7 β-galactosidase staining

Female flies fed with yeast for three days were dissected in PBS. Ovaries were dissected and fixed for 5 minutes in 4% p-Formaldehyde in PBT, then stained overnight in 100µl Staining Solution (10 mM Phosphate buffer, pH 7.0, 8 mM $K_3[Fe(CN)_6]$, 8 mM $K_4[Fe(CN)_6]$, 150 mM NaCl and 1 mM $MgCl_2$) to which 2.5 µl 8% X-Gal (5-Bromo-4-chloro-3-indolyl-β-D-galactoside) were added. The stained ovaries were rinsed in PBS and mounted in PBS/Glycerol (1:4).

2.5.8 Protein expression in bacterial cells

One method to get a solution of recombinant protein was by pelleting 4ml of induced BL21(DE3)Lys or XL1Blue cells (OD_{600}= 1.5) containing the pGEX-3X or pRSETC expression vector with the recombinant DSTPK61 coding sequence. The pellet was resuspended in 1ml PBS, mixed with Lysozyme (33µg/ml culture) and incubated on

ice for 40 minutes. Then the suspension was sonicated at varying conditions and centrifuged to remove the cell debris. Protein extracts from uninduced cells of the same density or from induced bacterial cells containing only the expression vector without the *dstpk61* sequence were used as controls for the Western blots.

2.5.8.1 General protocol for GST-fused protein expression

The protocol of the manufacturer (GST gene fusion system- Pharmacia Biotech) was followed. Subsequently optimisation of conditions was tried, as described in table 6.3.1.

2.5.8.2 Protein isolation from inclusion bodies

A 1L culture was grown at 37°C until OD_{600}= 0.5 and protein expression was induced with IPTG (1mM final) and the cells grown for 3hr at 37°C. Induction levels were monitored by taking a 1ml sample every hour and running them on an SDS gel together with the uninduced control kept, to check the progress of induction.

The cells were collected by centrifuging at 5000rpm for 15 minutes at RT. The supernatant was discarded and the pellet with the cells was lysed by resuspending the cells in 3ml Lysis buffer/g of cells (Buffer compositions in Table 2.5.3). To this lysozyme (10mg/ml stock) was added at 80μl/g cells, as well as 1M Benzamidine at 3μl/g of cells. The cells were incubated in the lysis buffer on ice for 30 minutes with occasional stirring. Then Sodium Deoxycholate (4mg/g cells) was added with continuous stirring and the cells were incubated at 37°C until the lysate became viscous (~10 minutes). The solution was incubated on ice again. 1M $MgCl_2$ and 1M $MnCl_2$ were added at 30μl/g cells and DNase I (0.4mg/ml stock solution) was also added at 50μl/g of cells. Incubation on ice lasted until the solution was no longer viscous (~30 minutes).

To isolate the inclusion bodies the cell lysate was centrifuged at 12krpm for 15 minutes at 4°C and the pellet was resuspended in washing buffer (3ml/g of cells). A fraction of the supernatant was kept for control - supernatant 1. The cells were

incubated on ice for 5 min. and centrifuged again for 15 min. at 12krpm at 4°C (some supernatant 2 was kept for control).

The pellet was carefully resuspended in a large volume of refolding buffer (4ml/g of cells) containing 8M Urea and 7mM DTT. After 1 hr incubation of the solution at 4°C all undissolved material was removed by centrifugation at 12krpm for 15 min. at 4°C (keep some of pellet 1 for control). The solution was diluted 10-fold with refolding buffer at 4°C. The dilution was carried out using a leaky syringe at a rate of 40ml/hour. All precipitated material was removed by centrifugation at 12krpm for 15 min. at 4°C (at this point some pellet 2 was kept). The supernatant (supernatant 3) was stored at 4°C until dialysis.

2.5.8.3 Protein dialysis and concentration

Preparation of dialysis tubing: The tubing was boiled for 10 minutes in 0.05% EDTA to remove sulphur compounds and metal ions. Once cooled the tubing was washed with dH_2O and stored at 4°C in a 0.01% sodium azide solution.

For dialysis the treated dialysis tubing was filled ¾ with the protein solution and clamped at each end with plastic dialysis clamps, ensuring there were no air bubbles. The filled dialysis tubing was left O/N at 4°C in the required volume of dialysis buffer [to dialyse 150ml of a protein solution 5L dialysis buffer are necessary].

The large volumes of protein solution after dialysis were reduced by protein concentration using UFV5BTK25 Ultrafree-4 Centrifugal filters (Millipore) by ultracentrifugation, according to the manufacturer's instructions. The protein concentration was subsequently estimated by Bradford assay.

2.5.8.4 Purification of GST-fused proteins

Dry glutathione-agarose beads (Sigma, G4510) were rehydrated by washing several times in ddH_2O and allowed to settle. The purification was done either in batch (with the glutathione-agarose beads in eppendorf tubes or in columns (by packing the beads in a 1ml plastic syringe plugged with glasswool), according to the glutathione-

agarose accompanying protocol. The protein was eluted using a buffer with reduced glutathione (Sigma, G4251) according to the manual from Sigma or the GST gene fusion system manual (Pharmacia Biotech).

2.5.8.5 Purification of Histidine-tagged proteins

Ni-NTA columns (Qiagen) were used to purify Histidine-tagged fusion proteins according to the manufacturer's protocol. 2.5ml Ni-NTA agarose was placed in a 10ml syringe plugged with glass wool. The column was washed with 20ml buffer X1 and was stored overlaid with 10ml buffer X1.

The column was washed with 10ml buffer X1 and equilibrated with 10ml buffer X1U. The protein solution (in X1U) was passed three times through the column and 15ml Wash buffer was passed through the column to remove unbound proteins.

The recombinant protein was eluted with 10ml elution buffer and 1ml fractions of eluate were collected and analysed on an SDS-polyacrylamide gel.The fractions containing the recombinant protein would be combined and dialysed as before, to allow the protein to re-fold. Buffers used are shown in Table 2.5.3.

The denaturing buffers described here (with Urea and Imidazole) were also tested for protein isolation of GST –fused recombinant proteins which normally happens under native conditions, without major improvements in the results.

Buffer	Components/Preparation	Final concentration
Lysis buffer (IB)	Tris-HCl pH 8.0 NaCl EDTA	50mM 100mM 2mM
Washing buffer (IB)	Tris-HCl pH 8.0 NaCl $CaCl_2$ EDTA	50mM 100mM 20mM 2mM
Refolding buffer (IB)	A) for the 10x dilution: Tris-HCl pH 8.0 NaCl $CaCl_2$ EDTA	 50mM 200mM 20mM 2mM

	Glycerol	5%
	B) for the protein refolding:	
	Tris-HCl pH 8.0	50mM
	NaCl	50mM
	$CaCl_2$	20mM
	EDTA	2mM
	Urea	8M
	DTT	7mM
Dialysis buffer (IB)	Tris-HCl pH 8.0	50mM
	NaCl	200mM
	Glycerol	5%
Imidazole pH 8.0	1.36g Imidazole (Mw:68.08)	1M
	Adjust pH to 8.0 with cHCl	
	Adjust the volume to 20ml	
X1 Buffer	5ml 1M Tris-HCl pH 8.0	10mM
	1ml 1M Imidazole pH 8.0	2mM
	50ml 5M NaCl	500mM
	0.5ml Tween-20	0.1%
	Adjust the volume to 500ml with ddH_2O	
X1U Buffer	5ml 1M Tris-HCl pH 8.0	10mM
	1ml 1M Imidazole pH 8.0	2mM
	50ml 5M NaCl	500mM
	0.5ml Tween-20	0.1%
	36g Urea (Mw:60.06)	6M
	Adjust the volume to 500ml with ddH_2O	
Wash Buffer	1ml 1M Tris-HCl pH 8.0	10mM
	1ml 1M Imidazole pH 8.0	10mM
	10ml 5M NaCl	500mM
	1ml 10% Tween-20	0.1%
	36g Urea	6M
	Adjust the volume to 100ml with ddH_2O	
Elution Buffer	1ml 1M Tris-HCl pH 8.0	10mM
	1.36g Imidazole (adjust pH to 8.0 with cHCl)	200mM
	10ml 5M NaCl	500mM
	1ml 10% Tween-20	0.1%
	36g Urea	6M
	Adjust the volume to 100ml with ddH_2O	

Table 2.5.3 Solutions required for isolation of protein from inclusion bodies (IB) and His-tagged protein purification.

Chapter 3: Genetic analysis of *dstpk61*

3.1. Introduction

3.1.1. Analysis of potential *dstpk61* mutants

Several potential *dstpk61* mutants had been created in our laboratory by P-element-mediated mobilisation, in an attempt to generate the necessary tools for genetic studies following the identification of *dstpk61* (Clyde, 1999). The P-insertion fly line 833/11 from Peter Deak's collection in Dundee (Deak et al, 1997) was used to mobilise the P-element located near the *dstpk61* gene locus at position 61. At the time the information provided was that fly line 833/11 contained a single P-insertion and it was not known that it contains 3 P-elements in chromosome 3, two of which map to 61A and the other to 86E. The P-hop resulted in 9 white-eyed, probably excision fly lines (in these lines at least the *white* (w^+) gene is excised but possibly more of the P-element and some neighbouring DNA may be excised as well) and 75 red-eyed insertion lines (mobilisation of the P-element). In both white and red-eyed lines homozygous viable, homozygous lethal and homozygous male-lethal phenotypes were observed (Clyde, 1999).

Complementation tests (Fonfara, 2000 – report from an undergraduate project) between the homozygous lethal (mainly male-lethal) white-eyed lines suggested there were two complementation groups, W4 and [W1, W7, W9, W47, W58]. Similarly, crosses between the red-eyed homozygous male-lethal lines showed four complementation groups, R17, R28, R29 and [R19, R25, R38, R51]. Subsequent complementation crosses between the white-eyed fly lines W1, W4 and the red-eyed homozygous male-lethal fly lines R17, R28, R29, R38 were carried out in order to find the relative positions of the red-eyed homozygous male-lethal fly lines in relation to the possible deletions of the white-eyed fly lines (Fonfara, 2000). The results are summarised in Table 3.1.1. and Figure 3.1.1. (based on Fonfara, 2000).

	R17	R28	R29	R38
W1	-	-	-	-
W4	-	+	+	+

Table 3.1.1: Complementation between red and white-eyed potential mutant fly lines

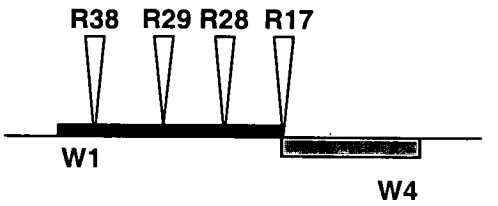

Figure 3.1.1: Diagram of relative positions of P-elements/deletions in potential mutant fly lines

Deletions W1 and W4 (indicated by a black and grey rectangle, respectively, in Fig. 3.1.1.) are in different positions since they do complement each other but the R17 P-element insertion must be located at the end of one and the beginning of the other deletion since it does not complement either of them. W1 must be a big deletion which includes the P-insertion sites (indicated by triangles in Fig. 3.1.1.) of all the red-eyed homozygous male-lethal fly lines. Inverse PCR on the red-eyed homozygous male-lethal fly lines had failed (Fonfara, 2000).

3.1.2 *dstpk61* mutants generated in other laboratories

In the time elapsed between the generation of the fly lines in our group and initial analysis of these potential *dstpk61* mutants and the beginning of my research, two other laboratories obtained mutants for the gene by imprecise excision of an EP element (Cho et al, 2001) and by EMS (chemically induced) mutagenesis (Rintelen et al, 2001) and they demonstrated a role for *dstpk61* in *Drosophila* as a regulator of cell and organism growth and apoptosis. Table 3.1.2 summarises the information regarding *dstpk61* mutants available to date.

Table 3.1.2: Mutants currently created for *dstpk61* and their phenotypes

***Dstpk61* mutant**	**Mutation location**	**How it was created**	**Phenotype**	**Reference**
dPDK1^{1}	P-element 711bp upstream of exon 4; disrupts translation of *Dstpk61*	EP line [EP(3)3091]– P element insertion	-embryonic lethal -no proper cuticles are formed -apoptosis is induced	Cho et al., 2001
dPDK1^{2}	10kb deletion that includes the first exon of *Dstpk61*	Imprecise excision of P element in line EP(3)0837	-embryonic lethal	Cho et al., 2001
dPDK1^{3}	amino acid change G352S in kinase subdomain VII (exon 4)	EMS-induced mutagenesis	-organ size reduction in mosaic animals	Rintelen et al., 2001
dPDK1^{4}	amino acid change P441L in kinase subdomain VIII (exon 4)	EMS-induced mutagenesis	-organ size reduction in mosaic animals -dPDK1$^{4/5}$ are viable, show developmental delay and reduced body size and weight due to cell size reduction. Males are almost completely sterile.	Rintelen et al., 2001
dPDK1^{5}	amino acid change Q437Z in kinase subdomain VIII (exon 4)	EMS-induced mutagenesis	-2nd instar larval lethal, as well as dPDK1$^{1/5}$ heteroalleles -Organ size reduction in mosaic animals	Rintelen et al., 2001
dPDK1^{1} (modified)		EP(3)3091 line recombined to remove all background mutations	-second instar larval lethal	Rintelen et al., 2001
UAS-PDK1^{A467V}	amino acid change A467V (gain of function) in kinase domain (exon 4)	Site-directed mutagenesis kit	-overexpression causes increase in cell size	Rintelen et al., 2001

Given these facts, my aim was to determine whether the potential mutants created in our lab were true mutants of *dstpk61* and if so, to analyse them further. Since my hypothesis is that there are roles for *dstpk61* that are likely to be sex-and tissue-specific, it would be of particular interest to dissect the function of *dstpk61* in male-lethal mutants, which apparently affect sexes in a different way. Knowing also that the original fly line used to create these mutants (833/11) has turned out to be much more complex than originally thought, made it crucial to start by mapping the exact

position of the P-elements in the red-eyed fly lines: I addressed this by inverse PCR. In parallel, I obtained the well-characterised *dstpk61* mutants created by other laboratories and used them in complementation tests with our own potential *dstpk61* mutants to investigate whether they disrupt the same function, i.e. the *dstpk61* gene locus and to help with mapping our red-eyed P-element insertion fly lines within the gene locus. The relative position of deletions represented by the white-eyed fly lines would be determined indirectly through the positions of the P-elements in the red-eyed lines.

3.2. Mapping of P-elements in red-eyed homozygous male-lethal potential dstpk61 mutants

Inverse PCR (Fig. 3.2.1) was used for fly lines R17, R28, R29, R38 and 833/11 to map the position of their P-elements. Lines R17, R28 and R38 have a single P-element insertion as only one product is present, whereas line R29 has two P-elements, indicated by the two bands, one of which is at the same size as those of the other red-eyed fly lines and one that is smaller (Fig. 3.2.2A). The original fly line used for the P-hop mutagenesis, line 833/11, has three P-element insertions as indicated by the presence of three bands after inverse PCR (Fig. 3.2.2B), in line with current knowledge regarding this fly line.

There were great difficulties in successfully isolating and purifying these PCR products and subsequently in obtaining good quality sequencing from them.

Sequencing R17 and the high MW product of R29 gave two inseparable sequences for each; therefore this data could not be processed further. The position and orientation of the inserted P-elements for fly lines R38, R28 and R29-2nd (low MW product) was determined by doing a Blastn search (Altschul et al, 1990) of the NCBI database with the sequenced DNA fragments.

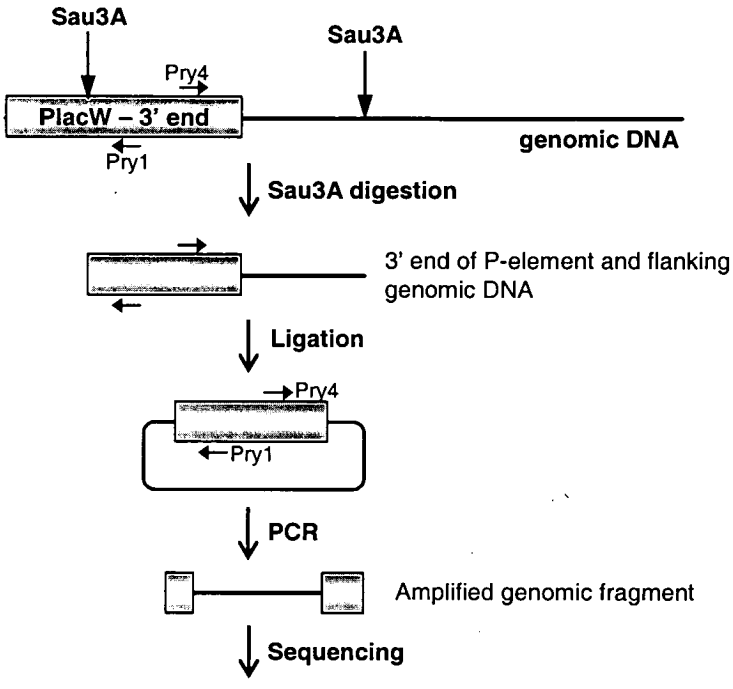

Figure 3.2.1: Inverse PCR technique
Genomic DNA containing P-elements (PlacW 3' end inverse PCR is shown here- the method applies to other P-elements and is similar for the 5-end) is isolated and digested with the restriction endonuclease *Sau3A*. *Sau3A* cuts every 256bp and there is a cutting site near the 3' end of the P-element, thus the genomic DNA flanking the P-element will be cut near the P-element insertion site. The linear fragments are ligated the genomic DNA fragment flanking the P-element 3' end is preferentially amplified by PCR using primers from the P-element sequence (Pry1 and Pry4 are indicated here). Sequencing with one of these primers and subsequent search of the genome database can reveal the exact position of P-element insertion as well as the orientation of the P-element.

The P-element of R28 and R38 is inserted in the right arm of chromosome 3, position 86E8. This is the 5' end of gene PGRP-LB, a defence/immunity protein (gi numbers: 41058118, 13760075) and the P-element has the same orientation as the gene. The second P-element of R29 is located on chromosome 2L, position 33E, within the big intron of gene CG5461 (bun), an RNA polymerase II transcription factor (gi:10728739). Therefore, none of these lines has a P-element inserted in *dstpk61* (chromosome 3L, position 61A) and they are not mutants of that gene. A Blastn search for the first P-element (top band) of 833/11 showed that it is located at position 86E on chromosome 3, in gene PGRP-LB (gi:24645945, 13027509) and for

the third P-element (lowest band) only P-element sequence, but not any flanking genomic sequence, was retrieved.

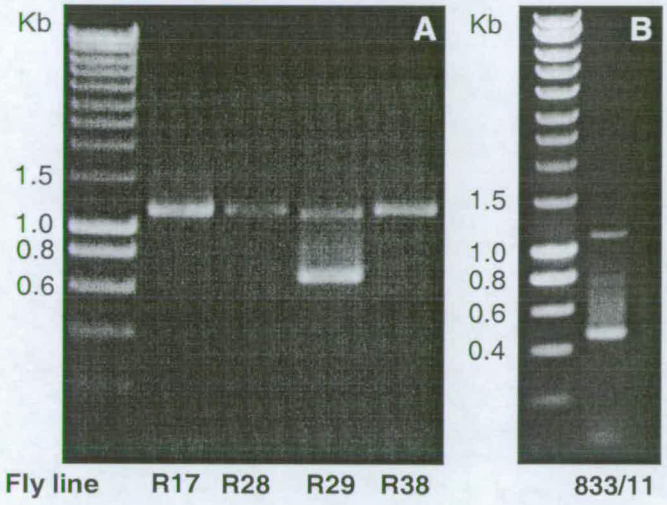

Figure 3.2.2: Inverse PCR
PCR under optimised conditions for the potential *dstpk61* red-eyed homozygous male lethal fly lines (A) and the original fly line used for the P-element mobilisation (B). Line R29 shows two bands and line 833/11 shows three bands, indicating that they have two and three P-elements, respectively. The high MW band runs similarly in all lines, possibly representing the same P-element. Bands were excised from the gel, purified and sequenced. The marker is Hyperladder I (Bioline).

The results from my inverse PCR analysis map the P-element of fly lines R28 and R38 at position 86. Taking into account the complementation analysis done previously (Fig. 3.1.1) that shows all the red-eyed fly lines falling within the deletion of white-eyed line W1 which lies next to the deletion of W4, I have to assume that all the mutants we have (R17, R28, R29, R38, W1 and W4) will map at position 86 and possibly affect the gene PGRP-LB. The fact that the four different red-eyed lines have a band of the same MW by inverse PCR, which, when sequenced for two of the lines gave the same P-element insertion position, supports this assumption.

3.3. Complementation analysis of P-insertion fly lines and mutants of dstpk61

The principle of complementation crosses is that if two mutations or deficiency lines disrupt the same function, an individual inheriting an allele for each from its parents will be essentially equivalent to a line homozygous for the mutation and will die. This result is non-complementation, since the two mutant alleles do not complement each other. If on the other hand the two mutations disrupt different functions, complementation will occur as each parent will contribute a wild-type allele for the mutation inherited by the other parent and the individual will be viable.

In parallel with the molecular analysis in the previous section, the *dstpk61* mutant fly lines dPDK1(1), dPDK1(5) and dPDK1(5ex) (which is line dPDK1(5) recombined to lose EP(3)837) (Rintelen et al, 2001) Ire crossed with each of the red-eyed P-element insertion lines R17, R28, R29 and R38. The crossing scheme is described in Fig. 3.3.1 and the results are presented in Tables 3.3.1 and 3.3.2.

P	***dstpk61 mutant*** **(dPDK1(1, 5 or 5ex))** / ***TM6B (Tb, e)***	x	***P[w⁺]*** **(R17-R38)** / ***TM3 (Sb, e)***	
F1	***dstpk61⁻*** / ***P[w⁺]***	; ***dstpk61⁻*** / ***TM3, Sb, e***	; ***P[w⁺]*** / ***TM6B, Tb, e***	; ***TM3, Sb, e*** / ***TM6B, Tb, e***
	Heteroallelic mutant **Viable?**	Heterozygous Stubble (Sb) **Viable**	Heterozygous Tubby (Tb) **Viable**	Heterozygous balancer Sb,Tb, e **Viable**

Figure 3.3.1: Complementation cross
Flies mutant for *dstpk61* (lines dPDK1(1), dPDK1(5) or dPDK1(5ex)) are crossed with the red-eyed P-element insertion lines R17, R28, R29, R38. The heterozygous balanced progeny are viable and can be distinguished by the presence of a marker on the balancer chromosome (*Sb* or *Tb*). Similarly, the progeny containing two balancer chromosomes has both *Sb* and *Tb* markers as well as *ebony (e)* which makes the fly body darker. If the red-eyed lines are *dstpk61* mutants the heteroallelic mutant progeny will die (non-complementation) – or at least the male progeny, since the red-eyed lines are homozygous male lethal. If the red-eyed lines disrupt a different function than the dPDK1 mutant lines complementation will occur and the heteroallelic mutants will be viable (wild-type phenotype).

Cross ♀ x ♂	dPDK1/ TM3		dPDK1/ P[w+]		P[w+]/ TM6		TM3/ TM6		Total progeny
	M	F	M	F	M	F	M	F	
R17 x dPDK1(1)	7	10	10	22	14	4	1	8	76
dPDK1(1) x R17 heterozygous	4	16	11	12	13	19	7	9	91
dPDK1(1) x R17 homozygous	n/a	n/a	44	37	35	22	n/a	n/a	139
R17 x dPDK1(5ex)	11	9	8	14	13	18	12	5	90
dPDK1(5) x R17	10	13	40	42	26	35	6	3	178
R28 x dPDK1(1) homozygous	n/a	n/a	3	2	20	16	n/a	n/a	41
dPDK1(1) x R28	23	14	30	27	18	18	10	11	151
R28 x dPDK1(5ex)	9	5	21	12	4	15	5	5	76
R28 x dPDK1(5)	16	24	21	31	13	8	6	12	130
dPDK1(5) x R28	9	3	5	7	6	3	9	4	46
R29 x dPDK1(1)	0	0	2	4	1	6	1	0	14
dPDK1(5) x R29 homozygous	Failed- no progeny								
dPDK1(1) x R38	26	34	28	29	8	6	9	9	149
dPDK1(5) x R38	25	28	31	36	17	14	11	15	177

Table 3.3.1: Results of complementation crosses
The red-eyed fly lines complement the different *dstpk61* mutant lines in all successfully completed crosses. The genotype of progeny that should be lethal had the two mutations been disrupting the same function is shown in the grey shaded column. Both male (M) and female (F) heteroallelic mutants are viable. In the case of non-complementation this genotype should be second instar larval lethal (at least for males).

	dPDK1(1)	dPDK1(5)	dPDK1(5ex)	R17	R28	R29	R38
dPDK1(1)	-	-		+	+	+	+
dPDK1(5)	-	-		+	+	failed	+
dPDK1(5ex)			-		+		
R17	+	+		-	+	+	-
R28	+	+	+	+	-	-	-
R29	+	failed		+	-	-	-
R38	+	+		-	-	-	-

Table 3.3.2: Complementation analysis of *dstpk61* mutants and potential mutants
The results of the current complementation analysis are combined with data from (Rintelen et al,2001) and (Fonfara, 2000) to summarise what is known about *dstpk61* mutants. The red-eyed lines, each one representing a complementation group, can all complement the two characterised *dstpk61* mutants dPDK1(1) and dPDK1(5). Note that line dPDK1(5ex) is the same as dPDK1(5) but cleaned from a background mutation.

All crosses produce viable (*dstpk61* mutation)/P(Red-eyed fly line) male and female progeny, thus complementation does occur and the red-eyed fly lines disrupt a different function from the three *dstpk61* mutants. This is consistent with the mapping data (section 3.2).

3.4. Effect of dstpk61 on organism size

My inverse PCR and complementation cross approaches showed that we did not have any *dstpk61* mutants; however we did have sets of transgenic flies to investigate function by mis-expression. These were used in the beginning of this study to investigate whether *dstpk61* mis-expression had any effect on the size of the flies (since mutations or mis-expression of other components of the insulin/IGF signalling

pathway had been shown previously to affect organism size- Leevers et al, 1996; Bohni et al, 1999; Brogiolo et al, 2001; Stocker et al, 2002).

Fly lines which express sense and antisense sequences of one of the *dstpk61* cDNAs ($cDNA^A$) had been created in the laboratory (Clyde, 1999). The DNA was subcloned in a plasmid (pCaSpeR, which also contains a marker for red eye colour) under the control of the *Drosophila* Heat Shock promoter. Thus, expression of the cloned fragment can be induced by heatshock. The gene is ectopically over-expressed in the sense transgenic fly lines whereas it is "knocked-out" or knocked down in antisense fly lines. To investigate the effect of the overexpressed or the knocked-out gene in the phenotype of the adult fly when the gene was expressed in different developmental stages, I used the experimental layout described below.

3.4.1. Heatshock-induced *dstpk61* mis-expression does not affect whole organism size significantly

The experimental design is presented in Figure 3.4.1. On day 1 (t=0) the parental generation of each fly line was placed in a fresh vial. The flies were allowed to lay eggs in this vial for 24 hours before being transferred to a new vial. On the eleventh day, after the parents were transferred to a new vial, all vials (t=0 – t=10) were heatshocked in an incubator twice at 39°C for 45 minutes each time, with a 30 minute interval between the heatshocks for the flies to recover at the temperature at which they grow. In this way, the flies in vial t=0 are pupae ready to eclose while the flies in the last vial are freshly laid eggs when they are subject to heatshock and $cDNA^A$ is either overexpressed or its expression is reduced in them. In all vials in between, there are flies in different stages of development (eggs, embryos, larvae, pupae, adult flies). After heatshock, flies in all vials were allowed to eclose, they were transferred to a different vial for 2-3 days to mature and then their phenotype was checked. The wings, legs, abdomens and overall external phenotype were checked, as well as the gonads. The size (body length) of 20 male and 20 female flies from each vial was measured from the base of the antennae to the end of the

abdomen. In each case, *OrR* wild type flies were used as a control and were subject to exactly the same treatment as the mis-expression fly lines. One of the traits of sexual dimorphism in *Drosophila* is that male flies are normally smaller than females. By separating male and female flies for the measurements I would be able to see the relative change between male and female size in mis-expression lines compared to the controls as well as any actual size (length) changes between mis-expression and control flies.

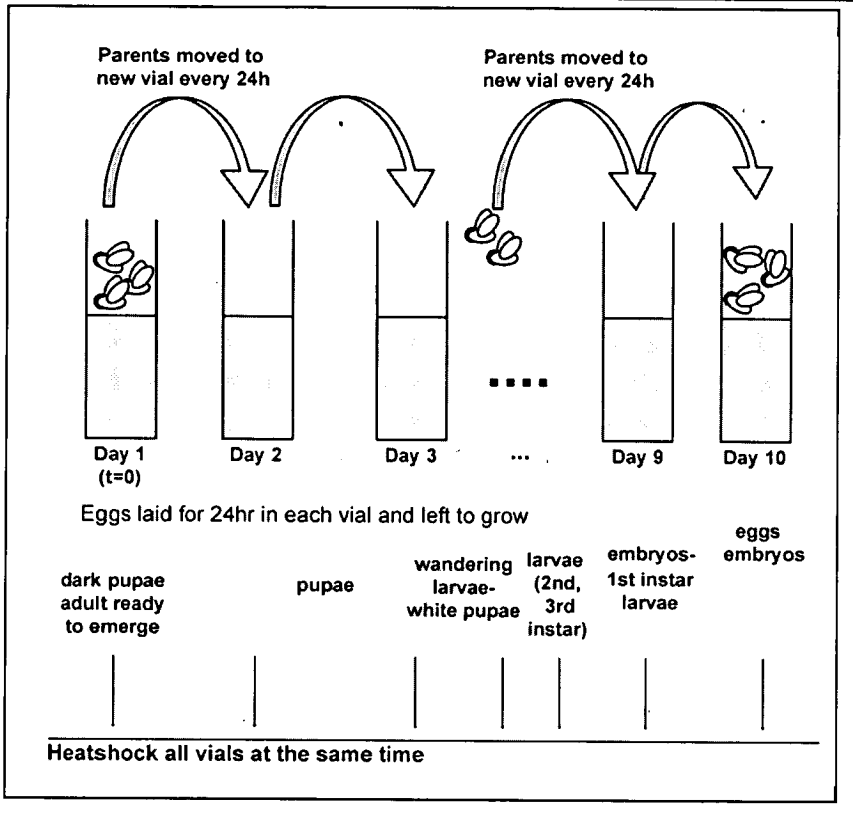

Figure 3.4.1 Diagram of experimental set-up
The parents for each mis-expression fly line tested were left in a vial with fresh food to lay eggs for 24hr. Then the parents were moved to a new vial and allowed to lay eggs for 24hr –this was repeated for 10 days. All vials were kept at 25°C- batch A- (or 18°C – batch B- with times altered accordingly) and were all heatshocked simultaneously on day 11. In this way all developmental stages from laid egg to dark pupa were heatshocked. The vials were left at 25°C (or 18°C) until the progeny emerged- the phenotype of these F1 flies was checked and their body size was measured.

There were two batches of fly lines tested, the first one (A) growing at 25°C following the described procedure and the second one (B) growing at 18°C. For the flies growing at 18°C (batch B) the protocol was slightly altered in that parents were

transferred to a new vial every 2 days approximately and the heatshock was done on the 16th day, after some F1 flies started to eclose. On the charts therefore (Figure 3.4.2) , time expressed as 1 to 9, refers to units of time which represent days 1, 3, 5, 7, 9, 11, 13, 15 and 16 from the beginning of the experiment, respectively. Sense fly lines HS/S CR29, CR30, CR40, CR41, CR44 in batch A and CR36 and CR39 in batch B, as well as antisense lines HS/AS CR4, CR6, CR18, CR23 in batch A and CR1 and CR25 in batch B were tested. The first time (batch A) the experiment started with 40 parent flies in each vial (30 female and 10 male flies). This number proved to be too high as it resulted in progeny that numbered hundreds of flies in some cases, making it difficult to distinguish whether the small flies observed were the result of mis-expression of *Dstpk61* or they were due to nutritional shortage since there were far too many flies in a vial. When the experiment was repeated (batch B) with four new fly lines, 20 flies (15 females and 5 males) were used as parents and the situation of over crowding of progeny in the vials was very much improved. In all cases the flies were completely fertile.

Even with the new experimental conditions for batch B, the results do not provide sufficient evidence to support a relationship between organism size and mis-expression of *dstpk61*. As shown in figure 3.4.2, the size of the heatshocked flies is similar to that of the control flies. Furthermore, the size of males and females does not overlap in any case and even in the cases where there seems to be a dynamic pattern of organism size in relation to developmental stage at which the gene was expressed under heatshock (i.e. a peak in female fly size at relative time 4 for CR36 and CR1 fly lines), almost the same pattern occurs in the wild type flies, so this pattern is not significant. In the antisense fly line CR25, heat-shocked male flies are bigger than the non-heatshocked control CR25 flies; for CR25 females this applies to flies that were early larvae (t = 6-8) or dark pupae (t = 1-2) when heatshocked. In the sense fly line CR36 it is essentially female flies that exhibit an increase of body size upon heatshock, rather than the males. In the sense line CR39 only female flies of certain vials (dark pupae – t=1, 2 and larvae in their wandering phase- t=4 when they were heatshocked) are significantly bigger than the non-heatshocked control flies. However, there is not enough evidence to allow a correlation between increased body

size and a specific developmental stage at which DSTPK61 was overexpressed (or knocked-down in CR25) to be made. Cho et al, 2001 and Rintelen et al, 2001 observed that overexpression of dPDK1 in the eye and in the head, using the Gal4-UAS ectopic expression system, leads to increased cell and organ size. It is not possible though to suggest that overexpression of DSTPK61 induced by heatshock in this experiment, increases body size, because white eyed flies which do not contain the extra *Dstpk61* sense or antisense gene also have bigger bodies when heatshocked, especially female flies, in comparison to a non-heatshock control.

Figure 3.4.3 shows some of the results obtained from batch A of mis-expression fly lines studied. The body size of adult flies of a sense (Fig. 3.4.3A) and an antisense (Fig. 3.4.3B) line are shown. The very wide variability in female control flies of line CR18 must have been caused by environmental factors, since it was not observed again in eight independent measurements (results not shown). This particular fly line can have a marginal difference in size between the bigger males and the smaller females. Also in this batch (A) abnormalities in the abdominal cuticle were observed (figure 3.4.3C- these flies were fully viable and fertile), in contrast with batch B. As abnormalities I listed deviations from the wild-type pattern of parallel abdominal segment plates when viewed dorsally. These included shorter segments (not spanning the whole width of the abdomen) and fused segments to various degrees. It is not certain whether this is connected to over-expression of *Dstpk61*. At the time I did not observe this phenotype in the control flies (HS or non-HS *OrR*) but later I would see fused abdominal segments in adult flies of various stocks, including the wild-type, at percentages from 0.1- 1%.

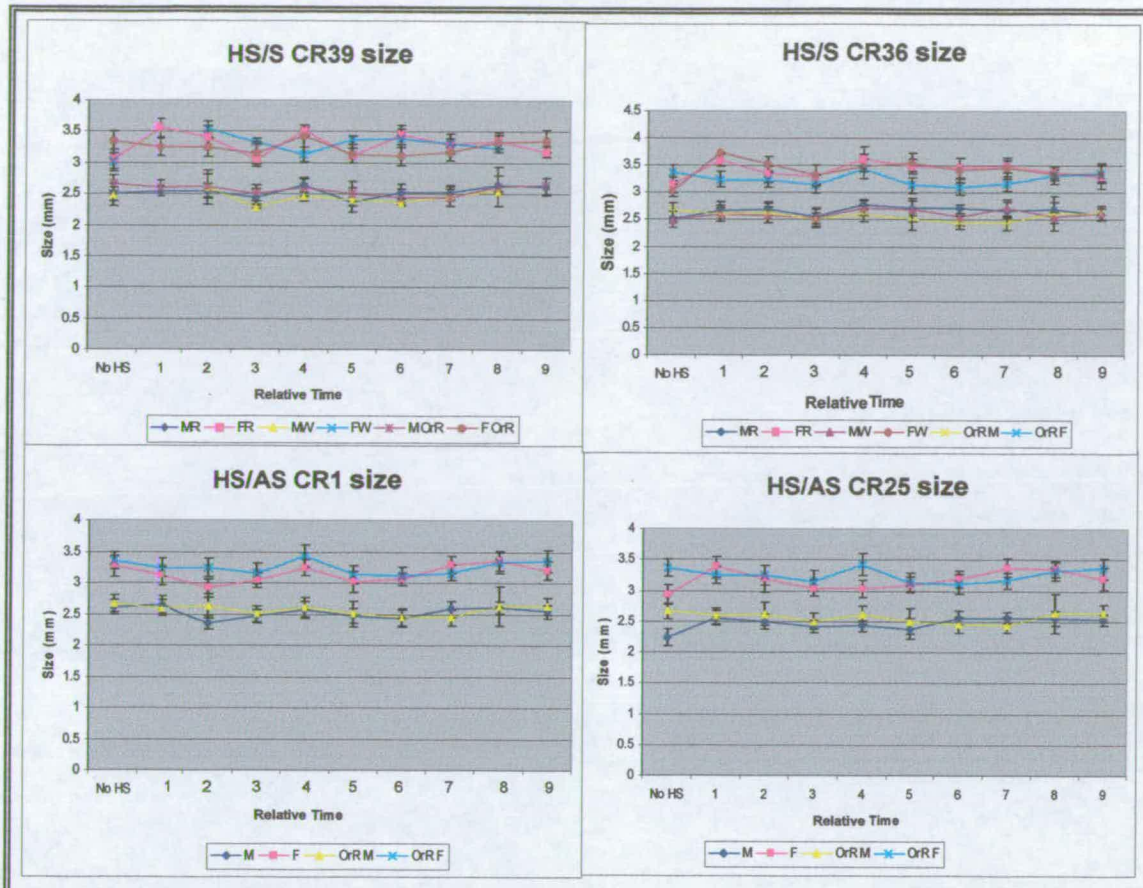

Figure 3.4.2: Batch B, grown at 18°C

Body size of adult flies of batch B in relation to the developmental stage during which expression of *dstpk61* was induced by heat shock (time units 1-9, see text). HS/S indicates sense lines, in which the gene is overexpressed whereas HS/AS indicates antisense lines where the gene is knocked down. In the chart legends, M or MR=male and F or FR=female flies with red eyes (thus containing the heatshock-inducible gene); MW and FW are male and female flies respectively with white eyes, which do not contain the gene and can be used as a control; OrR M and OrR F are male and female wild-type flies (Oregon R) which serve as an negative control. No HS is the average size of flies from the stock, which were not heat shocked and do not mis-express *dstpk61*. Y axis shows the actual body size in millimetres and the values are the average of all measurements. The standard deviation for each value is also shown.

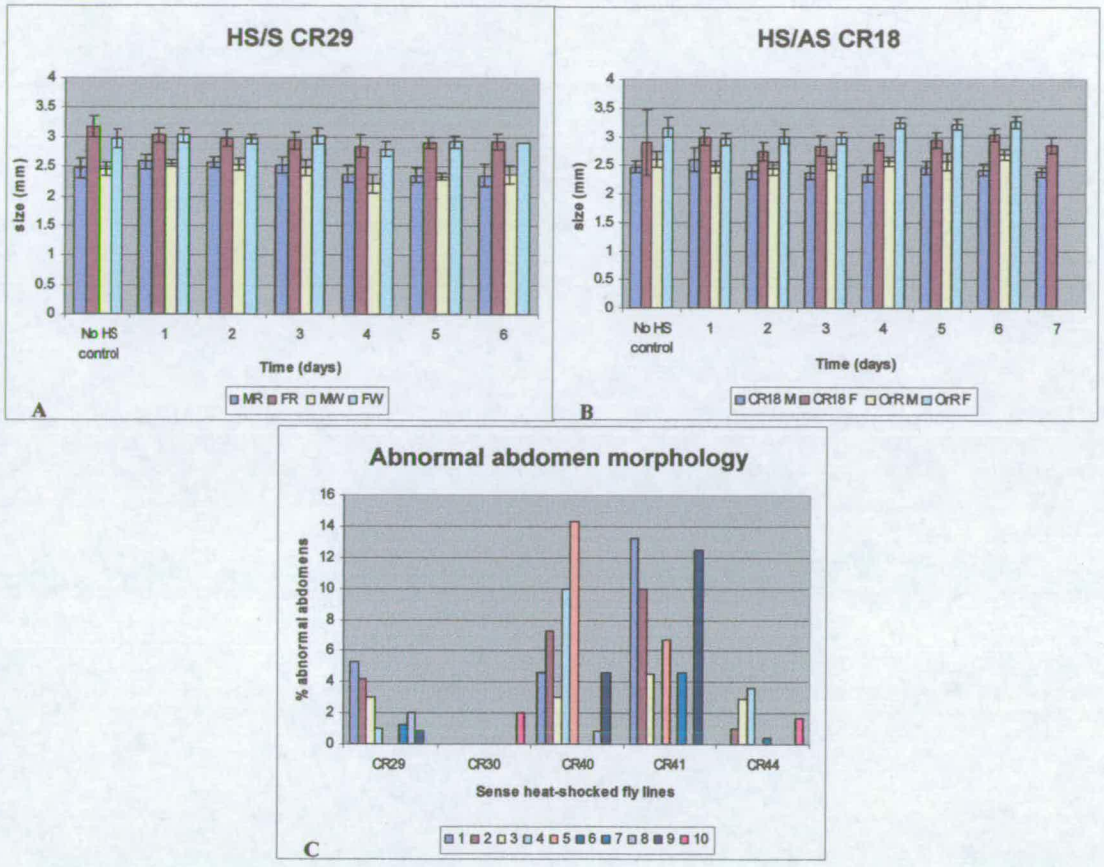

Figure 3.4.3: Batch A, grown at 25°C
(A, B): Body size of a sense (A) and an antisense (B) mis-expression line from batch A. On the X axis time is in days from the beginning of the experiment. No HS control are flies from the original stock. MR, FR = male and female flies with red eyes, MW, FW = flies with white eyes. In (A) white eyed CR29 flies are used as the control whereas in (B) the control is wild type Oregon R flies (OrR Male and Female). (C): Percentage of flies with abnormally formed abdomens for the sense lines of the first study group. Different colours indicate time as coded in the legend (as days from the beginning of the experiment).

Overall body size is a character dependent upon many factors, including nutritional shortage (Clancy et al, 2002) which may be a consequence of increased population size, therefore I could not draw any final conclusions from batch A of experiments on the possible effects of *dstpk61* mis-expression on body size. The fact that many factors contribute to size determination is demonstrated by the observation that flies with white eyes have variant size in different fly lines and at different times of heatshock (results not shown). As white-eyed flies do not contain the extra *dstpk61* sense or antisense gene, any effect on their size would be related to the different genetic background. Since all the lines were induced in the same genetic background,

the latter should not contribute to the effect. The white eyed flies are identical in all respects, genetic and environmental, and they lack the P-insertion which differentiates the red-eyed flies into individual lines.

3.4.2. Mis-expression of *dstpk61* is induced by heatshock treatment

To confirm that *dstpk61* is indeed overexpressed or "knocked-out" in the heatshock sense and antisense misexpression lines used in the experiment above, Northern blot analysis was used.

Total RNA was isolated from *OrR* (wild-type), two of the tested heatshock sense fly lines (HS/S CR39 and HS/S CR41) and two of the antisense lines (HS/AS CR4 and HS/AS CR25). One sense and one antisense line from each batch of the "organism size measurement" experiment were thus included. RNA was isolated both from non-heatshocked flies as a control and from flies heatshocked twice for 45 minutes at 39°C, with a 30-minute interval at 25°C in between the heatshocks. This should activate expression of the sense or antisense construct for *dstpk61* in these fly lines. The isolation was done 45 minutes after the last heatshock, so that I would be able to detect the (presumably transient) RNA changes following the heatshock treatment. The concentration of the RNA samples was measured by spectrometry and 25μg RNA from each sample was run on a gel and transferred to a nylon membrane. Double-stranded cDNA^{A} (common for all *dstpk61* isoforms) and rp49 (negative control) probes were labelled with ^{32}P and used to hybridise to the membrane; the results were visualised by autoradiography (Fig. 3.4.4).

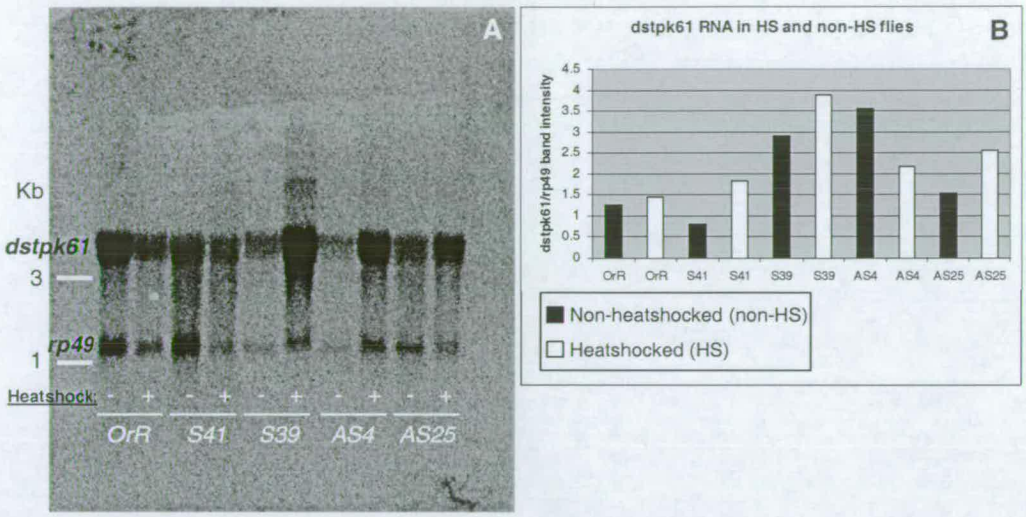

Figure 3.4.4. Northern blot on sense and antisense *dstpk61* fly lines
A: Nylon membrane with *dstpk61* and *rp49* (loading control) RNA as indicated. RNA from non-heatshocked (-) and heatshocked (+) wild-type *OrR*, *dstpk61* sense (*S41, S39*) and antisense (*AS4, AS25*) fly lines was used. The *rp49* bands do not have the same intensity between samples, indicating uneven loading.
B: Results from (A) normalised for *rp49*. Average band intensity for each *dstpk61* and *rp49* band and their respective backgrounds was measured using the ImageQuant TL software (Amersham Biosciences). Background values were subtracted from the samples and *dstpk61* band intensities were divided by the equivalent *rp49* band intensity, to remove any effect of uneven sample loading. Heatshock does not increase significantly *dstpk61* expression in *OrR*, but it does so for the two sense lines tested (*S41, S39*) and one of the antisense lines (*AS25*).

For three of the four *dstpk61* mis-expression lines tested (sense lines HS/S CR39, HS/S CR41 and antisense line HS/AS CR25) heatshock induced expression of the relevant construct, in contrast to the *OrR* wild-type control where heatshock does not seem to have any significant effect on *dstpk61* expression. For antisense fly line HS/AS CR4, after normalisation of the values with *rp49* to correct for uneven loading, there seems to be a decrease of *dstpk61* expression rather than an increase after heatshock. This may be reflect the fact that in this particular line *dstpk61* mis-expression is not induced by heatshock – a variability between different lines generated to contain a certain DNA construct is to be expected- or to be caused by the limitations of the normalisation method. It is also possible that the optimum time to look at RNA expression varies between different fly lines. Other possibilities would be that the chromosomal position of the insertion affects the levels of expression of a given construct or that some insertions are expressed in some tissues

and not in others. When the membrane hybridised with *dstpk61* and *rp49* probes was re-exposed for a different length of time, antisense line *AS4* (or HS/AS CR4) showed a slight increase of RNA expression instead of a decrease, the results for *OrR* and *AS25* were the same, *S41* showed an even higher increase of expression after heatshock and *S39* showed a slight decrease (results not shown). The difference could be attributed to saturation effects, but nonetheless it demonstrates that many factors affect the result after the normalisation procedure, including duration of exposure, amount of radioactivity and strength of background signal, which may mask signal or artificially enhance it.

3.5. Discussion

In this chapter the work related to *dstpk61* mutant and mis-expression fly lines is described. In order to characterise fully and subsequently use the *dstpk61* potential mutant fly lines generated previously in the lab, two approaches were used. Complementation crosses with known *dstpk61* mutants (a P-element insertion – dPDK1(1) or a point mutation in the kinase domain – dPDK1(5ex), dPDK1(5)) generated by other labs (Cho et al, 2001; Rintelen et al, 2001) demonstrated that our potential *dstpk61* mutants generated by P-hopping do not disrupt the same function as these mutants, since all heteroallelic progeny of the crosses are viable, meaning that complementation does occur (Tables 3.3.1 and 3.3.2). Therefore the homozygous male-sterile phenotype observed in the red-eyed potential *dstpk61* mutants must be caused by a background mutation, presumably the same for all red-eyed fly lines, located at position 86E and possibly disrupting gene PGRP-LB, according to my data from inverse PCR analysis.

Further evidence for this was provided by the second approach, inverse PCR, which was used to map the positions of the P-elements in the red-eyed potential *dstpk61* mutant fly lines. Even though sequencing was difficult, it revealed that in two independent fly lines, R28 and R38, the only P-element present (or at least the only one with the w^+ and the 3'end –part of the P-element not excised) is located very far

away from the *dstpk61* locus, at the other arm of the 3rd chromosome, at position 86E. In addition, inverse PCR on fly line 833/11, the line used to generate the mutants by P-element mobilisation, has three P-elements, one of which, the one that generates a DNA fragment running at the same position as the high MW band of the red-eyed lines, also maps at position 86E (Fig. 3.2.2). Therefore, it is reasonable to suggest that fly lines R17 and R29 (high MW band) for which sequencing failed, have the same P-element insertion at position 86E, since they generate a band that runs at the same MW as the one sequenced in fly lines R28, R38 and 833/11. The second P-element insertion of R29 maps at position 33E on the 2nd chromosome, again far away from *dstpk61*.

Given that the homozygous male-sterile red-eyed fly lines are not *dstpk61* mutants I decided to use different approaches to study the role of *dstpk61*, as described in the following chapters, and utilise the existing *dstpk61* mutants if necessary. I did not continue with the planned complementation crosses between the white-eyed P-element excision fly lines (W1 and W4 complementation groups) and the known *dstpk61* mutants or line 833/11, because knowing that the white-eyed fly lines have deletions (caused by excision of the P-elements) that cover the positions of the red-eyed fly lines (Fonfara, 2000) and that the red-eyed lines have their P-elements at distant positions to *dstpk61* means that the white-eyed lines are also far away from the *dstpk61* gene locus and thus they are not of interest for further study.

The study of the mis-expression heat shock inducible fly lines, used to investigate the effect of overexpression or "knock-out" of *dstpk61*, does not provide a clear enough picture. The present experimental design can probably be altered so that in each vial to be heat-shocked there are manually staged flies at different developmental stages, i.e. 3rd instar larvae, white pupae, dark pupae; thus the results may be more clear as the developmental stages heatshocked would be more clearly synchronised. Alternatively, it might be possible to see changes due to *dstpk61* mis-expression better by looking at wing length rather than the overall body size, or the GAL4-UAS system could be utilised for over-expression in specific tissues. Time limitations prevented further experimentation along these lines. GAL4-UAS sense and antisense

fly lines for cDNA^{A} are available in the laboratory and they could be used to test for sex-specific effects of *Dstpk61* mis-expression. For example, it would be interesting to see what happens if the gene is overexpressed in female larval gonads where it is normally not expressed. It would also be interesting to check if overgrowth occurs when this or one of the other isoforms is overexpressed in the wing blade or the eye.

The control Northern blot hybridisation was performed in order to confirm that the heatshock treatment used to induce overexpression of the sense *dstpk61* fly lines and *dstpk61* "knock-down" in the antisense lines, by overexpression of antisense RNA, actually does so. To keep the experiment in a manageable scale and due to time limitation, two sense and two antisense fly lines, one each from the two batches of fly lines, were used along with wild-type *OrR* control. Since the *dstpk61* radio-labelled probe used in the hybridisation was double-stranded DNA I would expect *dstpk61* upregulation in heatshocked (HS) flies compared to non-heatshocked (non-HS), both for sense and antisense lines, as they would hybridise with the antisense- and sense-radiolabelled probe, respectively. In wild-type *OrR* flies there should not be a difference in expression between HS and non-HS.

As described above, the result is as expected unequivocally at least for some of the fly lines tested, namely *OrR*, sense line *S41* and antisense line *AS25* (Fig. 3.4.4). Sense line *S39* shows significant upregulation upon heatshock (Fig. 3.4.4) but a repeat exposure showed a slight decrease upon HS (not shown), so these results should be treated with caution. Similarly, in Fig 3.4.4 antisense line *AS4* appears not to be upregulated upon HS, rather the opposite happens, but in the repeat of membrane exposure it is indeed upregulated. These observations suggest that i) it is not completely safe to assume that all mis-expression lines behave in the same way with respect to heatshock induction or that induction occurs at the same levels or at the same time for all, ii) an error can occur in several stages of the analysis of the results: Based on spectrometric estimation of RNA concentration of each sample, a supposedly equal amount of RNA was loaded per sample. This was obviously not correct since the picture of the RNA gel showed differences between samples (results not shown). This is why a loading control (*rp49* in this case) was necessary.

Furthermore, in the final picture after hybridisation with the radioactively labelled *dstpk61* and *rp49* probes, curiously enough not the same lanes that were previously under-loaded appear with lower signal now, presumably due to saturation of the signal in some of the bands. Only the earliest exposure –the clearest and not saturated- of the successful repeat of the experiment was used for band intensity measurements and normalisation of the *dstpk61* values to compensate for differences in *rp49* expression (it is assumed that *rp49* should be expressed at equal levels in all samples, HS and non-HS). Based on these facts one should be cautious regarding the interpretation of these data.

Nonetheless, even for the two fly lines that repeatedly show activation of the *dstpk61* construct, a trend in the overall organism size (body length) as a function of the developmental stage of the organism is not apparent and the results are clearly affected by exogenous factors, including environmental parameters such as overcrowding and the resulting nutritional shortage. If a different type of measurement were to be used, such as looking at an appropriate tissue or time, rather than the whole fly size, it should be accompanied by controls for every fly line used and in enough repeats to provide a clear result (confirming upregulation or otherwise) beyond any doubt. A suitable control experiment could be a Northern blot experiment similar to the one employed here, ideally with single-stranded RNA probes to recognise specifically the sense or antisense RNA from the construct. A Western blot, detecting the protein levels produced following sense and antisense RNA expression is a useful approach, although for DSTPK61 we are limited by the absence of a suitable specific antibody (Chapter 6, anti-DSTPK61. The new anti-E40 antibody would not be useful here since it is raised against a sequence not present in cDNA^{A}) The timing of when the RNA is highly expressed in the cell is also important and should probably be determined for each fly line tested, to ensure detection. That is because, even though a burst of antisense or sense RNA will possibly have long term developmental effects affecting final phenotypes, the RNA levels themselves would not be expected to be different for very long and certainly not inherited through subsequent cell division and differentiation.

Chapter 4: The Bioinformatics approach

4.1 Introduction

A different approach I used, complementary to experimental data such as RT-PCR and *in situ* hybridisation, was to analyse data regarding *dstpk61* generated by microarrays undertaken by Dr B. Oliver and Dr J. Terashima. Two sets of data from different microarray experiments were made available to me for further analysis.

The principle of DNA microarrays is hybridisation (base pairing) of the sample (the nucleic acid in solution, derived from the tissue of choice) to the "elements", or fixed nucleic acids to the microarray plate (Gupta and Oliver, 2003). The sample is usually cDNA or mRNA labelled with Cy3/Cy5 fluorescent dyes or with radioactive isotopes; the elements on the microarray can be cDNA clones, short (as in Affymetrix Gene Chips) or long oligonucleotides or genomic DNA represented by PCR amplicons. Microarray platforms can be designed to maximise *Drosophila* (or other species) genome coverage and hybridisation specificity or to bias for particular transcript sets, regions of the genome, tissues or developmental stages, according to the experimental design (Gupta and Oliver, 2003; Parisi et al., 2004).

The first data set was from a microarray screen aimed at analysis of transcription differences between the sexes and identification of sex-biased gene expression and further study of where these genes map, their predicted function and the tissues in which they are expressed. This array analysis was undertaken by Brian Oliver and co-workers, LCDB, NIH, USA (Parisi et al., 2004). I investigated whether there was differential expression of *dstpk61* between whole males and females, male and female carcasses (bodies after the removal of the gonads) and between ovaries and testes.

The second set of data was obtained from Dr Jun Terashima in our laboratory. He used a microarray approach to identify genes in the *Drosophila* ovary that show varied expression when comparing apoptotic and non-apoptotic conditions (represented by different nutritional treatments or hormonal treatments or a combination of the two) (Terashima and Bownes, 2005). Here I looked at how the expression of *dstpk61* may be affected by conditions promoting or preventing apoptosis in the ovary.

I have also regularly checked the EST (expressed sequence tags) database by similarity searches with the *Drosophila* genome (blastn, on the NCBI website, http://www.ncbi.nlm.nih.gov/blast/) (Altschul et al., 1997) and the Flybase website (http://www.flybase.bio.indiana.edu) for newly available *dstpk61* transcripts (Fig.1.1.3 shows what was known in the beginning of this study-2002). Based on their sequence and the sequence of the genomic DNA in the *dstpk61* locus I classified the transcripts according to their splicing pattern and the tissue in which they are present, following the classification introduced by Clyde and Bownes (2000). A full list of the currently available *dstpk61* transcripts is presented in Figure 4.1.1 (based on Clyde and Bownes, 2000, updated -2005- and corrected).

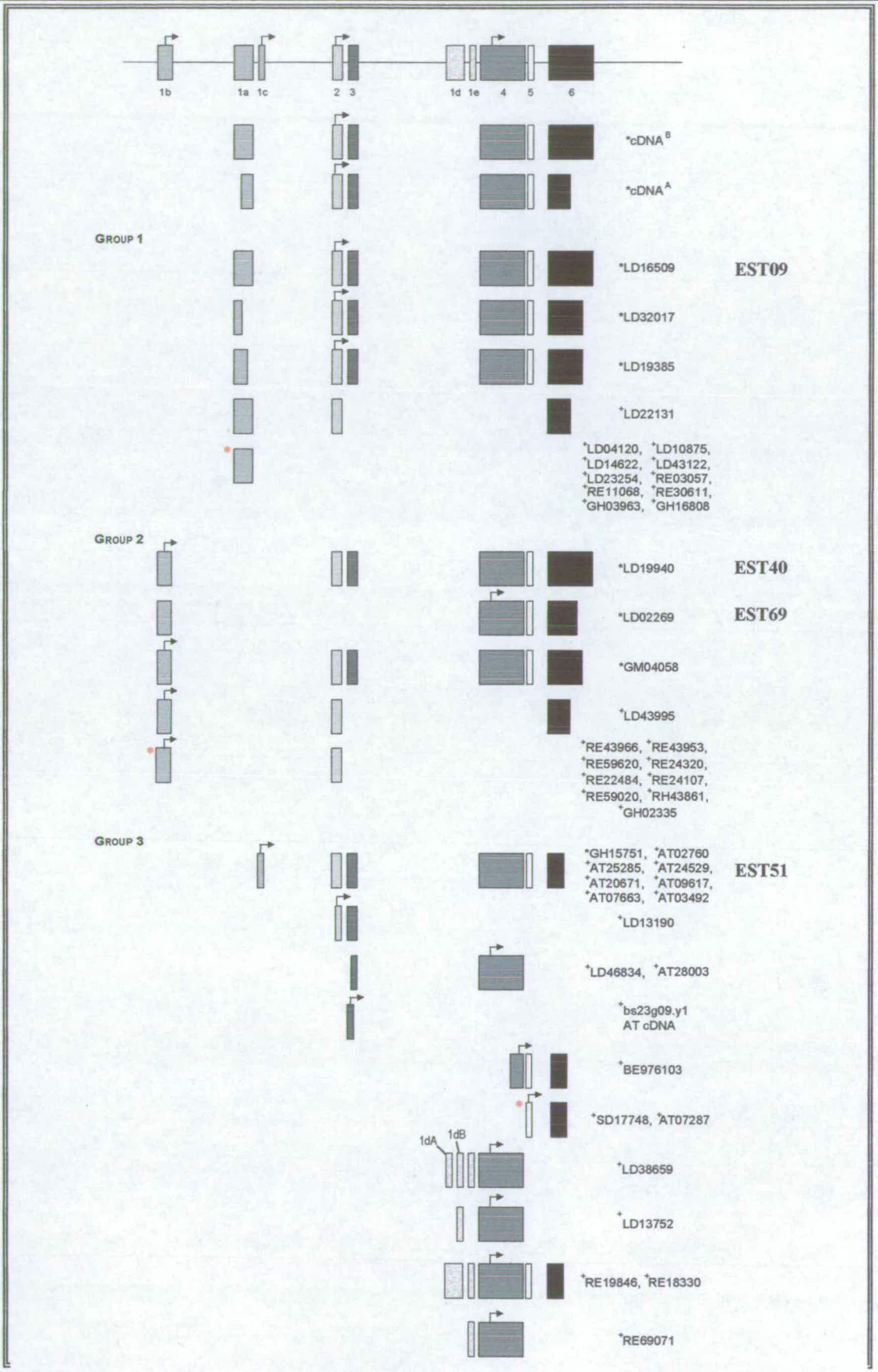
1b
1a 1c
2 3
1d 1e 4 5 6
*cDNA B
*cDNA A
GROUP 1
*LD16509
EST09
*LD32017
*LD19385
+LD22131
+LD04120, +LD10875, +LD14622, +LD43122, +LD23254, +RE03057, +RE11068, +RE30611, +GH03963, +GH16808
GROUP 2
*LD19940
EST40
*LD02269
EST69
*GM04058
+LD43995
+RE43966, +RE43953, +RE59620, +RE24320, +RE22484, +RE24107, +RE59020, +RH43861, +GH02335
GROUP 3
*GH15751, +AT02760, +AT25285, +AT24529, +AT20671, +AT09617, +AT07663, +AT03492
EST51
+LD13190
+LD46834, +AT28003
+bs23g09.y1 AT cDNA
+BE976103
+SD17748, +AT07287
1dA
1dB
+LD38659
+LD13752
+RE19846, +RE18330
+RE69071

Figure 4.1.1: *dstpk61* gene locus and transcripts
The exon structure of the three groups of *dstpk61* transcripts and of the *Dstpk61* gene locus. The numbers 1-6 correspond to the *dstpk61* exons. On the right, EST09, EST40, EST69 and EST51 indicate the transcripts that encode the respective protein isoforms. Group 1 contains all transcripts that have exon 1a, Group 2 the ones that have exon 1b and Group 3 the *dstpk61* transcripts that have exon 1c and all other combinations of alternative splicing not included in the first two groups. cDNAs marked * have been fully sequenced while the sequence of those marked + is incomplete sequence taken from the EST database The bent arrow (➦) indicates potential translational start sites. LD, RE = embryonic libraries, GH=adult head library, GM= ovary library, AT, BE = adult testes libraries. The red asterisk indicates that each of the different ESTs has exons with slightly variant 5' and 3' ends. (corrected and updated from Clyde and Bownes, 2000)

4.2 Differential spatial expression of dstpk61

4.2.1 Six *dstpk61* "elements" are present on the FlyGEM array platform

Parisi et al (2004) used pairs of mRNA samples (ovaries versus testes, females versus males, etc.) labelled with Cy3 or Cy5 fluorochromes, applied them to Incyte Fly Gene Expression Microarrays (FlyGEM) and analysed the extracted Cy3 and Cy5 values. For each experimental condition (pair of mRNAs) there was at least one biological replicate and for most also a dye reversal replicate (Parisi et al., 2004). Dye reversals, the labelling of Sample A with Cy5 and Sample B with Cy3, if originally Sample A was labelled with Cy3 and Sample B with Cy5, are a useful way of minimising errors due to bias introduced by dye incorporation (Gupta and Oliver, 2003). The FlyGEM microarray platform is a *Drosophila* transcriptome amplicon array containing 75% of the release 3.1 *Drosophila* genome predicted genes. Genomic DNA fragments were amplified by PCR with exon-specific primers so that most elements on the microarray monitor expression of only one fragment, in addition to the wide coverage of the genome (Johnston et al., 2004). All the array data is deposited at GEO, the Gene Expression Omnibus website (http://www.ncbi.nlm.nih.gov/geo) under accession number GPL20 (Parisi et al., 2004).

I was sent raw data and, later, a corrected version with natural log transformed data from three experimental datasets: whole females (F) versus males (M), female carcasses (FC) versus male carcasses (MC) and ovaries (ov) versus testes (te) for all elements of the array that correspond to *dstpk61*. Each data point was replicated in

each hybridisation and the experiments were done with a biological replicate and a dye reversal (M. Parisi, personal communication). Table 4.2.1 shows the resulting ratios of expression for each element (under "gene name") between each pair of samples after my analysis. The data points for each transcript hybridised with each sample were averaged, the Ln (natural logarithm) ratio of expression for each pair of samples was calculated (base =0) and these ratios were transformed back to natural numbers with base = 1. This means that a ratio of 1 in the male versus female comparison, for example, denotes no differential expression between the two samples. Only ratios higher than 1.5 were taken into account as evidence of significant differential expression, since for $P < 0.05$ measurements on the FlyGEM must be $\geq$ 1.5-fold (Parisi et al., 2004). For higher stringency a 2-fold criterion can be used (ratio > 2.0). The elements (transcripts) for which there is statistically significant differential expression are highlighted with grey on Table 4.2.1.

	Inverse LN ratio					
Gene name	**M Vs F**	**F Vs M**	**MC Vs FC**	**FC Vs MC**	**te Vs ov**	**ov Vs te**
CT42507	1.014726	0.9854882	0.930595	1.074582	0.527285	1.896509
CT42509	1.036036	0.9652176	1.099081	0.909851	0.822794	1.215371
CT42511	1.119634	0.8931486	0.888297	1.12575	1.579399	0.633152
CT42513	1.425101	0.7017047	1.012923	0.987241	2.009662	0.497596
CT1275	1.596856	0.6262307	0.941898	1.061686	2.81211	0.355605
CT2222	0.717665	1.3934072	0.852163	1.173484	0.545618	1.832784

Table 4.2.1: Ratios of males/females, male carcasses/female carcasses, testes/ovaries and vice versa for *dstpk61* elements on the FlyGEM microarray

Gene name is the name by which the relevant transcript amplicon is referred to on the array (see also table 4.2.2). M = males, F = females, MC = male carcasses, FC = female carcasses, te = testes, ov = ovaries, LN = natural logarithm. Values ≥ 1.5 indicate significant differential expression (in favour of the numerator) and are highlighted in grey. For more details see text.

In order to identify which *dstpk61* transcripts the "gene names" represent I searched the array platform GPL20 on the GEO database (http://www.ncbi.nlm.nih.gov/geo) and obtained the sequence of the amplicons used as elements on the array. I then did a Blastn (http://www.ncbi.nlm.nih.gov/blast/) similarity search between them and the

Drosophila genome around the *dstpk61* gene locus to find their exact position and to which transcript they belong. These data are summarised in Table 4.2.2.

Gene name	Transcript (GadFly II release)	*Drosophila* genome position (at 3L 61)	Position in *Dstpk61* gene (exon map)	Probe would recognise transcript:
CT42507	LD32017 Group 1	124179-124433	intron between exons 5-6 and exon 6	all
CT42509	EST 09 (LD16509)	112545-113194	exon 1a and some of the downstream intron	EST09 (1a)
CT42511	LD13752 Group 3	122434-122688	exon 4 (beginning until approx. 250bp downstream)	all
CT42513	LD38659 Group 3	122434-122688	exon 4 (beginning until approx. 250bp downstream)	all-same probe as CT42511
CT1275	EST 51 (GH15751)	116122-116506	exon 2 (whole)	all but E69
CT2222	EST 40 (LD19940)	110138-110552	exon 1b	E40

Table 4.2.2: *dstpk61* transcripts present in the FlyGEM microarray
The names of the *dstpk61* transcripts (as presented in Table 4.1.1) that correspond to the elements (gene name, column 1) in the FlyGEM array platform are given in the second column. The third column shows the element sequence position (numbers refer to the genomic sequence of 3L chromosome, position 61) and the fourth column explains where in the *dstpk61* gene this probe (element) lies. In the fifth column I give a prediction of which transcripts could be recognised by each element, based on the position of the element in the *dstpk61* locus. "All" is restricted to all transcripts that contain the particular exon/sequence within a group.

4.2.2 There is at least a testes-enriched *dstpk61* transcript

As only ratios higher than 1.5 are taken as evidence of significant differential expression only six pair-wise measurements fulfil this description (highlighted in Table 4.2.1) and the information related to them is presented in Table 4.2.3. From these transcripts only EST51 (CT1275) appears to be highly enriched in testes, with a ratio value of 2.81 in the testes versus ovaries experiment (value above the high stringency threshold of 2.0). The rest of the values above the 1.5 threshold are not very high (below or at 2.0), therefore these results should be considered indicative of a possible tissue-enrichment due to the high probability of false positives, or they could suggest very low levels (even absence) of differential expression for the transcripts involved.

Gene name - transcript (unique exon)	Enriched in:	Ratio
CT42507- LD32017 (1a)	ovaries	1.896509 ov/te
CT42511- LD13752 (1dB)	testes	1.579399 te/ov
CT42513- LD38659 (1dA; 1dB)	testes	2.009662 te/ov
CT1275 - EST 51 (1c)	males, testes	1.596856 M/F 2.81211 te/ov
CT2222 - EST 40 (1b)	ovaries	1.832784 ov/te

Table 4.2.3: Tissue-enriched *dstpk61* transcripts
The transcripts that show differential expression above the threshold ratio value of 1.5, with the exon specific to each of them shown in parenthesis next to their name. The tissue in which they are enriched and the ratio of expression for the relevant mRNA pair are shown in the second and third column, respectively.

The data support the existence of at least one testes-enriched transcript and one slightly ovary-enriched transcript. The strongest indication is that EST51 is a testes-enriched transcript, even though the sequence used from CT1275 is in exon 2, so in theory the element on the array could hybridise with transcripts from groups 1 (E09) or 2 (E40). However, CT1275 is the E51-encoding transcript and no transcript belonging to other groups shows similar differential expression, so it is quite likely that EST51 will encode the testes-enriched protein isoform (supported by EST database recent additions – Figure 4.1.1- and RT-PCR data discussed in following chapters). The fact that the transcript is also male-enriched is probably due to transcription in testes since the male carcasses do not show differential expression when compared to the female carcasses. Two other Group 3 transcripts, LD13752 and LD38659 show enriched expression in testes compared to ovaries, even though at lower levels than EST51. These transcripts are different in that they contain combinations of some small exons (1dA, 1dB and 1e for LD38659-CT42513; 1dB for LD13752-CT42511) which are usually spliced out as part of the big intron between exons 2-3 (Fig. 4.1.1). The transcripts do not have any of the upstream exons 1b – 3 and the potential protein encoded would share the same coding sequence with E69, the truncated DSTPK61 protein isoform. Again, theoretically any *dstpk61* transcript could hybridise to the element of CT42511 and CT42513 since the sequence used for both is in exon 4 (common to all groups).

Two other elements, CT42507 -LD32017, a Group 1 transcript, and CT2222 – LD19940 (EST40), the principal Group 2 transcript show some ovary-enriched expression. Based on the fact that the sequence of the CT2222 element on the array is the Group 2 transcript- and E40 isoform- specific exon 1b whereas the sequence used from CT42507 is from a common region, exon 6 and the intron between exons 5-6 (Table 4.2.2), I would tend to put more emphasis on the female gonad-enrichment of EST40 and Group 2, than of Group 1. To support this exercise of caution, element CT42509 is the transcript encoding E09, the Group 1 isoform, and the sequence used in the array was from the group- specific exon 1a. The results show a slightly enriched transcription in the ovary, but with a value below the threshold, and no differential expression between male and female flies and carcasses.

4.3 Expression of dstpk61 under apoptotic and non-apoptotic conditions

Dr J. Terashima used a microarray approach to identify genes in the ovary involved in the developmental decision of whether an egg chamber will continue developing into a mature egg or die by apoptosis, under different nutritional conditions. RNA from ovaries of flies under different experimental conditions was labelled in pairs with Cy3 and Cy5 and hybridised to a chip carrying 5364 *Drosophila* genes (http://www.flychip.org.uk/ Project/Protocols). There were three combinations of apoptotic and non-apoptotic conditions: Starved (S) versus Fed (F) flies, Starved (S) versus Juvenile Hormone analogue-treated (JH) and 20-hydroxyecdysone-injected (20E) versus Fed (F) and three replicates for each combination. Starved flies were transferred to a diet of sugar and water after three days on standard medium whereas fed flies were transferred to a diet of yeast after three days on standard medium (Terashima and Bownes, 2005). Injection of 20-hydroxyecdysone into fed flies triggers apoptosis in egg chambers at stages 8 and 9 of oogenesis, as does starvation. Conversely, application of Juvenile Hormone to starved flies restores the non-apoptotic phenotype and therefore permits development of the egg chamber as in fed flies. A control point or checkpoint is believed to exist at stage 8/9 of oogenesis

when the decision to either undergo apoptosis or continue to develop is made for individual egg chambers (Terashima and Bownes, 2005).

Two *dstpk61* transcripts were present as elements on the array: CT42511- LD13752, a group 3 transcripts with exon 1e, and LD22131, a group 1 (EST09) transcript. There were no differences in expression between the conditions compared for CT42511 (J. Terashima, personal communication). For LD22131 starvation seems to suppress *dstpk61* expression but application of Juvenile Hormone or injection of 20-hydroxyecdysone do not affect *dstpk61* expression (Table 4.3.1). The data (expression index, the log ratio of the pair of experimental conditions) were normalised for background signal before the average log ratio (ALR) was calculated.

S/F	JH/S	20E/F
-0.33 (0.002)	0.01 (0.423)	0.07 (0.094)

Table 4.3.1: Expression levels of *dstpk61* in response to apoptotic or non-apoptotic conditions (from Terashima and Bownes, 2005)
Values above zero indicate up-regulation and below zero down-regulation. The P-value is given in parenthesis for each sample. P<0.05 means there is a significant difference between the test sample and the control sample. S = starved, F = fed, JH = juvenile hormone-treated, 20E = 20-hydroxyecdysone-injected. The value is the average log ratio (ALR), calculated (for the first column) by the formula ALR = $\log_2$ (S average signal / F average signal). For columns two and three replace S/F average signals with JH/S and 20E/F, respectively.

4.4. Discussion

The major outcome from analysing the data on *dstpk61* from the FlyGEM set of arrays comparing sex-biased or –regulated gene expression (Parisi et al., 2004) is the strong indication of enriched expression of EST51 in male gonads (testes) versus ovaries. This information adds up to an increasing number of observations (Chapter 5 and below) confirming that the EST51 mRNA transcript (and thus the predicted E51 protein isoform) is highly enriched in *Drosophila* testes. EST51, a *dstpk61* transcript not well studied so far, seems to be currently the most promising aspect of the search for a role of *dstpk61* in development, due to its clear and reproducible presence preferentially in the testes, implicating it potentially in spermatogenesis.

Clone GH15751 (the EST51 *dstpk61* transcript), with the characteristic for EST51 exon 1c, became available in the EST database towards the end of the studies of the previous student working on *dstpk61* and as it comes from an adult head library there was no indication of any specific development-related localisation (Clyde and Bownes, 2000). Nowadays several EST clones from an adult testes library have the same sequence as GH15751 (Fig. 4.1.1) so a look at the EST database suggests that EST51 would be most likely present in testes. I did RT-PCR experiments with primers specific for EST51 to study expression of its mRNA (discussed in detail in Chapter 5) and they unequivocally confirm the high testes-enrichment of EST51. Furthermore, recently during a gain-of-function screen for identifying genes with potential roles in the regulation of male germline stem cells (GSC) maintenance and division and the early stages of germ cell differentiation by using EP lines, *dstpk61* was among the genes causing a reduced number of early germ cells in the testes when forcibly expressed in somatic cells (Schulz et al., 2004). This confirms the presence of *dstpk61* in the male gonad (although it is not informative at the transcript level) and gives some ideas about its function.

The FlyGEM array results give some indications of ovary or testes enrichment (no significant differential expression in the soma) but a general area of concern is that the sequence used sometimes is from a region common to many transcripts, even though the actual EST used for amplification of the spotted element is a very specific transcript. In cases such as EST51, it does not seem to matter eventually what the sequence of the probe (element) is; it picks up the specific transcript. In other cases though a small difference can be seen (ovary-enriched transcripts CT2222-EST40 and CT42507-Group 1 versus non significant enrichment of CT42509-EST09; for the two Group 1 transcripts there is also no differential expression between males and females (ratio around 1.0) whereas for the Group 2 CT2222 transcript there is a non- significant but slightly female-enriched expression)(Table 4.2.1). The other issue is that with the exception of EST51 the ratios indicating differential expression are too close to the threshold value and therefore should be treated as indications of a potential differential expression that needs to be verified by other means.

Transcripts LD13752 and LD38659 are potentially interesting. Especially if, as is the case for EST51, the probe sequence (common exon 4 in this case) matters less than what the transcript actually is, the indicated testes-enrichment of these transcripts which have exon 1d-1e combinations of alternative splicing and have so far been overlooked is highly intriguing. It is likely that exons 1dA-B and 1e in the 5'-UTR contain promoter elements that up-regulate expression of these transcripts in the male gonad. The absence of any of the other exons 1b, 1a, 1c, 2 or 3 at the 5'-end means that the putative encoded protein would have the amino acid sequence of E69 and be probably kinase inactive. If indeed this set of transcripts (which may form a distinct group) is expressed preferentially in testes as does EST51 which encodes a full-length, potentially kinase active isoform it would be a very interesting future direction to look at the relationship between the two types of transcripts and isoforms, whether they are spatially or temporally separated within the male gonad and if not, how they interact. Full sequencing of the transcripts should be followed by expression pattern analysis (such as via RT-PCR) to confirm or otherwise the spatial specificity indicated by the microarray analysis and ultimately functional analysis would provide some answers as to the role of *dstpk61* in the given tissue and the identification of its regulatory elements.

Regarding the effect of apoptotic or non-apoptotic conditions in the ovary on *dstpk61* expression, the microarray analysis from Dr. Terashima showed that *dstpk61* is suppressed in starved flies, but this suppression is not rescued by the application of Juvenile Hormone which restores many aspects of the non-apoptotic phenotype, neither is it observed when apoptotic conditions are caused by a hormonal stimulus (injection of 20-hydroxyecdysone) rather than trophic deprivation. However, the expression of Protein Kinase B (PKB/Akt) which is the principle substrate of *dstpk61* was found to be down-regulated by both starvation and 20E-injection and up-regulated by JH application (Terashima and Bownes, 2005), therefore giving a more consistent pattern of regulation of expression than *dstpk61*. PKB is a well known anti-apoptotic protein kinase (Vanhaesebroeck and Waterfield, 1999; Brazil et al., 2004) and *dstpk61* is a positive growth and cell-size regulator, mainly through regulating PKB and S6K activation (Rintelen et al., 2001).

Expression of *dstpk61* under apoptotic or non-apoptotic conditions is studied in further detail in Chapter 5. In situ hybridisation in ovaries with a Group 2 and a common (core) probe gave similar results for both fed and starved flies, namely expression in the nurse cell cytoplasm of egg chambers from stage 10 of oogenesis onwards. However, RT-PCR analysis on ovaries from 20E-injected and JH-treated flies resulted in higher expression of *dstpk61* in JH-treated flies, which was the non-apoptotic condition.

The initial discrepancy between the in situ hybridisation results and the microarray results when comparing fed and starved flies may be explained by the fact that the checkpoint for egg chambers to decide if they will develop or undergo apoptosis is at stages 8-9 of oogenesis and the *dstpk61* mRNA staining by in situ hybridisation begins at stage 10. It is possible that the lack of differential expression between fed and starved flies is due to the fact that in the starved flies only those egg chambers that pass the checkpoint will proceed to stage 10 and will therefore express *dstpk61* in the same way as the fed flies. The RT-PCR results show up-regulation under JH-treatment after normalisation, which is not observed in the microarray. This difference could reflect the different sensitivity of the methods, or even the effect of normalisation procedures (also discussed in Chapter 5) or types of analysis and their accuracy. Indeed, the same data set produced by the microarray without normalisation for background and with a different statistical analysis had shown no difference between apoptotic/ non-apoptotic conditions for any of the pairs compared, including starved/fed flies (J. Terashima, personal communication).

Finally, it is possible that in the kinase cascade of the Insulin Metabolism Pathway (IMP) *dstpk61* exerts its role as a positive regulator of growth and cell size and an anti-apoptotic role mainly via activation of its downstream targets, including PKB. Thus it is reasonable that such downstream genes would show more consistently the effects of apoptotic or pro-survival conditions on their expression, as is the case with PKB in Dr Terashima's microarray results.

Chapter 5: Expression analysis of *dstpk61* transcripts

5.1 Introduction

The *dstpk61* gene locus produces a multitude of transcripts through the use of alternative promoters, splicing and polyadenylation sites, as mentioned earlier (Introduction and Fig. 4.1.1). Four protein isoforms with variant N-termini are predicted to be encoded by these transcripts and for simplicity, I refer to the DNA, the mRNA transcript and the respective protein as E40, E51, E09 and E69 (Figure 5.1.1), as acronyms from the EST number representing each. The names EST40, EST51, EST09 or cDNA^{A} and EST69 also correspond to the same *dstpk61* transcripts.

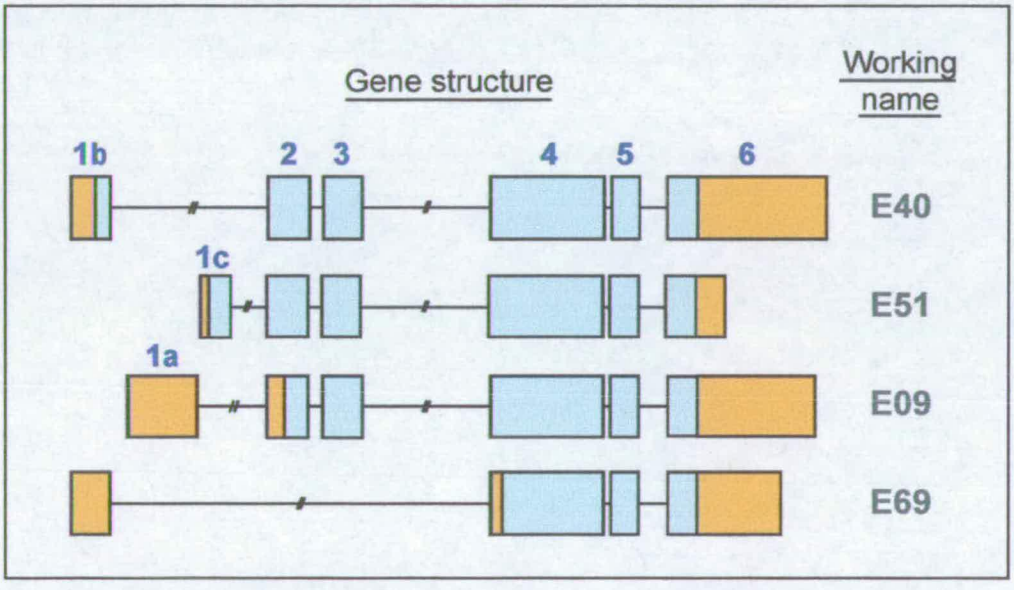

Figure 5.1.1 Exon/Intron structure of different *dstpk61* transcripts
Exons are numbered 1-6 and the name of each transcript is indicated on the right. Boxes represent exons and lines introns. The coding sequence is light blue and the 5' and 3' UTRs (untranslated regions) are orange.

Previous work in our laboratory suggested the presence of a female carcass-enriched, an ovary-enriched, a male testis-enriched and a non sex-specific transcript by Northern blot analysis (MacDougall et al, 1999). RT-PCR analysis showed E40 to be significantly female enriched, E69 to be present in both males and females and E09 in male and female carcasses (flies without gonads) and possibly in ovaries

(MacDougall et al, 1999; C. Mayor- Wellcome rotation project, 2001). In situ hybridisation experiments (Clyde, 1999) in different tissues and stages of development showed: 1. weak expression in embryos; 2. a transcript not of group 1 or 2 (i.e. not E40 or E09) in male but not female larval gonads, in spermatocytes but not spermatagonia; 3. group 2 (E40) transcripts in larval imaginal discs and brains; 4. a transcript (detected with a core region probe) in the adult testes along the inner edge of the coil in spermatocytes and postmeiotic spermatids, but not in the apical tip of the testis; 5. the presence of *dstpk61* transcripts (with all probes used) in adult ovaries. Subsequent in situ hybridisation experiments in ovaries by two students, Simah Khalid and Charlie Mayor, produced contradictory results as to where exactly *dstpk61* is expressed in the ovary; this is most likely to be in the oocyte and nurse cell cytoplasm [Simah had produced in situ hybridisations with clear expression in the nurse cell nuclei but did not have the time to repeat this to check if probes had been muddled up]. The probes used in the in situ hybridisation experiments described above included a core probe, common for all transcripts, a Group 1 and a Group 2 probes, specific for exons 1a and 1b, respectively (Figure 5.1.2).

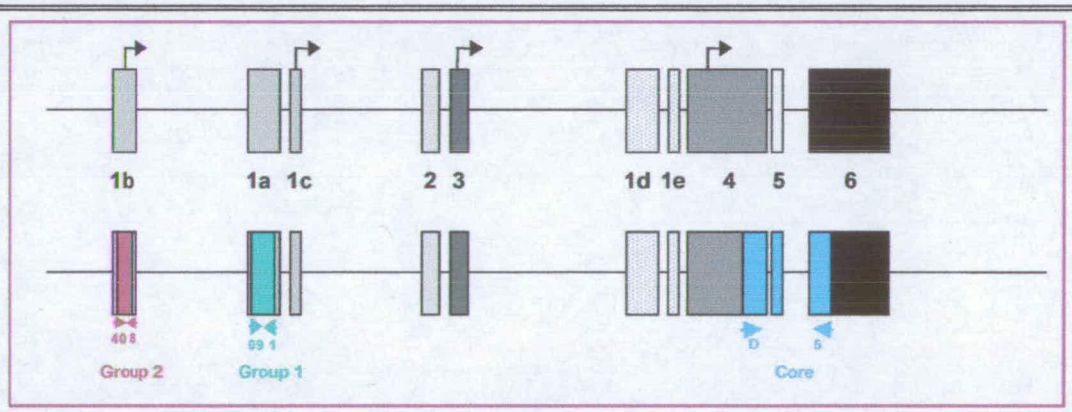

Figure 5.1.2 Position of probes used for in situ hybridisation and *dstpk61* exons they bind to
The coloured regions in the bottom drawing mark the DNA sequence for each probe, with its name and the primers used to make it underneath. These were all double stranded DIG-labelled DNA probes.

I decided to investigate the expression pattern of *dstpk61* transcripts by RT-PCR and in situ hybridisation, building on the existing data and taking into account additional

information that had become available, namely the testis-enrichment of E51 and potential ovary enrichment of Group1 transcripts suggested by B. Oliver's microarray results (Chapter 4) and the addition of seven EST's from an adult testis library that contained exon 1c to the EST database. My priority was to investigate whether E51 represented a real transcript and its localisation pattern in different tissues, since it was not previously included in an expression analysis. I needed to confirm if E51 is the testes-enriched transcript previously observed on Northern blots, initially by RT-PCR and possibly also by in situ hybridisation, if a suitable probe could be designed. RT-PCR for the other *dstpk61* transcripts was also repeated, to verify their expression patterns. In situ hybridisation experiments for the different groups of *dstpk61* transcripts (Group 1, Group 2, common core domain) in the ovaries were performed in order to clarify the contradictory results of previous studies concerning the mRNA expression pattern in this tissue.

Differences in spatial expression patterns of E40 and E09 transcripts between different sets of flies during repeats of experiments in my initial studies led me to believe that at least one other factor must regulate the *dstpk61* expression across different tissues. I then checked different conditions, including age, food deprivation or treatment with hormones to induce or prevent apoptosis, and investigated the effect of mating in males, in an attempt to identify additional factors that may affect *dstpk61* expression.

5.2 Different dstpk61 transcripts are expressed in different tissues

5.2.1 RT-PCR analysis

Total RNA was isolated from ovaries (ov), testes (te) and male (MC) and female (FC) carcasses of wild-type *OrR* flies (50 each males and females, and 50 pairs of gonads). Following determination of the RNA concentration by spectrometry, the same amount of RNA from each sample was used for RT reactions, followed by PCR with primers specific for exons 1a, 1b and 1c that would recognise transcripts E09, E40 and E51, respectively. Primer sequences and related information are in Chapter

2 (Materials and Methods). Several dilutions of template cDNA (usually corresponding to 100ng, 10ng and 2ng total RNA) were used per PCR. This was to ensure that amplification in the linear phase of the reaction would be observed for each sample, that between the three concentrations I would be able to confirm differential expression between tissues for a given transcript (i.e. in a dilution where no PCR product is detected for a specific sample, for another sample a PCR product is visible) and that I would have a band intensity directly comparable to the marker band intensity used for quantification. Relative quantification was done by comparison to the Hyperladder I marker (Bioline). The bands of this marker have a different, known amount of DNA each, when 5μl of marker are loaded in a 1% agarose gel. Based on this, I estimated the amount of DNA per μl of PCR product. A PCR with primers for the housekeeping gene *rp49*, encoding a ribosomal protein (Al-Atia et al, 1985), was used as a positive control and for normalisations of the results, as its expression should be constant throughout development (Till et al, 1998).

Figure 5.2.1 shows the results of this experiment. Transcript E51 is always highly enriched in testes. It is virtually absent from other tissues, but a very weak E51 band can be detected in ovaries and male carcasses after PCR with the highest template concentration (not shown); for this reason I do not refer to E51 as "testes-specific" but as "highly testes-enriched". Transcripts E40 and E09 are detected in all four tissues at the two higher template concentrations (bands marked A and C in Figure 5.2.1B, top). However, their expression pattern in the different tissues varied when different batches of flies were used in two independent repeats of the experiment (A' and B'). E40 is consistently enriched in ovaries. Its expression levels in the other tissues though vary between different batches of flies used for RNA isolation: E40 expression (after ovaries) can either be higher in female carcasses, followed by equally low levels in male carcasses and testes (Fig. 5.2.1C) or, in contrast, higher in male carcasses, significantly lower in female carcasses and slightly lower in testes (Fig.5.2.1.A). E09 can either be expressed at the highest level in the ovaries and at lower levels in female carcasses, male carcasses and testes (in that order) (Fig.5.2.1C) or to exhibit its highest level of expression in male carcasses, followed closely be ovaries and have low expression levels in female carcasses and testes (Fig.

5.2.1A and B, top). It must be noted that the overall expression levels of transcript E09 are lower than for transcript E40. Transcript E69 is expressed equally among tissues (result after normalisation for the *rp49* PCR product) at much lower levels than the other transcript groups (Fig. 5.2.1B, bottom). Figure 5.2.1D presents a comparison of the results of the two independent experimental repeats to demonstrate their variability.

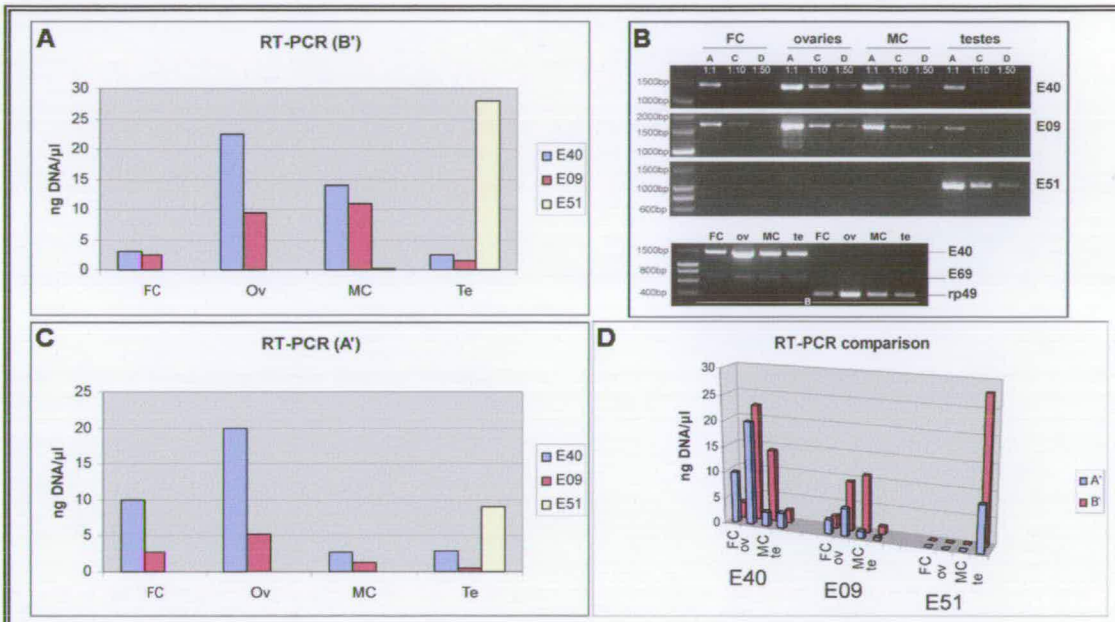

Figure 5.2.1 Differential expression of *dstpk61* transcripts in various tissues

In all pictures, FC and MC are female and male carcasses, respectively; ov are ovaries and te are testes. A' and B' (in A, C and D) correspond to two independent repeats of the experiment. Transcript E51 is consistently highly enriched in testes. Transcripts E40 and E09 are ovary-enriched and are present in all tested tissues. For both E40 and E09, expression is higher in the female carcasses than in male ones in repeat A' (C) but higher in male carcasses than in female, in repeat B' (A, B). Therefore, after the consistent between repeats ovary enrichment, the pattern changes for different batches of wild-type flies, but is similar for both transcripts.

In (A) and (C) the DNA concentration (ng/µl PCR product) is plotted for transcripts E40, E09 and E51 in all tissues, after normalisation for the expression of the housekeeping gene *rp49* that was used as a positive control (transcript expression/ *rp49* expression for each sample). In (D) the results from the two repeats A' and B' are compared.

In (B) the gels for repeat B' are presented. There are 3 bands for each sample, corresponding to different amount of cDNA template. A PCR with different primers, detecting E40 and E69 is shown at the bottom, together with the positive control *rp49*. Bands marked as A, B, C, D indicate template concentrations equivalent to 100ng, 40ng, 10ng and 2ng total RNA, respectively.

Apart from the novel and clear observation that transcript E51 is highly testes-enriched, there are two somewhat unexpected observations. Firstly, the inconsistency of the expression pattern among tissues for transcripts E40 and E09 (but not for E51 or E69). I used flies of similar age, not overcrowded in their vials, sufficiently fed and a mix of males and females so that mating could occur, to try to avoid obvious sources of variability. Practically, for all general purpose PCR and RT-PCR experiments and in situ hybridisations, I would add yeast to newly eclosed flies and allow them to grow at 25°C for 3 days before dissection. The discrepancy of the E09 and E40 expression patterns is due to the mRNA representation of each transcript in each set of RNA isolation and not a PCR mistake, since different RT-PCR reactions for all transcripts, following exactly the same protocol, were done using RNA from repeats A' and B' and showed the same results as the first time (not shown).

Secondly, the expression pattern I observed is different from what was reported earlier for transcripts E40 and E09 (Clyde, 1999; MacDougall et al, 1999; C. Mayor and M Bownes, unpublished work). A Group 2 transcript (E40 and other ESTs with exon 1b) was found to have very high expression in female and very weak expression in male carcasses. RT-PCR with Group 1 (E09)-specific primers on male and female carcasses was unsuccessful (Clyde, 1999; MacDougall et al, 1999). Charlie Mayor, a student doing a rotation project in our laboratory (2001) performed RT-PCRs on male and female carcasses, testes and ovaries for E09 and E40. He confirmed the presence of E40 in female carcasses and a weak signal in male carcasses, but observed no E40 expression in ovaries or testes. He detected E09 in male and female somatic tissues and in ovaries, but not in testes. However, in situ hybridisation experiments he did on ovaries showed some E40 expression in egg chambers (nurse cell cytoplasm); this raises a question as to how trustworthy the results of his RT-PCRs are since no E40 was detected in the ovaries.

I observed ovary-enrichment of E40 in both repeats, but report presence of the transcript in somatic and gonadal tissues of both male and female flies. I similarly observed E09 in all tested tissues but cannot define any tissue-enrichment related to this transcript (apart from the fact that its presence in testes is consistently very low)

as results vary between repeats. Since the previous attempts on RT-PCRs for *dstpk61* transcript groups, as described above, were either incomplete (not testing gonads), unsuccessful or raised questions, I was confident about the results of my analysis, but still concerned that the clearly demonstrated preferential Group 2 expression in female versus male gonads (MacDougall et al, 1999) was not reproduced. I designed new primers for all transcripts to conduct my analysis and one possibility was that the use of different oligonucleotides somehow affected the result (albeit the new primers were in close proximity to the old ones, for E40 and E09). To address this issue, I repeated the PCRs using the same primers, PCR conditions and template concentration as in MacDougall et al (1999), and *rp49* primers for a control. Use of this primer set allows visualisation of a band presumably corresponding to transcript E69, which I confirm that is expressed equally in all tissues. However, my results with the old conditions still show similar results to my PCRs with new primers. Expression of E40 is at least equal between male and female carcasses (normalising for *rp49*) and slightly enriched in ovaries (Figure 5.2.1B, bottom). Again, there are variations in the expression levels among tissues for different fly batches (not shown).

This variation for E09 expression levels and E40 male and female carcass expression levels led me to believe that some other factors affect the tissue-specificity (or the relative level of expression of a given transcript in a tissue) of *dstpk61* transcripts. Age and stress were the most obvious candidates to look at first (sections 5.3 and 5.4). Stress can include nutrient availability (such as food limitations in overcrowded situations, which affect egg production and fly size) and I used starvation and treatment with hormones in the ovaries as apoptotic conditions with respect to oocyte progression and development within the ovary (Bownes, 1989; Terashima and Bownes, 2004).

The results of all the different conditions used to study *dstpk61* transcript expression are summarised in Table 5.1 before section 5.6 (discussion).

5.2.2 In situ hybridisation for different *dstpk61* transcripts in ovaries

One other issue I had to clarify was the expression pattern of different *dstpk61* transcripts in ovaries, as there were contradictory results, especially for E40, as to whether it is expressed in the nurse cell and oocyte nucleus or the cytoplasm (S. Khalid and C. Mayor reports; Clyde, 1999). I prepared single stranded DIG-labelled DNA probes for the three different groups of *dstpk61* transcripts (E09- Group 1, E40-Group 2, E51) and a Core region, common to all transcripts. The antisense (AS) strand, usually generated by using the reverse primer during DIG-labelling by PCR, is the probe that will generate a signal, as it will hybridise to the (sense strand) mRNA in question. The sense (S) probe, usually generated by the forward primer, is used as a negative control.

A general difficulty occurring throughout the years of research on *dstpk61* in our laboratory is that the *dstpk61* transcripts are exceptionally rare, hence in situ hybridisation experiments have always proved problematic. Indeed, a lot of optimisation of the protocol was necessary to achieve some results, with staining being extremely weak more often than not, thus not allowing detailed observations.

Based on my results (Figure 5.2.2- see also Fig. 5.4.2) I confirm that any *dstpk61* mRNA presence in the ovary is in the nurse cell cytoplasm and not in the nuclei. The expression pattern is similar for Group 1 and 2 transcripts (Fig.5.2.2F-H and 5.4.2I-J) and the Core probe (very weak signal in Fig.5.2.2C- black arrow; also Fig.5.4.2H, K-L): *dstpk61* mRNA is expressed in nurse cell cytoplasm from stage 10-13 of oogenesis. These is a possibility that the same pattern is observed with the E51 probe (Fig. 5.2.2D), although it is difficult to confirm that since the differences from the background staining apparent in the negative controls (Fig.5.2.2A) are very subtle. Similarly, it is possible that there is some Group 1 expression in the germarium region 2B (Fig.5.2.2E) but the signal is too weak. *oskar* mRNA in situ was used as a positive control (Fig.5.2.2B, red arrows point to *osk* expression at the posterior of the oocyte).

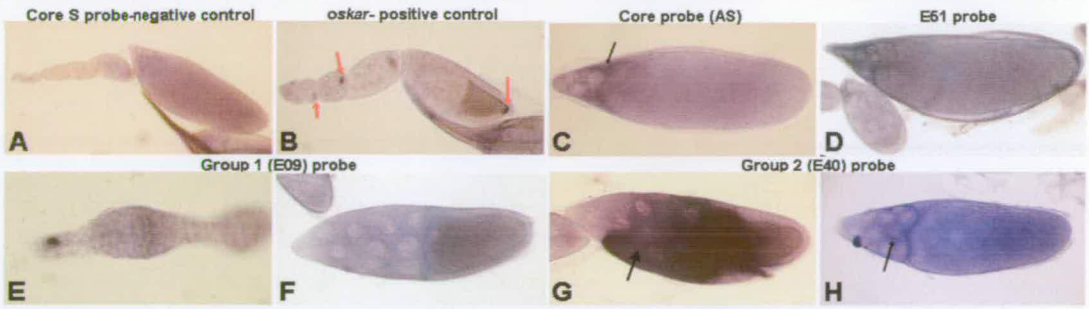

Figure 5.2.2 In situ hybridisation in ovaries for *dstpk61* transcripts
Expression is very weak but consistent in the nurse cell cytoplasm of stages 10-12 (F-H, C) with group 1, 2 and Core probes. No expression is detected in earlier stages of oogenesis, with the possible exception of region 2b in the germarium with group 1 probe (E). (A), negative control and (B), positive control (*oskar* staining= red arrows). Black arrows point to the *dstpk61* expression in mid-late oogenesis which is also possibly present with the E51 probe (D). (F, G)-stage 10; (H)-stage 11; (C-D and A-left)-stage 12. Egg chambers are under different magnifications.

Expression of *dstpk61* could not be undoubtedly observed in the follicle cells. The more ubiquitous staining covering also the nurse cell nuclei in Fig.5.4.2B, C and H is a strong indication that there is *dstpk61* expression (at least of Group 2 transcripts) in the follicle cell layer (The "fed" ovaries of the experiment presented in Figure 5.4.2 are from flies treated in exactly the same way as those for all in situ hybridisations, including those presented in Figure 5.2.2.). Expression levels of *dstpk61* transcripts in the follicle cells are probably below the level of detection by in situ hybridisation. However, antibody staining with an antibody against Dstpk61 protein isoform E40 shows E40 expression in follicle cell cytoplasm as well as nurse cell and oocyte cytoplasm throughout oogenesis (Chapter 6).

5.3 Fly age affects expression of E51 and E09 dstpk61 transcripts

To test the effects of the age of flies to the *dstpk61* transcript expression, I collected total RNA from male and female carcasses, ovaries and testes of wild-type *OrR* flies of different ages, as shown in Figure 5.3.1 legend. I was collecting newly eclosed flies (combined male and female), transferring them to a new bottle and dissecting the tissues after the required number of days at 25°C. I then reverse transcribed the

mRNA and did PCR for *dstpk61* transcripts E40, E09 and E51, and *rp49* as described before (section 5.1.1). I had 4 age groups for each fly tissue and transcript: A, B, C and D, corresponding to 0-1 day old, 1-3 days old, 4 days old and 6-7 days old flies, respectively.

The most striking variation of a transcript expression with age comes from the E51 transcript in testes (Figure 5.3.1C) where expression in very young (<24 hr old) and old flies (6-7 days old) is significantly (5.2x higher, in average) higher than that of 1-4 day old flies. Furthermore, the level of expression for these two age extremes is the highest observed among all the transcripts in all tissues (compare Fig.5.3.1C with A and B). For E09, a significant age-related differential expression occurs in female carcasses, where the expression levels are much higher in 0-24hr old female somatic tissues than in those of any other age (Fig. 5.3.1B). Expression of E09 does not vary much with age in other tissues (somewhat more in male carcasses than in ovaries-Fig.5.3.1B) and, apart from the peak in young female carcasses, is generally at lower levels than transcript E40 expression. Not much difference with respect to age is observed in any tissue for E40, with the expression levels being marginally higher in ovaries compared to male and female carcasses, and much lower in testes. In the latter, there is a several orders of magnitude scaled down version of the E51 phenomenon: E40 expression is higher in very young and very old fly testes, than in intervening ages.

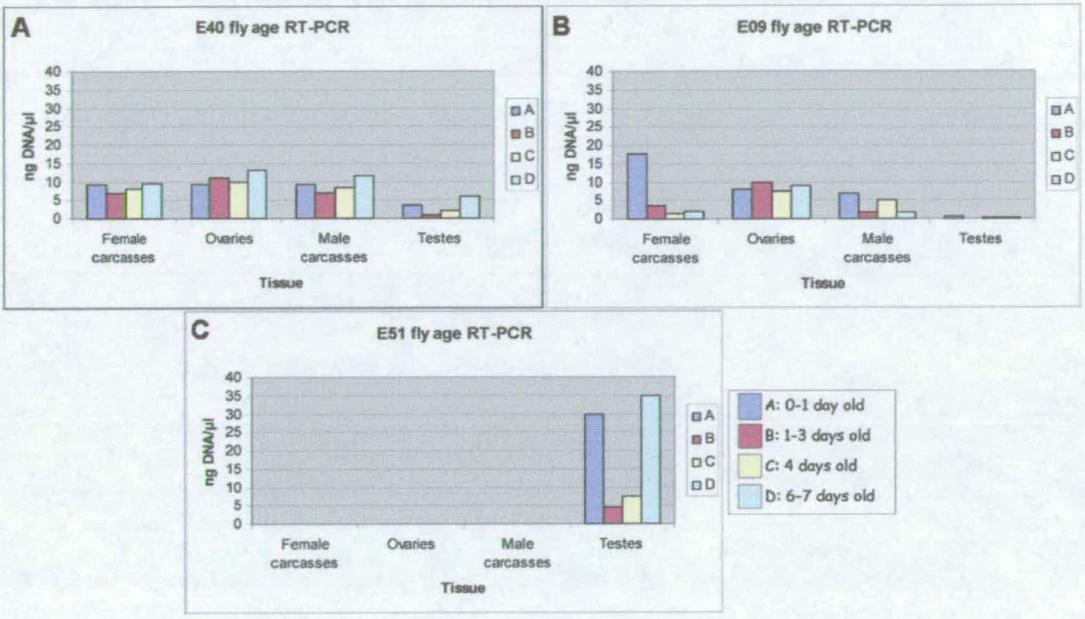

Figure 5.3.1 Expression of *dstpk61* transcripts in flies of different age
(A) Expression of E40 does not vary significantly in fly tissues of different ages.
(B) E09 is expressed in high levels in young female carcasses, while the expression levels drop in older female carcasses. There is not much age-dependent variation in ovaries and testes, with a bit more fluctuation in E09 expression levels in male carcasses.
(C) Expression levels of E51 are very high in testes of the two age extremes (0-1 day and 6-7 day old flies) and significantly lower in 1-4 day old fly testes.
Expression levels for E09 are generally lower than for E40.

5.4 Apoptotic Vs non-apoptotic conditions in the ovaries affect dstpk61 expression levels

Activity of the insulin/IGF signalling pathway (ISP) has been linked with nutrient availability in numerous reports; female sterility, reduced body weight through reductions in cell size and number, increased life-span and growth retardation have been observed in *chico* and *Dilp* (*Drosophila insulin-like peptides*, the fly homologues to insulin) mutant flies but also in flies starved during development (Bohni et al, 1999; Brogiolo, 2001; Clancy et al, 2001; Ikeya et al, 2002) and a similar situation has been reported in mice, with IRS mutant and starved mice having similar phenotypes (Butler and Le Roith, 2001). Moreover, starvation was shown to reduce the activity of the ISP in vivo (Britton et al, 2002). Since the ISP is probably

related to nutrient response pathways, from the several environmental stresses for *Drosophila* I selected nutritional shortage to look at how it may affect *dstpk61* expression. I worked on *Drosophila* ovaries and used starvation directly, or treatment with 20-hydroxyecdysone, the concentration of which is elevated in flies under nutritional shortage (Bownes, 1989) as conditions that would promote apoptosis during early vitellogenesis (Terashima and Bownes, 2004).

Apoptosis, or programmed cell death (PCD) is a normal component of development, necessary for forming or deleting structures, controlling cell numbers or eliminating abnormal cells (Baehrecke, 2002). In oogenesis, apart form the nurse cell cytoplasm being transported into the oocyte as the nurse cells undergo PCD in late oogenesis (Buszczak and Cooley, 2000), there is mid-oogenesis cell death (stages 7 and 8) in response to nutrient deprivation (i.e. starvation), other external factors (such as mating, overcrowding or heat stress) or developmental abnormalities caused by mutations in the genes controlling the checkpoint (like ecdysone response genes *E74, E75* and *Broad-Complex*) (Soller et al, 1999; Laundrie et al, 2003; Terashima and Bownes, 2004, 2005).

Apoptosis in mid-oogenesis is the result of a checkpoint where the nutritional status and other environmental factors determine how many mature eggs can be made and monitor the state of the egg chambers before investing in vitellogenesis (Soller et al, 1999; Buszczak and Cooley, 2000). Apoptosis commitment occurs at stage 5-6 of oogenesis and is marked by the differential expression of Broad-Complex (Br-C) isoforms (Terashima and Bownes, 2004); then there is a checkpoint control at stage 8-9 after which all egg chambers committed undergo apoptosis – mediated by *reaper, hid* and *grim* (Grether et al, 1995; White et al, 1996; Chen et al, 1996)- unless they are rescued (Terashima and Bownes 2004, 2005).

This checkpoint controls vitellogenic oocyte progression as well as fat body synthesized-yolk protein uptake and *yolk protein* gene expression in the ovary (Soller et al, 1997). Mating, through the transfer of the Sex Peptide, a product of the male accessory glands, to the female promotes oocyte progression through this control point at stage 9 (Soller et al, 1997), most likely through the induction of Juvenile

hormone (JH) biosynthesis which increases yolk protein uptake from the hemolymph and yolk protein synthesis in the ovary (Soller et al, 1999). In virgin and starved females the level of 20-hydroxyecdysone (20E) is high in the hemolymph and this mediates the resorption of stage 9 oocytes when the ovaries are filled with stage 14 eggs or slowing down of the progression of stage 10 oocytes when the nutrients are low. Therefore the balance of JH and 20E in the hemolymph regulates whether oocytes will progress through the stage 9 control point or undergo apoptosis (Soller et al, 1999). Thus, ovaries from flies treated with 20E as well as starved flies are considered to be under conditions that induce apoptosis whereas flies treated with juvenile hormone or fed flies are under conditions that permit growth and inhibit apoptosis (Soller et al, 1999; Terashima and Bownes, 2004).

5.4.1 RT-PCR for *dstpk61* transcripts on 20E and JH-treated fly ovaries

I used RNA from flies injected with 20-hydroxyecdysone (20E) or treated with Juvenile Hormone (JH) (kindly provided by Dr J. Terashima) to do an RT-PCR analysis, as described before, to ovary RNA with primers for all *dstpk61* transcripts. 20E-injected flies represented the apoptotic conditions and JH-treated flies the non-apoptotic conditions. Two template concentrations were used for the PCR, marked 1:1 and 1:10 in Figure 5.4.1-top, corresponding to 100ng and 10ng of initial RNA used for the RT reaction, respectively.

After normalisation of the results for *rp49* expression, which should be equal in all samples (Fig.5.4.1top), I found that under non-apoptotic conditions (JH-treated flies) expression of transcripts E09, E40 and a Core *dstpk61* domain (common to all transcripts) is higher than under apoptotic conditions (2.1-2.5 times more). There was no expression detected with primers for E51, as expected since the only tissue tested was ovaries- so E51 served as a negative control (Figure 5.4.1bottom).

As before, transcript E40 is expressed at higher levels than E09. The higher amounts of PCR product produced with the Core domain primers are very close to equalling the added products of E09 and E40 (Fig. 5.4.1bottom); expression of E69 may make

up for the remaining DNA produced by the Core PCR. This observation increases my confidence to the, admittedly crude, method of quantification by comparing sample band intensity to the intensity of marker bands of known DNA quantity.

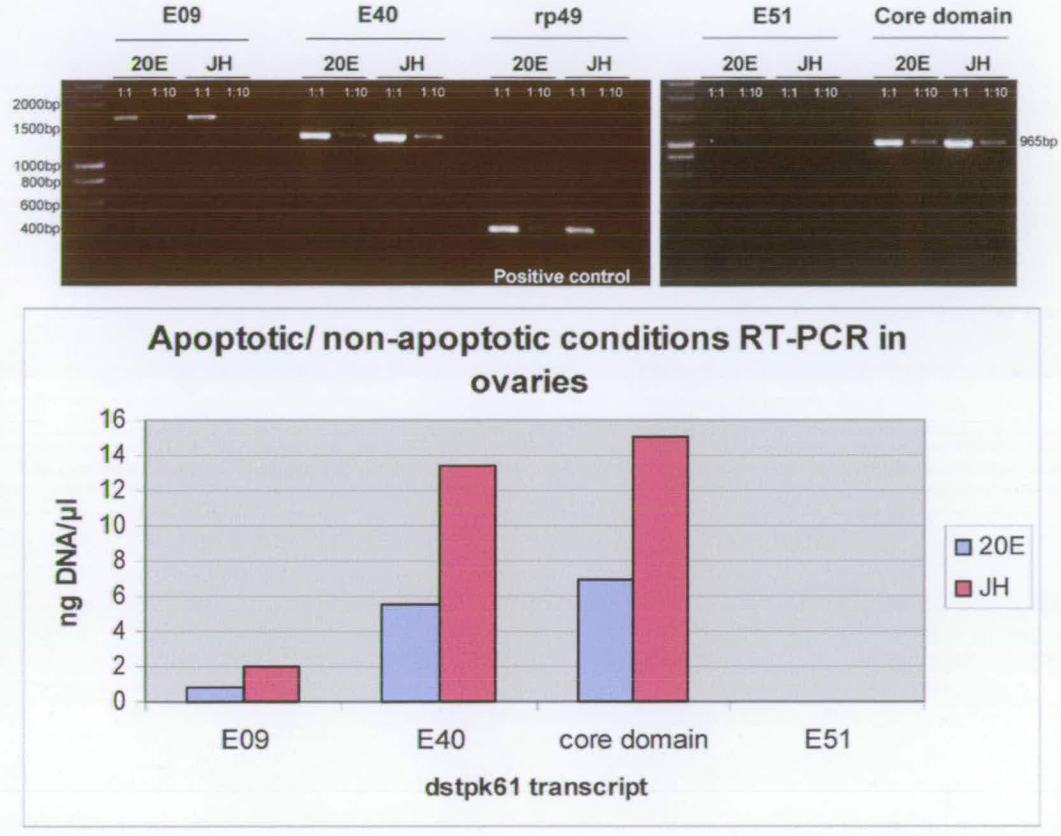

Figure 5.4.1 *dstpk61* transcript expression under apoptotic or non-apoptotic conditions
(Top): PCR on 20E and JH fly ovaries with primers specific for E09, E40, E51 or a common (Core) domain of *dstpk61*. Two template concentrations 1:1, 1:10 were used for each sample. PCR for the *rp49* gene product was used as a positive control.
(Bottom): Chart of expression levels of each transcript in apoptotic (20E) and non-apoptotic (JH) conditions after normalising the values with respect to the positive control. The expression is higher in JH-treated flies for all ovary-represented transcripts.

5.4.2 Transcript localisation in oogenesis under apoptotic and non-apoptotic conditions

In situ hybridisation with DIG-labelled single strand DNA probes for transcript groups 1, 2 and a common domain (Core probe) was undertaken with ovaries of fed and starved flies as examples representative of non-apoptotic and apoptotic

conditions, respectively. For the fed flies, 0-24hr eclosed flies were transferred to a new vial/bottle with yeast, and dissected 3 days later (same as standard procedure). The starved flies were 0-24hr eclosed flies transferred to a vial with sucrose medium (sucrose, agar and water), left for 3 days and then dissected. In situ hybridisation with a Group 1 probe was unsuccessful, so the probes used are shown in Figure 5.4.2i.

dstpk61 mRNA is present in the nurse cell cytoplasm from stage 10 of oogenesis onwards, in both starved and fed flies (Fig. 5.4.2ii). The absence of differential expression between fed and starved flies is expected at these stages, since only the egg chambers passing the checkpoint control earlier, during stages 8-9, will continue to develop. Had *dstpk61* expression been detected by in situ techniques in stages earlier that 10, there may have been a difference between the two conditions- apoptotic and non-apoptotic (as the key differences are usually around oogenetic stages 7, 8 and 9 for the checkpoint or even earlier st.5 vs 6 for *BrC* that is involved in apoptosis commitment- Terashima and Bownes, 2004). Dr J. Terashima's microarray results show *dstpk61* is suppressed in starved flies (Terashima and Bownes, 2005) (chapter 4) and provide an indication that such a difference may be true.

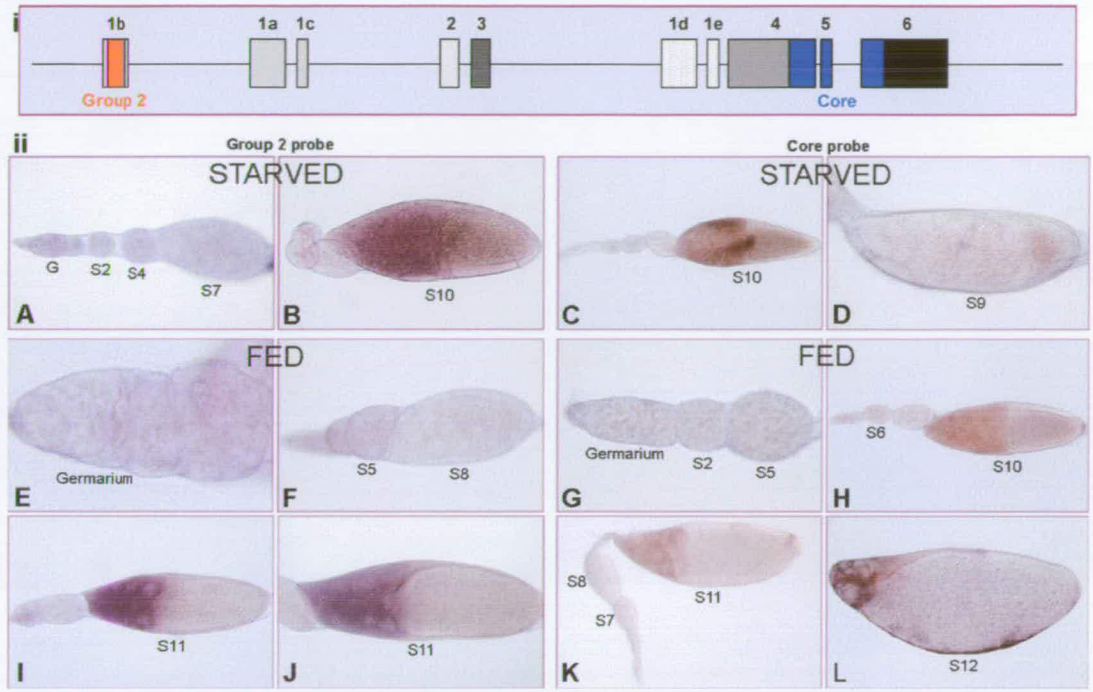

Figure 5.4.2 In situ hybridisation in ovaries of fed and starved flies
In (i) the position of the probes used for the in situ hybridisation are shown on the *dstpk61* gene locus. In (ii) the results of in situ hybridisation with Group 2 (for E40) and Core (for all transcripts) probes on both starved (A-B, C-D) and fed (E-F-I-J, G-H-K-L) flies are shown, as indicated. Egg chamber stages are marked as G or germarium and S(x) with a number for the corresponding stage.
The pattern is the same for both sets of probes in both fed and starved flies: No *dstpk61* mRNA is detected in the germarium or early stages of oogenesis, up to and including stage 9 (D). Expression is observed in the nurse cell cytoplasm of fed and starved egg chambers from stage 10 onwards. (B, C, H show stage 10, I-K stage 11 and L stage 12 egg chambers). It is not clear if there is expression in the columnar follicle cells- it is quite likely though (see expression in B, H).

5.5 The E51 dstpk61 transcript in the male gonad

So far, I have shown that E51 is a transcript very highly enriched in testes, with consistent expression in the male gonad and it is virtually absent from the other tissues using several repeats of experiments and different experimental set-ups. Therefore, I believe that E51 is indeed the testis-specific transcript described by MacDougall et al (1999), and, given that during my study, none of the other *dstpk61* transcripts exhibited such an unequivocal tissue and, most notably, sex specificity, it

appears to be the highest priority target for further studies into the field of sex-specific transcripts and isoforms of *dstpk61* and their role.

5.5.1 E51 expression levels in the male gonad are affected by the age and mating status of the fly

We already saw that E51 expression in the testis is at its highest in very young and in old flies, but drops dramatically in flies aged 1-4 days. Apart from age, I decided to look into how mating, whether the male flies were kept virgin or were allowed to copulate, may affect E51 testes expression. Sperm will move across to females and would need to be remade in mated flies so differences in E51 expression between mated and non-mated male flies may reflect potential differential requirements for it in spermatogenesis.

A minimum of 100 virgin male wild-type *OrR* flies were collected every day. The method of collection was similar to female virgin collections: every 4-5 hours newly eclosed flies were collected from bottles that were previously emptied from any eclosed flies. Newly eclosed flies can also be identified by their pale body colour, folded wings if they are very young, and the presence of a dark spot in their abdomen (meconium). From the male flies selected, 50 were kept in a bottle with food and yeast without any females, whereas the other 50 were transferred to a yeasted food bottle together with their female siblings and were allowed to mate. RNA was isolated (Trizol method) from the testes of mated and non-mated (virgin) males after different amounts of time, up to the time that the progeny of the mated flies were just about to eclose (one life cycle). Due to the scale of the experiment, mated and non-mated male flies were left to grow at 18°C, where the life cycle is extended to 21 days compared to 10 days at 25°C. The virgin flies were collected from bottles kept at 25°C.

RT reactions and PCR were performed as before, starting with the same amount of RNA (determined by spectrometry) from each sample. PCR with primers for E51 cDNA was done for two template concentrations per sample, corresponding to 10ng and 2ng initial RNA, since the bands on the gels with the highest concentration were

oversaturated in all previous experiments (e.g. Fig. 5.2.1B). Primers for *rp49* were used as a positive control for subsequent normalisation.

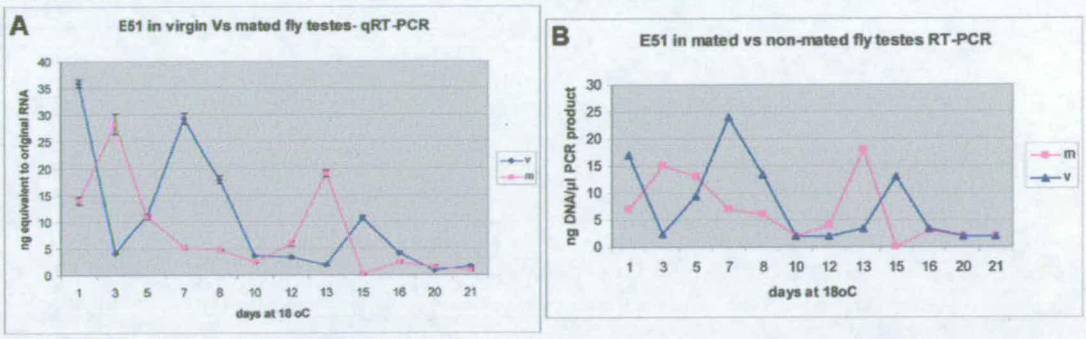

Figure 5.5.1 E51 transcript expression levels in testes vary depending on the age and mating state of the male fly

Two different methods, real time PCR (qPCR-quantitative) (A) and conventional PCR with two template concentrations (B) and quantification of bands compared to the Hyperladder marker, give almost identical patterns of E51 expression in the testes of mated versus non-mated (virgin) male flies over time. Standard error bands in (A) represent the standard error amongst E51 triplicates for each sample.

These patterns are contrasting, with virgin male testes having peaks of maximum expression on days 1, 7 and, to a lower extend, 15, and mated male testes having peaks of minimum E51 expression on days 1, 10 and 15. Mated male testes have their maximum E51 expression levels on days 3 and 13, which are the days virgin male testes E51 is at its lowest, together with day 10.

After quantification and normalisation, the results were plotted as the E51 PCR product concentration for mated (m) and non-mated (v) male flies over time (Figure 5.5.1B). Interestingly, the E51 expression levels fluctuate a lot and usually have the opposite trend in mated and virgin males, apart from two time points, one in the middle of the life cycle (10-12 days at 18°C) and one at the end, in old flies (16-21 days at 18°C). Otherwise, virgin males start with a high E51 expression level which drops to a minimum by day 3 (in 1 day at 25°C) and then rises again to reach a maximum at day 7 (day 3-4 at 25°C). E51 expression falls again to a minimum at day 10 and remains in low levels until day 12-13 when it starts rising again to a peak at day 15 (day 7 at 25°C). It drops for a third time quickly and stays at very low levels for the last 6 days (days 8-10 at 25°C). In contrast, mated males express E51 at moderately high levels when they are very young and expression levels elevate to peak at day 3, before they start falling gradually but steadily to reach a low point at day 10 (day 5 at 25°C). E51 expression gets higher slowly by day 12 and then quite dramatically increases within 1 day at 18°C to reach a maximum by day 13. Then

rapidly all the transcript is turned over by day 15, increases slightly by day 16 and from then on stays at low levels until day 21, sharing the same expression level and pattern for the last days.

In order to increase the accuracy of my calculations, I repeated the experiment by real-time (quantitative-q) PCR, using SYBR Green as the fluorescent dye indicating amplification. Due to the different method and principle, several new pairs of primers were designed and tested, together with two *rp49* sets of primers and a β-Tubulin one, as positive controls. Because SYBR Green binds to any double stranded DNA, test PCRs were ran to select a suitable pair of primers for E51 and one for control, that would amplify well and not produce secondary bands or primer dimers. Each sample was tested in triplicate and a standard curve was made for *rp49* and E51 for calculations and normalisation. The final result from the qPCR (Fig. 5.5.1A) is almost identical to the curves I get from the conventional PCR and quantification (Fig.5.5.1B) and shows the same trends with slightly different values and peak sizes.

The fact that a more accurate method like qPCR and my quantification method of a conventional PCR give so similar results proves the efficiency of my method and increases the significance factor of this and my other results and the likelihood that what I observe reflects the real situation.

5.5.2 In situ hybridisation for E51 in adult testes

Although previous reports (Clyde, 1999) stress the technical difficulty of testes in situ hybridisation experiments and hence only the common *dstpk61* Core was ever used for testes in situ hybridisation, I decided to use my single stranded DIG-labelled E51 RNA probes to look at the expression of E51 mRNA in testes.

Using a protocol by Dr. H. White-Cooper (Materials and Methods) and high concentrations of probes, since *dstpk61* transcripts are generally very weak, I observed Alkaline Phosphatase staining throughout the testis (Figure 5.5.2A-B, C', D, E), including the apical tip of the testis (blue arrows in Fig.5.5.2A and E), but not

in the accessory glands (Fig.5.5.2C, C'-red arrowheads). Probes for two cell cycle regulatory genes with known patterns of expression in the testis, *Cyclin B* and *twine* (White-Cooper et al, 1998) were used as positive controls (Fig. 5.5.2G and H, respectively). The E51 sense probe was the negative control (Fig.5.5.2F).

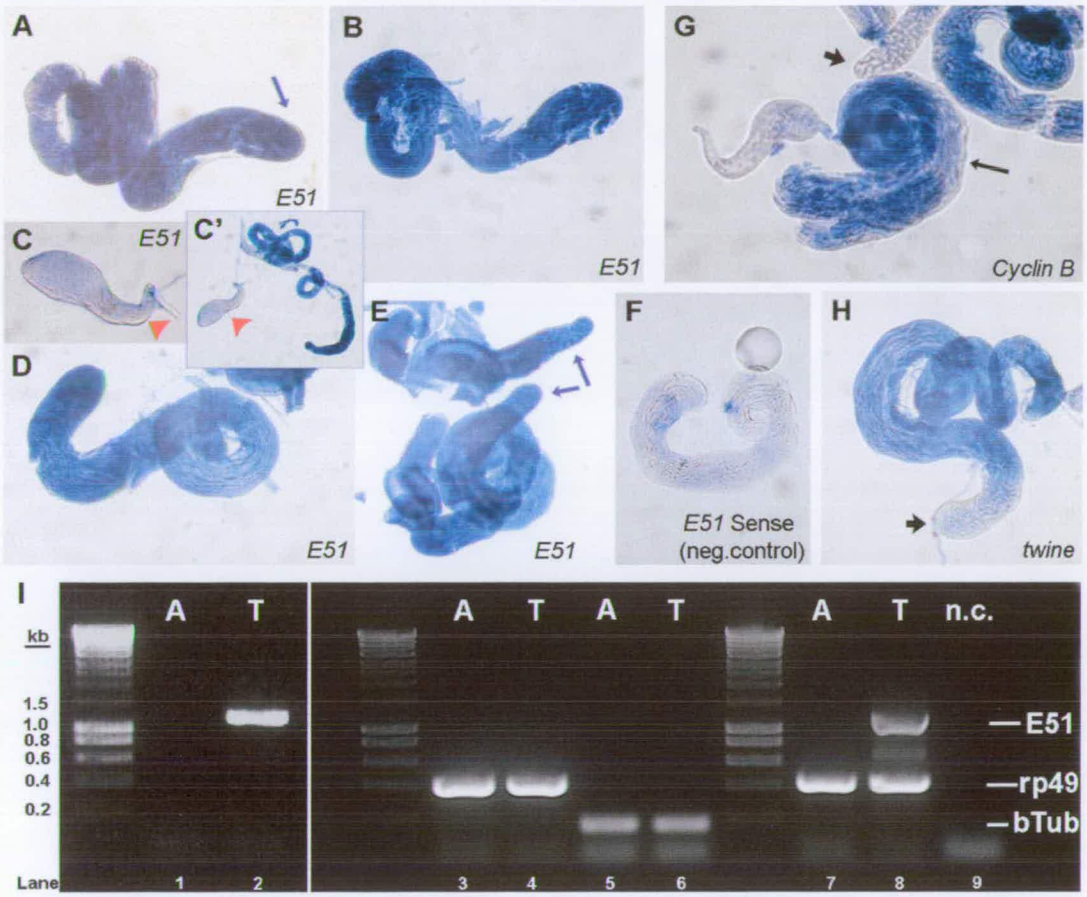

Figure 5.5.2 Transcript E51 is expressed in testes but not in male accessory glands

(A-H) In situ hybridisation for E51 in testes shows that E51 *dstpk61* mRNA is present throughout the testis (A, B, C', D, E), from the apical tip (blue arrows) where the mitotic divisions occur through to mature spermatids, but it is not expressed in the accessory glands (C, C') (red arrowheads). (F) E51 negative control. Positive control mRNAs for *Cyclin B* (G) and *twine* (H) are not expressed in the apical tip of the testis (black arrows), or are present in very low levels, and are expressed in primary spermatocytes and sometimes not in post-meiotic cells (black thin arrow). Neither is expressed in the accessory glands.

(I) RT-PCR on separated testes (marked "T") and accessory glands ("A") RNA. Transcript E51 is present only in testes and not in accessory glands (lanes 2, 8 compared to 1, 7). cDNA for *rp49* (lanes 3-4 and 7-8) or β-Tubulin (lanes 5-6) were used as positive controls and show that the same amount of cDNA is loaded in lanes "A" and "T". The lowest band appearing on the gel (not marked) is primer dimers. Lane 9 (n.c.) = negative control; on the left, band size for the Hyperladder I marker bands, in kilobases.

The mRNA for *Cyclin B* and *twine* is not expressed either in the accessory glands (not shown) and its distribution is less ubiquitous than that of E51. No expression (or very little) is observed at the apical tip of the testis with these two genes (Fig.5.5.2G, H- black short arrows). In some testes stained with *CyclinB* there is less expression at the outer edge of the coil, where the postmeiotic cysts are (thin black arrow). It is true that the coil of the testis with the elongating and mature spermatids appears stained for these two genes where it was not reported so (White-Cooper et al, 1998). This could reflect over-staining or high background, but still, since the apical tip, accessory glands and parts of the coil remain unstained for *Cyclin B* and *twine* but the whole of the testis is stained for E51, including consistently the apical tip, it must be of some importance. Time limitations did not allow for repeats of the experiment and optimisation of the protocol, which would enable me to investigate in further detail the exact pattern of E51 mRNA expression in the testis, and possibly compare it with the expression pattern of mRNA for the other *dstpk61* transcripts, to see if and where they may co-localise.

5.5.3 The E51 *dstpk61* transcript is present in the testes but not the accessory glands of adult male flies

To address the subject of whether the *dstpk61* E51 transcript is present in the testes or/and in the accessory glands (although the in situ results suggest it is not expressed in the accessory glands) I used RT-PCR, as a more sensitive method to in situ hybridisation. Until now, in all the testes dissections I was using the pair of testes with the seminal vesicles, the pair of accessory glands and as little of the anterior ejaculatory duct as possible (see Fig. 1.2.2.1 for anatomy), where the other organs were connected. This time, during the dissection I separated the testes and seminal vesicles (marked "T", to distinguish from the term "te" used before) from the accessory glands (marked "A" in Figure 5.5.2I) and isolated total RNA from each. The RT reaction and PCR was done as before, with two template concentrations.

E51 is present only in the testes and not in the accessory glands (Figure 5.5.2I-lanes 1 vs 2; 7vs 8), at either concentration. Primers for *rp49* and *β-Tubulin* (*bTub*) were used as positive controls and demonstrate that equal amounts of cDNA were used from the two tissues (Fig.5.5.2I- lanes 3-4 for *rp49*, lanes 5-6 for *beta-Tubulin* and lanes 7-8 for a multiplex PCR with *rp49* and E51 primers).

	***dstpk61* transcript**		
Conditions:	**E40**	**E09**	**E51**
Tissue-variable expression RT-PCR (A', B' repeats vary for E40, E09)	Ov>FC>>MC=Te (A') Ov>MC>FC≥Te (B') **E69:** equal low level of expression in all tissues	Ov>FC>MC=Te (A') MC≥Ov>>FC>Te (B') Lower expression levels than E40	Te>>>>MC, ov, FC Very consistent High expression levels
In situ hybridisation in ovaries	In nurse cell cytoplasm of stages 10-13	In nurse cell cytoplasm of stages 10-13. Possibly also in germarium region 2b (?) – not clear	In nurse cell cytoplasm of stages 10-13? – not clear staining
Effect of age in different tissues RT-PCR Reproducible	In all tissues, not significant variation with age; in 0-24hr and 6-7 day Testes> 2-4 day old. Ov>=MC≥FC>Te Higher expression levels than E09 (apart from E09 0-24hr FC)	In all tissues, not significant variation in ov, te with age; in FC 0-24hr old>>>2-7 day old; in MC 0-24hr and 4 day>2-3 and 6-7 day old. Overall: Ov>MC>FC>Te (average- but FC 0-24hr old is highest)	Only in testes 0-24hr and 6-7 day-old >>>> 2-3 day and 4 day old. Very high expression levels in very young and old flies
20E Vs JH –treated ovaries RT-PCR	JH> 20E (2.4 times more)	JH > 20E (2.1 times more)	No expression
	Core domain: JH > 20E (2.2 times more) Expression levels: Core> E40>> E09		
Starved Vs Fed flies ovary in situ hybridisation No difference detected since staining is after st.9 apoptosis control point.	In nurse cell cytoplasm of stages 10 onwards, in both fed and starved flies. Also in follicle cell cytoplasm?	Did not work	n/a
	Core domain: In nurse cell cytoplasm of stages 10 onwards, in both fed and starved flies. Possibly staining in follicle cell cytoplasm, too (?) –not clear. No early staining for core or E40.		
Mated Vs virgin male flies – testes RT-PCR Similar pattern obtained with conventional and real-time PCR	n/a	n/a	Dynamic pattern of expression varies with age- opposite trends of expression between mated and virgin males- 2 peaks of high E51 for mated, 3 peaks

			for virgin flies.
Testes in situ hybridisation for E51	n/a	n/a	Ubiquitous E51 expression in the testes- no expression in accessory glands.
Testes Vs accessory glands RT-PCR for E51	n/a	n/a	E51 expression only in testes, not in accessory glands.

Table 5.1 Summary of results for *dstpk61* transcript expression under different conditions
FC: female carcasses; MC: male carcasses; ov: ovaries; te: testes; Vs: versus

5.6 Discussion and future work

5.6.1 The expression patterns of the various *dstpk61* transcripts

The four putative protein isoform-encoding transcripts of *dstpk61* vary greatly in their spatial and temporal expression pattern and their relative levels of expression.

5.6.1.1 E51

E51 mRNA is highly testes-enriched under all conditions tested and its expression in the testes is significantly higher in very young and old flies. There is striking fluctuation of the mRNA in flies of different age, with contrasting expression patterns between mated and non-mated males. The mRNA was shown to be present throughout the adult testis, but was not detectable in the accessory glands by in situ hybridisation. RT-PCR on separated testes and accessory glands verified the specific localisation of E51 in the testis versus the accessory glands. The pattern observed in the mated/non-mated experiment (Fig.5.5.1) does not contradict the early and late pattern of E51 expression in the experiment investigating the effects of age (Fig.5.3.1C); rather, it verifies it. The peaks of E51 expression in the testes of mated day 13 (at 18°C) flies and virgin day 1 plus mated day 3 (at 18°C) flies in the former experiment correspond well to the 6-7 day old (at 25°C) and 0-24hr old (at 25°C) flies with high E51 expression that drops in between age groups of the latter experiment. This is because the *D. melanogaster* life cycle is around 9-10 days at 25°C but extends to around 19-21 days at 18°C (Ashburner, 1989; Greenspan, 1997)

so the age groups mentioned above should be at the equivalent developmental stages. Also, since in the experiment investigating the effects of age I was keeping female and male flies of the same age in the same bottle until dissections, I make the assumption that after 6-7 days (at 25°C) in the presence of females, the E51 expression pattern will reflect that of mated males rather than virgins, and I would not expect to observe any of the peaks of E51 expression in older non-mated flies seen in the mated/non-mated experiment. However, the 0-24hr sample in the experiment investigating the effects of age would include virgin as well as mated flies since male and female flies are sexually immature for several hours after eclosion. Therefore the 0-24 hour high E51 expression could be due to E51 elevated expression in virgin as well as the high expression in mated very young males.

5.6.1.2 E40

The E40 transcript is ovary enriched but is also present at lower levels in female and male carcasses and testes. It generally has higher expression levels than E09 and its expression can be higher in either male or female carcasses, depending on the batch of flies and, presumably, some factor related to the environment that affects the transcriptional levels. Age does not seem to influence E40 mRNA levels of expression significantly, as I observe only minor fluctuations between different age groups for all tested tissues. It is interesting that in the experiment investigating the effects of age E40 expression levels are not much higher in ovaries than in male and female carcasses – testes expression is significantly lower. This only stresses the fact that differences in expression levels for E40 (and E09, see below) between tissues can be subtle and dynamic.

5.6.1.3 E09

Transcript E09 is also present in male and female somatic and gonadal tissues, with the lowest expression levels always in testes and the highest in the ovaries or male carcasses, but varying in level between different batches of flies. Female carcass E09 expression can be either higher or lower than that of male carcasses, but is always lower than ovarian expression. Interestingly, an exception to the lower female

carcass E09 expression levels is that 0-24hr old female fly carcasses express E09 at extremely high levels (compared to the overall expression in all tissues and age groups), dropping dramatically in older flies. To lesser extent, E09 expression in 0-24hr old male carcasses is also high and drops in 1-3-day old tissue, to rise again in 4-day old and drop in 6-7 day old carcasses. Age does not affect significantly E09 expression in ovaries or testes. In all tissues, expression levels of E09 are lower than of transcript E40. This applies also to ovaries under apoptotic or non-apoptotic conditions, (represented by 20E or JH hormone application) where E09, E40 and a core *dstpk61* domain are all expressed in higher levels under non-apoptotic conditions (2.1-2.5 times more than under apoptotic conditions). E09, as well as E40, a core domain, and possibly E51, are localised to the nurse cell cytoplasm of egg chambers of stage 10 and older, as detected by in situ hybridisation in ovaries.

5.6.1.4 E69

Transcript E69, which encodes the putative kinase-inactive, truncated Dstpk61 isoform and belongs to Group 2 transcripts, is detected in equal levels in all tissues tested, and is expressed at much lower levels than the other three transcripts. Its ubiquitous low-level expression verifies earlier observations (MacDougall et al, 1999; Clyde, 1999). I did not persist in its study and worked with the other transcripts, E40, E09 and E51, instead, since it exhibited no spatial differentiation and its sequence is fully included in that of the other transcripts. The core domain probes used for in situ hybridisation and primers used for PCR would pick up E69 transcripts as well as all other *dstpk61* transcripts.

5.6.2 Effects of apoptotic conditions in *dstpk61* transcript expression in oogenesis

Injection of flies with 20-Hydroxyecdysone (20E) and treatment of flies with Juvenile Hormone (JH) was used to induce apoptotic and non-apoptotic conditions, respectively. RT-PCR in the ovaries of these flies showed increased expression of *dstpk61* transcripts E40 and E09 and the core domain, which represents all

transcripts, in JH-treated flies, i.e. in non-apoptotic conditions. Microarray analysis (Terashima and Bownes, 2005) showed that *dstpk61* is suppressed in starved flies (apoptotic conditions) but not when apoptotic conditions are induced by 20E injection. My results are consistent for the three sets of *dstpk61* probes (no E51 was expressed in either condition) with respect to the pattern and scale of differential expression between the two conditions and the difference is only accentuated after normalisation. The varying outcomes of RT-PCR and microarray (Chapter 4) could reflect the different sensitivity of the methods or the analysis used (see also 5.6.3). Confirmation of the RT-PCR results, perhaps using additional positive controls, should clarify the matter.

In adult ovaries, E40 (Group 2 transcripts) mRNA can be seen in the nurse cell cytoplasm of egg chambers of stage 10 onwards (and possibly in the follicle cells but results are not clear). Due to this, relatively late, expression pattern, no differences were seen for E40 or a core *dstpk61* probe in ovaries of starved and fed flies that should be under apoptotic and non-apoptotic conditions, respectively. The checkpoint control for apoptosis is earlier in oogenesis, during stages 8-9 with apoptosis commitment occurring earlier, at stages 5-6.

The fact that E40 protein was observed in all stages of oogenesis in the nurse cell and oocyte cytoplasm and in the follicle cells cytoplasm with a peptide antibody designed against E40 (Chapter 6), leads me to believe that E40 mRNA (if not mRNA of other *dstpk61* transcripts as well) must be expressed earlier on in oogenesis, than what is observed by in situ hybridisation. Two directions can be taken in any future work regarding this project:

For the investigation of how *dstpk61* transcripts are affected under conditions of nutrient deprivation, antibody staining of ovaries of fed and starved flies with the E40-specific antibody I now have should allow detection of the E40 isoform in egg chambers at the developmental stage of interest (st.8-9) and potential differences in protein expression between the non-apoptotic and apoptotic conditions can be observed. Additionally, an RT-PCR approach (since the technique is arguably more sensitive than in situ hybridisation) can be taken to verify if there is expression of

E40 and the other *dstpk61* transcripts in earlier stages of oogenesis and if this changes between apoptotic and non-apoptotic conditions. Ovaries from fed and starved flies or also 20E and JH-treated flies can be dissected further, to first remove stage 10 and later stages egg chambers (which can be kept as a positive control, since *dstpk61* transcripts, perhaps even E51, are detected there) and then from the remaining ovarioles separate the germaria and very early oogenetic stages (up to st.4-5) from stage 5-6 to stage 9 egg chambers. RT-PCR with primers for E40 and E09 on RNA from these separated egg chamber stages should shed light on any differences in expression caused at the time of the apoptosis checkpoint control and confirm the presumed earlier expression of *dstpk61* in oogenesis.

For the improvement of in situ hybridisation experiments, techniques optimised extensively for the *extramacrochaetae* project (Chapter 7) can be adopted for the study of *dstpk61*. Fluorescent in situ hybridisation (FISH) utilising the Tyramide Signal Amplification (TSA) technique (Materials and Methods), optimising conditions for *dstpk61* probes, can help to increase the resolution of in situ hybridisation and allow observation of *dstpk61* mRNA in other stages of oogenesis. Also, use of single-stranded RNA DIG-labelled probes as opposed to the single-stranded DNA-probes used in the current investigation, may improve the results. In the past, double stranded probes for in situ hybridisation were used and it was reported that there was no difference between DNA and RNA *dstpk61* probes, with both giving similar weak signal (Clyde, 1999); hence I had decided to work with DNA probes, changing from double stranded to single stranded ones to include an internal negative control. My work on the *extramacrochaetae* gene (Chapter 7) though, showed dramatic improvement of in situ hybridisation experiments when DNA probes were replaced by RNA probes, when used in conjuction with the TSA amplification method. Therefore, I suggest that use of RNA probes along with TSA amplification for *dstpk61* may also have an impact on the success of *dstpk61* in situ hybridisation experiments. I have already made such RNA probes for all *dstpk61* transcripts (and used the E51 ones for the testes in situ hybridisation) but time restrictions prohibited me from repeating in situ hybridisations for *dstpk61* within the course of this PhD work. Protocol optimisation, through incorporation of RNA

probes and the TSA protocol, can improve both general in situ hybridisation experiments for *dstpk61* transcript distribution and those ones aimed at differential *dstpk61* expression between apoptotic and non-apoptotic conditions.

5.6.3 *rp49*- the importance of normalisation in result interpretation

Internal controls are essential for normalising differences in sample concentration and loading, when comparing RNA levels of the gene under investigation (*dstpk61* here) among different samples for a relative quantification. Thus it is important that the internal control is expressed at constant levels across all samples; the expression of many housekeeping genes that are usually used as controls, such as *β-actin,* or *GAPDH* in mammals, are shown to have different expression levels in different tissues whereas ribosomal RNAs are found to be more similarly distributed among diverse tissues (Ambion Technical bulletin #151, www.ambion.com). The gene encoding ribosomal protein 49 (*rp49*, also known as *RpL32* in Flybase) has been traditionally used in our laboratory as a positive internal control in Northern blot and PCR experiments. It is a single copy gene that is expressed throughout development at constant levels (Aguadé, 1988; Till et al, 1998).

I normalised my results for the quantifications presented as graphs in this chapter by dividing *dstpk61* transcript expression by the relevant *rp49* expression for each sample. The normalisation procedure sometimes had a decisive role on the final results and in other occasions affected the first-observed results only mildly, causing minor changes in the values but not affecting the expression pattern. For instance, when testing E51 mRNA expression in testes versus accessory glands, normalisation did not alter at all the result, since both controls used, *rp49* and *β-Tubulin,* were equally expressed in the two tissues (Fig.5.5.2H). Similarly, had I not normalised for *rp49* in the experiments comparing E51 expression in mated versus non-mated male flies of different age on testes (Fig. 5.5.1), the pattern of the curves in both conditions would have remained the same, only their numerical values and in some occasions the relative distance between the two curves would have changed very slightly. In the

case of ovaries from the JH versus 20E-treated flies *rp49* is expressed much more strongly in 20E ovaries than JH ones. Higher expression levels of *dstpk61* transcripts E09 and E40 are clearly observed in JH samples than in 20E ones (more subtle difference favouring JH treatment in the core domain samples) (Fig. 5.4.1). Normalisation here increased the difference already observed, making the *dstpk61* transcript expression significantly higher in JH- than in 20E-treated samples. In the experiments comparing expression of different *dstpk61* transcripts across tissues normalisation has a bigger impact on the final result, since generally *rp49* was found to be expressed more strongly in the ovaries than in other tissues. This could reflect the fact that ovaries are more transcriptionally active than adult tissues and the final results presented in graphs (Fig. 5.2.1) were corrected for this and other tissue variations. Lack of normalisation would make the E09 transcript expressed in ovaries slightly higher than in male carcasses with female carcasses and testes expression both significantly lower in repeat B'. In both repeats A' and B' the ovary-enrichment for E40 and E09 would be more pronounced, but still both transcripts would show the second highest expression in female carcasses for repeat A' and male carcasses for repeat B'. E51 testes-enriched expression would not be affected, only its value slightly lowered. For the experiment investigating the effect of age (Fig.5.3.1) absence of normalisation would increase relative ovary expression for both E40 and E09 but would not affect age differences for any tissue or relative expression levels in the rest of the results.

Validation of an internal control for each experimental system is recommended (www.ambion.com). I cannot exclude the possibility that *rp49* is not normally expressed in the same levels between males and females, somatic tissue and gonads, or after different treatments of the same tissue. Therefore I suggest that prior to any publication or additional experiments to confirm my results, an experiment using the same conditions and tissues be made with 3-4 replicates for each sample using the *rp49* primers, to evaluate whether *rp49* expression is consistent among different tissues or treatments. Furthermore, additional candidate control genes should be tested, such as *beta-Tubulin*, so that there will be at least one suitable control gene that can be undoubtedly used for normalisation and quantification of the *dstpk61*

results. Nonetheless, as I discussed earlier, I believe that should any problems regarding the use of *rp49* occur, the key observations made regarding expression of *dstpk61* transcripts, namely the testes-enrichment of E51 and its expression pattern relative to fly age and mating state; the expression of E40 and E09 in all tissues, with relative abundance of E40 transcripts and the variation between fly batches; and the up-regulation of E40, E09 and core *dstpk61* under non-apoptotic conditions are not affected. The most likely outcome would be a more definite ovary-enrichment of E40 and E09 transcripts.

5.6.4 Future directions regarding the highly testes-enriched E51 *dstpk61* transcript

As transcript E51, being highly enriched in testes, absent from accessory glands and virtually absent from adult tissues and ovaries and having an intriguing age-dependent expression pattern, severely influenced by whether the fly has mated or not, seems to be the most interesting subject for subsequent study relevant to sex-related *dstpk61* transcripts, there are several approaches for answering key questions about the role of E51 in the testis in the future.

Whether E51 is expressed in the germline or the somatic cells of the testis should be investigated. One way of studying this is through the use of *tudor* (*tud*) mutant flies (Schupbach and Wieschaus, 1986). The progeny of homozygous *tud* female flies do not have germline cells in their gonads. Therefore, in situ hybridisation and RT-PCR in testes of *tud* mutant progeny compared to wild-type *OrR* should determine if E51 is expressed in the germline, in which case E51 should be absent from *tud* RT-PCR, or the somatic cells of the testes, which would result in E51 expression both in *tud* mutant and wild-type testes and in detection of E51 by testes in situ. I attempted to do this experiment, using two *tudor* fly stocks (*tud*^{1} *bw sp/CyO* and *cn tud*^{1} *bw sp/CyO*, both from E. Wieschaus). I was unable to collect enough homozygotes (they were 2-3‰ at best and not surviving long enough to lay eggs) and crossing the two stocks to improve homozygote escaper survival rates by clearing the genetic

background of other mutations did not succeed. The experiment should be attempted on a much larger scale, to improve chances for selection of enough homozygote flies that will survive throughout; time limitations prevented me from doing this. A recent publication by the Fuller group (Schulz et al, 2004) lists an EP line driving expression of *dstpk61* among those causing a reduced number of early male germ cells when forcibly expressed in somatic cyst cells but not in germ cells. EP(3)3091 line has a P-element insertion in the 4th intron of *dstpk61,* with the opposite orientation to that of *dstpk61* transcription (Cho et al, 2001) and thus must disrupt expression of all *dstpk61* transcripts. This observation may indicate that E51 is expressed in somatic rather than in germline cells in the male, but in any case this must be investigated; E40 and E09 (and E69) are also expressed in the testis, albeit at much lower levels, and Schulz et al (2004) observation may depend on their contribution as well.

The in situ hybridisation experiments in the testes must be repeated for E51, to verify the ubiquitous distribution I observed and to clarify the issue of late expression of positive controls *twine* and *Cyclin B*, which is not reported in the literature (White-Cooper et al, 1998); is this real expression, an artefact (and so, also for E51), or caused by potential overexposure or too high probe concentration? They should also be extended to the other *dstpk61* transcripts, E40 and E09, and, together with antibody staining for E40 in testes, should reveal the expression pattern of these *dstpk61* transcripts -and E40 protein- in testes and whether it is the same as for E51 or different. D. Clyde in her PhD thesis (1999) reports expression in spermatocytes along the inner side of the gyre (coil), but not in spermatagonia at the apical tip of adult testes and in spermatocytes, but not spermatagonia in the male larval gonad, using a double stranded DIG-DNA core *dstpk61* probe. The difference with the pattern I observed may be due to the different probes used or the different protocols. In any case the protocols and conditions for testes in situ should be optimised for maximum efficiency and resolution with minimum background staining- the currently used protocol uses RNA probes, and these should be used for the other *dstpk61* transcripts apart from E51, as well. Use of the TSA system mentioned above (and Chapter 7) could be beneficial as well, especially for detection of E40 and E09

in the testes, since both these transcripts expression levels are expected to be significantly lower than those of E51.

In situ hybridisation in the male and female larval gonads with the E51 probe (and potentially the others) can also be informative. Initially this experiment would serve to verify that E51 is male gonad-specific, which, after the work presented here, I believe cannot be doubted much now. The advantage of a male larval gonad in situ hybridisation in the future, provided that the technique is well optimised, would be to study the details of where exactly *dstpk61* is in it- in spermatagonia or cyst progenitor cells, as well as confirming that E51 is expressed during that stage.

Finally, the potential role of E51 transcript and protein in the testis should be investgated. Towards this goal, the expression pattern of E51 mRNA in the testes should be compared with that of other male specific or testes-enriched genes, and genes with a similar pattern should be identified and looked at. Also, a search for genes with age-related or mating-related differential distribution, similar to E51 would identify genes that may be related to the same process or regulated by the same mechanisms as E51. Looking at the 5' UTR and promoter region of *dstpk61* E51 (exon 1c) for specific regulatory elements or consensus sequences may provide useful information. Comparisons with the 5' UTRs of the other *dstpk61* transcripts could show if something present only in E51 5'UTR is potentially important for the transcript localisation and, should some regulatory elements be identified, a search for genes sharing these sequences would be helpful. After identifying genes potentially regulated or expressed in similar ways to E51, an idea of the process or pathway in which it participates, should be apparent. Already, we know that overexpression of *dstpk61* in somatic cyst cells affects the number of germ cells in the testes (Schulz et al, 2004) although it is not certain whether E51 alone is responsible for this. Using mutants for these potential E51-interacting genes can contribute towards understanding the role of E51.

Unfortunately, the *dstpk61* mutants available so far (Cho et al, 2001; Rintelen et al, 2001) are either point mutations in the kinase domain (exon 4) which is common to all *dstpk61* transcripts or P-element insertions affecting again all transcripts, or

deletions of an area affecting more than one transcripts. So no work targeting specifically E51 can be done using these mutants (e.g. for generating mosaic flies). New mutants must be generated for this purpose, targeting specifically exon 1c (point mutations) or its 5'UTR without affecting the expression of other *dstpk61* transcripts. Alternatively, E51 over-expression constructs can be generated, under the regulation of the Gal4-UAS system, or GFP-tagged functional and mutant E51 constructs and fly lines generated by P-element-mediated transformation.

Chapter 6: Protein expression analysis

6.1 Introduction

The detailed study of the different DSTPK61 protein isoforms in an attempt to elucidate the function of each isoform was originally my main priority. The variety of *dstpk61* transcripts (8 according to the 3rd release of the *Drosophila* genomic annotation) encodes, to date, only four different DSTPK61 protein isoforms that vary in their N-termini (Figure 6.1.1). Many of the transcripts vary in their 5' and 3' untranslated regions (UTRs), hence the number of protein isoforms is smaller than that of transcripts.

The four protein isoforms contain all or some of the following domains and motifs: a kinase domain, essential for the role of DSTPK61 as a signalling molecule; a pleckstrin homology domain which is involved in membrane and protein:protein interactions; an OPA repeat/DNA binding domain- OPA repeat domains in *Drosophila* are mainly found in proteins with developmentally restricted expression patterns; nuclear localisation signals; and a mitochondrial intermembrane space targeting sequence (see figure 6.1.1) . It is possible that the isoforms are structured so as to target the protein to different parts of the cell, probably undertaking different functions, and also that specific isoforms are expressed in different tissues or developmental stages (Clyde & Bownes, 2000).

I was particularly interested in the potential role of DSTPK61 in developmental processes, since some of the gene products appeared to be sex-specific (MacDougall et al, 1999) and others tissue-enriched (Chapter 5). My working hypothesis is that different isoforms are necessary for different events, some isoforms being specific for a particular function while others have a more general function. Given that the isoforms are predicted to contain variant localisation signals (DSTPK61^{836}/E40 has a mitochondrial targetting sequence in addition to the nuclear localisation signal common to all isoforms), it is possible that locating the protein to different subcellular compartments might ensure that it interacts in one signalling pathway rather than another. Another hypothesis is that low levels of kinase activity could be needed for cell growth and higher levels for sex-specific events.

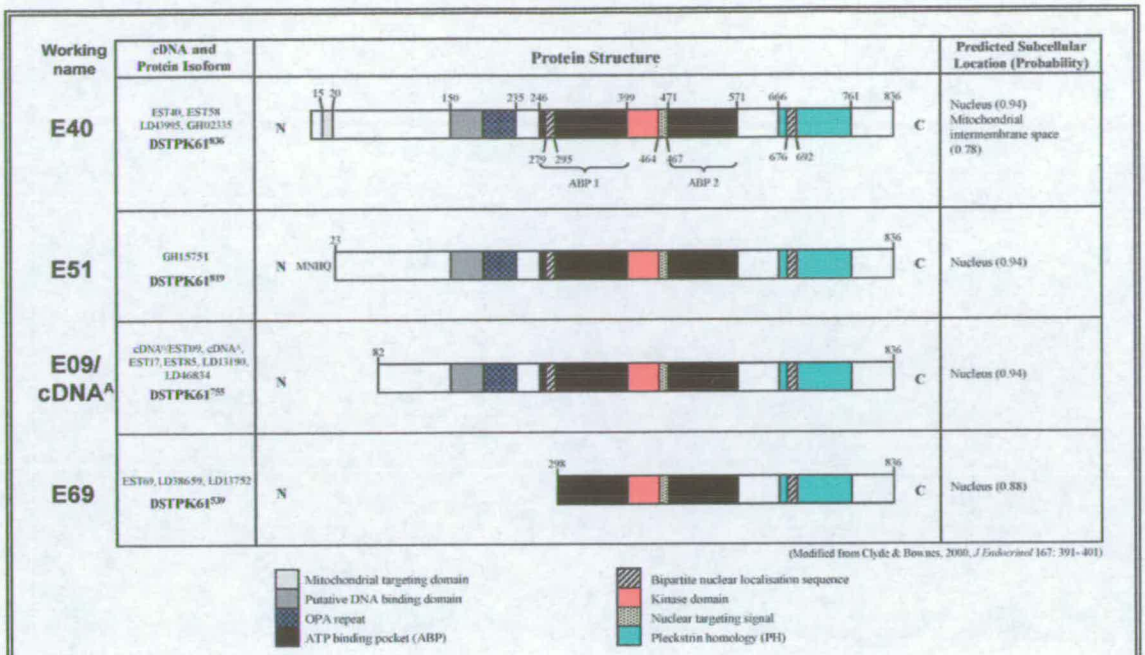

Figure 6.1.1 Structure of the four predicted DSTPK61 isoforms
The main *dstpk61* EST cDNAs encoding these isoforms and the original name of each isoforms are given in the second column. The names I am using here to refer to the DSTPK61 isoforms are in the first column, under "Working name". The motifs and domains of the proteins are coded according to the key above. The drawing is from Clyde and Bownes, 2000, with minor corrections and modifications.

To test these hypotheses, I aimed to express all four DSTPK61 isoforms to investigate if they are all enzymatically active (it has been suggested that the truncated E69 isoform may be kinase-inactive and act as a competitive inhibitor of kinase-active isoforms – Clyde, 1999) and if they all participate in the same signalling pathways (i.e. do they all have the same substrates?), by kinase activity assays. To determine the temporal and spatial expression profiles of the different isoforms in development and their location within the cell, antibodies should be raised against each isoform.

6.2 Antibodies against DSTPK61

6.2.1 The existing anti-DSTPK61 is non-specific

An antibody against DSTPK61 had been generated in our laboratory, prior to the beginning of my project, using a recombinant protein with the $cDNA^{A}$ sequence as the immunogen (D. Clyde, N. Dzhindzhev). The antibody was raised in sheep. I used this antibody initially in all my experiments to monitor the expression of the DSTPK61 isoforms from bacterial cells carrying the appropriate expression vector (see section 6.3) and to detect DSTPK61 in different fly tissues by Western blot. With the generation of more, isoform-specific, antibodies against DSTPK61 pending, this was the only available antibody recognising the *Drosophila* DSTPK61 sequence. One anti-PDK1 against the human protein was available at the time, and several are available now; however, these antibodies are designed against peptides from sequences (usually the C-terminal end) that are conserved among mammals but not between mammals and *Drosophila*, so they could not be used for my study.

Western blot analysis on wild-type (Oregon-R) fly tissues with anti-DSTPK61 antibody did not give a clear picture (Figure 6.2.1). Whole male and female adult flies, male and female carcasses without gonads, ovaries and testes were used. The protein expression patterns in each tissue were different (Fig. 6.2.1A), but it was obvious that the antibody we have is not DSTPK61-specific as it recognised an array of other proteins. I believed however that it is likely to be kinase-specific since it did not simply react with all the proteins present on the membrane or even the most abundant proteins (Fig.6.2.1A); instead it interacted strongly with proteins that were not abundant (Fig. 6.2.1B, bands labelled with +) indicating that is has some degree of antigen specificity.

It was clear from the Western blot analyses that our existing antibody was not suitable for further investigation as it is not specific for DSTPK61 and it certainly cannot be used for immunohistochemistry. Even for identification of DSTPK61 isoforms under denaturing conditions as in a Western blot, results such as those in figure 6.2.1 do not allow for matching specific isoforms with specific tissues

unambiguously. It was later found out that the anti-DSTPK61 antibody was actually raised against the kinase domain of cDNA[A] (Nikola Dzhindzhev, personal communication), which explains the multitude of bands observed in Western blot, since it would recognise at least conserved serine/ threonine protein kinases or ACG family kinases, in which DSTPK61 belongs.

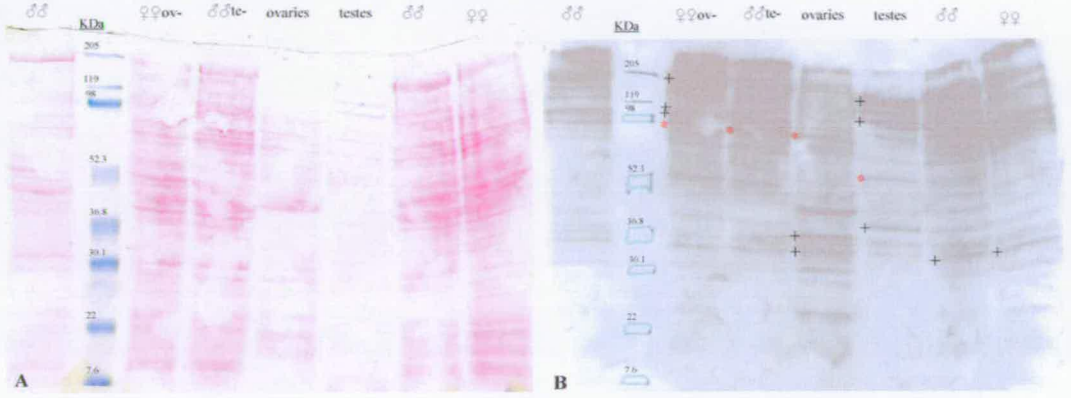

Figure 6.2.1 Western blot on fly tissues with anti-DSTPK61 antibody
(A) Ponceau S staining of the membrane after proteins had been transferred from the SDS-polyacrylamide gel and (B) the protein pattern after Western blot with the anti-DSTPK61 existing antibody. The bands that give the strongest signal are not always the more abundant proteins. Indicated with + are the non-abundant bands that give a strong signal (B) but the protein was not expressed at such high level (A). A red asterisk (*) indicates bands that are probably DSTPK61 isoforms (according to their size). ♂♂, males; ♀♀, females; ♂♂te-, male carcasses; ♀♀ov-, female carcasses.

In Western blots for monitoring the expression of the DSTPK61 isoforms by bacterial cells upon induction (Fig. 6.3.3), the lack of specificity of anti-DSTPK61 was compensated for, in some degree, by stripping the membrane and hybridising with an anti-GST antibody. In this way the bands representing DSTPK61 were recognised indirectly, since only the fusion proteins overexpressed by the plasmid construct would contain GST (Glutathione S-Transferase) (section 6.3.1).

One way of making this antibody more useful is to purify it by affinity chromatography. For this to be done though, the protein isoforms should be expressed (which was not eventually achieved during the course of this study-section 6.3) so that there will be DSTPK61 protein available to be used in a column for the antibody to bind to. Another method of antibody purification would be to use

another serine/threonine protein kinase to block the anti-DSTPK61 antibody with; a small fraction of the serum antibodies, containing DSTPK61-specific, non- kinase recognising antibodies should be left. Protein kinase B (PKB) has already been used to block anti-DSTPK61 (C. Fonfara, practical term project, 2000) without increasing the antibody specificity.

6.2.2 Design of peptide antibodies

Isoform specific antibodies are necessary in order to investigate the localisation of each isoform in various tissues and developmental stages. To address my needs for isoform-specific antibodies, the options were either to create constructs containing specific domains of each isoform, such as the amino-terminal domains of the longest isoforms E40 and E51, to be used as antigens, or to design synthetic peptide antigens for the isoform-specific domains. Given that the four potential DSTPK61 isoforms encode the same protein and only have variant N-termini, it is not possible to obtain a sequence that will be unique for each isoform. E40 has an amino-terminal 22 amino acid- long unique sequence, E51 has only five unique amino acids, MNIIQ, at the N-terminal and the entire sequence of E69 is contained in that of the other three isoforms, and the entire sequence of E09 lies within the sequence of E40 and E51 (Figure 6.1.1). Thus I could only design isoform-specific antibodies for isoforms E40 and E51. Ideas for other antibodies include an antibody specific for a region within amino acids 82-298 of the protein sequence (where a putative DNA binding domain and the OPA repeat domain are located) to recognise also E09 and one specific for a domain common to all isoforms, possibly the PH domain or a non-domain-containing region to ensure the antibody will be specific only for DSTPK61.

I selected several parts of the sequence that would be appropriate for synthetic peptide design, to be used as antigens (Angeletti, 1999). The amino acid sequence and their position within DSTPK61 sequence is shown in figure 6.2.2.

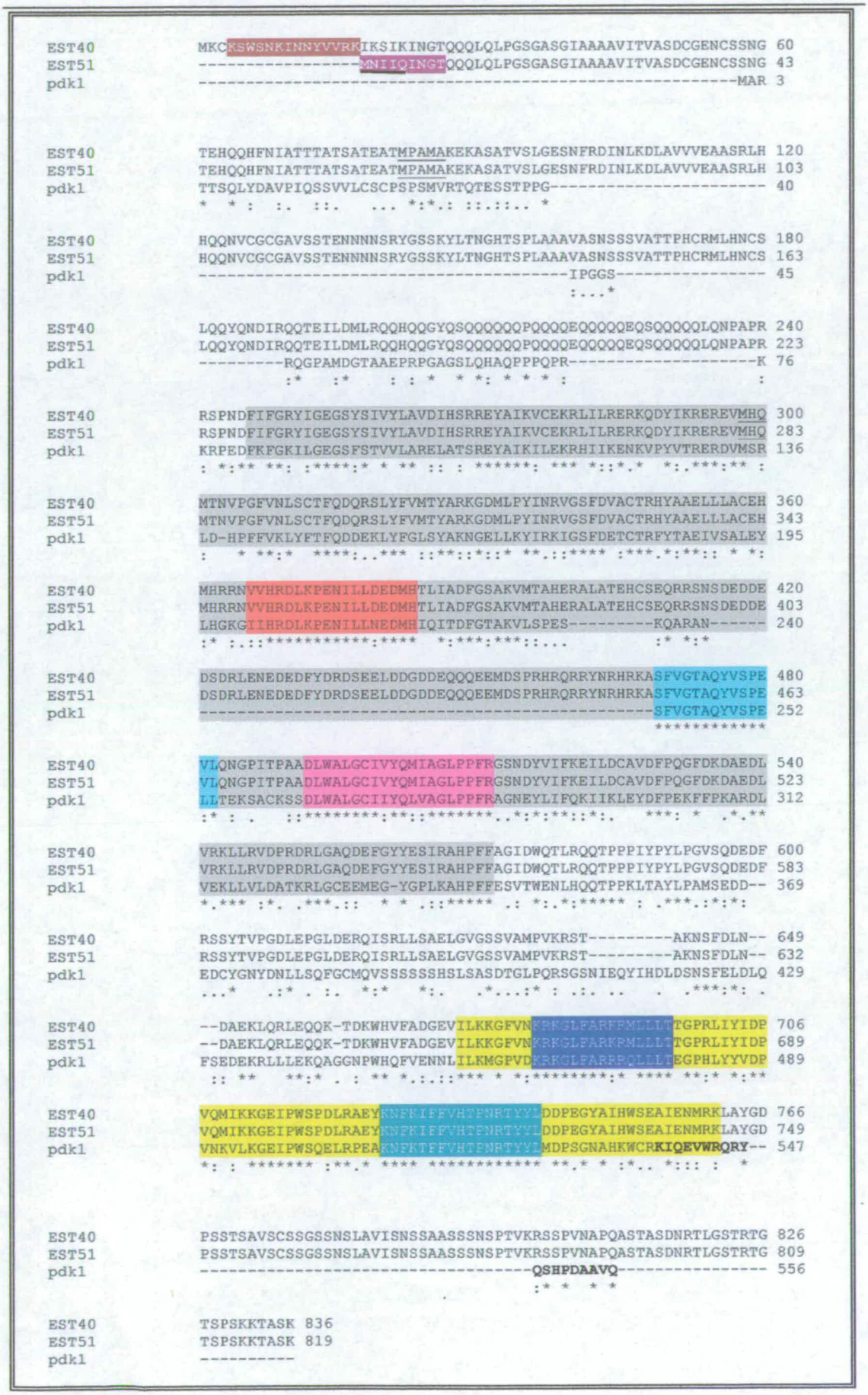
EST40 MKCKSWSNKINNYVVRKIKSIKINGTQQQLQLPGSGASGIAAAAVITVASDCGENCSSNG 60
EST51 ----------MNIIQINGTQQQLQLPGSGASGIAAAAVITVASDCGENCSSNG 43
pdk1 ----------MAR 3
EST40 TEHQQHFNIATTTATSATEATMPAMAKEKASATVSLGESNFRDINLKDLAVVVEAASRLH 120
EST51 TEHQQHFNIATTTATSATEATMPAMAKEKASATVSLGESNFRDINLKDLAVVVEAASRLH 103
pdk1 TTSQLYDAVPIQSSVVLCSCPSPSMVRTQTESSTPPG---------- 40
EST40 HQQNVCGCGAVSSTENNNNSRYGSSKYLTNGHTSPLAAAVASNSSSVATTPHCRMLHNCS 180
EST51 HQQNVCGCGAVSSTENNNNSRYGSSKYLTNGHTSPLAAAVASNSSSVATTPHCRMLHNCS 163
pdk1 ----------IPGGS---------- 45
EST40 LQQYQNDIRQQTEILDMLRQQHQQGYQSQQQQQQPQQQQEQQQQQEQSQQQQQLQNPAPR 240
EST51 LQQYQNDIRQQTEILDMLRQQHQQGYQSQQQQQQPQQQQEQQQQQEQSQQQQQLQNPAPR 223
pdk1 ---------RQGPAMDGTAAEPRPGAGSLQHAQPPPQPR----------K 76
EST40 RSPNDFIFGRYIGEGSYSIVYLAVDIHSRREYAIKVCEKRLILRERKQDYIKREREVMHQ 300
EST51 RSPNDFIFGRYIGEGSYSIVYLAVDIHSRREYAIKVCEKRLILRERKQDYIKREREVMHQ 283
pdk1 KRPEDFKFGKILGEGSFSTVVLARELATSREYAIKILEKRHIIKENKVPYVTRERDVMSR 136
EST40 MTNVPGFVNLSCTFQDQRSLYFVMTYARKGDMLPYINRVGSFDVACTRHYAAELLLACEH 360
EST51 MTNVPGFVNLSCTFQDQRSLYFVMTYARKGDMLPYINRVGSFDVACTRHYAAELLLACEH 343
pdk1 LD-HPFFVKLYFTFQDDEKLYFGLSYAKNGELLKYIRKIGSFDETCTRFYTAEIVSALEY 195
EST40 MHRRNVVHRDLKPENILLDEDMHTLIADFGSAKVMTAHERALATEHCSEQRRSNSDEDDE 420
EST51 MHRRNVVHRDLKPENILLDEDMHTLIADFGSAKVMTAHERALATEHCSEQRRSNSDEDDE 403
pdk1 LHGKGIIHRDLKPENILLNEDMHIQITDFGTAKVLSPES---------KQARAN------ 240
EST40 DSDRLENEDEDFYDRDSEELDDGDDEQQQEEMDSPRHRQRRYNRHRKASFVGTAQYVSPE 480
EST51 DSDRLENEDEDFYDRDSEELDDGDDEQQQEEMDSPRHRQRRYNRHRKASFVGTAQYVSPE 463
pdk1 ----------SFVGTAQYVSPE 252
EST40 VLQNGPITPAADLWALGCIVYQMIAGLPPFRGSNDYVIFKEILDCAVDFPQGFDKDAEDL 540
EST51 VLQNGPITPAADLWALGCIVYQMIAGLPPFRGSNDYVIFKEILDCAVDFPQGFDKDAEDL 523
pdk1 LLTEKSACKSSDLWALGCIIYQLVAGLPPFRAGNEYLIFQKIIKLEYDFPEKFFPKARDL 312
EST40 VRKLLRVDPRDRLGAQDEFGYYESIRAHPFFAGIDWQTLRQQTPPPIYPYLPGVSQDEDF 600
EST51 VRKLLRVDPRDRLGAQDEFGYYESIRAHPFFAGIDWQTLRQQTPPPIYPYLPGVSQDEDF 583
pdk1 VEKLLVLDATKRLGCEEMEG-YGPLKAHPFFESVTWENLHQQTPPKLTAYLPAMSEDD-- 369
EST40 RSSYTVPGDLEPGLDERQISRLLSAELGVGSSVAMPVKRST---------AKNSFDLN-- 649
EST51 RSSYTVPGDLEPGLDERQISRLLSAELGVGSSVAMPVKRST---------AKNSFDLN-- 632
pdk1 EDCYGNYDNLLSQFGCMQVSSSSSSHSLSASDTGLPQRSGSNIEQYIHDLDSNSFELDLQ 429
EST40 --DAEKLQRLEQQK-TDKWHVFADGEVILKKGFVNKRKGLFARFFMLLLTTGPRLIYIDP 706
EST51 --DAEKLQRLEQQK-TDKWHVFADGEVILKKGFVNKRKGLFARFFMLLLTTGPRLIYIDP 689
pdk1 FSEDEKRLLLEKQAGGNPWHQFVENNLILKMGPVDKRKGLFARRFQLLLTTEGPHLYYVDP 489
EST40 VQMIKKGEIPWSPDLRAEYKNFKIFFVHTPNRTYYLDDPEGYAIHWSEAIENMRKLAYGD 766
EST51 VQMIKKGEIPWSPDLRAEYKNFKIFFVHTPNRTYYLDDPEGYAIHWSEAIENMRKLAYGD 749
pdk1 VNKVLKGEIPWSQELRPEAKNFKTFFVHTPNRTYYIMDPSGNAHKWCRKIQEVWRQRY-- 547
EST40 PSSTSAVSCSSGSSNSLAVISNSSAASSSNSPTVKRSSPVNAPQASTASDNRTLGSTRTG 826
EST51 PSSTSAVSCSSGSSNSLAVISNSSAASSSNSPTVKRSSPVNAPQASTASDNRTLGSTRTG 809
pdk1 ----------QSHPDAAVQ---------- 556
EST40 TSPSKKTASK 836
EST51 TSPSKKTASK 819
pdk1 ----------

Figure 6.2.2 Protein sequence of *Drosophila* DSTPK61 E40 and E51 isoforms and human PDK1, with potential peptide antigens shown
Alignment of protein sequence of *Drosophila* DSTPK61 isoforms E40, E51 and human PDK1. The beginning of the DSTPK61 isoforms other than E40 is underlined; MNIIQI for EST51, MPAMA for cDNA[A] (EST09), MHQ for EST69. The colour code is as follows:
Highlighted with:
grey: Serine/Threonine protein kinases catalytic domain (as determined by SMART for E40- http://smart.embl-heidelberg.de/)
yellow: Pleckstrin homology domain
dark red: Peptide antigen specific for E40
violet: Peptide antigen specific for E51
red: candidate 1
turquoise: candidate 2
pink: candidate 3
blue: candidate 4
green: candidate 5
bold: PDK1 peptide antigen commercially available
Candidates 1-3 are within the kinase domain, 4-5 are within the PH domain.
All candidates are common to all 4 isoforms of DSTPK61.

The peptides designed for E40 and E51 contain, apart from the highlighted sequence in figure 6.2.2, a Cysteine residue at their carboxy-terminal end to facilitate conjugation with a carrier protein. In general, synthetic peptides need to be conjugated to a suitable highly immunogenic carrier protein (usually KLH or BSA) to ensure that an immunogenic response will occur when the peptide coupled to the carrier will be injected to the host for antibody production.

All peptides designed were checked for similarity or identity with other unrelated proteins using the BLAST programme (both for nucleotide and amino acid sequence) and searching the available databases (http://www.ncbi.nlm.nih.gov/BLAST/). The peptides for E40 and E51 are not contained in any other known protein. The five peptides termed candidates 1-5 were designed to recognise both *Drosophila* DSTPK61 and human PDK1, and they represent all possible sequence regions that have high homology between the two species. From those candidates, the 1st and 3rd are not suitable for a peptide antigen because they are recognised by many other kinases apart from PDK1 homologues. Apparently these regions are conserved not only between species but also within the kinase family. Candidates 2, 4 and 5 are specific for DSTPK61 and its mammalian homologues. Candidate 2 lies within the kinase domain but since it does not contain enough charged residues, some

modifications should be made on the sequence to obtain a good antigen. According to its sequence, candidate 4 should be a good antigen and candidate 5 contains a marginal number of hydrophilic residues, which may not be sufficient for production of a soluble peptide. Both of these potential antigens are in the Pleckstrin Homology domain of DSTPK61. With respect to the isoform specific peptides, the peptide sequence selected for E40 should provide a satisfactory antigen, but the sequence for E51 is problematic, as it contains many hydrophobic residues which will decrease peptide solubility and may not allow production of antibodies against its epitope. In the case of E51 it would not sensible to proceed with the production of a synthetic peptide and production of an antibody that will most likely not be useful. Indeed, the E51 unique peptide sequence was verified as being unsuitable for production of a peptide antibody by experts in protein synthesis (Dr Lu Jaing, Edinburgh Centre for Protein Technology - Albachem, personal communication). Designing a construct that will contain a bigger part of the N-terminus of E51, expressing this fusion protein and using it as an immunogen would be a more advisable choice.

6.2.3 Production, verification and use of the E40 antibody

6.2.3.1 Peptide synthesis and rabbit immunisation programme

The synthesis of the peptide for E40, used as an antigen after conjugation to BSA (bovine serum albumin) and the production of the antibody against DSTPK61 E40 were undertaken by Sigma. Pre-immune serum from the two rabbits used for the antibody production was isolated and sent to me for control purposes. The animals were immunised six times with the antigen and serum was collected four times, seven days after each of the final four antigen injections, during a 77-day protocol (www.sigma-genosys.co.uk/custom_antisera/). The E40 peptide (Fig. 6.2.3A for its relative position) that was not used for immunisation was sent to me and it could be used for control experiments and potentially for affinity purification of the antibody.

6.2.3.2 Control experiments with anti-E40 serum

Western Dot-Blot analysis was used to test the serum from each bleed and the pre-immune serum. The E40 peptide used as an antigen for immunisation of the animals (6μg/slot – in TBS buffer), bacterial cell lysate from XL1Blue cells in TBS (control) and TBS buffer (negative control) were spotted onto nitrocellulose membranes. The membranes were incubated either with the pre-immune serum or with serum from the immune bleed (all four immune bleeds were tested (not shown) with similar results - results from the dot blot with the second immune bleed are shown in Figure 6.2.3B) at various concentrations. The westerns were processed as described in Materials and Methods (Chapter 2).

The dot-blots confirm that only the immune bleed reacts with the antigen peptide (Figure 6.2.3B). Both animals react with bacterial lysate, but animal A at a higher level than animal B. This indicates that the immunised rabbits must have had some infections in the past and had produced antibodies against bacterial proteins; these antibodies were present in their blood. The serum contains all isotypes of immunoglobulins (IgG, IgA, IgM) as it is unpurified. Having animals with some antibody background is not uncommon; one of the advantages of using two or more animals to produce an antibody is that the "cleaner" animal serum can be used, i.e. the serum that presents the highest response against the antigen combined with the lowest background (better signal-to-noise ratio). In my case, the serum from animal B was used in all subsequent experiments (Fig. 6.2.3B, better signal-to-noise ratio) and specifically the serum from the second and third bleeds, as these had the strongest signal and lowest background from all four bleeds. The serum was blocked by incubation with BSA before use (BSA was used as a carrier protein and anti-BSA antibodies had a strong presence in the serum-not shown), to minimise background. Also, when used on fly tissues, bacterial cell lysate was also used to block the antibody and minimise non-specific background.

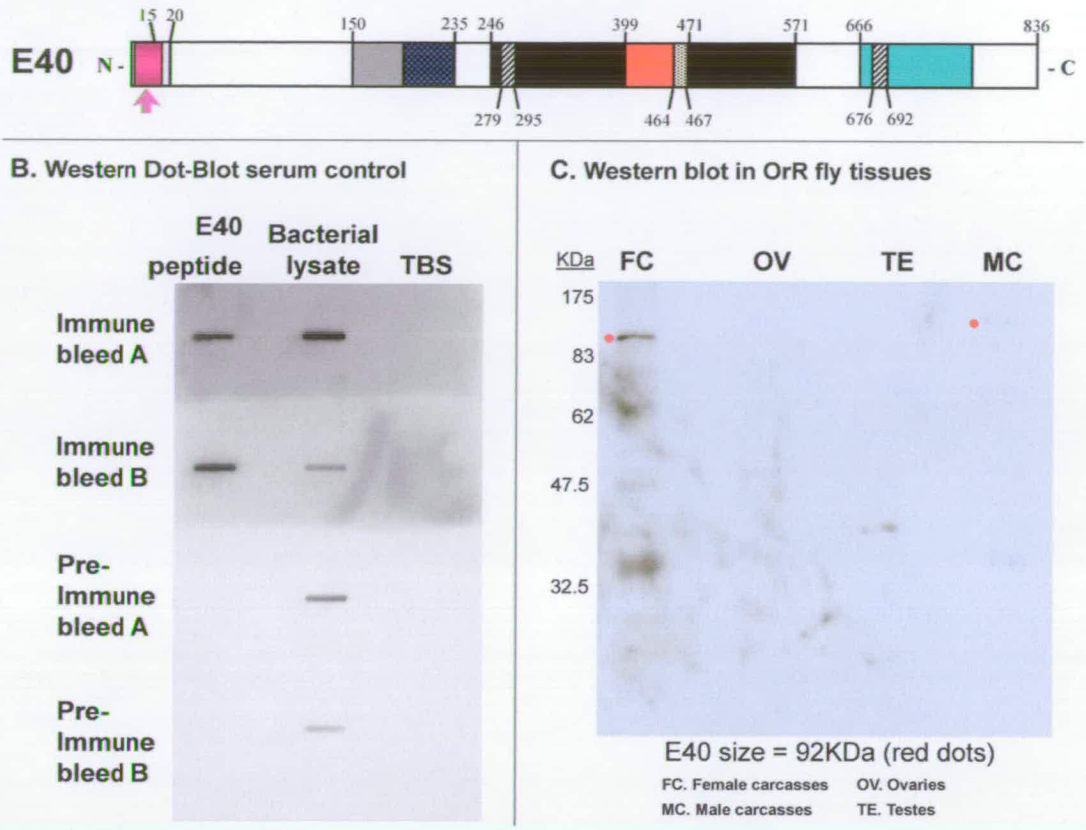

Figure 6.2.3 Western blots with the E40 antibody and its position
(A) The purple colour and arrow point to the amino acid sequence of the E40 isoform that was used to generate an antibody.
(B) Serum from both animals A and B contains antibody recognising the E40 peptide which was used as an antigen after the immunisation (top two rows, left) but not before (bottom two rows, left). The serum of both animals contains also antibodies against other proteins (signal in the bacterial lysate lanes, centre), with a higher background for animal B than for A. Buffer TBS was used as a negative control. Serum was used at 1:500 in TBS.
(C) A band corresponding to the size of E40 DSTPK61 isoform is detected in female and male carcasses by western blot with the E40 antibody (serum from animal B, which has a better signal-to-noise ratio). Other bands of lower MW that are detected may represent E40 degradation products or unrelated proteins recognised by other antibodies contained in the serum.

6.2.3.3 Detection of wild-type E40 in adult tissues with the new antibody

To test if the E40-specific new antibody would be capable of recognising the wild-type E40 DSTPK61 protein from *Drosophila* tissues, I prepared protein extracts from *OrR* male and female carcasses, ovaries and testes (see Materials and Methods). The

proteins were separated by SDS-PAGE and transferred to a PVDF membrane. The membrane was blocked in Blocking buffer and the anti-E40 SBB (second bleed from animal B) serum, pre-blocked with two volumes XL1Blue cell lysate and 3 volumes BSA (1.5μg/μl) was added at 1:20000 in TBS. The membrane was washed and then incubated with the secondary antibody (anti-Rabbit IgG conjugated with HRP, used at 1:4000), followed by ECL detection.

The antibody recognised a protein of the expected size for wild-type E40 in male and female carcasses (Figure 6.2.3C, bands marked with red dots). This band was not recognised in ovaries or testes [however, the E40 antibody reacted with ovary and testes protein lysates in a Dot blot- not shown]. Background was generally low (in contrast to when the antibody was used in bacterial cell cultures to monitor the expression of recombinant proteins, where background was very high -not shown), with a few lower MW bands recognised, that may represent degradation products.

6.2.3.4 Immunolocalisation of DSTPK61 E40 in *Drosophila* ovaries

Antibody staining with anti-E40 serum in *OrR* ovaries (method described in Chapter 2) showed a ubiquitous expression of DSTPK61 E40 protein isoform in nurse cell and follicle cell cytoplasm in all stages of oogenesis (Figure 6.2.4B-G). Stronger expression is observed in the cell membrane of nurse cells (Fig. 6.2.4E) and nurse-cell-associated (or stretched) follicle cells (Fig. 6.2.4F) and corresponds well to the function of DSTPK61 as a protein kinase docked to the cell membrane via its Pleckstrin Homology domain binding to PIP3 at the membrane (Alessi et al, 1997a). Staining was also observed in the oocyte cytoplasm, mainly visible in early stage egg chambers (Fig. 6.2.4B-C, early stages) before yolk accumulation in the oocyte.

This staining pattern was consistent and was never observed when the pre-immune serum was used (Fig. 6.2.4A) or when only the secondary, FITC-conjugated antibody was used (not shown) as negative controls.

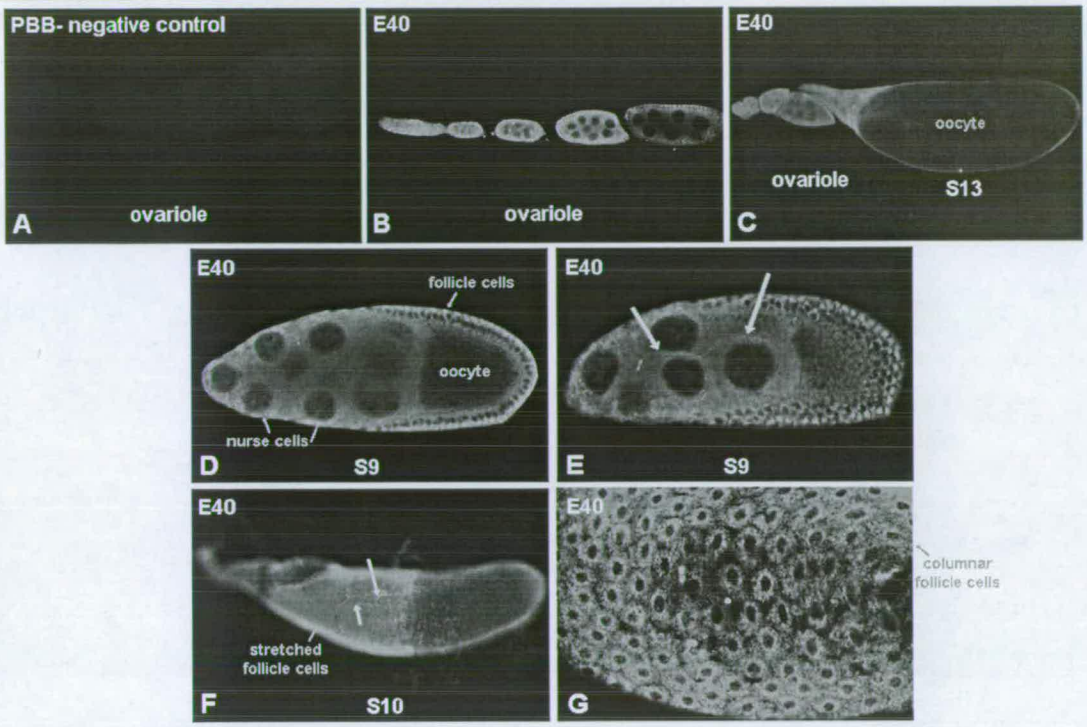

Figure 6.2.4 DSTPK61 E40 expression during *Drosophila* oogenesis
Antibody staining with anti-E40 and a FITC-labelled secondary antibody was used to detect the position of E40 protein isoform in wild-type *OrR* ovaries. Pictures were taken in a Leica confocal microscope.
(A) The pre-immune bleed serum (PBB) gave no staining, consistent with its absence of recognition of the E40 peptide in Dot-blots.
(B-G) E40 indicates that the immune serum containing anti-E40 antibody was used. S9, S10, S13 or ovariole correspond to the stage of oogenesis or cover the stages from germarium to stage 8, respectively. Staining is observed throughout oogenesis in the somatic follicle cell (B-G) and the germline nurse cells (B-E) and oocyte (B-C) cytoplasm. Large white arrows in (E) and (F) indicate E40 staining in the cell membranes between nurse cells and stretched follicle cells over the nurse cells, respectively.

6.3 Expression of DSTPK61 protein isoforms

6.3.1 GST-tagged constructs

For the biochemical assays of different DSTPK61 isoforms, the full-length protein isoforms needed to be expressed, isolated and purified. I was utilising the GST- gene fusion system (Pharmacia Biotech) for the chemically induced protein expression in *E.coli*.

6.3.1.1 Work with the existing protein expression constructs

One of the isoforms (cDNA^{A}) had already been expressed, used in biochemical assays and used to make the anti-DSTPK61 antibody (Alessi et al, 1997b) and a second (E69) was expressed but could not be purified at the time. Constructs for the remaining two isoforms (E40 and E51) had been made in our laboratory before the beginning of this study (Tim Wood, Omanma Adighibe).

The method used for the creation of constructs, summarised in Figure 6.3.1, involves the amplification of the DNA copy of the insert contained within the appropriate library plasmid via PCR, using primers that recognise the ends of the open reading frame and contain restriction endonuclease recognition sites. The PCR product is digested with these restriction enzymes, as is the expression vector, to create sticky ends in their sequence so as to allow ligation of the insert and the vector. The expression vector used (pGEX-3X) is designed for inducible, high-level intracellular expression of genes as fusions with glutathione-S-transferase (GST). Fusion proteins can be purified upon binding to glutathione-sepharose or glutathione-agarose beads and subsequently eluted by their higher affinity for reduced glutathione present in the elution buffer; they can be detected by enzymatic (with CDNB, a GST substrate) or immunological assay (using anti-GST antibodies).

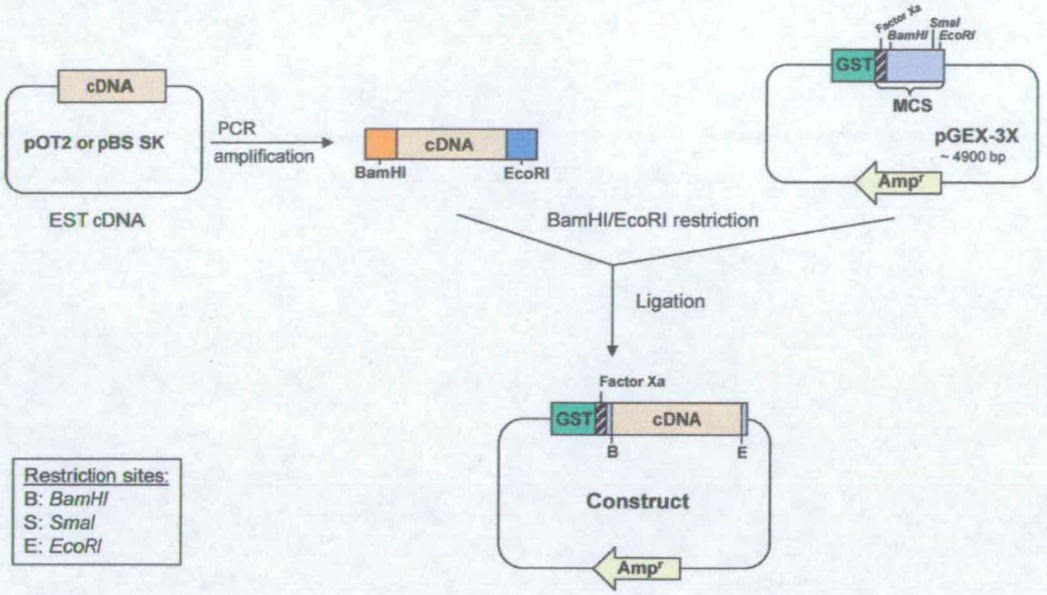

Figure 6.3.1 Generation of GST-fused constructs for protein expression
cDNA from the appropriate EST was amplified by PCR with primers that introduce enzyme cutting sites. Both the PCR fragment and the expression vector (pGEX-3X here) which has the GST coding sequence next to the multiple cloning site (MCS) are digested with the appropriate enzymes and ligated, so that the cDNA is in frame with GST. This construct is transformed into bacterial cells and the GST-fused protein can be expressed at high levels upon induction with IPTG.

I sequenced the 5' and 3' ends of the constructs for E40 and E51 which were made last, to check if the insert is in the same open reading frame as the vector, to make sure that the protein of interest will be expressed. The inserts in both cases were in frame with the vector. Three base substitutions were observed for E40; these lead to amino acid substitutions Q155/H in exon 2 before the kinase domain and E684/G and F700/L substitutions in exon 5 in the PH domain. Four amino acid substitutions were observed for E51 (S147/G and HEH183-185/QQR at the 5'-end – exon 2); also a stop codon was introduced at the 3'-end in exon 6, which would result in a protein 98 amino acids shorter than E51 (Summarised in Figure 6.3.2). There is a possibility that some of the nucleotide changes may represent polymorphisms; checking for that though was beyond the scope of my study. These substitutions were not in an important protein region, and even the shorter E51 caused by introduction of a stop codon would probably still be suitable for antibody production and kinase assays, so at the beginning it was decided to proceed with these constructs.

Subsequently, I had been trying to optimise conditions for protein expression, experimenting with different temperatures and time allowed for bacterial growth, concentration of IPTG used to induce protein expression and different methods for cell lysis, including varying the length and power of sonication and different lysis buffers (Table 6.3.1).

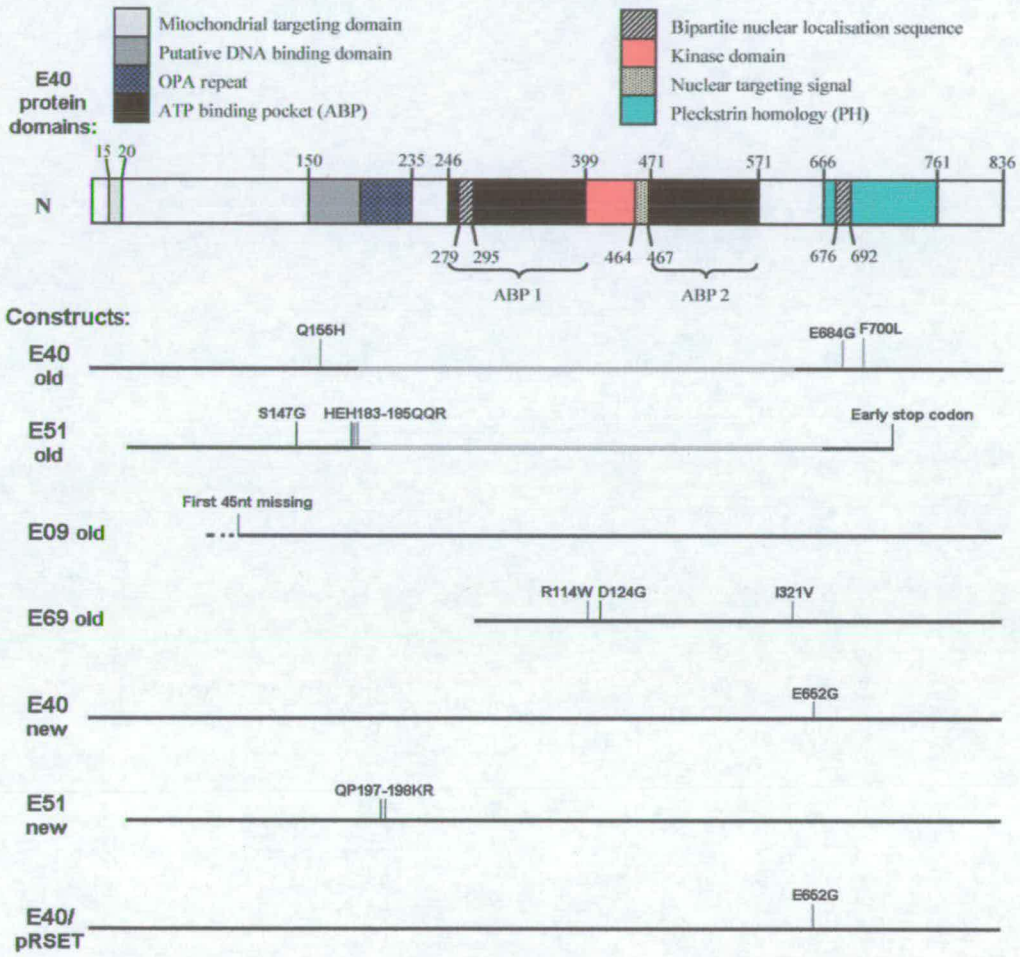

Figure 6.3.2 Sequencing of all used protein expression constructs and amino acid substitutions occurring

The E40 (longest) DSTPK61 isoform with the relative positions of various domains on it is shown at the top (from Clyde and Bownes, 2000).

At the bottom, each horizontal line represents the sequence of the DSTPK61 component of each fusion protein expression construct. The first 6 are GST-fused and the last one (E40/pRSET) is 6xHis-fused. All constructs are in frame with their tag and the fusion protein can be expressed.

The grey region in E40 old and E51 old lines indicates the part of the construct that was not sequenced.

For all other constructs, the nucleotide substitutions that lead to amino acid substitutions are listed; the amino acid change is indicated for each substitution using the single letter code as original amino acid-its position in the isoform protein sequence- new amino acid. nt: nucleotides (the change in E09 old construct corresponds to a 15 amino acid shorter protein at the N-end).

The expected molecular weight of the GST-DSTPK61 fusion protein is 118 KDa for E40, 117KDa for E51 (106.1 KDa if truncated due to the new stop codon), 109.9 KDa for E09 and 85.9 KDa for E69. However, only E69- (which is over-expressed even in uninduced cells – there is leaky expression of this construct) and E09-expressing cells had a product of the size anticipated for the fusion protein. E51 had GST-fused proteins of smaller size than expected (Figure 6.3.3B), but previously in a similar experiment it contained a fusion protein of the correct size (Figure 6.3.4). E40 though, repeatedly showed a band of approximately 75 KDa as the major product, indicating that DSTPK61 fused to GST is truncated in this case. For all four isoforms there were additional GST-DSTPK61 bands on the gel (figure 6.3.3C), which probably represent degraded versions of the protein or different phosphorylation levels which would alter the speed at which each protein runs. As mentioned earlier, the only method to distinguish which of all these bands represent DSTPK61 is indirect, by stripping the filter membrane and hybridising it with an anti-GST antibody. Since only the fusion protein over-expressed by the plasmid construct will contain GST, the proteins bound to the membrane that are recognised by both antibodies are the DSTPK61 isoforms.

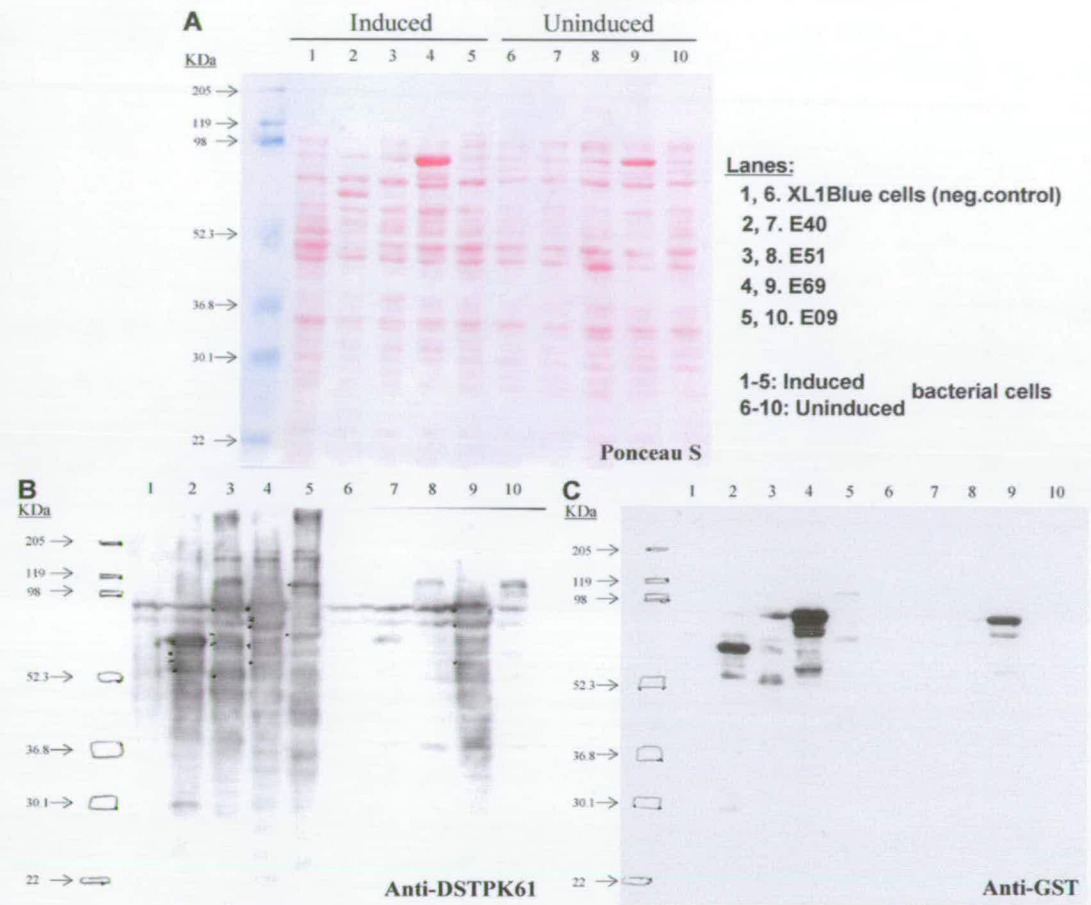

Figure 6.3.3 Western blot analysis of the four expressed DSTPK61 isoforms
(A) Ponceau S staining of the nitrocellulose membrane shows the proteins present on the membrane. Proteins recognised by the anti-DSTPK61 antibody are shown in (B) and those recognised by the anti-GST antibody in (C). The bands marked with a dot in (B) are the proteins also recognised by the anti-GST antibody and must correspond to DSTPK61 GST-fusion proteins and their degradation products.

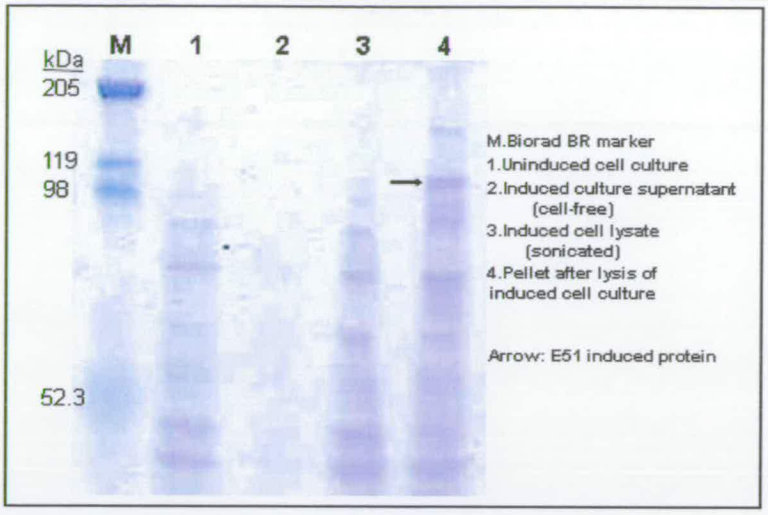

Figure 6.3.4 SDS-PAGE for E51 expressed in XL1Blue cells
A protein with a MW between 100-115 kDa, most likely E51, is expressed following IPTG induction (arrow). The protein remains in the pellet after cell lysis (lane 4) and is absent from the cell lysate (lane 3) that would be used for protein purification. This indicated that a different protocol should be employed, to achieve isolation of soluble induced fusion proteins.

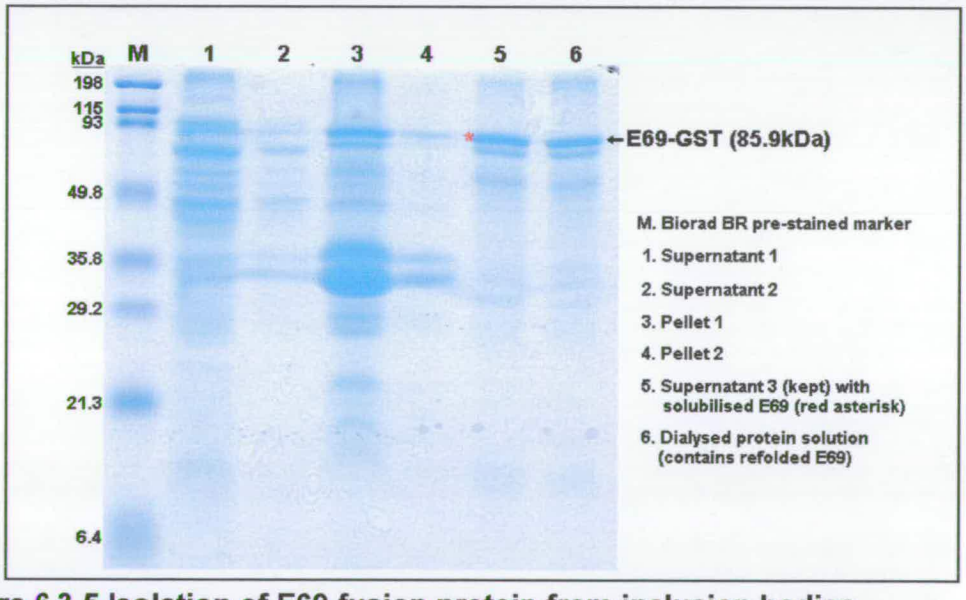

Figure 6.3.5 Isolation of E69 fusion protein from inclusion bodies
The cells were lysed and the remaining pellet was washed and treated with urea to denature the proteins. Solubilised proteins must be properly refolded to regain function. Denaturant was removed by dialysis to allow protein refolding. Lanes 1-4 contained supernatants and pellets discarded during the procedure (controls), lane 5 contained the E69 solubilised protein (red asterisk) and lane 6 contained refolded E69 after dialysis.

The next step was the purification of the protein isoforms, starting with E69 and E09 cells which expressed the full size product. No elution was observed; this was because most of the protein remained in the bacterial pellet after cell lysis instead of the cleared cell lysate (not shown). I tried several protocols to increase the efficiency of cell lysis (using lysozyme, different composition of PBS buffer and sonication time, urea lysis buffer-Table 6.3.1). Using different procedures, elution of four bands for E69 (one of ~ 88-90KDa and three of much lower MW) and two bands (the biggest being ~ 52 KDa) for E09 was possible (results not shown). The two E69 protein bands with the higher molecular weight and the higher MW band of E09 were excised from the gel and sequenced by MALDI-TOF. This revealed that the ~90KDa E69 band is a serine/threonine kinase which matches DSTPK61 sequence from the database and the ~50 KDa E69 band is a strong hit for GST and part of DSTPK61, therefore it is a degraded product of DSTPK61 expression. The E09 sample was contaminated. Upon verification that E69 DSTPK61 isoform was purified, I attempted a large-scale purification but the results were not reproducible and most of the protein remained in the post-sonicate pellet. Eventually, using a protocol for protein isolation from inclusion bodies, it was possible to isolate soluble fusion protein for E69, as shown in Figure 6.3.5.

6.3.1.2 Generation of new E40 and E51 constructs and sequencing

Since the longest protein isoform, E40, was always present as a truncated version instead of the full-length protein and E51 lately did not produce a full-length product either, I created new constructs for these isoforms, using *Pfu turbo* polymerase instead of Taq polymerase for the PCR reaction, lowering the PCR cycle number at the same time, to increase the accuracy of cDNA amplification. E40 and E51 cDNAs were subcloned into pGEX-3X as in Figure 6.3.1 and the bacterial strain BL21Lys (optimised for protein expression) as well as XL1Blue were transformed with the constructs.

Sequencing of the 5' and 3' prime ends of the vector confirmed that the inserted EST40 or EST51 cDNA is in the correct open reading frame for expression as fusion with GST and that there is a stop codon in frame at the end of the protein coding

sequence. These new constructs were used for induced protein expression and purification of the proteins from inclusion bodies, with the protocol proved to work for E69 (Fig. 6.3.5). However, this method worked at a very low efficiency for E40 and failed for E51 (not shown).

At this point, since results were not reproducible when using the optimised protocols at a larger scale or for the other DSTPK61 isoforms, I decided to fully sequence all the constructs I was using, rather than just the ends. This was to ensure that when the fusion protein expression and purification would be achieved, all four protein isoforms would have the correct predicted amino acid sequence, for the kinase assays indicating activity and the searches for potential differential substrate use to be of any significance.

As shown in Figure 6.3.2, the existing E69 construct has mistakes leading to 2 amino acid substitutions in the kinase domain and 1 substitution in the region between the kinase and the PH domains. The construct for E09 does not contain any base substitutions but is missing the first 45bp of the predicted coding sequence (resulting in a protein 15 amino acids shorter at the N-terminus; the protein can still be expressed because the preceding GST tag contains the ATG sequence required). The new E51 construct (E51pfu) has 3 nucleotide substitutions resulting in 2 amino acid substitutions in the OPA repeat domain and the new E40 construct (E40pfu) has one substitution in the region between the kinase and PH domains.

Following this, I believed that it is crucial to obtain constructs with perfect sequence before attempting any other optimisations on the fusion protein expression in bacterial cells or any alternative protein expression methods (discussed in sections 6.4.1-2). A method by which I could correct some of the existing constructs by altering their point mutations to the correct base, is by using a site-directed mutagenesis kit. I obtained the Quickchange XL Site-Directed Mutagenesis kit (Stratagene) planning to use it initially on the E40pfu and E51pfu constructs. Time limitations though prevented me from proceeding with this work.

6.3.2 His-tagged constructs

I also used the His-tag system (Histidine-tagged) for expression of E40 and E51 isoforms. The principle for construct generation is similar to the GST-tagged system (Fig. 6.3.1) but the coding sequence for six Histidine amino acids (6xHis) is used as a tag at the N-end of the protein, instead of GST, and the purification and detection, based on the recognition of 6xHis varies accordingly (Materials and Methods).

I used the pRSETC expression vector (Invitrogen) and made constructs with cDNA encoding full length E40 and E51 DSTPK61 isoforms. The E40/pRSET plasmid was fully sequenced and one nucleic acid substitution was detected between the kinase and PH domains, leading to E652G. Protein purification and elution using Ni-NTA agarose columns (QIAgen) was unsuccessful, since the protein could not be eluted from the column (not shown). Two attempts at ligating the E51 fragment to the pRSET C expression vector failed, resulting only in re-ligated vector. The results from my protein expression experiments are summarised in Table 6.3.1. The generation and attempts at expression of His-tagged fusion proteins was done together with Beth Pearce, a summer student.

Conditions tested	Comments- Results
GST-fused proteins: standard protocol	
Induction: - IPTG concentration 30μM, 100μM, 200μM, 500μM - OD_{600} of cultures when induced: 0.5-0.6 or 1.0-1.6 - Growth temperature during induction: a) 25°C for 16hr b) 37°C for 1-2hr c) 37°C for 4hr	Some induction observed for E40, not E51. Better results with 100μM IPTG for 2hr. E51, E09 induced sometimes but not consistently. Leaky expression of E69 and consistently high induction of it. (from Alessi et al, 1997b – 30μM IPTG) (from Pharmacia GST manual-100μM IPTG) (from G. Tzolovsky- 100 or 500μM IPTG)
Cell lysis: -Various sonication conditions (3-10 x 10", 4-10 x 20", 4 x 1', power levels 3-5) - Addition of Lysozyme (33μg/ml culture)	The lowest sonication condition that gives more proteins in the cell lysate than the remaining pellet was selected (6 x 10", power 3.5). Sonication generally does not result to the cloudy solution becoming clear lysate. Addition of lysozyme did not change results. The major problem seems to be absence of induction and presence of the protein (when induced) in the remaining pellet.
Buffers used: - for native conditions (GST manual protocol)	In Materials and Methods. No improvement by using denaturing conditions, so continue

- with urea/ imidazole (denaturing conditions) Bradford assays for protein quantification: – test if induction is sufficient – Use equal protein amounts from each sample for all subsequent western blots.	with native conditions (no protein refolding necessary) Dot-blots with anti-GST reacted with induced but not uninduced cell cultures for E51, E40 GST-fused proteins. Lower MW bands observed in Western blots usually. Inconsistency of successful induction of protein expression. Non-reproducable results.
Bacterial strains: XL1Blue and BL21Lys	Not big difference. BL21Lys is supposedly optimised for protein expression but both strains have the same problems in successful induction of the fusion proteins and subsequently the proteins are in the pellet. Easier to get transformed colonies from Bl21Lys though.
Purification and elution of fusion proteins: - batch purification in eppendorf tubes - Column purification	Not a big difference between the two. Possibly column purification and elution is slightly better but this must be verified. Conditions that are optimised for small scale elution (i.e. E69) are not reproducible when moving to the large scale experiment. **The expressed proteins were in the pellet rather than the cell lysate- presumably toxic for the cell and packed in inclusion bodies. Try a suitable protocol.**
Isolation from inclusion bodies (IB) Denaturing conditions – protocol in Materials and Methods	Method worked well for E69; very little amount of E40 was isolated (induction at much lower levels than E69); E51 was not isolated but induction was not good to start with (even though the same method that had worked before was used).
His-tagged proteins (with Beth Pearce)	
Generation of appropriate PCR fragments for ligation with expression vector pRSETC	E40- transformation successful; fully sequenced – 1 substitution (Fig.6.3.2) E51- transformation failed (two attempts, onl re-ligated vector)
E40 purification/elution	Ni-NTA agarose columns were used- did not work. Protein must have bound to the column (since it is not in the protein flowthrough) but was not eluted. Small scale expression showed some induction and Western with anti-His-tag showed a band of lower MW than expected.

Table 6.3.1.Summary of variant conditions used and optimisation protocols tried for protein expression

6.4 Discussion and future directions

6.4.1 Constructs without mistakes are essential for subsequent expression analysis

Given that the main purpose of expression of GST- (or His-) tagged fusion proteins for all DSTPK61 isoforms is to obtain native purified protein from each to be used in biochemical assays to determine the kinase activity and potential substrate specificity of each isoform, I believe it is necessary that the *in vitro* expressed proteins are identical (as far as we can control this) to the isoforms predicted to be expressed in *Drosophila in vivo*. Base substitutions during generation of the cDNA fragment to be subcloned that cause amino acid substitutions in the final protein sequence should be avoided. These amino acid substitutions, even though they may be present in regions of the protein that do not have functional domains (i.e. no kinase or PH domain), can cause changes in the tertiary folding of the protein and potentially affect its activity or affinity for substrates. That is because the side-chains of different amino acids vary greatly in size and charge and a substitution can alter significantly the conformation of the resulting protein.

The most obvious example is the construct for E69, the shortest DSTPK61 isoform. Even though this was the construct for which expression of the fusion protein and its isolation was the most successful, after full sequencing I found that there are two amino acid changes in the kinase domain (Fig. 6.3.2). The changes are quite drastic, too: a positively charged, hydrophilic Arginine residue is replaced by a highly hydrophobic Tryptophan at position 114 and a negatively charged hydrophilic Aspartic Acid residue at position 124 is replaced by a Glycine, the side chain of which is only a Hydrogen molecule. Since the hypothesis is that this protein isoform which lacks part of the kinase domain may be kinase inactive (Clyde and Bownes, 2000) it is essential that we do not risk that any putative kinase inactivity is due to mistakes in the sequence of the protein expressing construct. Similarly, even in cases such as E09 where the first 15 amino acids seem to be missing from the protein but they are in a region without recognised domains it would only be good practice to

express a full size protein with which to proceed with biochemical analysis [The existing constructs with base substitutions may still prove useful for use as mutant *dstpk61* and generation of appropriate transgenic flies].

6.4.2 Alternative approaches for successful protein expression

Protein expression has so far proved problematic. I did extensive optimisation of the protocol used trying several different conditions (Table 6.3.1), but when a particular set of conditions was giving a desirable result, upon repeating the experiment at a large scale (necessary to obtain the required amounts of protein) or for the other DSTPK61 fusion proteins the results ceased to be reproducible. Even expressing E09, which had been successful in the past (Alessi et al, 1997b – even though the authors point out how much more difficult the isolation of the *Drosophila* protein was, compared to the human recombinant protein) was not successful, with a band of the correct size for the fusion protein obtained sometimes but not consistently. I stopped my attempts at expressing the proteins while I worked on the full sequencing of the constructs. After confirming that specific base substitutions had been introduced, which would cause amino acid changes in the expressed protein, I decided to postpone any further optimisation of the protein expression procedure until correct constructs were made available.

I considered several alternative methods to achieve protein expression, given the lack of significant progress with the expression of fusion proteins in bacterial cells, under either native (GST-fusion proteins) or denaturing (6xHis-tagged proteins) conditions. Due to time limitations I did not proceed with them; however, I am listing them here as alternative options that may help overcome some of the problems observed so far with protein expression, such as the potential toxicity of the kinase DSTPK61 to the host cells.

The protein isoforms could be expressed in cells other than of bacteria. The Baculovirus expression system is widely-used and involves the introduction of the foreign gene into a non-essential region of the viral genome by homologous

recombination, transfection of insect cells (Sf9, Sf21 cell lines) with the recombinant baculovirus and harvesting the baculovirus expressing the protein of interest (www.invitrogen,com, www.bdbiosciences.com). Another interesting and probably effective solution is expression in *Drosophila* Dmel-2 (S2) cells, using vectors tagged with the V5 14-amino acid epitope (such as the vector pAcV5-His6 for constitutive expression- Dr R. Kohanski, pers. comm., www.invitrogen.com). Both these systems combine the advantage of expressing the protein in eukaryotic cells with high levels of expression and eucaryotic post-translational modifications that should yield a native functional protein. Another attractive option is the use of a cell-free expression system. Several companies, including Roche (the RTS, Rapid Translation System) and Promega, provide kits for cell-free expression, which use a continuous-exchange, cell-free system for high yield expression of proteins using an *E.coli* cell lysate reaction mix. There are typically two chambers in a cell-free protein expression system, separated by a membrane which allows only small molecules (< 10 kDa) to pass through it; the smaller reaction space with the reaction solution where translation takes place and the protein is produced and folded and the larger feeding space where substrates, amino acids, chaperones and inhibitory by-products diffuse through the membrane. The coding sequence of interest is cloned into a special vector which contains a T7 promoter and a ribosomal binding site (RBS) upstream of the coding sequence and a T7 terminator downstream of the stop codon. The T7 RNA polymerase transcribes the gene and the mRNA produced (including the RBS) is translated utilising the components of the *E. coli* lysate.

6.4.3 Future plans

The major aim of expressing all four potential DSTPK61 isoforms for biochemical studies still remains, although I believe that, by demonstrating how difficult the expression of this particular gene's products in bacterial cells is and by having explored many possibilities for optimisation and recorded the results I have contributed towards achieving this target. I suggest a radical change of expression

system such as trying expressing in *Drosophila* cell culture or in a cell-free translation system as the most likely ways to get the DSTPK61 isoforms expressed.

Kinase activity assays will determine which isoforms are enzymatically active and phosphorylation studies should determine the *in vitro* substrates of DSTPK61 and reveal any differential substrate specificity for the different DSTPK61 isoforms, something that could be confirmed by immunodetection with isoform- specific antibodies. The isoforms can also be tested for their ability to phosphorylate mammalian substrates. E09 (cDNA^{A}) has already been shown to phosphorylate human PKB *in vitro* (Alessi et al, 1997b). On the long term, it would be interesting to investigate the phosphorylation profiles of recombinant DSTPK61 isoforms that lack the PH domain or the opa repeat domain. This should provide information on their probable *in vivo* roles.

I produced an isoform-specific antibody against E40, raised against the N-terminal peptide sequence unique to E40. The antibody recognises bands of the correct size in female and male carcasses in Western blots, binds to protein lysate from ovaries and testes in a Dot-blot (not shown) and is suitable for immunohistochemistry, as E40 antibody staining in ovaries demonstrated. This antibody should be further used for detection of the E40 protein expression pattern in testes, as discussed in Chapter 5; also to detect the E40 fusion protein on Western blots for future protein expression experiments. The developmental expression profile of E40 DSTPK61 isoform can be investigated by a developmental Western with the E40 antibody, on embryos, different stage larvae and pupae and adult flies. Even though the background of E40 was very low in Western blots of fly tissues (when the antibody is blocked with BSA and bacterial cell lysate), it may be beneficial to proceed with affinity purification of the serum containing the E40 antibody, to increase its specificity. For this purpose the unconjugated peptide I have (the same that was used as an antigen) can be bound to a column, the immune serum to be passed from the column so that the E40 antibody will be retained and subsequently eluted from the column.

Antibodies against other regions of the DSTPK61 protein can be generated by expressing parts of the protein, such as the amino-terminal part of E51 (since

production of an antibody against an E51-specific peptide is not possible) and of E09 or the sequence between the OPA repeat domain and the ATP binding pocket (see figure 6.1.1) as GST fusion proteins to be used as antigens. The antibodies should be used in Western blots from different *Drosophila* tissues and from different stages of development. They should also be used for *in situ* antibody staining to identify the localisation of each isoform within the tissue. Antibodies could also be used in immuno-co-precipitation experiments to verify the DSTPK61 substrates identified so far by their genetic interactions and possibly to identify further potential substrates.

Another approach that would facilitate the study of the *in vivo* localisation of the various isoforms is the creation of GFP-tagged recombinant proteins and their expression in flies following P-element transformation. With this method it can be determined if specific amino acid sequences, in particular the mitochondrial targeting domain of the longest isoform, or the opa repeat domain, direct differential subcellular localisation of DSTPK61. One of the advantages of GFP-tagged proteins is that they can be easily detected by using a commercially available anti-GFP antibody and by their fluorescence in living tissue; therefore it may be useful to express even a whole isoform and detect it indirectly through GFP if an antibody against the isoform is not sufficiently specific. I started generating the constructs for this with a summer student, Beth Pearce- we have a core domain GFP-DSTPK61 construct (lacking the first 100 amino acids of E40) ready, subcloned into the pUASP vector (Rorth, 1998) for expression in the germline; the majority of it is sequenced without displaying any base substitutions (not shown).

Chapter 7: The gene *extramacrochaetae* is expressed throughout oogenesis and is involved in dorsal appendage formation

7.1 Introduction

The gene *extramacrochaetae* (*emc*) was isolated in our laboratory during an enhancer-trap screen for genes with interesting expression patterns in follicle cells. The *lacZ* enhancer-trap fly line *261/31* was selected for analysis based on its temporally and spatially restricted β-galactosidase expression pattern in the follicle cell layer surrounding the germline cells in oogenesis (Figure 7.2.1). This line was provided from Peter Deak's collection (Deak et al, 1997). A fragment of genomic DNA isolated following plasmid rescue of *261/31* was sequenced, used to screen cDNA libraries and found to correspond to the known gene *extramacrochaetae* (*emc*). The *P{lacW}* element insertion is in the 5' UTR of *emc*, 72 base pairs from the first exon, as identified by homology searches of the rescued fragment. Full length cDNA was obtained from Garrell and Modolell (1990) and used in all subsequent experiments. Whole mount in situ hybridisation in ovaries (with alkaline phosphatase detection) was used to determine the *emc* mRNA expression pattern during oogenesis (see Figure 7.2.2).

To investigate further the role of *emc* in oogenesis transgenic fly lines expressing sense and antisense RNA (as in Deng et al, 1999) were generated. Full-length *emc* cDNA in either the sense (s) or antisense (as) orientation was expressed under a heatshock (hs) promoter, by ligating the appropriate *emc* fragment to the *pCaSpeR-hs* plasmid and introducing the constructs into w^{1118} flies by P element mediated germline transformation (Spradling, 1986). From the eight heatshock-sense-*emc* (*hs-s-emc*) lines and 12 heatshock-antisense-*emc* (*hs-as-emc*) lines established, lines *s1*, *s7b* and *as10c* were selected for further study since they showed the highest egg abnormality rates when heatshocked. Eggs with abnormal dorsal appendage formation were classified as "abnormal eggs". Dorsal appendage phenotypes varied from small eggs with fused appendages to wild-type eggs showing variable levels of fusion (Figure 7.1.1). Different heatshock methods affected the number of abnormal eggs laid and the exact phenotypes observed. Generally the heatshocked antisense *emc* lines laid abnormal eggs much later than the heatshocked sense *emc* lines, showing that disruption early in oogenesis has a greater phenotypic effect.

Presumably this reflects the time needed for the already expressed *emc* RNA and protein to be turned over and disrupted by the antisense *emc* expression.

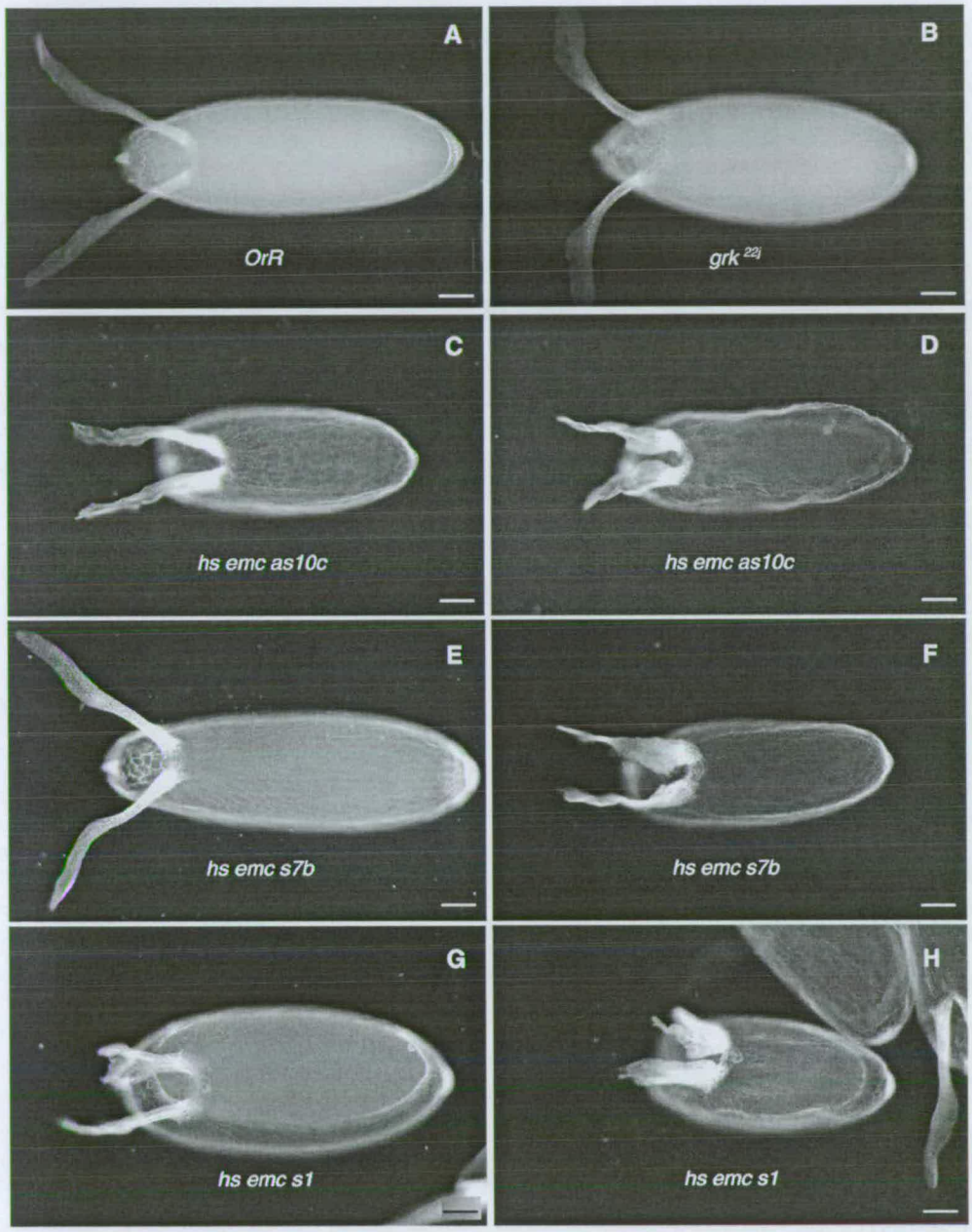

Figure 7.1.1: Dorsal appendage phenotypes
The phenotypes observed in *OrR*, *grk*^{22j} and *emc* sense and antisense eggs. A: wild-type *OrR*. B: Grk over-expression line *grk*^{22j} with the dorsal appendages pushed further away from the dorsal midline. C, D: Heatshocked *emc as10c* have appendages that are thicker and pushed closer to the dorsal midline. E-H are from two *emc* sense lines, *s7b* in (E) and (F) and *s1* in (G) and (H); they show the varying thickness and length of appendages and their abnormal tip morphology – these egg chambers are also ventralised. Note the wider and shorter cells between the appendages in (B). Scale bar = 50 µm. Transgenic eggs are generally smaller than wild-type. Pictures C-H are from Dr. G. Tzolovsky.

The specificity of the *emc* constructs was tested by investigating their effects on bristle development in the thorax. Known *emc* mutations (Huang et al, 1995; Moscoso del Prado and Garcia-Bellido, 1984) show distinct bristle patterns and if the *emc* sense and antisense constructs were generating phenotypes corresponding to them it would demonstrate that the constructs do indeed affect *emc* expression. Heatshock inducible lines *s1* (sense *emc*) and *as10c* (antisense *emc*) were used. Females were allowed to lay eggs for 24 hours, and then transferred to a new vial; this was repeated for 10 days to collect all developmental stages. The vials were then all heatshocked at once and the resulting flies were scored for bristle phenotypes. Many flies had missing dorsocentral and scutellar bristles. However, the control wild-type flies frequently had these phenotypes as well, when heatshocked. The heatshocked *emc* sense and antisense flies also showed phenotypes typical of *emc* mutations (Huang et al, 1995): extra dorsocentral and scutellar bristles, two bristles (scutellar and/or postalar) coming from one socket and short thick bristles in several locations. There were also flies with scutellar bristles facing in the wrong orientation. Some of the phenotypes observed are shown in Figure 7.1.2B-D compared to the *OrR* phenotype (Fig. 7.1.2A).

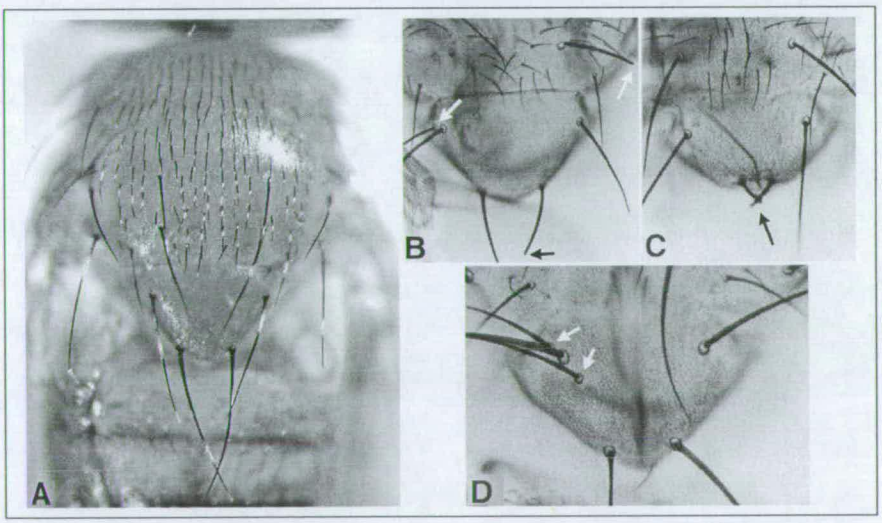

Figure 7.1.2: Bristle phenotypes of *emc* sense and antisense fly lines compared to wild-type *OrR*

A: Wild-type bristle pattern (*OrR*). B: One extra scutellar bristle and truncated thickened bristles. C: Short abnormal scutellar bristles. D: Two additional scutellar bristles. Abnormal bristles are marked with arrows. Pictures B-C are from the sense fly line *hs emc s1* and D is from the antisense line *hs emc as10c*. Pictures B-D are from Drs K. Leaper and D. Zhao.

Western blot analysis was used to confirm the effect of the induced sense and antisense constructs on the levels of the Emc expression (Emc has a predicted molecular weight of 22 kDa). As shown in Figure 7.1.3A (by G. Tzolovsky), Emc protein levels are highly elevated in heatshocked sense flies (lines s1 and s7b) in comparison to the low endogenous Emc expression in wild-type OrR flies, whereas in antisense flies (line as10c) Emc protein is essentially undetectable in comparison to beta-Tubulin. Figure 7.1.3B shows a quantification of the results of the Western blot in Fig. 7.1.3A. Similar results were obtained with immunohistochemistry with Emc antibody (Figure 7.3.1A-C), as described below.

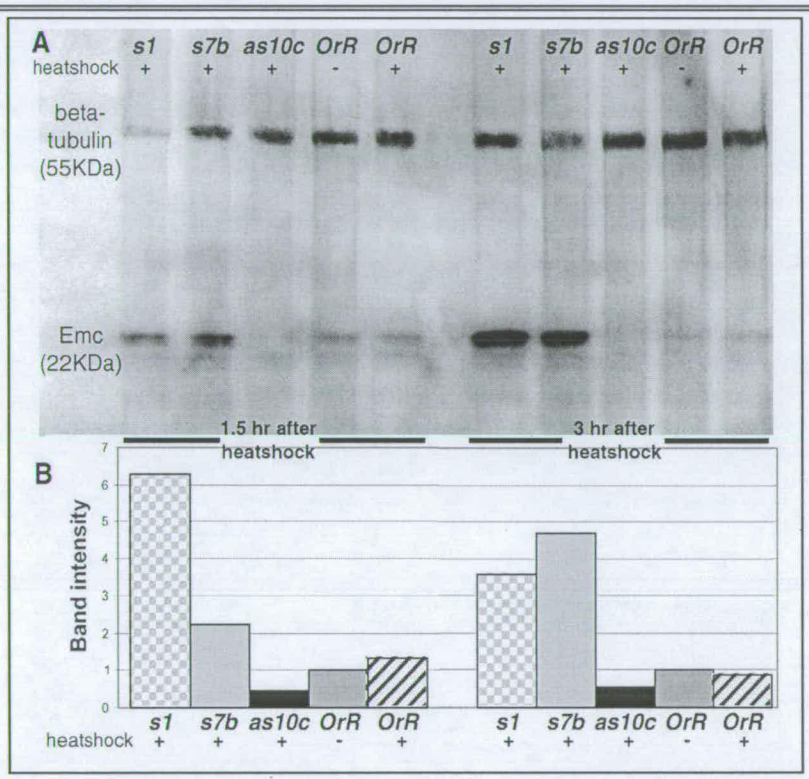

Figure 7.1.3: The efficiency of *emc* sense and antisense constructs is demonstrated by Western blot

A: Western blot with Emc antibody and anti-β-Tubulin (loading control) to ovaries from wild-type, *emc* sense (*s1, s7b*) and antisense (*as10c*) fly lines. In lanes 1-5 the ovaries were dissected 1.5 hours after heatshock and in lanes 6-10 the ovaries were dissected 3 hours after heatshock. The low endogenous level of Emc in wild-type flies is not affected significantly by the heatshock treatment. Emc protein expression is significantly increased in heatshocked *s1* and *s7b* flies (lanes 1 and 2) and stays at high levels with time (lanes 6, 7). In contrast, no Emc protein is detected in the heatshocked *emc* antisense line as10c, neither 1.5 nor 3hours after heatshock (lanes 3 and 8). B: The graph shows the relative intensity of bands after normalising for β-Tubulin [(Emc intensity – background)/ (β-tubulin intensity-background)]. All values are expressed relative to the non-heatshocked *OrR* sample (negative control; value = 1). Picture A is from Dr G. Tzolovsky.

The nature of the phenotypic changes in the appendages was investigated in more detail by measuring the spacing between the appendages in eggs laid by females expressing *emc as10c* (standard heatshock regime) to see how much the appendages had moved, compared to wild type *OrR* eggs and to eggs laid by *gurken*^{22j} (*grk*^{22j}) females. The *grk*^{22j} flies have four copies of the wild type *grk* gene and the positioning on the appendages is influenced by *grk* via the EGFR pathway (Neuman-Silberberg and Schüpbach, 1994). Misexpression of *grk* causes a broader area of the egg to be dorsalised and the appendages are pushed further apart (Fig. 7.1.1B). The distance between appendages was found to be bigger for the *grk*^{22j} line by approximately 17 microns compared to *OrR*, whereas in hs *emc as10c* the distance was smaller, i.e. the appendages are closer together, by approximately 15 microns. There is an interesting phenomenon showing that once the appendages get closer together than approximately 20 microns they fuse rather than form separately. Studying the organisation of cells between the appendages showed that wild-type eggs have elongated follicle cells between the dorsal appendages, the *emc* knock-out antisense eggs have a similar cellular shape, however, the cells between the *grk*^{22j} appendages are shorter and wider than in the *emc* antisense eggs and the wild type (data not shown). It was thus suggested that *emc* mutants do not change the shape of cells, but the number of cells between the appendages.

Mosaic flies were generated and eggs with abnormal appendage phenotypes, similar to the mis-expression analysis, were observed. However it was not possible to observe the clones in oogenesis when dissecting ovaries from the heatshocked flies laying the abnormal eggs with the methods used.

Another interesting phenotype observed previously in our laboratory was the absence of an oocyte or the presence of two oocytes in early stage egg chambers in flies expressing sense and antisense *emc* constructs. This was detected by in situ hybridisation with a probe for *oskar* mRNA (Ephrussi et al, 1991) that marks the oocyte position. The number of germline cells was counted in egg chambers with two oocytes and was normal; this ruled out the possibility that the "two oocyte" phenotype was the result of fusion of two egg chambers. Wild-type *OrR* egg

chambers always had a single oocyte whereas in *emc* sense lines *s1* and *s7b* 2.6-2.8% of egg chambers had two oocytes and 1.3- 3.8% had no oocyte (no *oskar* localisation). In antisense *emc* fly line *as9* 3.3% of egg chambers had two oocytes and 5.8% had none; in *as10c* 3.8% of egg chambers had no oocyte (K. Leaper and E. Asscher, unpublished observations). The two oocytes were mostly located at the posterior and anterior poles of the egg chamber. These abnormal egg chambers subsequently underwent apoptosis. Based on these observations a hypothesis that *emc* has a role in oocyte selection was formed: it was suggested that *emc* is involved in the selection of which of the two pro-oocytes will become the oocyte rather than in selecting an oocyte from all 16 cells in the germ cell cluster, since both reduced *emc* expression and overexpression/misexpression of *emc* can cause defects in oocyte selection.

Some of the work described in the section above was undertaken by G. Tzolovsky, K. Leaper, D. Zhao, P. Taylor, G. Kirk, E. Asscher and D. Clyde in our laboratory and the figures are courtesy of them where so stated.

My work on the *extramacrochaetae* project had two aims: firstly, to undertake an *emc* clonal analysis at two levels. To generate follicle clones of *emc* null cells in oogenesis and demonstrate that the abnormal appendage phenotypes are caused by disruption in *emc* expression; also to generate germline *emc* clones and study the effect of disrupting normal *emc* expression in the germline, investigating the potential role of *emc* in oocyte selection. Secondly, to position *emc* in a signalling pathway, by studying how *emc* mRNA expression is affected by mutations in other genes that are components of the EGFR signalling pathway which participates in the dorso-ventral axis determination and is involved in dorsal appendage formation. This was done by in situ hybridisation. The principle is that if a gene is upstream of *emc* in a signalling pathway, the *emc* mRNA expression pattern would be altered. If a gene is downstream of *emc*, the *emc* mRNA expression pattern should remain unaffected by mutations in that gene.

In order to proceed with the mutant background analysis I first needed to study in detail the *emc* expression pattern in wild-type flies and confirm (or otherwise) the

previously observed pattern, to use is as a basis for comparisons with the *emc* expression pattern in the various mutant backgrounds.

7.2 The dynamic expression pattern of emc in oogenesis

7.2.1 *emc-lacZ* expression

The β-galactosidase expression pattern in fly line *261/31* is very likely to mimic some or all of the normal expression of *emc* since the P-element carrying the *lacZ* gene is located in the 5' UTR of the *emc* gene. β-galactosidase expression in *261/31* was detected throughout *Drosophila* oogenesis with particularly strong expression from stage 2 to 11. Initially, staining is detected in all follicle cells (stages 2 to 6 – Fig. 7.2.1A-C). At stages 7-8 follicle cells over the oocyte are stained more intensely (Fig. 7.2.1A-C) and at stage 9 *lacZ* is highly expressed in a band of follicle cells at the boundary between the oocyte and the nurse cells and in the migrating follicle cells that cover the anterior two thirds of the oocyte (results not shown), as well as in the stretched follicle cells that remain over the nurse cells. During stages 10-11 *lacZ* expression is localised to the centripetal follicle cells, the nurse cell-associated follicle cells and the dorsal anterior follicle cells; in the latter, at stage 10A expression in the columnar follicle cells becomes restricted to the region over the dorsal anterior of the oocyte (Fig. 7.2.1A-C). This expression pattern remains until stage 11 when two distinct subsets of stained follicle cells are defined (Fig. 7.2.1C-D). As the dorsal-ventral axis is established during this stage, the dorsal-anterior expression of this gene suggested a potential role in dorsal-ventral patterning of the egg. At stage 12 expression is localised in two discrete groups of dorsal anterior follicle cells on either side of the dorsal midline (Fig. 7.2.1E), which move anteriorly over the forming dorsal appendages as the oocyte develops (stage 13) but are now connected as one band covering the dorsal midline (Fig. 7.2.1F).

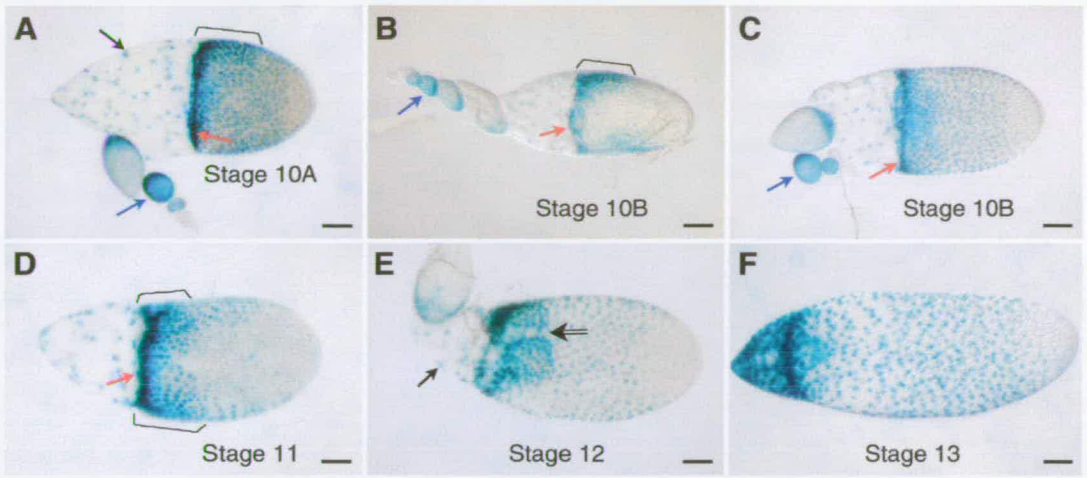

Figure 7.2.1 Expression pattern of *emc-lacZ* in follicle cells
β-galactosidase staining pattern in egg chambers of the enhancer-trap line *261/31*. A: An ovariole containing the germarium (not stained), egg chambers in early stages of oogenesis (stages 3, 6 and 8 are presented here) and a stage 10A egg chamber (main picture). B, C: ovarioles with early stage egg chambers as before and a stage 10B egg chamber, with dorsal anterior *lacZ* expression. Blue arrows indicate ubiquitous *emc* expression in follicle cells covering the germline cells in the early stages of oogenesis (stages 5-6 are indicated); red arrows point to the centripetal follicle cell expression; black arrows indicate expression in stretched follicle cells over the nurse cells and brackets, in the area over the dorsal anterior of the oocyte. D: Stage 11 egg chamber with *lacZ* expression localised in the centripetal cells (red arrow) and in two groups of lateral dorsal anterior follicle cells (brackets). E: In a stage 12 egg chamber, the two groups of dorsal anterior follicle cells are separated by a gap on the dorsal midline (double black arrow). Expression is also retained in a ring of follicle cells at the border between the oocyte and nurse cells. F: Strong *lacZ* expression in follicle cells over the forming dorsal appendages and in a small area over the dorsal midline (stage 13). A and B are lateral views while C, D, F are top views (dorsal is at the top) and in E dorsal is marked by the direction of the arrow. Scale bars = 50 μm. In all figures anterior is to the left.

7.2.2 Expression pattern of *emc* mRNA and Emc protein (with Dr G. Tzolovsky)

In situ hybridisation to ovaries with *emc* double stranded DNA probes and alkaline phosphatase detection was used previously to observe *emc* expression in the follicle cell layer. However, several attempts using this protocol and optimisations of it failed to give a clear picture of the staining pattern in follicle cells. Staining denoting *emc* mRNA expression was always observed in the nurse cell nuclei and presumably was masking any subtle expression differences in the surrounding follicle cells. In situ hybridisation with single stranded DNA probes gave the same germline cell *emc*

expression result when the antisense probe was used and only background with the sense (negative control) probe (results not shown). We therefore tried several protocols and modifications to obtain a clear, reproducible *emc* expression pattern by in situ hybridisation. This was eventually achieved by using RNA *emc* probes and an in situ hybridisation protocol with TSA (tyramide signal amplification) detection [based on a protocol from Ilan Davis' laboratory (http://homepages.ed.ac.uk/ilan/tech.html) and modified – see Materials and Methods].

As figure 7.2.2A-F shows, the *emc* mRNA expression pattern is largely similar to the beta-galactosidase staining. Expression of *emc* is detected in all somatic follicle cells from stage 1 (in region 3 of the germarium) until stage 6 (Fig. 7.2.2A and not shown). Subsequently *emc* expression becomes restricted to a tight band of follicle cells at the nurse cell-oocyte boundary and to the stretched follicle cells over the nurse cells at stage 10A and 10B (Fig. 7.2.2B-C). During stage 11 expression is refined to two subsets of follicle cells either side of the dorsal midline (Fig. 7.2.2D-E). Expression persists in these follicle cells as they migrate anteriorly, secreting the dorsal appendages, but *emc* is now expressed in a single larger area covering the dorsal midline (Fig. 7.2.2.F). By stage 14 expression is limited to a small group of follicle cells located between the dorsal appendages (data not shown).

Emc protein follows the mRNA expression pattern and is detected by immunostaining with an *emc* antibody in follicle cells of all stages, starting from the germarium (Fig. 7.2.2G and H-inset). Protein is not expressed very strongly at stages 7-8. It is present in all germline cell nuclei in mid- and late oogenesis (st.8-13) (Fig. 7.2.2I), in the centripetal cells at stage 10 and in the posterior polar cells (st.10-11). At stages 11 and 12 Emc is expressed in two dorsal anterior subsets of follicle cells either side of the dorsal midline (Fig. 7.2.2J), during stage 12 these dorsal follicle cells migrate anteriorly and at stage 13 Emc is only detected in the follicle cells of the developing dorsal appendages (data not shown and Fig. 7.3.1A).

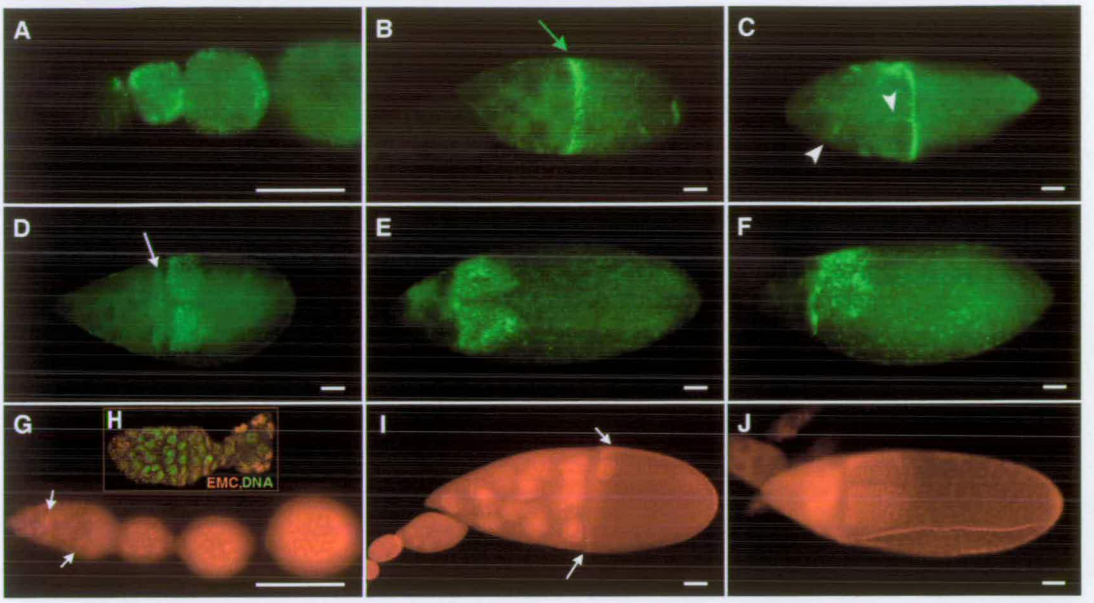

Figure 7.2.2 Expression pattern of *emc* mRNA (A-F) and Emc protein (G-J) in *OrR* ovaries

A: *emc* mRNA (green) is expressed ubiquitously in stages 1 (germarium region 3) - 6 of oogenesis, in the follicle cells and the nurse cell cytoplasm. Occasionally expression was also observed in region 2 of the germarium (not shown). B-C: At stage 10A (B) *emc* expression is very strong in a band of follicle cells that cover the anterior of the oocyte (green arrow). There is a low level of expression in the nurse cell cytoplasm that continues in later stages. The stretched follicle cells over the nurse cells also express *emc* (arrowheads in C – stage 10B egg chamber). D: By stage 11 *emc* is expressed in the centripetal cells (arrow) and in two discrete groups of lateral dorsal anterior follicle cells either side of the dorsal midline. E: Towards stage 12 these two groups of follicle cells become restricted to dorsal anterior positions on either side of a thin gap along the dorsal midline and (F) later in stages 12-13 there is a continuous area of *emc* expression covering the dorsal anterior of the developing oocyte, including the dorsal midline.
G: Emc protein (red) is expressed in the germarium (arrows) and in the follicle cells surrounding early stage egg chambers. Inset (H), magnified germarium with Emc (red) and Sytox Green (green, DNA stain). Emc expression in follicle cells. I: The nurse cell and oocyte nuclei strongly express Emc. In the follicle cells Emc expression is stronger in the centripetal and dorsal anterior cells (arrows). J: At stage 12 Emc is expressed in two dorsal anterior patches of follicle cells and the nurse cell nuclei. D-E are dorsal views, F and J are dorso-lateral and (I) is a lateral view. Scale bar = 50 µm. H (inset in G) is magnified 1.2x. Pictures B, E and I are from Dr G. Tzolovsky.

7.3 Confirmation of specificity of emc constructs

Emc antibody staining in ovaries of wild type *OrR*, sense *s7b* and antisense *as10c* fly lines was used to confirm the specificity of the *emc* constructs and effectiveness of the heatshock regime, in addition to the bristle pattern and the Western blot analyses

used (see 7.1-introduction). Emc is observed ectopically in the heatshocked sense line *s7b* (Fig. 7.3.1B – note the lateral/posterior follicle cells stained on the oocyte) compared to the wild type Emc expression pattern (Fig. 7.3.1A). At the same time there is absence of Emc staining from the heatshocked antisense line *as10c* (Fig. 7.3.1C) consistent with the "knock-out" effect of the antisense construct.

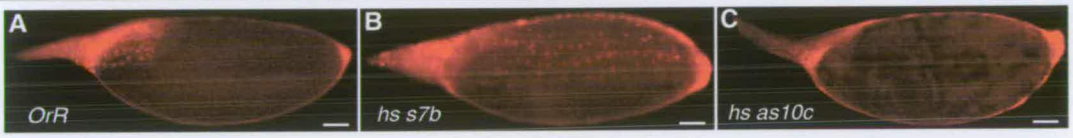

Figure 7.3.1 Emc expression is affected in sense and antisense mis-expression fly lines
Immunohistochemistry with Emc antibody using stage 13 egg chambers. (A) Wild type Emc expression in the dorsal anterior using *OrR* ovaries. (B) Ectopic Emc in follicle cells laterally and posteriorly apart from the dorsal anterior in *hs s7b* sense *emc* flies. (C) Absence of Emc staining, even on the dorsal anterior in *emc* antisense flies *hs as 10c*. Scale bars: 50μm.

7.4 Disruption and misexpression of emc affects egg chamber formation (with Dr G. Tzolovsky)

In heatshocked sense and antisense *emc* ovaries we detected egg chambers fused to various extents (Figure 7.4.1A-D). Sometimes there are 32 germline nuclei, presumably resulting from the fusion of two egg chambers, but usually there is incomplete fusion, resulting in one abnormally large egg chamber with an irregular number of nurse cell nuclei (e.g. 28 nurse cells- Fig. 7.4.1B) linked to an atrophic or underdeveloped egg chamber. These egg chambers were undergoing apoptosis but there were cases where development appeared to proceed to some extent (stage 11 egg chamber in Fig.7.4.1D). This fused egg chamber phenotype was observed more in sense *emc* lines than in antisense *emc* and wild-type flies never exhibited it, even when they were subjected to the same heatshock treatment as *emc* transgenic flies and the number of egg chambers undergoing apoptosis in their ovaries was increased (Fig. 7.4.1E).

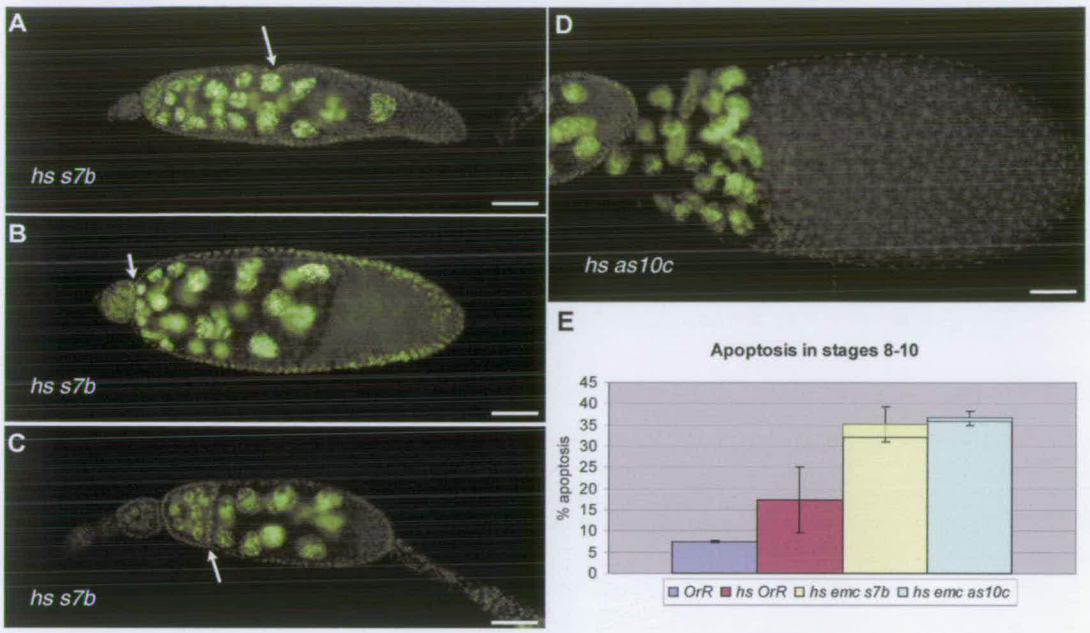

Figure 7.4.1: Fused egg chambers and high levels of apoptosis in *emc* mis-expression fly lines
A-D: Fused egg chambers from heatshocked sense and antisense *emc* fly ovaries. Nuclei are stained in green. A: Arrow indicates a groove in the follicle cell layer where presumably this egg chamber should have been separated in two. B-C: Arrows point to the irregular separation of two egg chambers. D: A stage 11 fused egg chamber with more than fifteen nurse cells. The names of the fly lines used are written on each picture. E: Graph showing the percentage of apoptotic egg chambers in wild-type and *emc* transgenic flies during stages 8-10. Vertical lines denote the standard deviation. Darker coloured boxes in the *s7b* and *as10c* columns represent the fraction of apoptotic egg chambers that also exhibit a fused phenotype. For heatshocked and non-heatshocked wild-type *OrR* flies this equals zero. Scale bars = 50 µm. Pictures A-D are from Dr G. Tzolovsky.

7.5 Eggs with emc[1] homozygous mutant follicle cell clones have abnormal dorsal appendages and are smaller than wild-type

Mosaic flies with *emc* homozygous clones were generated in order to investigate the effect of *emc* mutant clones in oogenesis and to confirm that the abnormal appendage phenotypes seen in the antisense analysis were due to perturbations in *emc* expression. The crossing scheme for generating follicle cell clones is presented in Figure 7.5.1.

I:

P ♂ ♀

$\frac{y^1\ w^{1118}\ P\{ry^{+t7.2}=70FLP\}3F}{Dp(1;Y)y^+}$; $\frac{TM2}{TM6C,\ Sb^1}$ x w^{1118}; $\frac{P\{w^{+mC}=Ubi\text{-}GFP(S65T)nls\}3L\ P\{ry^{+t7.2}=neoFRT\}80B}{TM3,\ Sb^1}$

(hsFLP; Sb) (FRT-nlsGFP/ Sb)

Select F1 ♀ $\frac{y^1\ w^{1118}\ P\{ry^{+t7.2}=70FLP\}3F}{w^{1118}}$; $\frac{P\{w^{+mC}=Ubi\text{-}GFP(S65T)nls\}3L\ P\{ry^{+t7.2}=neoFRT\}80B}{TM6C,\ Sb^1}$

II: (hsFLP;FRT-nlsGFP/Sb) and cross with ♂ $\frac{w^*;\ emc^1P\{ry^{+t7.2}=neoFRT\}80B}{Y\qquad TM6B,\ Tb^1}$ (FRT-emc^1/Tb)

Select ♂ hsFLP/Y; FRT-emc^1/ FRT-nlsGFP (non-Sb, non-Tb)

III: Cross these ♂ ($\frac{hsFLP;\ FRT\text{-}emc^1}{Y\quad FRT\text{-}nlsGFP}$) to ♀ $\frac{w^*;\ emc^1P\{ry^{+t7.2}=neoFRT\}80B}{TM6B,\ Tb^1}$ (FRT-emc^1/Tb)

Select non-Tb larvae and from the eclosed flies select non-Sb female flies of the genotype:

$\frac{y^1\ w^{1118}\ P\{ry^{+t7.2}=70FLP\}3F}{w^*}$; $\frac{emc^1\ P\{ry^{+t7.2}=neoFRT\}80B}{P\{w^{+mC}=Ubi\text{-}GFP(S65T)nls\}3L\ P\{ry^{+t7.2}=neoFRT\}80B}$

Heatshock these ♀ hsFLP; FRT-emc^1/ FRT-nls GFP to activate the FLP recombinase and induce mitotic recombination between the FRT sites. This results in clones of cells homozygous for *emc^1* that are identified by the absence of green fluorescence in the cell nucleus, since they do not have the nls-GFP gene any more.

Figure 7.5.1 Genetic crosses for generation of mosaic *emc* mutant flies
Only the genotypes of progeny selected from each cross are shown and a name summarising the key genes present is given in parentheses, for simplicity. Note that even though the desired hsFLP; FRT-emc^1/FRT-GFP female flies are present in the progeny of the second cross, the third cross is necessary to ensure all selected female flies will be homozygous for hsFLP; the FRT-emc^1/FRT-GFP females from the second cross are 50% homozygous for hsFLP but cannot be distinguished from the heterozygous hsFLP/w*.

Follicle cell clones were observed in the ovaries of heatshocked *FLP; emc^1, FRT 80B/ nlsGFP, FRT80B* flies as shown in Figure 7.5.2A-B. Occasionally the follicle cells within the clone would appear denser and smaller compared to their neighbours, even in quite large areas of the follicle cell monolayer (Fig. 7.5.2B) but this does not seem to have an immediately obvious morphological effect during oogenesis. However, the eggs laid by the heatshocked flies having *emc* clones in their ovaries

have a high percentage of abnormal dorsal appendages. The most pronounced phenotype associated with the *emc* mutant clones is dorsal appendages with split ends ("antler"-type) to various degrees (Fig. 7.5.2D-H). Many other types of abnormally formed dorsal appendages were observed, ranging from complete absence of appendages with only some dorsal appendage material on the eggshell to appendages closer together or fused at base. Some of the phenotypes were also observed in eggs laid by heatshocked *OrR* flies but at a much lower percentage than the *emc* clones (Table 7.5.1); the "antler"-type appendages though were unique to *emc* clones. The *emc* clones were induced by heatshock mainly during stage 8 of oogenesis or later [as shown in Table 7.5.1, eggs with abnormal dorsal appendages caused by *emc* clones were laid 0- 26hr after heatshock, with the peak at 21- 25hr after heatshock, which would correspond the egg chambers being at stage 8 at the time of heatshock. In egg chambers heatshocked earlier, between st.5-8 and st.3-5, abnormalities in dorsal appendages are also caused by *emc* clones but there is a higher probability that heatshock itself can cause them (calculations based on Spradling, 1993)]. Further evidence that these eggs came from egg chambers which had *emc* clones was the observation of abnormally large or misshapen cell imprints on the eggshell of the eggs with abnormal appendages (Figure 7.5.2I). This was never observed in heatshocked *OrR* flies, not even when they had abnormal dorsal appendages. Furthermore, the flies producing eggs with *emc* homozygous mutant clones also had extra (mostly dorsocentral) bristles in the notum (Fig. 7.5.2J-L), characteristic of *emc* mutations (Moscoso del Prado and Garcia-Bellido, 1984; Huang et al, 1995) (compare with the wild-type bristle pattern in Figure 7.1.2). To observe clones in the notum that lead to defects in bristle pattern, wandering larvae/light pupae were heatshocked (39°C, 1hr in an incubator or 37°C, 1hr in a waterbath) and the bristles were observed when the flies eclosed. To observe clones in developing egg chambers throughout oogenesis, flies were heatshocked twice or up to four times (37°C, 1hr in a waterbath) with 4 hr minimum interval between heatshocks. Ovaries were dissected 3-5 days after heatshock, therefore the "egg chambers" were prior to stage 2, in the germarium, at the time of the first heatshock (Development from a stem cell to a stage 2 egg chamber that has left the germarium

takes about 7 days and from stage 2 to the end of stage 14 – mature egg – another 2.65 days – Spradling, 1993).

The size of the emc^1 mosaic eggs was generally smaller than the *OrR* wild-type eggs (compare Fig. 7.5.2D-H to Fig. 7.5.2C), as is the case with the *emc* sense and antisense mis-expression fly lines (Fig. 7.1.1). Also a large percentage of mosaic egg chambers showed a distinct phenotype where the oocyte and surrounding follicle cells proceed through the last stages of oogenesis and the dorsal appendages are formed, but the nurse cells have not dumped their cytoplasmic material to the oocyte and are still present and occupying a large part of the egg chamber (Figure 7.5.3D, E, G-I). This can result in a very small, round egg (Figure 7.5.3F). Around 50% of egg chambers exhibited this phenotype which was not observed in control heatshocked *OrR* flies (or observed in 1-3% of egg chambers in an independent experiment). This phenotype is likely to be caused by defects in both antero-posterior and dorsoventral patterning which would result in defects in centripetal cell migration and nurse cell dumping (like *cup* mutants – Berg, 2005). Fused egg chambers during the early stages of oogenesis were also observed in ovaries of heatshocked FLP; FRT-emc/FRT-GFP flies, like the ones from sense and antisense *emc* fly lines.

Collection time (hours)	Eggs with abnormal dorsal appendages (%)	
	hs *OrR*	**hs mosaic *emc*^{1}**
0-26	**2.76**	**8.01 ***
26-38	**9.75**	**13.93**
38-52•	**0.0**	**2.68**

Table 7.5.1: Percentage of eggs with abnormal dorsal appendages from heatshocked wild-type *OrR* and mosaic *emc*^{1} flies with follicle cell clones, at different times after heatshock

Within the 0-26 hour interval, the peak of eggs with abnormal DA laid from both fly lines was between 21-25 hours after heatshock (data not shown). Statistical analysis (chi-square test) showed that the results are statistically significant at the 0.1% level for the 0-26 hours after heatshock collection (chi-square = 19.41, $p < 0.001$), as indicated by the asterisk, but not for the 26-38 hours and 38-52 hours after heatshock collections (chi-square = 0.71 and 0.24, respectively; it should be ≥ 3.84 for significance at the 5% level). This means that for the last two samples the difference in the percentage of abnormality between mosaic and control flies may well be caused by the heatshock treatment but during the first 26 hours after heatshock the abnormal appendage phenotypes in the mosaic flies are caused by the presence of follicle cell clones since the difference from the control flies is significant.
The relatively low percentage of eggs with abnormal dorsal appendages can be explained as only a small proportion of egg chambers would be at the correct developmental stage during the heatshock. Furthermore, not all of the egg chambers would have *emc* homozygous mutant clones covering the specific subpopulations of follicle cells that affect appendage formation.

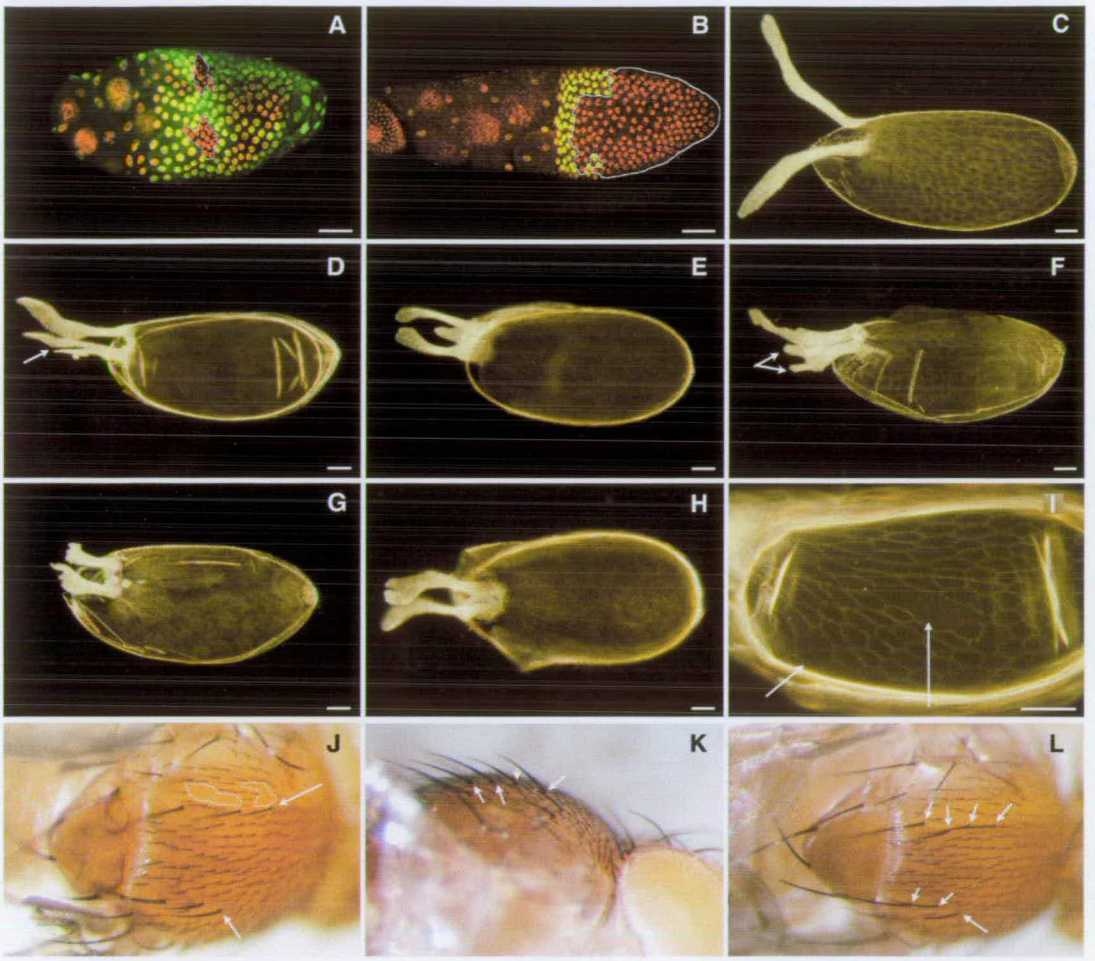

Figure 7.5.2: Mosaic flies with *emc*$^{1-/-}$ follicle cell clones
Phenotypic effects of *emc* follicle cell clones. A-B: Confocal micrographs of *emc* clones in ovaries. Nuclear GFP is green and all nuclei are in red (TO-PRO 3). Cells homozygous for *emc*^{1} do not express GFP and appear red rather than yellow in the overlays (clones circled with a white line). C: Wild-type egg morphology. D-H: Eggs from flies with *emc* follicle cell clones in ovaries. The dorsal appendages are closer together or fused at the base, have split ends (arrows), are thicker or occasionally shorter than wild type and sometimes have extra material. I: Follicle cell imprints on the eggshell of a mosaic egg. Arrows point to the abnormally shaped large clones as opposed to the regular follicle cell pattern. J-L: Mosaic flies have extra dorsocentral bristles (arrows) in the notum and the pattern of microchaetae can be disrupted in areas of *emc* clones (microchaetae absent from areas circled with a white line in J). Scale bars: 50µm.

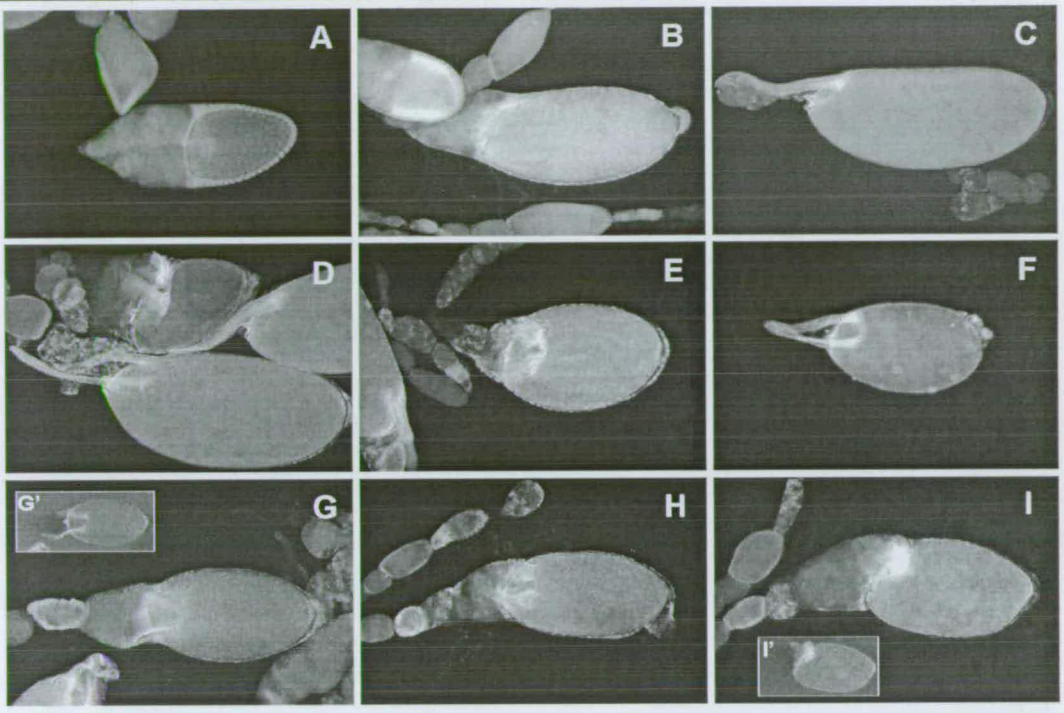

Figure 7.5.3 Small eggs and incomplete nurse cell cytoplasm dumping in ovaries with *emc* follilcle cell clones

Normal-sized (as in wild-type) egg chambers of stage 10 (A), 12 (B) and 14 (C) for size comparison in the first row. Egg chambers where dorsal appendages are developed (as in stage 14) but there is also nurse cell material that was not dumped into the oocyte (D, E, G, H, I). (F) shows an egg with normal dorsal appendages but is smaller and more round than wild-type. In (D, E, H, I) the dorsal appendages formed are short and wide, close together (E) or covering the dorsal midline in one continuous accumulation of dorsal appendage material (I). In (D) comparison of the malformed egg chamber (top left) can be readily made with a wild-type-looking egg (bottom half of picture). The insets (G') and (I') show in greater detail the morphology of the dorsal appendages of (G) and (I), respectively. All pictures (A-I) are at the same magnification with insets (G', I') being 0.25x of the original size.

7.6 The Grk/EGFR pathway and emc

The dynamic late expression pattern of *emc* in oogenesis with the localisation in two dorsal anterior patches at stage 12 that correspond to the stage 12 expression pattern of Broad-Complex and the effect of *emc* mis-expression, knock-out or clones on the egg dorsal appendage formation led us to suspect a link between *emc* and the Grk/EGFR pathway which is responsible for the establishment of the dorso-ventral (D-V) axis of the oocyte. I used in situ RNA hybridisation to investigate the position of *emc* with respect to genes that are well-known components of the Grk/EGFR (Grk/DER) signalling pathway.

7.6.1 *emc* must lie downstream of *gurken, Egfr and fs(1)K10*

As shown in Figure 7.6.1C, in the ovaries of grk^{ED11} homozygous mutant flies *emc* ceases to be expressed in two distinct subsets of dorsal-anterior follicle cells at stages 11 and 12 and is instead expressed in a broad dorsal-anterior region covering the dorsal midline (compare with Fig. 7.6.1A). Mutant $gurken^{ED11}$ flies (Neuman-Silberberg and Schüpbach, 1993) lay ventralised eggs with the dorsal appendages being closer together and thinner than in the wild type (Fig. 7.6.1B); their phenotype ranges from a smaller distance between the appendages to appendages fused at the base (Figure 7.6.1D), completely fused or a single very short appendage on the dorsal midline. *emc* mRNA is not expressed in the early stages of oogenesis and it is present in the centripetal cells at stages 9-10b (results not shown) but from stage 11 onwards its expression pattern changes to cover the dorsal midline in a single band in a manner reminiscent of the future appendage appearance of the laid egg. Therefore I suggest that *emc* lies downstream of *gurken* in oogenesis.

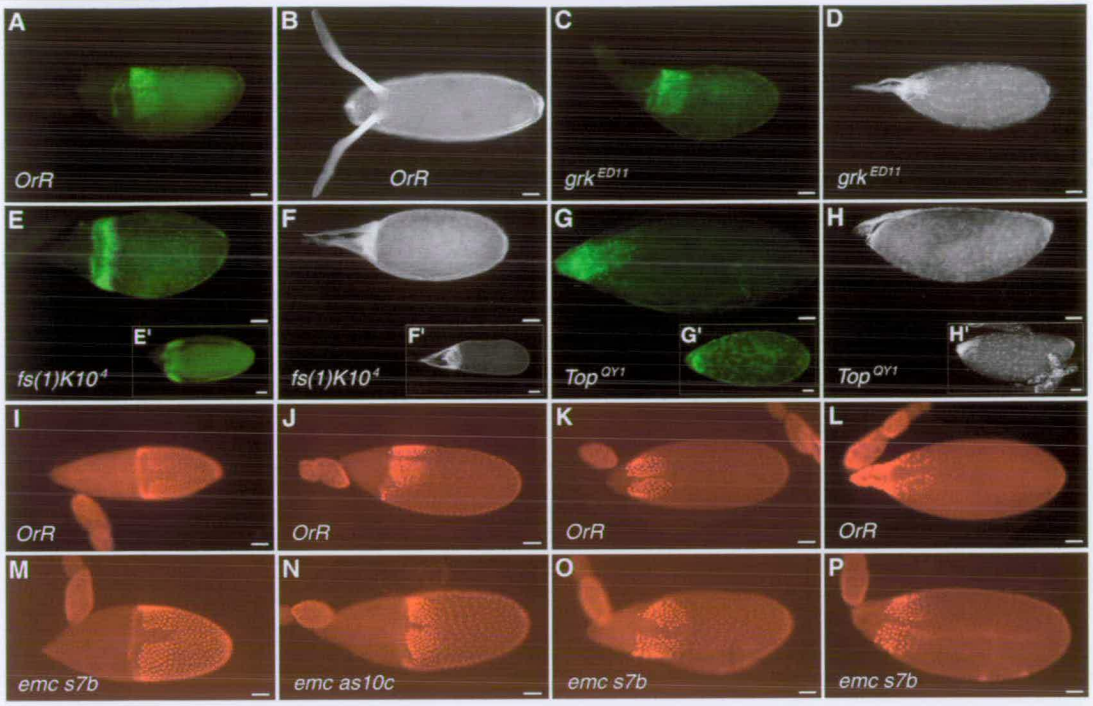

Figure 7.6.1: *emc* late expression pattern is altered in ovaries of flies mutant for *grk, Egfr* and *fs(1)K10* and *emc* mis-expression affects Br-C late oogenesis expression

A-H': In situ hybridisation with *emc* RNA on mutant backgrounds. A, C, E, E', G, G' show *emc* expression (green) in stage 12 egg chambers and B, D, F, F', H, H' show the corresponding dorsal appendage phenotype for each fly line. In (A) *emc* is expressed in two dorsal anterior subsets of follicle cells either side of a thin gap at the dorsal midline in wild-type *OrR* flies. *OrR* eggs have normal dorsal appendages (B). In grk^{ED11} mutant flies *emc* is expressed in a single broad dorsal anterior area covering the dorsal midline (C) and the eggs laid (D) have thin, shorter dorsal appendages fused at base (ventralised eggs) and are smaller than wild-type. *emc* is expressed in a ring of follicle cells all around the dorsal anterior (E) or in two lateral and a wide dorsal anterior patches (E') in $fs(1)K10^{4}$ mutants, resulting in dorsalised eggs shorter and more round than wild-type, with four appendages all around the anterior (F) or two wide lateral appendages with appendage material connecting them (F'). In Top^{QY1} mutants *emc* is expressed in a single patch over the dorsal midline (G) or is absent from follicle cells (G'). The corresponding eggs (ventralised) have either one very short, thin dorsal appendage (H) or very little chorionic appendage material at the anteriormost region of the egg (H').

I-P: Immunohistochemistry with a Br-C antibody. (I-L) show the expression pattern of Broad-Complex in *OrR* flies at stages 10 (I), early (J) and late (K) stage 12 and stage 13 (L). (M-P) show Br-C in *emc* sense and antisense fly lines. Normal Br-C expression is not disrupted in mid-oogenesis in the sense line *s7b* (M), but later at stage 12 the shape of the patches of follicle cells expressing Br-C is affected (O, P). Disruption of normal Emc expression in the antisense line *emc as10c* does not inhibit Br-C expression and disrupts the shape of the Br-C – expressing patches only mildly (N). Scale bars = 50 μm. Pictures M-P by G. Tzolovsky.

Similarly, *emc* transcript expression pattern is disrupted by mutations in *fs(1)K10* and *Egfr* (*Torpedo*) genes (Figure 7.6.1E-H'). Fs(1)K10 is required in the oocyte nucleus to restrict *grk* expression to the dorsal part of the anterior oocyte, most likely by interaction with Squid and Bruno proteins (Kelley, 1993; Norvell et al, 1999). Eggs mutant for $fs(1)K10^{4}$ are dorsalised, having two very wide lateral respiratory appendages (due to the -dorsal- region of *grk* expression expanding towards the ventral side) or an even more extreme phenotype of a ring of dorsal appendage material all around the anterior of the egg (Fig. 7.6.1F, 7F') because of *grk* transcripts being translated throughout the anterior of the oocyte. As shown in Figure 7.6.1E *emc* transcripts are present in a ring all around the oocyte anterior at stage 12 instead of being restricted to two dorsal anterior follicle cell subsets, or, in milder phenotypes, *emc* is expressed in two lateral and a wide dorsal anterior follicle cell patch (Fig. 7.6.1E'). Top^{QY1} mutant flies (Schüpbach, 1987) laid ventralised eggs with a central, very thin and short dorsal appendage (Fig. 7.6.1H) or very little dorsal appendage material (Fig. 7.6.1H'). The expression of *emc* is altered, with *emc* mRNA being present in one dorsal anterior group of follicle cells, thinner and longer compared to the grk^{ED11} mutants, covering the dorsal midline at stage 12 (Fig. 7.6.1G); alternatively, *emc* is expressed in even smaller dorsal-anterior spots or is absent from the follicle cells at stage 12 (Fig. 7.6.1G'), presumably reflecting the various degrees of ventralisation of the egg caused by the absence of EGFR signalling. These results suggest that *emc* expression is involved in the commitment to dorsal appendage fate of the follicle cells in which it is expressed, and that it is downstream of the *fs(1)K10* and *Egfr/Top* genes in the Grk/EGFR signalling pathway.

7.6.2 Broad-Complex expression pattern is disrupted in *emc* sense and, to a lower extent, antisense transgenic flies (with G. Tzolovsky)

Since the *emc* late expression pattern in oogenesis is reflected in the dorsal appendage phenotype observed, we used an antibody against the Broad-Complex (Br-C) core domain (Tzolovsky et al., 1999) on *emc hs as10c* and *s7b* fly lines. The

Br-C locus is required for dorsal appendage morphogenesis and is an effector of the Grk/EGFR pathway on D-V axis formation while Dpp signalling is necessary for its correct expression along the A-P axis (Deng and Bownes, 1997b). *Br-C* expression pattern is quite different from that of *emc* in early and mid-oogenesis (Fig. 7.6.1I) up to stage 12 where *Br-C* is expressed in two subsets of dorsal anterior follicle cells either side of the dorsal midline exactly like *emc*. The same pattern is followed by Br-C and Emc proteins at stage 12 and 13 (Fig. 7.6.1J-L). In the sense *emc* line *s7b* the late Br-C protein expression pattern is disrupted more often than in the antisense *emc* line *as10c* (Figures 7.6.1O-P, compared with 7.6.1J-K), suggesting that *emc* affects *Broad-Complex* expression with respect to the dorsal appendage-producing follicle cells. Its function must be one of refining the dorsal appendage position rather than determining whether there will be dorsal appendages produced or not, since in *emc* antisense heatshocked flies BR-C was still expressed, even though Emc was knocked-out, and the BR-C expression pattern was usually normal (Fig. 7.6.1N); Br-C was also not affected in Emc null follicle cell clones (Fig. 7.6.2). In the sense *emc* flies, where *emc* was ectopically expressed, Br-C was likely to be expressed in extra follicle cells, suggesting that *emc* needs to be correctly localised for the correct localisation of Br-C in the follicle cells producing the dorsal appendages, but that there must be other genes responsible for regulating the expression itself of BR-C acting on those subsets of follicle cells. Expression of Br-C during early and mid-oogenesis was not affected by *emc* misexpression (Fig. 7.6.1M compared to 7.6.1I).

7.6.3 Broad-Complex (Br-C) expression is not affected by *emc* homozygous mutant clones

Antibody staining for Broad-Complex (Br-C) using *emc* mosaic flies shows that Br-C expression is not disrupted by the absence of *emc* from a clone of cells (Fig. 7.6.2). This is true not only in stages 9-10 (Fig. 7.6.2A) when one could argue that Emc and Br-C do not co-localise (Fig 7.6.1I), thus they would not be expected to be interacting, but also in stages 12 and 13 (Fig. 7.6.2B-C) where they would be expressed in the same subsets of dorsal anterior follicle cells.

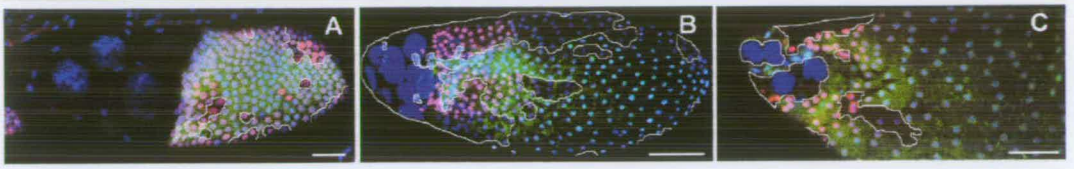

Figure 7.6.2 Broad-Complex expression in egg chambers with *emc* clones
Confocal microscope overlays of *emc* clones (absence of green nuclear GFP staining), Broad-Complex antibody staining (red) and DNA staining (blue). The Broad-Complex expression pattern is not affected by the presence of *emc* clones; clones are circled with a white line. A: Stage 10; B: Stage 12 and C: stage 13 egg chamber. Scale bars = 50 µm.

This suggests that *emc* expression is not required for allowing Br-C to be expressed in the late stages of oogenesis. The way by which it seems to cause expression of Br-C in some extra cells apart from the usual clusters of dorsal appendage-forming cells in *emc* sense fly lines must be sought elsewhere. One possibility is that it could be by interactions with other genes involved in the formation of the tube that is the dorsal appendage, such as by affecting the genes that form the border between roof (Br-C)-inducing and floor (Rho)-inducing cells (Ward and Berg, 2005).

7.6.4 *emc* mRNA expression in other mutant backgrounds

In addition to flies with the mutations for *grk*, *Egfr* and *fs(1)K10* described above, a series of other fly lines with mutations for genes involved in the dorso-ventral axis patterning or inducing ectopic expression or knock-out of such genes was used to study how *emc* expression would be affected. The results were not as clear as for the aforementioned genes but due to time limitations it was not possible to continue and clarify the matter. A summary of the findings so far is presented in Table 7.6.1.A-B and Figure 7.6.3.

Genetic background (source)/ expected function	Egg chamber/ laid egg phenotype	*emc* mRNA expression	Comments
UAS kekkon[1] $4R^{+}$ TM/ T155 Gal4 (Musacchio et al, 1996) Ectopic Kekkon	Ventralised eggs: St.14 egg chambers and laid eggs do not have dorsal appendages or have very small ones, non-extending beyond	No early stage staining. Only dorsal staining over centripetal cells at st.9-10, also non-stained st.9 egg chambers. No st.11-12 staining (dorsal anterior patches).	Very weak staining generally. *Kekkon* could be upstream of *emc* but results need to be confirmed.

expression in all follicle cells.	egg length.		
UAS Egfr[B]/ T155 Gal4 Ectopic expression of Egfr.B in all follicle cells	Normal-looking dorsal appendages (or slightly closer together – dorsalisation)	No early stage *emc* staining. Wild-type expression in st.9-10 (anterior fc over centripetal cells stained); occasionally two dorsal anterior patches stained in st.10. Normal *emc* expression in st.11. No dorsal anterior patches in st.12 but staining between dorsal appendages in st.14.	Results need to be confirmed and staining pattern in mid-oogenesis clarified.
HS as Rho (Ruohola-Baker et al, 1993) Heatshock-induced antisense over-expression = Rho knock-out	Shorter, more round egg chambers than wild-type (wt). Several egg chambers are undergoing apoptosis	No early stage staining. Dorsal anterior staining across centripetal cells at st.10 as in wild-type. Two dorsal anterior patches in st.11-12 like wt, but also st.12 without *emc* on these patches	Unclear if Rho knockout phenotype is absence of *emc* expression in the two dorsal anterior fc subsets or *emc* presence but with a smaller dorsal midline gap (ventralisation). Control non-HS as Rho flies had wild-type *emc* expression, starting from st.2 fc.
HS s Rho Heatshock-induced sense over-expression = ectopic Rho expression	Several apoptotic egg chambers. Laid eggs –normal size, occasionally with da closer together.	Usually no early stage staining. Two dorsal anterior patches at st.12, sometimes also a line across the ventral anterior fc.	The results indicating no effects on the cells that will produce da must be confirmed – are the st 12 patches exactly the same as in wt eggs or do they contain different number of cells/ have slight modifications?
UAS-dpp/ T155 Gal4 Ectopic *decapentaplegic* expression in all follicle cells	Ventralised eggs – no dorsal appendages or da material, or very little dorsal appendage material. Malformed chorion Many fused egg chambers	Very strong staining in all early stages up to st.10, also appears to be in nurse cell cytoplasm. In st.12 the dorsal anterior patch seems to have moved anteriorly, over the nurse cells.	Too strong staining to distinguish features- confirmation of results needed. Extremely low survival rates. Female larval lethal for T155♀ x UASdpp♂ at 25°C and 18°C. Very few

			females eclose at 18°C from UASdpp♀ x T155♂ cross, after a long developmental delay.
UASdpp/ hs Gal4 Ectopic *decapentaplegic* expression in all follicle cells, induced by heatshock	Malformed egg chambers: nurse cell nuclei everywhere, fc in fragmented layers. Some fused early egg chambers. Laid eggs with normal-looking da in some ovaries but also ventralised eggs without da material (95%) or very short da (5%)	Early stages stained (st.2-st.6, not st.7) St. 8-9 are very strongly stained but look malformed at the same time- must be apoptotic. *emc* staining between da in st. 13-14.	Very few flies survive from this cross
dpp[e87] Lethal *dpp* allele, conditional temperature-sensitive			No homozygous dpp[e87] escapers isolated from the dpp[e87]/CyO stock at either 25°C or 18°C.
UAS pntP1/ T155 Gal4			1^{st}-2^{nd} instar larval lethal at both 25°C and 18°C
UAS pntP2/ hs Gal4	Occasionally some apoptotic egg chambers. Wild-type –looking laid eggs.	Strong staining in early stages up to st.8. Wild-type *emc* staining line in st.9. Uniform strong *emc* staining in follicle and nurse cells, not in laid eggs.	All available ovaries were too small even in very well-fed flies – not all stages represented (only very early stages and a few laid eggs)
grk[3] (Schüpbach, 1987) Strong mutant *grk* allele - Ventralised eggs			No homozygous grk[3]$^{-/-}$ escapers in the grk[3]/CyO stock.
grk[22j] (Neuman-Silberberg and Schüpbach, 1994) Grk overexpression	Dorsalised eggs- da thicker than wt, further apart between them	Normal *emc* anterior expression in st.9-10. St.9: also strong expression in stretched fc cytoplasm and nurse cells. St. 11 continuous anterior line of staining (no patches) St. 12: never two patches, *emc* staining looks more anterior and continuous	grk[22j] flies have four copies of *grk*. Very weak staining overall.

		over nurse cells as well. St.13 possibly 2 micropyles forming in an egg chamber.	
Hs Argos (Zhao et al, 1999) Ectopic Argos expression after heatshock	Ventralised eggs Laid eggs are normal or have very thin appendages, close together with thick bases, or are bottleneck (no da)	No early stages staining. St.9: nurse cells are stained. St.11: no *emc* fc patches, only nurse cells stained. St.12: very anterior tip stained.	Abnormalities (ventralisation) in laid egg phenotypes confirm that heatshock induces *aos* oversexpression. *emc* staining not clear.
Hs Z1 (Br-C) (Deng and Bownes, 1997b)	Many apoptotic st.8-9 egg chambers	Some weak early stage staining (up to st.6) or no early staining. Patches at st.11 seem to be further apart and there is anterior *emc* expression in st.12.	Not very clear pictures- difficult to see if the patches are further apart than wild-type or if there is background staining.
UAS lacZ/T155 Gal4	β-galactosidase staining to monitor the expression pattern of T155 Gal4 fly line. Uniform staining of follicle cells around the germline cells.		
UAS lacZ/ hs Gal4	β-galactosidase staining to monitor the expression pattern of hs Gal4 fly line and the efficiency of heatshock in inducing Gal4 expression. Staining of all follicle cells observed. Strong expression from st. 7-8 in all follicle cells, weaker expression in fc of earlier stages.		

Table 7.6.1A: In situ hybridisation with *emc*T7 probe on fly lines with mutations or overexpression of genes related with the Grk/Egfr pathway and D-V axis patterning

Information regarding mutant backgrounds Grk^{ED11}, Top^{QY1} and $fs(1)K10^{4}$ was omitted from the table as it was presented above (section 7.5.2). wt, wild-type; da, dorsal appendages; fc, follicle cells; nc, nurse cells.

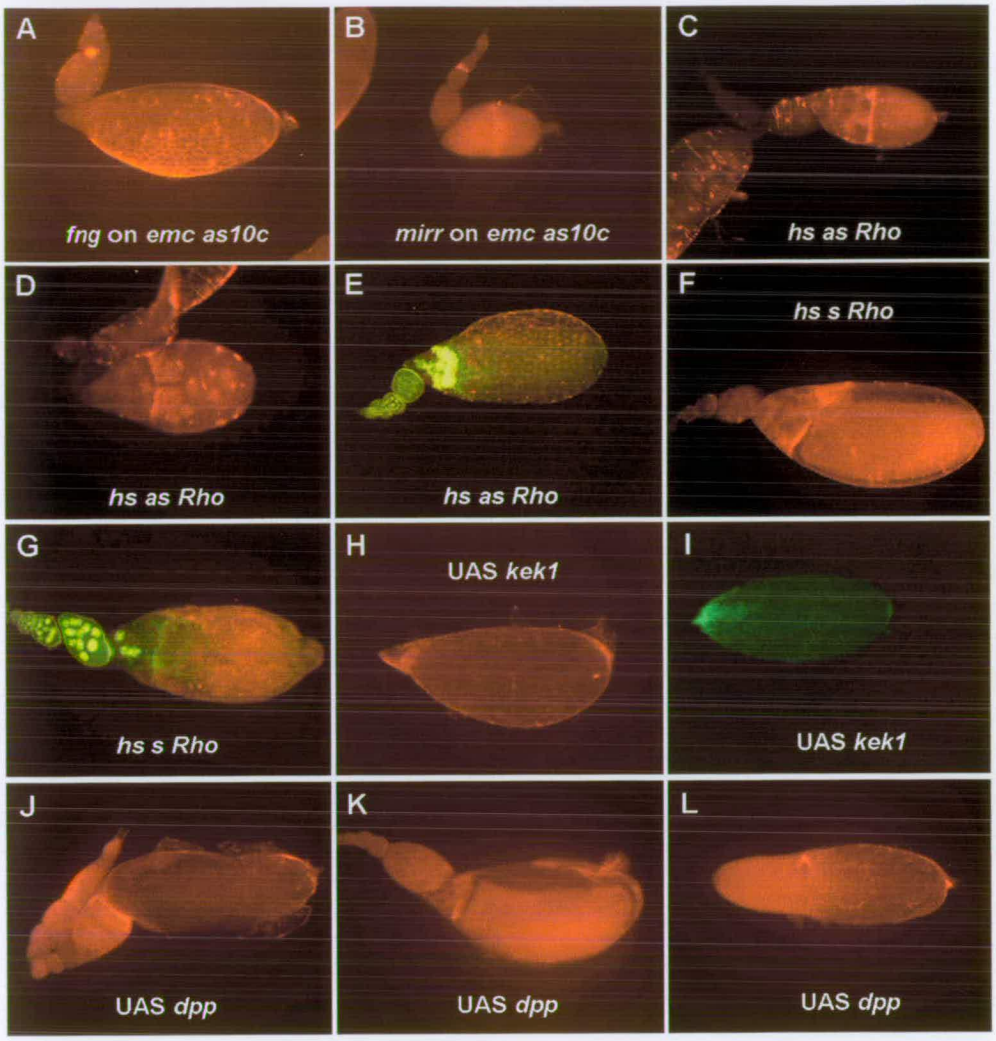

Figure 7.6.3: *emc* expression in mutant backgrounds and *fringe, mirror* expression in *emc* knock-out fly lines
Some phenotypes from the in situ hybridisation experiments presented in table 7.6.1. For details, see tables. (A, B) are in situ hybridisations with *fringe* and *mirror* probes, respectively (red staining), on *emc as10c* antisense fly ovaries. (C-L) are all in situ hybridisation experiments with *emc* probe on the genetic backgrounds written on each picture. In (C-H) and (J-L) the *emc* mRNA expression pattern is in red (TSA-Cy3). In (E) and (G) green indicates DNA (in cell nuclei). In (I) *emc* mRNA is in green (TSA-FITC). All pictures are with the same magnification.

7.7 Investigation of a role for emc in oocyte selection

7.7.1 Analysis of *emc* germline clones

To observe the effect of *emc* clones in the germline cells *FLP; ovoD1, FRT/ emc*^{1}, *FRT* flies were heatshocked to induce mitotic recombination and allowed to lay eggs.

Heatshock was performed once or more on wandering L3 larvae (39°C, 1hr) or from early third instar larvae until early pupae; flies eclosed around 4 days after heatshock and were dissected 6-12 days after heatshock, after observing the notum bristle phenotype and monitoring the flies for egg laying (fertility). At the time of heatshock the differentiation of ovarioles would have began and the ovaries would contain oogonia, which ultimately provide the stem cells of the germaria (King, 1970). The crossing scheme is presented in Figure 7.7.1. The principle of using the dominant female sterile *ovoD1* mutation is that *ovoD1* flies do not lay eggs and their ovaries are atrophic, containing only previtellogenic egg chambers (Perrimon, 1998; Mevel-Ninio et al, 1991); when a given mutation becomes homozygous after mitotic recombination only the egg chambers homozygous for that mutation will mature and become embryos since any egg chamber containing *ovoD1* cannot complete oogenesis. No eggs were laid from the heatshocked *ovoD1/emc*^{1} flies and in all ovaries dissected (from 501 flies) there were no egg chambers bigger than what would be equivalent in size to stage 6 of oogenesis (See Fig. 7.7.2A-C for mosaic ovaries). Egg chambers were fused or devoid of germline cells, or undergoing apoptosis. However, extra bristles were observed on the notum of these heatshocked flies (Figure 7.7.2D-F and 7.7.2H) indicating that *emc* mutant clones were induced at least in the notum and the head and produced extra bristles in the same manner observed in *emc* mutants (Moscoso del Prado and Garcia –Bellido, 1984) and, as shown above, in *emc* follicle cell clone-producing flies and in *emc* sense and antisense transgenic flies (compare with Fig. 7.5.2J-L). Therefore I suggest that the early function of *emc* in oogenesis is essential for the normal development of the egg since absence of *emc* from the germline cells cannot rescue the *ovoD1* phenotype and egg chambers cannot develop beyond stage 6 and into vitellogenic stages.

I:

P ♂ ♀

$$\frac{w^{*};\ P\{w^{+mC}=ovoD1\text{-}18\}3L\ P\{w^{+mW.hs}=FRT^{w[hs]}\}2A}{Y;\ TM3,\ Sb^{1}} \times \frac{P\{ry^{+t7.2}=hsFLP\}1,\ y^{1}\ w^{1118};\ Dr^{Mio}}{P\{ry^{+t7.2}=hsFLP\}1,\ y^{1}\ w^{1118}\ \ TM3,\ ry\ Sb^{1}}$$

(ovoD1-FRT/Sb) – (orange eyes, Sb) (hsFLP; Dr^{Mio}/Sb) – (white Dr^{Mio} eyes, Sb)

Select F1 ♂ $\frac{P\{ry^{+t7.2}=hsFLP\}1,\ y^{1}\ w^{1118}}{Y};\ \frac{P\{w^{+mC}=ovoD1\text{-}18\}3L\ \ P\{w^{+mW.hs}=FRT^{w[hs]}\}2A}{Dr^{Mio}}$ or $\frac{P\{w^{+mC}=ovoD1\text{-}18\}3L}{P\{w^{+mW.hs}=FRT^{w[hs]}\}2A\ \ TM3,\ ry\ Sb^{1}}$

Option A **Option B**

(yellow ♂; either orange Dr^{Mio} eyes, non-Sb, or orange normal eyes, Sb)
= (hsFLP; ovoD1)

II:

(e.g Option B) ♂ ♀

$$\frac{P\{ry^{+t7.2}=hsFLP\}1,\ y^{1}\ w^{1118}}{Y};\ \frac{P\{w^{+mC}=ovoD1\text{-}18\}3L\ \ P\{w^{+mW.hs}=FRT^{w[hs]}\}2A}{TM3,\ ry\ Sb^{1}} \times \frac{w^{*};\ emc^{1}P\{ry^{+t7.2}=neoFRT\}80B}{w^{*}\ \ TM6B,\ Tb^{1}}$$

(hsFLP; ovoD1-FRT/Sb) (FRT-emc^{1}/Tb)

Select ♀ (hsFLP/w^{*}; ovoD1-FRT/ FRT-emc^{1}) = (non-Tb, non-Sb) of the genotype:

$$\frac{P\{ry^{+t7.2}=hsFLP\}1,\ y^{1}\ w^{1118}}{w^{*}};\ \frac{P\{w^{+mC}=ovoD1\text{-}18\}3L\ \ P\{w^{+mW.hs}=FRT^{w[hs]}\}2A}{emc^{1}P\{ry^{+t7.2}=neoFRT\}80B}$$

and heatshock to activate the FLP recombinase and induce mitotic recombination between the FRT sites.

Practically: Separate Tb from non-Tb larvae in progeny of cross II. Heatshock all non-Tb larvae to induce mitotic recombination, select the non-Sb females when they eclose. Only the recombinants emc^{1}/emc^{1} (*ovoD1* removed) will have vitellogenic stage egg chambers and produce laid eggs, provided that *emc* does not affect normal development.

Figure 7.7.1 Genetic crosses for generation of flies with *emc* mutant clones in the germline

Only the genotypes of progeny selected from each cross are shown and a name summarising the key genes present as well as the phenotype used for selection are given in parentheses, for simplicity. For cross II separate crosses were set with both options A and B for males crossed with FRT-emc^{1} females, to maximise the number of progeny produced.

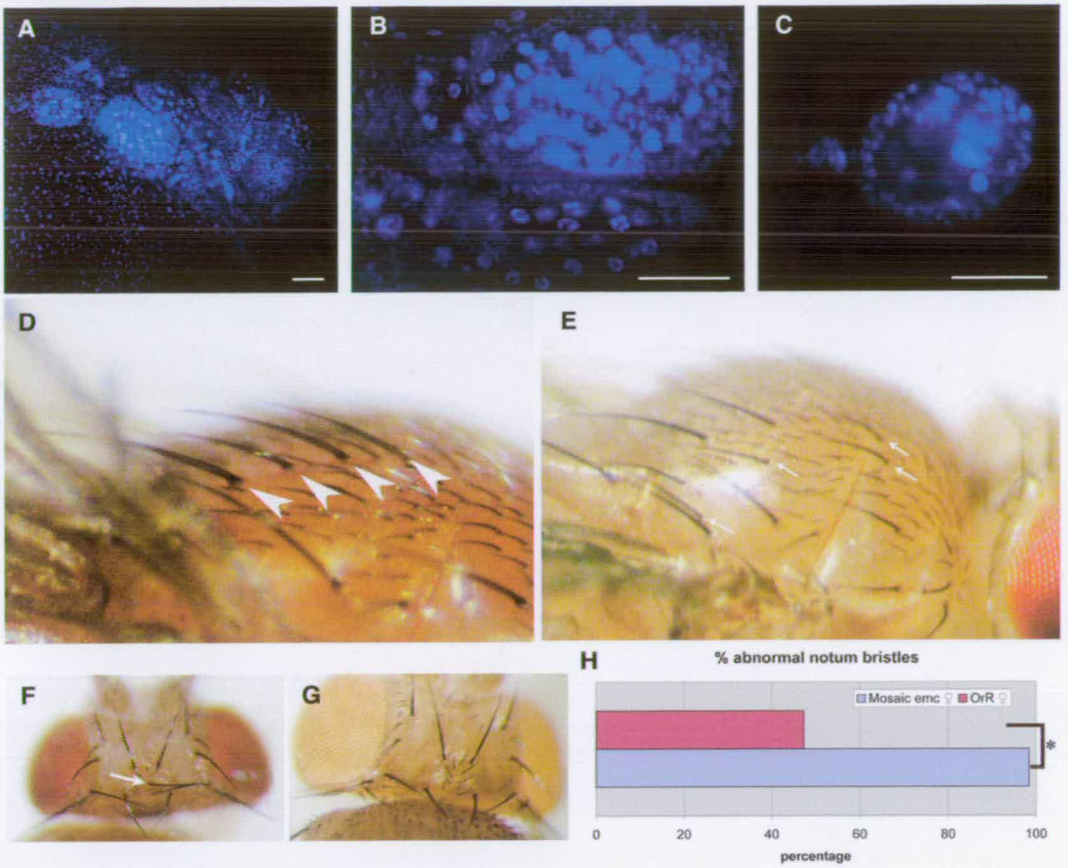

Figure 7.7.2 *emc* germline clones
(A-C) Atrophic ovaries from flies with *emc* germline clones; DNA is stained with Hoechst 33258. (A) Whole ovary- there are no normally developing egg chambers. (B) shows fused egg chambers (with more than 16 polyploid nuclei) and (C) an apoptotic egg chamber. Scale bars = 50 µm. The general phenotype of the mosaic ovaries is very similar to that of *ovoD1* mutant flies, so the emc^1 homozygous mutant egg chambers cannot be distinguished morphologically from the *ovoD1*-expressing egg chambers. (D-F) Extra bristles in the notum of mosaic flies. Four dorsocentral bristles instead of two in (D) (arrowheads) and extra macrochaetae in the notum (arrows) in (E). (F) shows an extra bristle in the head (arrow) compared to the wild-type phenotype in (G). (H) Table showing the percentage of flies with emc^1 germline clones having abnormal bristles compared to similarly treated *OrR* flies. Note that the abnormalities in the wild-type *OrR* flies are mainly missing bristles and occasionally extra bristles on the sides of the notum, whereas the abnormalities in the mosaic flies refer to the presence of extra bristles, mainly extra dorsocentral bristles. The asterisk indicates that the results are statistically significant at the 0.1% level (chi-square = 327.95, $p<0.001$).

7.7.2 Following the oocyte position with *oskar* in situ hybridisation

I used *oskar* (*osk*) mRNA as a marker for the oocyte position and performed in situ hybridisation to ovaries of heatshocked and non-heatshocked *OrR* wild-type flies and

heatshocked *emc* sense and antisense mis-expression fly lines (s7b and as10c). Ovaries were dissected 6- 26hr after heatshock (37°C, 1hr in a waterbath) and expression of *oskar* was detected by alkaline phosphatase or Tyramide Signal Amplification and fluorescent probes. The number of early stage egg chambers (up to stage 10) was counted for each fly line and the numbers of egg chambers without an oocyte (marked by absence of *osk* staining) or with two oocytes (two dots of staining) were scored (see Figure 7.7.3A-B). Following the Alkaline Phosphatase signal detection, the abnormal egg chambers were checked in a phase-contrast microscope to look for the oocyte nucleus and check whether even if there is no *osk* staining there is an oocyte or not. Visualisation of the oocyte nucleus with this method is possible from stage 7 onwards. There is a high percentage of heatshocked *OrR* egg chambers showing no obvious *osk* staining, much higher than the equivalent sense *emc* and not significantly smaller than *emc* antisense (Table 7.7.1). For egg chambers with two oocytes the percentage is very low for all fly lines but the heatshocked *OrR* figure is actually higher than the *emc* mis-expression lines. Therefore, based on these results I cannot confirm that mis-expression of *emc* affects oocyte selection since there is no significant difference to the control. It must be noted though that it is not always easy to assess whether a given egg chamber lacking *oskar* staining contains 16 nurse cells or 15 nurse cells and an oocyte which, for whatever reason, was not stained. Similarly, for *oskar* staining in two places in an egg chamber, situations where one dot was clearly an artefact were not taken into account, but there may still be some false-positives.

	% of egg chambers up to st.10	
Fly line	**No oocyte**	**Two oocytes**
Non-HS *OrR*	0.0	0.0
HS *OrR*	25.13	2.18
HS *emc* s7b	4.14	1.30
HS *emc* as10c	36.29	1.54

Table 7.7.1 Percentage of egg chambers with oocyte number defects
Early egg chambers (germarium- stage 10) from control and *emc* mis-expression fly lines were counted and scored for number of oocytes/egg chamber (0, 1, 2 or more) based on *oskar* staining. The egg chambers were not fused with others and the number of germline cells was counted (in as many as possible) and equalled 16. 183-917 egg chambers were counted per fly line.

In order to investigate how oocyte determination may be affected in *emc* homozygous mutant clones in the ovary, I used in situ hybridisation with *oskar* mRNA on mosaic ovaries containing $emc^{1-/-}$ and *ovoD1/ovoD1* egg chambers. The parental fly lines of the germline clone-generating cross were used as controls (females that are sterile from the *ovoD1-FRT/Sb* stock, females from the *FRT-*emc^{1}*/Tb* stock – see Fig. 7.7.1) as well as wild-type *OrR*. *oskar* mRNA is present in its expected expression pattern in one germline cell (the oocyte) of each egg chamber, and localised at the posterior of the oocyte from stage 3 in both *OrR* and *FRT-*emc^{1} ovaries (Fig. 7.7.3C-D). The sense *osk* DIG-labelled RNA used as a negative control on *OrR* did not give any staining (not shown). Staining was also absent in the *ovoD1-FRT* ovaries (Fig. 7.7.3I) whereas in mosaic ovaries (Fig. 7.7.3E-F) only very few egg chambers were stained for *oskar*; in some cases there were two oocytes in an egg chamber (Fig. 7.7.3G-H), although this could be due to fusion between egg chambers, which was observed at high levels in the mosaic ovaries. It is intriguing why the dominant female sterile *ovoD1* ovaries do not show any *oskar* expression. There is the possibility that the in situ hybridisation simply did not work well, although it did work as expected in two other fly lines with the same probes and conditions. Nonetheless, with the "mother" *ovoD1* fly line not showing *osk* expression it is not possible to identify those egg chambers in the mosaic (*ovoD1-FRT/*emc^{1}*-FRT*) ovaries that would not express the *osk* oocyte marker due to a potential effect of the *emc* homozygous clones. How *emc* may be involved in oocyte determination and what roles it may have in relation to the germline cells remains to be investigated. Several approaches that would help to overcome the current problems are discussed below (section 7.8).

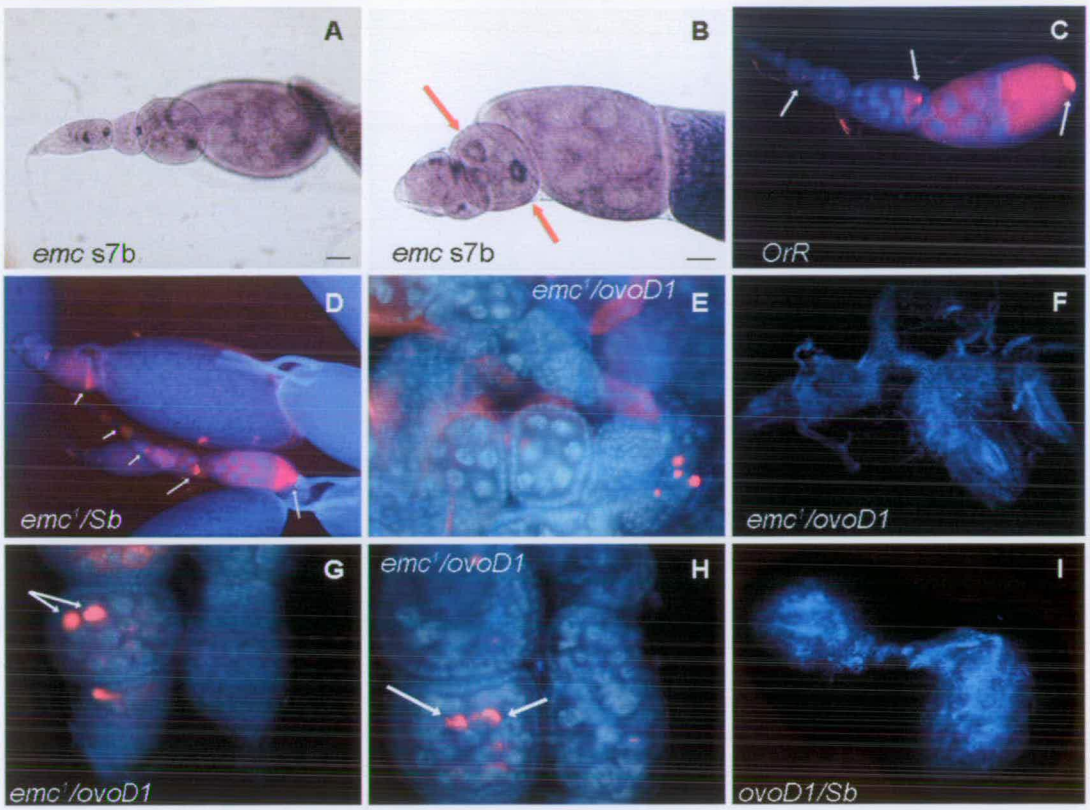

Figure 7.7.3 *oskar* mRNA in situ hybridisation on mosaic *emc* mutant and mis-expression fly lines
(A) wild-type *oskar* expression pattern, detected by alkaline phosphatase. The oocyte expresses *osk* and is localised at the posterior of the cyst. (B) Two stained areas in a sense *emc*-expressing fly line may represent two oocytes and are indicated by red arrows. (C, D) Normal expression of *osk* in wild-type *OrR* and a heterozygous balanced emc^1 fly line, respectively. Ovaries from flies mosaic for emc^1 and *ovoD1* (E-H). The mosaic ovaries look very much like ovaries from *ovoD1* flies (I), but can have more "normal"-looking egg chambers (E) than *ovoD1* ones, even though they have many fused egg chambers and cysts without germline cells. Occasionally there is *osk* staining in two cells of the same egg chamber; this can indicate two oocytes (G) or may be attributed to partial fusion of egg chambers (H, likely). No *osk* was expressed in *ovoD1* ovaries (I). Scale bars = 20µm in A - B. E, G, H are magnified 2x compared to C, D, F and I. White arrows = *osk* expression.

7.8 Discussion

emc appears to have a key role in cell fate determination in somatic cells during the process where follicle cells surround the oocyte and in dorsal appendage positioning.

I have shown using β-galactosidase staining of an enhancer-trap line, in situ hybridisation to mRNA and antibody staining that *emc* has a dynamic expression pattern in oogenesis. Expression is observed both in the germ cells and in the somatic follicle cells. Maternal Emc is already known to be essential for sex determination in embryogenesis (Younger-Shepherd et al., 1992) thus the expression observed in the nurse cell nuclei was expected.

Ectopic *emc* overexpression using heatshock sense fly lines leads to a large number of fused egg chambers that eventually undergo apoptosis. Most of the abnormal egg chambers seem to be fused longitudinally, as they appear to be very long and thin. A different type of fusion is present using antisense *emc* knock-out: fusion seems to happen laterally since egg chambers that can proceed up to stage 11 of oogenesis with a normally developing oocyte and double the number of nurse cells were observed. This phenotype was not observed in heatshocked *OrR* flies. These phenotypes suggest abnormalities during enveloping of the germline cysts in germarium region 2, when egg chambers become assembled and are characteristic of mutants for *Notch*, *Delta*, *daughterless* and of ectopic *hedgehog* expression (Goode et al, 1996; Forbes et al, 1996). Similar phenotypes were observed in ovaries of flies with *emc* follicle cell clones. Thus *emc* would be implicated in enveloping the germ cell cluster, consistent with presence of the protein in the germarium and with recent findings by Adam and Montell (2004) who observe similar fused egg chambers following overexpression of *emc*. They confirm the relationship of *emc* with the Notch signalling pathway in oogenesis by identifying *emc* as an effector of Notch signalling in the differentiation of follicle cells and suggest that the fused phenotypes are caused by the failure of polar cells to differentiate (polar cells are required to induce stalks which separate developing egg chambers in the ovariole) (Adam and Montell, 2004). Such a relationship is not surprising, given that *emc* is known to interact with the *Notch-Delta* pathway in the developing eye (*hedgehog* is involved as well) and wing disc and to be involved in the regulation of the bHLH Daughterless in sensory organ formation and sex determination (van Doren et al, 1991, Younger-Shepherd et al, 1992; Cabrera et al, 1994; de Celis, 1998; Baonza and Freeman, 2001).

Emc also functions later in development in the follicle cells, during the regulation of dorsal appendage formation, a procedure controlled by the Grk/EGFR pathway. The chorionic appendages are moved closer together and often fuse when *emc* levels are reduced by antisense expression. Similar results are seen when *emc* is removed in clones of cells, where the appendages are frequently split at their ends. I have demonstrated that *emc* mRNA expression is affected by the disruption of the normal dorso-ventral axis formation caused by mutants for *fs(1)K10*, *gurken* and *Egfr*. Specifically, the *emc* expression pattern follows the ventralisation caused by grk^{ED11} and Top^{QY1} and the dorsalisation caused by $fs(1)K10^{4}$. Therefore *emc* functions downstream of *fs(1)K10*, *gurken* and *Egfr* and upstream of the finally formed dorsal appendages.

Further support for the role of *emc* in dorsal appendage morphogenesis comes from our finding that *emc* ectopic expression affects the expression pattern of Broad-Complex, a transcription factor that regulates dorsal appendage formation (Deng and Bownes, 1997b). In *emc* sense transgenic lines Br-C protein is expressed in a more irregular pattern than normal, mainly at stages 12-13. Br-C protein expression pattern coincides with that of *emc* mRNA at stage 12 of oogenesis as they are both expressed in two dorsal anterior subsets of concentrated follicle cells either side of the dorsal midline (these "patches" of follicle cells are discrete and visible also with nuclear markers) and in late stage 12-13 they follow the same pattern of being expressed in the migrating follicle cells that are forming the dorsal chorionic appendages. In *emc* sense flies the borders of Br-C expression are irregular and there are follicle cells in the gap between the two patches or around their borders that express Br-C. So *Br-C* must lie downstream of *emc* since its expression is affected by *emc* misexpression. However, *emc* is not the gene that activates *Br-C* since Br-C protein is expressed in the normal wild-type pattern in *emc* homozygous mutant follicle cell clones and in *emc* antisense lines where *emc* is knocked-out (or there are minor disruptions in the Br-C expression area in antisense compared with sense lines); rather, it seems that *emc* must be necessary for modulating *Br-C* within the areas of *emc* expression.

Further work would be necessary to define in greater detail the position of *emc* in the dorso-ventral axis formation pathway and to establish a link with other genes that are key players in this process. Preliminary work with *emc* expression in various other mutant backgrounds shows that it is likely that *emc* is downstream of *kek1* -which makes sense since *kekkon-1* is an inhibitor of Egfr (Musacchio et al, 1996; Ghiglione et al, 1999) and *Egfr* is shown to be upstream of *emc*. Expression of *mirror* in wild-type, *hs emc s7b* and *hs emc as10c* at stage 10 is localised to dorsal anterior cells. *mirr* is activated by Grk/EGFR and suppresses *fng* expression in dorsal anterior follicle cells (Zhao et al, 2000a). For *fringe*, the expression pattern in all follicle cells except the dorsal anterior (Zhao et al, 2000b) seems to be present in both sense and antisense *emc* lines in stages 9-12, suggesting that *fng* may not be affected by *emc* mis-expression. Therefore *emc* is likely to lie downstream of *mirr* and *fng*. These patterns must be confirmed in order to clarify the interaction of *emc, kek1, fng* and *mirr* and further work on *dpp, pointed, Rhomboid* and *argos* must be undertaken.

In several of these genetic backgrounds in situ hybridisation with *emc* shows absence of early stage *emc* staining. This presumably is important for a different *emc* function in oogenesis. Eventually I concentrated on the late *emc* expression in oogenesis, related with dorsal appendages formation regulation, and did not continue with studies for the early function after some preliminary work on generation of *emc* clones in the germline and in situ hybridisations aimed at following the oocyte fate with *oskar* as a marker. The study of the role of *emc* in early oogenesis can be an independent new project- *emc* roles in follicle cells and in the germline during early oogenesis are possibly different from its role(s) later in oogenesis.

My work on early oogenesis showed that *emc* germline clones generated using the *ovoD1* mutation fail to proceed through oogenesis and die during the early stages. Although no embryos were obtained, I am confident that the *ovoD1*-like phenotype I observed after clone induction is significant and denotes failure of *emc* germline clones to proceed with development in the ovary, since clones were observed in other tissues of the treated flies (e.g. induction of extra bristles). This confirms that the heatshock treatment for clone induction was efficient and statistically significant

compared to control wild-type flies. Therefore *emc* early function must be crucial for normal egg chamber development. Adam and Montell (2004) already showed *emc* to be an effector of *Notch* in early oogenesis linked to follicle cell differentiation and we also observe defects in germline cyst enveloping by follicle cells, marked by the high percentage of fused egg chambers in *emc*-defective fly lines with absence of intervening polar and stalk cells.

Regarding the effects of *emc* mis-expression in oocyte number, I observed egg chambers that had two oocytes or no oocyte (marked by the presence of two stained spots or absence of *oskar* mRNA, respectively) from both heatshocked sense and antisense *emc* fly lines. However, heatshocked wild-type *OrR* flies also exhibited these phenotypes and the difference in frequency of occurrence was not always statistically significant. The ratio of abnormal phenotypes in *emc* mis-expression lines can vary depending on how long after induction of mis-expression by heatshock treatment the ovaries are dissected. Previous work in our laboratory had shown that low levels of abnormal egg chambers with two or no oocytes were present in both sense and antisense *emc* heatshocked flies but not in *OrR*. I also performed *oskar* mRNA in situ hybridisation in ovaries of flies with *emc* germline clones in an *ovoD1* background. The expression pattern of *osk* was normal in wild-type and FRT-emc^1 flies, there was no *osk* staining detected in *ovoD1*-FRT flies and in mosaic flies with emc^1 clones *osk* staining was observed occasionally, sometimes with two oocytes in an egg chamber. Based on these results I cannot confirm without reservation that *emc* affects oocyte determination through a role in the selection of which of the two pro-oocytes will become the oocyte. The clonal analysis in the germline was meant to shed light on the role of *emc* in oocyte determination, but I would need a positive clone marker and an oocyte marker that will consistently work (also in *ovoD1* flies), to be able to draw any conclusions and quantify the potential abnormal oocyte phenotypes of *emc* mutant egg chambers in mosaic flies. It is possible that optimisation of the timing of the ovary dissections after heatshock, or the heatshock conditions themselves, may improve the percentage of defective egg chambers and the clarity of the phenotypes observed. Any such experiments should be carefully controlled though, to ensure any resulting phenotypes are due to *emc* mis-expression

and not to the effect of heatshock or other factors. Furthermore, even though I used phase-contrast microscopy to count the number of cell nuclei in egg chambers with two oocytes in order to confirm that these egg chambers are not the product of fusion, it would be useful to also count the number of germline cells in egg chambers flanking those with two oocytes. This would give extra confidence in the results as it would rule out the possibility that the second oocyte is from an adjacent cell and is the product of irregular fusion. Further work would be necessary to elucidate the potential relationship of *emc* with oocyte determination.

Since Emc can bind to multiple partners misexpression of Emc could lead to developmental defects by interacting with partners that may normally be functioning in rather different developmental processes. Thus the phenotypes resulting from misexpression of *emc* may be generated using different HLH proteins to those partners used during its normal role in oogenesis. A candidate gene for potential interaction with *emc* is *Rbp9* (Park et al, 1998). Rbp9 is an RNA binding protein found mainly in the adult central nervous system and it binds to poly-U sequences. Rbp9 binds to the 3'-UTR of *emc* mRNA and it is necessary for downregulation of *emc* (Park et al, 1998). In a different study Rbp9 was shown to be present in the cytoplasm of cystocytes during oogenesis and by stage 3 of oogenesis Rbp9 is expressed only in small amounts in the oocyte. It downregulates BAM (bag-of-marbles) expression in early oogenesis by binding to *bam* 3'-UTR and Rbp9 function is required for proper oocyte determination and positioning (Kim-Ha et al, 1999). It is reasonable to assume that there may be an interaction of Rbp9 and *emc* mRNA in early oogenesis as well, since *emc* is a known target of Rbp9, but this issue remains to be investigated. I observed normal *emc* expression pattern throughout oogenesis in egg chambers of the only available *Rbp9* stock from Bloomington Stock Centre- the only possible difference was that the dorsal anterior patches of expression in stage 12 seemed to be bigger than in wild-type. However, no information is available on this stock (UAS, P-insertion, etc.) so its effect on normal Rbp9 expression is unclear (results not shown).

Another interesting aspect of the late expression of *emc* in oogenesis was to look at whether *emc* expression is conserved and related to dorsal appendage formation in other species with different numbers of dorsal appendages (with Dr G. Tzolovsky). *Rho* and *argos* are expressed in four domains and *Br*-C is reported to be expressed in four groups of follicle cells at stage 12 in *Drosophila virilis*, a species with four dorsal appendages, as opposed to two in *D. melanogaster* (Nakamura and Matsuno, 2003). We observed this expression pattern using a Br-C core antibody, albeit very weakly, but immunohistochemistry with the Emc antibody was not successful in *D. virilis* and *Zaprionus badyi* (Kwiatowski and Ayala, 1999), two distinct species with four dorsal appendages (results not shown). Optimisation of experimental conditions would be necessary to proceed with this investigation.

Future directions of research could be to investigate how the role of *emc* acting downstream of *Notch* (Adam and Montell, 2004) may be interlinked with its interaction with the Grk/EGFR pathway I report here. In other tissues such as the developing eye and wing *emc* is required for a number of processes and acts in parallel or is regulated by many different signals, including the EGFR and the Notch signalling pathways (de Celis, 1998; Baonza and Freeman, 2001). An important question is to identify which of the bHLH proteins may be antagonised by Emc in the ovary, since negative regulation of bHLH proteins by formation of inactive heterodimers with *emc* is the only method of *emc* function described so far. In addition, using a different system to interfere with *emc* expression, such as UAS-sense and antisense *emc* constructs instead of the heatshock promoter-driven ones we have used so far, can provide useful additional information by allowing for expression of sense or antisense *emc* in specific populations of cells or times through the use of appropriate Gal4 lines. For example, it may help clarify if the *emc* phenotype is cell autonomous or not. Also the role of *emc* in early oogenesis needs further in-depth investigation. Since the *ovoD1* mutation proved not to be a sufficient marker to identify *emc* mutant clones in the germline, a different method must be employed to reveal *emc* germline function. GFP-marked germline clones should be easier to be followed and analysis of the germline clone phenotype would be possible. For instance, antibodies against Orb or Oskar could be used to analyse *emc*

requirement for oocyte development and the issue of whether the severe early defects in germline clones are caused by defects in oocyte determination or in other processes, such as follicle cell differentiation, would be addressed. I did not obtain clear enough results with *oskar* mRNA in situ hybridisation to confirm unequivocally the phenotype of two oocytes or none in fly lines mis-expressing *emc* that was reported. Staining with different early markers for oocyte determination like *Orb* and *Bic* should help in clarifying the matter. Further investigation of the multiple roles of *emc* in oogenesis and their specific timing should help to unravel the complexities of producing a viable, morphologically normal, egg.

A large part of this study has now been published in Mechanisms of Development (Papadia et al, 2005) and is presented in this thesis as Appendix A.

References

Adam, J. C. and Montell, D. J. (2004). A role for extra macrochaetae downstream of Notch in follicle cell differentiation. *Development* **131**, 5971-80.

Al-Atia, G. R., Fruscoloni, P. and Jacobs-Lorena, M. (1985). Translational regulation of mRNAs for ribosomal proteins during early Drosophila development. *Biochemistry* **24**, 5798-803.

Alberts, B. (2002). Molecular biology of the cell, (ed. New York: Garland Science.

Alessi, D. R., Andjelkovic, M., Caudwell, B., Cron, P., Morrice, N., Cohen, P. and Hemmings, B. A. (1996). Mechanism of activation of protein kinase B by insulin and IGF-1. *Embo J* **15**, 6541-51.

Alessi, D. R., Deak, M., Casamayor, A., Caudwell, F. B., Morrice, N., Norman, D. G., Gaffney, P., Reese, C. B., MacDougall, C. N., Harbison, D. et al. (1997). 3-Phosphoinositide-dependent protein kinase-1 (PDK1): structural and functional homology with the Drosophila DSTPK61 kinase. *Curr Biol* **7**, 776-89.

Alessi, D. R., James, S. R., Downes, C. P., Holmes, A. B., Gaffney, P. R., Reese, C. B. and Cohen, P. (1997). Characterization of a 3-phosphoinositide-dependent protein kinase which phosphorylates and activates protein kinase Balpha. *Curr Biol* **7**, 261-9.

Alessi, D. R., Kozlowski, M. T., Weng, Q. P., Morrice, N. and Avruch, J. (1998). 3-Phosphoinositide-dependent protein kinase 1 (PDK1) phosphorylates and activates the p70 S6 kinase in vivo and in vitro. *Curr Biol* **8**, 69-81.

Alnemri, E. S. (1999). Hidden powers of the mitochondria. *Nat Cell Biol* **1**, E40-2.

Altschul, S. F., Gish, W., Miller, W., Myers, E. W. and Lipman, D. J. (1990). Basic local alignment search tool. *J Mol Biol* **215**, 403-10.

Anderson, K. E., Coadwell, J., Stephens, L. R. and Hawkins, P. T. (1998). Translocation of PDK-1 to the plasma membrane is important in allowing PDK-1 to activate protein kinase B. *Curr Biol* **8**, 684-91.

Angeletti, R. H. (1999). Design of useful peptide antigens. *J Biomol Tech* **10**, 2-10.

Ashburner, M. (1989). *Drosophila* A laboratory handbook: Cold Spring Harbor Laboratory Press.

Atchley, W. R. and Fitch, W. M. (1997). A natural classification of the basic helix-loop-helix class of transcription factors. *Proc Natl Acad Sci U S A* **94**, 5172-6.

Baehrecke, E. H. (2002). How death shapes life during development. *Nat Rev Mol Cell Biol* **3**, 779-87.

Balendran, A., Casamayor, A., Deak, M., Paterson, A., Gaffney, P., Currie, R., Downes, C. P. and Alessi, D. R. (1999). PDK1 acquires PDK2 activity in the presence of a synthetic peptide derived from the carboxyl terminus of PRK2. *Curr Biol* **9**, 393-404.

Baonza, A., de Celis, J. F. and Garcia-Bellido, A. (2000). Relationships between extramacrochaetae and Notch signalling in Drosophila wing development. *Development* **127**, 2383-93.

Baonza, A. and Freeman, M. (2001). Notch signalling and the initiation of neural development in the Drosophila eye. *Development* **128**, 3889-98.

Basu, S., Totty, N. F., Irwin, M. S., Sudol, M. and Downward, J. (2003). Akt phosphorylates the Yes-associated protein, YAP, to induce interaction with 14-3-3 and attenuation of p73-mediated apoptosis. *Mol Cell* **11**, 11-23.

Belham, C., Comb, M. J. and Avruch, J. (2001). Identification of the NIMA family kinases NEK6/7 as regulators of the p70 ribosomal S6 kinase. *Curr Biol* **11**, 1155-67.

Belham, C., Wu, S. and Avruch, J. (1999). Intracellular signalling: PDK1--a kinase at the hub of things. *Curr Biol* **9**, R93-6.

Benezra, R., Davis, R. L., Lockshon, D., Turner, D. L. and Weintraub, H. (1990). The protein Id: a negative regulator of helix-loop-helix DNA binding proteins. *Cell* **61**, 49-59.

Berg, C. A. (2005). The Drosophila shell game: patterning genes and morphological change. *Trends Genet* **21**, 346-55.

Bertrand, L., Alessi, D. R., Deprez, J., Deak, M., Viaene, E., Rider, M. H. and Hue, L. (1999). Heart 6-phosphofructo-2-kinase activation by insulin results from Ser- 466 and Ser-483 phosphorylation and requires 3-phosphoinositide- dependent kinase-1, but not protein kinase B. *J Biol Chem* **274**, 30927-33.

Bevan, P. (2001). Insulin signalling. *J Cell Sci* **114**, 1429-30.

Biondi, R. M. (2004). Phosphoinositide-dependent protein kinase 1, a sensor of protein conformation. *Trends Biochem Sci* **29**, 136-42.

Biondi, R. M., Cheung, P. C., Casamayor, A., Deak, M., Currie, R. A. and Alessi, D. R. (2000). Identification of a pocket in the PDK1 kinase domain that interacts with PIF and the C-terminal residues of PKA. *Embo J* **19**, 979-88.

Biondi, R. M., Kieloch, A., Currie, R. A., Deak, M. and Alessi, D. R. (2001). The PIF-binding pocket in PDK1 is essential for activation of S6K and SGK, but not PKB. *Embo J* **20**, 4380-90.

Bohni, R., Riesgo-Escovar, J., Oldham, S., Brogiolo, W., Stocker, H., Andruss, B. F., Beckingham, K. and Hafen, E. (1999). Autonomous control of cell and organ size by CHICO, a Drosophila homolog of vertebrate IRS1-4. *Cell* **97**, 865-75.

Botas, J., Moscoso del Prado, J. and Garcia-Bellido, A. (1982). Gene-dose titration analysis in the search of trans-regulatory genes in Drosophila. *Embo J* **1**, 307-10.

Bownes, M. (1989). The roles of juvenile hormone, ecdysone and the ovary in the control of *Drosophila* vitellogenesis. *J Insect Physiol* **35**, 409-413.

Bownes, M. (1994). Interactions between germ cells and somatic cells in *Drosophila melanogaster*. *Seminars in Developmental Biology* **5**, 31-42.

Bownes, M. and Hames, B. D. (1978). Analysis of the yolk proteins in Drosophila melanogaster. Translation in a cell free system and peptide analysis. *FEBS Lett* **96**, 327-30.

Brand, A. H. and Perrimon, N. (1994). Raf acts downstream of the EGF receptor to determine dorsoventral polarity during Drosophila oogenesis. *Genes Dev* **8**, 629-39.

Brazil, D. P., Yang, Z. Z. and Hemmings, B. A. (2004). Advances in protein kinase B signalling: AKTion on multiple fronts. *Trends Biochem Sci* **29**, 233-42.

Brennan, M. D., Weiner, A. J., Goralski, T. J. and Mahowald, A. P. (1982). The follicle cells are a major site of vitellogenin synthesis in Drosophila melanogaster. *Dev Biol* **89**, 225-36.

Britton, J. S., Lockwood, W. K., Li, L., Cohen, S. M. and Edgar, B. A. (2002). Drosophila's insulin/PI3-kinase pathway coordinates cellular metabolism with nutritional conditions. *Dev Cell* **2**, 239-49.

Brogiolo, W., Stocker, H., Ikeya, T., Rintelen, F., Fernandez, R. and Hafen, E. (2001). An evolutionarily conserved function of the Drosophila insulin receptor and insulin-like peptides in growth control. *Curr Biol* **11**, 213-21.

Brunet, A., Bonni, A., Zigmond, M. J., Lin, M. Z., Juo, P., Hu, L. S., Anderson, M. J., Arden, K. C., Blenis, J. and Greenberg, M. E. (1999). Akt promotes cell survival by phosphorylating and inhibiting a Forkhead transcription factor. *Cell* **96**, 857-68.

Burke, T., Waring, G. L., Popodi, E. and Minoo, P. (1987). Characterization and sequence of follicle cell genes selectively expressed during vitelline membrane formation in Drosophila. *Dev Biol* **124**, 441-50.

Burnett, P. E., Barrow, R. K., Cohen, N. A., Snyder, S. H. and Sabatini, D. M. (1998). RAFT1 phosphorylation of the translational regulators p70 S6 kinase and 4E-BP1. *Proc Natl Acad Sci U S A* **95**, 1432-7.

Buszczak, M. and Cooley, L. (2000). Eggs to die for: cell death during Drosophila oogenesis. *Cell Death Differ* **7**, 1071-4.

Cabrera, C. V., Alonso, M. C. and Huikeshoven, H. (1994). Regulation of scute function by extramacrochaete in vitro and in vivo. *Development* **120**, 3595-603.

Campuzano, S. (2001). Emc, a negative HLH regulator with multiple functions in Drosophila development. *Oncogene* **20**, 8299-307.

Cardone, M. H., Roy, N., Stennicke, H. R., Salvesen, G. S., Franke, T. F., Stanbridge, E., Frisch, S. and Reed, J. C. (1998). Regulation of cell death protease caspase-9 by phosphorylation. *Science* **282**, 1318-21.

Carmeliet, P. (1999). Developmental biology. Controlling the cellular brakes. *Nature* **401**, 657-8.

Carpenter, A. T. (1994). Egalitarian and the choice of cell fates in Drosophila melanogaster oogenesis. *Ciba Found Symp* **182**, 223-46; discussion 246-54.

Casamayor, A., Morrice, N. A. and Alessi, D. R. (1999). Phosphorylation of Ser-241 is essential for the activity of 3- phosphoinositide-dependent protein kinase-1: identification of five sites of phosphorylation in vivo. *Biochem J* **342**, 287-92.

Casamayor, A., Torrance, P. D., Kobayashi, T., Thorner, J. and Alessi, D. R. (1999). Functional counterparts of mammalian protein kinases PDK1 and SGK in budding yeast. *Curr Biol* **9**, 186-97.

Chen, C., Jack, J. and Garofalo, R. S. (1996). The Drosophila insulin receptor is required for normal growth. *Endocrinology* **137**, 846-56.

Chen, P., Nordstrom, W., Gish, B. and Abrams, J. M. (1996). grim, a novel cell death gene in Drosophila. *Genes Dev* **10**, 1773-82.

Chen, P. S., Stumm-Zollinger, E., Aigaki, T., Balmer, J., Bienz, M. and Bohlen, P. (1988). A male accessory gland peptide that regulates reproductive behavior of female D. melanogaster. *Cell* **54**, 291-8.

Cho, K. S., Lee, J. H., Kim, S., Kim, D., Koh, H., Lee, J., Kim, C., Kim, J. and Chung, J. (2001). Drosophila phosphoinositide-dependent kinase-1 regulates apoptosis and

growth via the phosphoinositide 3-kinase-dependent signaling pathway. *Proc Natl Acad Sci U S A* **98**, 6144-9.

Chou, M. M., Hou, W., Johnson, J., Graham, L. K., Lee, M. H., Chen, C. S., Newton, A. C., Schaffhausen, B. S. and Toker, A. (1998). Regulation of protein kinase C zeta by PI 3-kinase and PDK-1. *Curr Biol* **8**, 1069-77.

Christerson, L. B. and McKearin, D. M. (1994). orb is required for anteroposterior and dorsoventral patterning during Drosophila oogenesis. *Genes Dev* **8**, 614-28.

Clancy, D. J., Gems, D., Hafen, E., Leevers, S. J. and Partridge, L. (2002). Dietary restriction in long-lived dwarf flies. *Science* **296**, 319.

Clancy, D. J., Gems, D., Harshman, L. G., Oldham, S., Stocker, H., Hafen, E., Leevers, S. J. and Partridge, L. (2001). Extension of life-span by loss of CHICO, a Drosophila insulin receptor substrate protein. *Science* **292**, 104-6.

Clark, K. A. and McKearin, D. M. (1996). The Drosophila stonewall gene encodes a putative transcription factor essential for germ cell development. *Development* **122**, 937-50.

Clyde, D. (1999). Characterisation of a novel gene (*Dstpk61*) encoding a serine/threonine protein kinase in *Drosophila melanogaster*. In *Institute of Cell and Molecular Biology*, (ed. Edinburgh: University of Edinburgh.

Clyde, D. and Bownes, M. (2000). The Dstpk61 locus of Drosophila produces multiple transcripts and protein isoforms, suggesting it is involved in multiple signalling pathways. *J Endocrinol* **167**, 391-401.

Cooley, L. and Theurkauf, W. E. (1994). Cytoskeletal functions during Drosophila oogenesis. *Science* **266**, 590-6.

Cooperstock, R. L. and Lipshitz, H. D. (2001). RNA localization and translational regulation during axis specification in the Drosophila oocyte. *Int Rev Cytol* **203**, 541-66.

Cox, R. T. and Spradling, A. C. (2003). A Balbiani body and the fusome mediate mitochondrial inheritance during Drosophila oogenesis. *Development* **130**, 1579-90.

Cross, D. A., Alessi, D. R., Cohen, P., Andjelkovich, M. and Hemmings, B. A. (1995). Inhibition of glycogen synthase kinase-3 by insulin mediated by protein kinase B. *Nature* **378**, 785-9.

Cubas, P., Modolell, J. and Ruiz-Gomez, M. (1994). The helix-loop-helix extramacrochaetae protein is required for proper specification of many cell types in the Drosophila embryo. *Development* **120**, 2555-66.

Currie, R. A., Walker, K. S., Gray, A., Deak, M., Casamayor, A., Downes, C. P., Cohen, P., Alessi, D. R. and Lucocq, J. (1999). Role of phosphatidylinositol 3,4,5-trisphosphate in regulating the activity and localization of 3-phosphoinositide-dependent protein kinase-1. *Biochem J* **337**, 575-83.

Davis, R. L., Cheng, P. F., Lassar, A. B. and Weintraub, H. (1990). The MyoD DNA binding domain contains a recognition code for muscle-specific gene activation. *Cell* **60**, 733-46.

De Celis, J. F. (1998). Positioning and differentiation of veins in the Drosophila wing. *Int J Dev Biol* **42**, 335-43.

de Cuevas, M. and Spradling, A. C. (1998). Morphogenesis of the Drosophila fusome and its implications for oocyte specification. *Development* **125**, 2781-9.

Deak, M., Casamayor, A., Currie, R. A., Downes, C. P. and Alessi, D. R. (1999). Characterisation of a plant 3-phosphoinositide-dependent protein kinase- 1 homologue which contains a pleckstrin homology domain. *FEBS Lett* **451**, 220-6.

Deak, P., Omar, M. M., Saunders, R. D., Pal, M., Komonyi, O., Szidonya, J., Maroy, P., Zhang, Y., Ashburner, M., Benos, P. et al. (1997). P-element insertion alleles of essential genes on the third chromosome of Drosophila melanogaster: correlation of physical and cytogenetic maps in chromosomal region 86E-87F. *Genetics* **147**, 1697-722.

Deng, W., Leaper, K. and Bownes, M. (1999). A targeted gene silencing technique shows that Drosophila myosin VI is required for egg chamber and imaginal disc morphogenesis. *J Cell Sci* **112 (Pt 21)**, 3677-90.

Deng, W. and Lin, H. (1997). Spectrosomes and fusomes anchor mitotic spindles during asymmetric germ cell divisions and facilitate the formation of a polarized microtubule array for oocyte specification in Drosophila. *Dev Biol* **189**, 79-94.

Deng, W. M. and Bownes, M. (1997). Two signalling pathways specify localised expression of the Broad-Complex in Drosophila eggshell patterning and morphogenesis. *Development* **124**, 4639-47.

Deng, W. M. and Bownes, M. (1998). Patterning and morphogenesis of the follicle cell epithelium during Drosophila oogenesis. *Int J Dev Biol* **42**, 541-52.

Deng, W. M., Zhao, D., Rothwell, K. and Bownes, M. (1997). Analysis of P[gal4] insertion lines of Drosophila melanogaster as a route to identifying genes important in the follicle cells during oogenesis. *Mol Hum Reprod* **3**, 853-62.

Deprez, J., Bertrand, L., Alessi, D. R., Krause, U., Hue, L. and Rider, M. H. (2000). Partial purification and characterization of a wortmannin-sensitive and insulin-stimulated protein kinase that activates heart 6-phosphofructo- 2-kinase. *Biochem J* **347 Pt 1**, 305-12.

Deprez, J., Vertommen, D., Alessi, D. R., Hue, L. and Rider, M. H. (1997). Phosphorylation and activation of heart 6-phosphofructo-2-kinase by protein kinase B and other protein kinases of the insulin signaling cascades. *J Biol Chem* **272**, 17269-75.

Dimmeler, S., Fleming, I., Fisslthaler, B., Hermann, C., Busse, R. and Zeiher, A. M. (1999). Activation of nitric oxide synthase in endothelial cells by Akt- dependent phosphorylation. *Nature* **399**, 601-5.

Dobens, L. L. and Raftery, L. A. (2000). Integration of epithelial patterning and morphogenesis in Drosophila ovarian follicle cells. *Dev Dyn* **218**, 80-93.

Dong, L. Q., Landa, L. R., Wick, M. J., Zhu, L., Mukai, H., Ono, Y. and Liu, F. (2000). Phosphorylation of protein kinase N by phosphoinositide-dependent protein kinase-1 mediates insulin signals to the actin cytoskeleton. *Proc Natl Acad Sci U S A* **97**, 5089-94.

Dong, L. Q. and Liu, F. (2005). PDK2: the missing piece in the receptor tyrosine kinase signaling pathway puzzle. *Am J Physiol Endocrinol Metab* **289**, E187-96.

Dong, L. Q., Zhang, R. B., Langlais, P., He, H., Clark, M., Zhu, L. and Liu, F. (1999). Primary structure, tissue distribution, and expression of mouse phosphoinositide-dependent protein kinase-1, a protein kinase that phosphorylates and activates protein kinase Czeta. *J Biol Chem* **274**, 8117-22.

Dorman, J. B., James, K. E., Fraser, S. E., Kiehart, D. P. and Berg, C. A. (2004). bullwinkle is required for epithelial morphogenesis during Drosophila oogenesis. *Dev Biol* **267**, 320-41.

Downward, J. (1998). Mechanisms and consequences of activation of protein kinase B/Akt. *Curr Opin Cell Biol* **10**, 262-7.

Downward, J. (1999). How BAD phosphorylation is good for survival. *Nat Cell Biol* **1**, E33-5.

Du, K., Herzig, S., Kulkarni, R. N. and Montminy, M. (2003). TRB3: a tribbles homolog that inhibits Akt/PKB activation by insulin in liver. *Science* **300**, 1574-7.

Dutil, E. M., Toker, A. and Newton, A. C. (1998). Regulation of conventional protein kinase C isozymes by phosphoinositide-dependent kinase 1 (PDK-1). *Curr Biol* **8**, 1366-75.

Ellenberger, T., Fass, D., Arnaud, M. and Harrison, S. C. (1994). Crystal structure of transcription factor E47: E-box recognition by a basic region helix-loop-helix dimer. *Genes Dev* **8**, 970-80.

Ellis, H. M., Spann, D. R. and Posakony, J. W. (1990). extramacrochaetae, a negative regulator of sensory organ development in Drosophila, defines a new class of helix-loop-helix proteins. *Cell* **61**, 27-38.

Ephrussi, A., Dickinson, L. K. and Lehmann, R. (1991). Oskar organizes the germ plasm and directs localization of the posterior determinant nanos. *Cell* **66**, 37-50.

Ephrussi, A. and Lehmann, R. (1992). Induction of germ cell formation by oskar. *Nature* **358**, 387-92.

Feng, J., Park, J., Cron, P., Hess, D. and Hemmings, B. A. (2004). Identification of a PKB/Akt hydrophobic motif Ser-473 kinase as DNA-dependent protein kinase. *J Biol Chem* **279**, 41189-96.

Filippa, N., Sable, C. L., Hemmings, B. A. and Van Obberghen, E. (2000). Effect of phosphoinositide-dependent kinase 1 on protein kinase B translocation and its subsequent activation. *Mol Cell Biol* **20**, 5712-21.

Findley, S. D., Tamanaha, M., Clegg, N. J. and Ruohola-Baker, H. (2003). Maelstrom, a Drosophila spindle-class gene, encodes a protein that colocalizes with Vasa and RDE1/AGO1 homolog, Aubergine, in nuage. *Development* **130**, 859-71.

Flynn, P., Mellor, H., Casamassima, A. and Parker, P. J. (2000). Rho GTPase control of protein kinase C-related protein kinase activation by 3-phosphoinositide-dependent protein kinase. *J Biol Chem* **275**, 11064-70.

Fonfara, C. (2000). Project report: Genetic and molecular analysis of a novel serine/threonine kinase gene in *Drosophila melanogaster*, (ed.: Insitute of Cell and Molecular Biology, University of Edinburgh.

Forbes, A. J., Lin, H., Ingham, P. W. and Spradling, A. C. (1996). hedgehog is required for the proliferation and specification of ovarian somatic cells prior to egg chamber formation in Drosophila. *Development* **122**, 1125-35.

Franke, T. F., Kaplan, D. R. and Cantley, L. C. (1997). PI3K: downstream AKTion blocks apoptosis. *Cell* **88**, 435-7.

Freeman, M., Klambt, C., Goodman, C. S. and Rubin, G. M. (1992). The argos gene encodes a diffusible factor that regulates cell fate decisions in the Drosophila eye. *Cell* **69**, 963-75.

Frodin, M., Jensen, C. J., Merienne, K. and Gammeltoft, S. (2000). A phosphoserine-regulated docking site in the protein kinase RSK2 that recruits and activates PDK1. *Embo J* **19**, 2924-34.

Fruman, D. A., Rameh, L. E. and Cantley, L. C. (1999). Phosphoinositide binding domains: embracing 3-phosphate. *Cell* **97**, 817-20.

Fuller, M. T. (1993). Spermatogenesis. In *The development of Drosophila melanogaster*, vol. 1 (ed. M. Bate, Martinez-Arias, A), pp. 71-148: Cold Spring Harbor Laboratory Press.

Fuller, M. T. (1998). Genetic control of cell proliferation and differentiation in Drosophila spermatogenesis. *Semin Cell Dev Biol* **9**, 433-44.

Fulton, D., Gratton, J. P., McCabe, T. J., Fontana, J., Fujio, Y., Walsh, K., Franke, T. F., Papapetropoulos, A. and Sessa, W. C. (1999). Regulation of endothelium-derived nitric oxide production by the protein kinase Akt. *Nature* **399**, 597-601.

Gao, X. and Pan, D. (2001). TSC1 and TSC2 tumor suppressors antagonize insulin signaling in cell growth. *Genes Dev* **15**, 1383-92.

Garrell, J. and Modolell, J. (1990). The Drosophila extramacrochaetae locus, an antagonist of proneural genes that, like these genes, encodes a helix-loop-helix protein. *Cell* **61**, 39-48.

Ghabrial, A., Ray, R. P. and Schupbach, T. (1998). okra and spindle-B encode components of the RAD52 DNA repair pathway and affect meiosis and patterning in Drosophila oogenesis. *Genes Dev* **12**, 2711-23.

Ghabrial, A. and Schupbach, T. (1999). Activation of a meiotic checkpoint regulates translation of Gurken during Drosophila oogenesis. *Nat Cell Biol* **1**, 354-7.

Ghiglione, C., Carraway, K. L., 3rd, Amundadottir, L. T., Boswell, R. E., Perrimon, N. and Duffy, J. B. (1999). The transmembrane molecule kekkon 1 acts in a feedback loop to negatively regulate the activity of the Drosophila EGF receptor during oogenesis. *Cell* **96**, 847-56.

Giannakou, M. E., Goss, M., Junger, M. A., Hafen, E., Leevers, S. J. and Partridge, L. (2004). Long-lived Drosophila with overexpressed dFOXO in adult fat body. *Science* **305**, 361.

Gilbert, S. F. (2003) Developmental Biology 7th edition, Sinauer Associates Inc., p.271-277.

Goberdhan, D. C., Paricio, N., Goodman, E. C., Mlodzik, M. and Wilson, C. (1999). Drosophila tumor suppressor PTEN controls cell size and number by antagonizing the Chico/PI3-kinase signaling pathway. *Genes Dev* **13**, 3244-58.

Godt, D. and Tepass, U. (1998). Drosophila oocyte localization is mediated by differential cadherin-based adhesion. *Nature* **395**, 387-91.

Gonzalez-Reyes, A., Elliott, H. and St Johnston, D. (1995). Polarization of both major body axes in Drosophila by gurken-torpedo signalling. *Nature* **375**, 654-8.

Gonzalez-Reyes, A., Elliott, H. and St Johnston, D. (1997). Oocyte determination and the origin of polarity in Drosophila: the role of the spindle genes. *Development* **124**, 4927-37.

Gonzalez-Reyes, A. and St Johnston, D. (1994). Role of oocyte position in establishment of anterior-posterior polarity in Drosophila. *Science* **266**, 639-42.

Gonzalez-Reyes, A. and St Johnston, D. (1998). The Drosophila AP axis is polarised by the cadherin-mediated positioning of the oocyte. *Development* **125**, 3635-44.

Goode, S., Melnick, M., Chou, T. B. and Perrimon, N. (1996). The neurogenic genes egghead and brainiac define a novel signaling pathway essential for epithelial morphogenesis during Drosophila oogenesis. *Development* **122**, 3863-79.

Greenspan, R. J. (1997). Fly Pushing
The theory and practice of *Drosophila* genetics: Cold Spring Harbor Laboratory Press.

Grether, M. E., Abrams, J. M., Agapite, J., White, K. and Steller, H. (1995). The head involution defective gene of Drosophila melanogaster functions in programmed cell death. *Genes Dev* **9**, 1694-708.

Grieder, N. C., de Cuevas, M. and Spradling, A. C. (2000). The fusome organizes the microtubule network during oocyte differentiation in Drosophila. *Development* **127**, 4253-64.

Gupta, V. and Oliver, B. (2003). Drosophila microarray platforms. *Brief Funct Genomic Proteomic* **2**, 97-105.

Hennig, K. M. and Neufeld, T. P. (2002). Inhibition of cellular growth and proliferation by dTOR overexpression in Drosophila. *Genesis* **34**, 107-10.

Hicks, J. L., Deng, W. M., Rogat, A. D., Miller, K. G. and Bownes, M. (1999). Class VI unconventional myosin is required for spermatogenesis in Drosophila. *Mol Biol Cell* **10**, 4341-53.

Hill, M., Feng, J. and Hemmings, B. (2002). Identification of a Plasma Membrane Raft-Associated PKB Ser473 Kinase Activity that Is Distinct from ILK and PDK1. *Curr Biol* **12**, 1251.

Huang, F., van Helden, J., Dambly-Chaudiere, C. and Ghysen, A. (1995). Contribution of the gene *extramacrochaete* to the precise positioning of bristles in *Drosophila*. *Roux's Arch. Dev. Biol.* **204**, 336-343.

Huang, H., Potter, C. J., Tao, W., Li, D. M., Brogiolo, W., Hafen, E., Sun, H. and Xu, T. (1999). PTEN affects cell size, cell proliferation and apoptosis during Drosophila eye development. *Development* **126**, 5365-72.

Huynh, J. R. and St Johnston, D. (2004). The origin of asymmetry: early polarisation of the *Drosophila* germline cyst and oocyte. *Curr Biol* **14**, R438-49.

Ikeya, T., Galic, M., Belawat, P., Nairz, K. and Hafen, E. (2002). Nutrient-Dependent Expression of Insulin-like Peptides from Neuroendocrine Cells in the CNS Contributes to Growth Regulation in Drosophila. *Curr Biol* **12**, 1293.

Ito, N. and Rubin, G. M. (1999). gigas, a Drosophila homolog of tuberous sclerosis gene product-2, regulates the cell cycle. *Cell* **96**, 529-39.

Jensen, C. J., Buch, M. B., Krag, T. O., Hemmings, B. A., Gammeltoft, S. and Frodin, M. (1999). 90-kDa ribosomal S6 kinase is phosphorylated and activated by 3-phosphoinositide-dependent protein kinase-1. *J Biol Chem* **274**, 27168-76.

Johnston, L. A. and Gallant, P. (2002). Control of growth and organ size in Drosophila. *Bioessays* **24**, 54-64.

Johnston, R., Wang, B., Nuttall, R., Doctolero, M., Edwards, P., Lu, J., Vainer, M., Yue, H., Wang, X., Minor, J. et al. (2004). FlyGEM, a full transcriptome array platform for the Drosophila community. *Genome Biol* **5**, R19.

Jordan, K. C., Clegg, N. J., Blasi, J. A., Morimoto, A. M., Sen, J., Stein, D., McNeill, H., Deng, W. M., Tworoger, M. and Ruohola-Baker, H. (2000). The homeobox gene mirror links EGF signalling to embryonic dorso-ventral axis formation through notch activation. *Nat Genet* **24**, 429-33.

Kandel, E. S. and Hay, N. (1999). The regulation and activities of the multifunctional serine/threonine kinase Akt/PKB. *Exp Cell Res* **253**, 210-29.

Kawakami, Y., Nishimoto, H., Kitaura, J., Maeda-Yamamoto, M., Kato, R. M., Littman, D. R., Leitges, M., Rawlings, D. J. and Kawakami, T. (2004). Protein kinase C betaII regulates Akt phosphorylation on Ser-473 in a cell type- and stimulus-specific fashion. *J Biol Chem* **279**, 47720-5.

Kelley, R. L. (1993). Initial organization of the Drosophila dorsoventral axis depends on an RNA-binding protein encoded by the squid gene. *Genes Dev* **7**, 948-60.

Keyes, L. N. and Spradling, A. C. (1997). The Drosophila gene fs(2)cup interacts with otu to define a cytoplasmic pathway required for the structure and function of germ-line chromosomes. *Development* **124**, 1419-31.

Kiger, A. A., Jones, D. L., Schulz, C., Rogers, M. B. and Fuller, M. T. (2001). Stem cell self-renewal specified by JAK-STAT activation in response to a support cell cue. *Science* **294**, 2542-5.

Kim, A. H., Khursigara, G., Sun, X., Franke, T. F. and Chao, M. V. (2001). Akt phosphorylates and negatively regulates apoptosis signal-regulating kinase 1. *Mol Cell Biol* **21**, 893-901.

Kim-Ha, J., Kerr, K. and Macdonald, P. M. (1995). Translational regulation of oskar mRNA by bruno, an ovarian RNA-binding protein, is essential. *Cell* **81**, 403-12.

Kim-Ha, J., Kim, J. and Kim, Y. J. (1999). Requirement of RBP9, a Drosophila Hu homolog, for regulation of cystocyte differentiation and oocyte determination during oogenesis. *Mol Cell Biol* **19**, 2505-14.

Kim-Ha, J., Smith, J. L. and Macdonald, P. M. (1991). oskar mRNA is localized to the posterior pole of the Drosophila oocyte. *Cell* **66**, 23-35.

King, R. C. (1970). Ovarian development in *Drosophila melanogaster*. New York: Academic Press.

Kitamura, T., Kitamura, Y., Kuroda, S., Hino, Y., Ando, M., Kotani, K., Konishi, H., Matsuzaki, H., Kikkawa, U., Ogawa, W. et al. (1999). Insulin-induced

phosphorylation and activation of cyclic nucleotide phosphodiesterase 3B by the serine-threonine kinase Akt. *Mol Cell Biol* **19**, 6286-96.

Knowles, B. A. and Cooley, L. (1994). The specialized cytoskeleton of the Drosophila egg chamber. *Trends Genet* **10**, 235-41.

Kobayashi, T. and Cohen, P. (1999). Activation of serum- and glucocorticoid-regulated protein kinase by agonists that activate phosphatidylinositide 3-kinase is mediated by 3- phosphoinositide-dependent protein kinase-1 (PDK1) and PDK2. *Biochem J* **339**, 319-28.

Kops, G. J., de Ruiter, N. D., De Vries-Smits, A. M., Powell, D. R., Bos, J. L. and Burgering, B. M. (1999). Direct control of the Forkhead transcription factor AFX by protein kinase B. *Nature* **398**, 630-4.

Kozma, S. C. and Thomas, G. (2002). Regulation of cell size in growth, development and human disease: PI3K, PKB and S6K. *Bioessays* **24**, 65-71.

Kwiatowski, J. and Ayala, F. J. (1999). Phylogeny of Drosophila and related genera: conflict between molecular and anatomical analyses. *Mol Phylogenet Evol* **13**, 319-28.

Lane, M. E. and Kalderon, D. (1994). RNA localization along the anteroposterior axis of the Drosophila oocyte requires PKA-mediated signal transduction to direct normal microtubule organization. *Genes Dev* **8**, 2986-95.

Lantz, V., Chang, J. S., Horabin, J. I., Bopp, D. and Schedl, P. (1994). The Drosophila orb RNA-binding protein is required for the formation of the egg chamber and establishment of polarity. *Genes Dev* **8**, 598-613.

Larkin, M. K., Holder, K., Yost, C., Giniger, E. and Ruohola-Baker, H. (1996). Expression of constitutively active Notch arrests follicle cells at a precursor stage during Drosophila oogenesis and disrupts the anterior-posterior axis of the oocyte. *Development* **122**, 3639-50.

Laundrie, B., Peterson, J. S., Baum, J. S., Chang, J. C., Fileppo, D., Thompson, S. R. and McCall, K. (2003). Germline cell death is inhibited by P-element insertions disrupting the dcp-1/pita nested gene pair in Drosophila. *Genetics* **165**, 1881-8.

Lawlor, M. A. and Alessi, D. R. (2001). PKB/Akt: a key mediator of cell proliferation, survival and insulin responses? *J Cell Sci* **114**, 2903-10.

Lawlor, M. A., Mora, A., Ashby, P. R., Williams, M. R., Murray-Tait, V., Malone, L., Prescott, A. R., Lucocq, J. M. and Alessi, D. R. (2002). Essential role of PDK1 in regulating cell size and development in mice. *Embo J* **21**, 3728-38.

Le Good, J. A., Ziegler, W. H., Parekh, D. B., Alessi, D. R., Cohen, P. and Parker, P. J. (1998). Protein kinase C isotypes controlled by phosphoinositide 3-kinase through the protein kinase PDK1. *Science* **281**, 2042-5.

Leevers, S. J., Weinkove, D., MacDougall, L. K., Hafen, E. and Waterfield, M. D. (1996). The Drosophila phosphoinositide 3-kinase Dp110 promotes cell growth. *Embo J* **15**, 6584-94.

Li, J., DeFea, K. and Roth, R. A. (1999). Modulation of insulin receptor substrate-1 tyrosine phosphorylation by an Akt/phosphatidylinositol 3-kinase pathway. *J Biol Chem* **274**, 9351-6.

Lin, H., Yue, L. and Spradling, A. C. (1994). The Drosophila fusome, a germline-specific organelle, contains membrane skeletal proteins and functions in cyst formation. *Development* **120**, 947-56.

Lizcano, J. M. and Alessi, D. R. (2002). The insulin signalling pathway. *Curr Biol* **12**, R236-8.

Lynch, D. K., Ellis, C. A., Edwards, P. A. and Hiles, I. D. (1999). Integrin-linked kinase regulates phosphorylation of serine 473 of protein kinase B by an indirect mechanism. *Oncogene* **18**, 8024-32.

MacDougall, C. N., Clyde, D., Wood, T., Todman, M., Harbison, D. and Bownes, M. (1999). Sex-specific transcripts of the Dstpk61 serine/threonine kinase gene in Drosophila melanogaster. *Eur J Biochem* **262**, 456-66.

Mach, J. M. and Lehmann, R. (1997). An Egalitarian-BicaudalD complex is essential for oocyte specification and axis determination in Drosophila. *Genes Dev* **11**, 423-35.

Mahajan-Miklos, S. and Cooley, L. (1994). Intercellular cytoplasm transport during Drosophila oogenesis. *Dev Biol* **165**, 336-51.

Maira, S. M., Galetic, I., Brazil, D. P., Kaech, S., Ingley, E., Thelen, M. and Hemmings, B. A. (2001). Carboxyl-terminal modulator protein (CTMP), a negative regulator of PKB/Akt and v-Akt at the plasma membrane. *Science* **294**, 374-80.

Margaritis, L. H. (1986). The eggshell of *Drosophila melanogaster*. II. New staging characteristics and fine structural analysis of choriogenesis. *Can. J. Zool.* **64**, 2152-2175.

Margaritis, L. H. M., M. (1998). Structure of the egg. In *Microscopic anatomy of invertebrates*, vol. 11C: Insecta, pp. 995-1037: Wiley-Liss.

Margolis, J. and Spradling, A. (1995). Identification and behavior of epithelial stem cells in the Drosophila ovary. *Development* **121**, 3797-807.

Massari, M. E. and Murre, C. (2000). Helix-loop-helix proteins: regulators of transcription in eucaryotic organisms. *Mol Cell Biol* **20**, 429-40.

Mevel-Ninio, M., Terracol, R. and Kafatos, F. C. (1991). The ovo gene of Drosophila encodes a zinc finger protein required for female germ line development. *Embo J* **10**, 2259-66.

Micklem, D. R., Dasgupta, R., Elliott, H., Gergely, F., Davidson, C., Brand, A., Gonzalez-Reyes, A. and St Johnston, D. (1997). The mago nashi gene is required for the polarisation of the oocyte and the formation of perpendicular axes in Drosophila. *Curr Biol* **7**, 468-78.

Miller, A. (1950). The internal anatomy and histology of the imago of *Drosophila melanogaster*. In *Biology of Drosophila*, (ed. M. Demerec), pp. 424-442: John Wiley & Sons, New York.

Miron, M., Verdu, J., Lachance, P. E., Birnbaum, M. J., Lasko, P. F. and Sonenberg, N. (2001). The translational inhibitor 4E-BP is an effector of PI(3)K/Akt signalling and cell growth in Drosophila. *Nat Cell Biol* **3**, 596-601.

Montagne, J., Stewart, M. J., Stocker, H., Hafen, E., Kozma, S. C. and Thomas, G. (1999). Drosophila S6 kinase: a regulator of cell size. *Science* **285**, 2126-9.

Montell, D. J., Rorth, P. and Spradling, A. C. (1992). slow border cells, a locus required for a developmentally regulated cell migration during oogenesis, encodes Drosophila C/EBP. *Cell* **71**, 51-62.

Mora, A., Davies, A. M., Bertrand, L., Sharif, I., Budas, G. R., Jovanovic, S., Mouton, V., Kahn, C. R., Lucocq, J. M., Gray, G. A. et al. (2003). Deficiency of PDK1 in cardiac muscle results in heart failure and increased sensitivity to hypoxia. *Embo J* **22**, 4666-76.

Mora, A., Komander, D., van Aalten, D. M. and Alessi, D. R. (2004). PDK1, the master regulator of AGC kinase signal transduction. *Semin Cell Dev Biol* **15**, 161-70.

Morimoto, A. M., Jordan, K. C., Tietze, K., Britton, J. S., O'Neill, E. M. and Ruohola-Baker, H. (1996). Pointed, an ETS domain transcription factor, negatively regulates the EGF receptor pathway in Drosophila oogenesis. *Development* **122**, 3745-54.

Morris, J. and Lehmann, R. (1999). Drosophila oogenesis: versatile spn doctors. *Curr Biol* **9**, R55-8.

Moscoso del Prado, J. a. G.-B., A. (1984). Genetic regulation of the achaete-scute complex of Drosophila melanogaster. *Roux's Arch. Dev. Biol.* **193**, 242-245.

Mouzaki, D. G. (1991). Comparative study of choriogenesis in insects of economic importance. In *Biology Department*, (ed. Athens, Greece: National and Capodistrian University of Athens.

Murre, C., McCaw, P. S. and Baltimore, D. (1989). A new DNA binding and dimerization motif in immunoglobulin enhancer binding, daughterless, MyoD, and myc proteins. *Cell* **56**, 777-83.

Murre, C., McCaw, P. S., Vaessin, H., Caudy, M., Jan, L. Y., Jan, Y. N., Cabrera, C. V., Buskin, J. N., Hauschka, S. D., Lassar, A. B. et al. (1989). Interactions between heterologous helix-loop-helix proteins generate complexes that bind specifically to a common DNA sequence. *Cell* **58**, 537-44.

Musacchio, M. and Perrimon, N. (1996). The Drosophila kekkon genes: novel members of both the leucine-rich repeat and immunoglobulin superfamilies expressed in the CNS. *Dev Biol* **178**, 63-76.

Myers, M. P., Stolarov, J. P., Eng, C., Li, J., Wang, S. I., Wigler, M. H., Parsons, R. and Tonks, N. K. (1997). P-TEN, the tumor suppressor from human chromosome 10q23, is a dual- specificity phosphatase. *Proc Natl Acad Sci U S A* **94**, 9052-7.

Nakamura, Y. and Matsuno, K. (2003). Species-specific activation of EGF receptor signaling underlies evolutionary diversity in the dorsal appendage number of the genus Drosophila eggshells. *Mech Dev* **120**, 897-907.

Nave, B. T., Ouwens, M., Withers, D. J., Alessi, D. R. and Shepherd, P. R. (1999). Mammalian target of rapamycin is a direct target for protein kinase B: identification of a convergence point for opposing effects of insulin and amino-acid deficiency on protein translation. *Biochem J* **344 Pt 2**, 427-31.

Neuman-Silberberg, F. S. and Schupbach, T. (1993). The Drosophila dorsoventral patterning gene gurken produces a dorsally localized RNA and encodes a TGF alpha-like protein. *Cell* **75**, 165-74.

Neuman-Silberberg, F. S. and Schupbach, T. (1994). Dorsoventral axis formation in Drosophila depends on the correct dosage of the gene gurken. *Development* **120**, 2457-63.

Niederberger, C. and Schweingruber, M. E. (1999). A Schizosaccharomyces pombe gene, ksg1, that shows structural homology to the human phosphoinositide-dependent protein kinase PDK1, is essential for growth, mating and sporulation. *Mol Gen Genet* **261**, 177-83.

Norvell, A., Kelley, R. L., Wehr, K. and Schupbach, T. (1999). Specific isoforms of squid, a Drosophila hnRNP, perform distinct roles in Gurken localization during oogenesis. *Genes Dev* **13**, 864-76.

Oldham, S. and Hafen, E. (2003). Insulin/IGF and target of rapamycin signaling: a TOR de force in growth control. *Trends Cell Biol* **13**, 79-85.

Oldham, S., Montagne, J., Radimerski, T., Thomas, G. and Hafen, E. (2000). Genetic and biochemical characterization of dTOR, the Drosophila homolog of the target of rapamycin. *Genes Dev* **14**, 2689-94.

Oldham, S., Stocker, H., Laffargue, M., Wittwer, F., Wymann, M. and Hafen, E. (2002). The Drosophila insulin/IGF receptor controls growth and size by modulating PtdInsP(3) levels. *Development* **129**, 4103-9.

Ozes, O. N., Akca, H., Mayo, L. D., Gustin, J. A., Maehama, T., Dixon, J. E. and Donner, D. B. (2001). A phosphatidylinositol 3-kinase/Akt/mTOR pathway mediates and PTEN antagonizes tumor necrosis factor inhibition of insulin signaling through insulin receptor substrate-1. *Proc Natl Acad Sci U S A* **98**, 4640-5.

Papadia, S., Tzolovsky, G., Zhao, D., Leaper, K., Clyde, D., Taylor, P., Asscher, E., Kirk, G. and Bownes, M. (2005). emc has a role in dorsal appendage fate formation in Drosophila oogenesis. *Mech Dev* **122**, 961-74.

Paradis, S., Ailion, M., Toker, A., Thomas, J. H. and Ruvkun, G. (1999). A PDK1 homolog is necessary and sufficient to transduce AGE-1 PI3 kinase signals that regulate diapause in Caenorhabditis elegans. *Genes Dev* **13**, 1438-52.

Parisi, M., Nuttall, R., Edwards, P., Minor, J., Naiman, D., Lu, J., Doctolero, M., Vainer, M., Chan, C., Malley, J. et al. (2004). A survey of ovary-, testis-, and soma-biased gene expression in Drosophila melanogaster adults. *Genome Biol* **5**, R40.

Park, J., Leong, M. L., Buse, P., Maiyar, A. C., Firestone, G. L. and Hemmings, B. A. (1999). Serum and glucocorticoid-inducible kinase (SGK) is a target of the PI 3-kinase-stimulated signaling pathway. *Embo J* **18**, 3024-33.

Park, S. J., Yang, E. S., Kim-Ha, J. and Kim, Y. J. (1998). Down regulation of extramacrochaetae mRNA by a Drosophila neural RNA binding protein Rbp9 which is homologous to human Hu proteins. *Nucleic Acids Res* **26**, 2989-94.

Partovian, C. and Simons, M. (2004). Regulation of protein kinase B/Akt activity and Ser473 phosphorylation by protein kinase Calpha in endothelial cells. *Cell Signal* **16**, 951-7.

Pause, A., Belsham, G. J., Gingras, A. C., Donze, O., Lin, T. A., Lawrence, J. C., Jr. and Sonenberg, N. (1994). Insulin-dependent stimulation of protein synthesis by phosphorylation of a regulator of 5'-cap function. *Nature* **371**, 762-7.

Paz, K., Liu, Y. F., Shorer, H., Hemi, R., LeRoith, D., Quan, M., Kanety, H., Seger, R. and Zick, Y. (1999). Phosphorylation of insulin receptor substrate-1 (IRS-1) by protein kinase B positively regulates IRS-1 function. *J Biol Chem* **274**, 28816-22.

Peri, F. and Roth, S. (2000). Combined activities of Gurken and decapentaplegic specify dorsal chorion structures of the Drosophila egg. *Development* **127**, 841-50.

Potter, C. J., Huang, H. and Xu, T. (2001). Drosophila Tsc1 functions with Tsc2 to antagonize insulin signaling in regulating cell growth, cell proliferation, and organ size. *Cell* **105**, 357-68.

Pullen, N., Dennis, P. B., Andjelkovic, M., Dufner, A., Kozma, S. C., Hemmings, B. A. and Thomas, G. (1998). Phosphorylation and activation of p70s6k by PDK1. *Science* **279**, 707-10.

Queenan, A. M., Ghabrial, A. and Schupbach, T. (1997). Ectopic activation of torpedo/Egfr, a Drosophila receptor tyrosine kinase, dorsalizes both the eggshell and the embryo. *Development* **124**, 3871-80.

Radimerski, T., Montagne, J., Rintelen, F., Stocker, H., van Der Kaay, J., Downes, C. P., Hafen, E. and Thomas, G. (2002). dS6K-regulated cell growth is dPKB/dPI(3)K-independent, but requires dPDK1. *Nat Cell Biol* **4**, 251-5.

Rane, M. J., Coxon, P. Y., Powell, D. W., Webster, R., Klein, J. B., Pierce, W., Ping, P. and McLeish, K. R. (2001). p38 Kinase-dependent MAPKAPK-2 activation functions as 3-phosphoinositide-dependent kinase-2 for Akt in human neutrophils. *J Biol Chem* **276**, 3517-23.

Razzini, G., Ingrosso, A., Brancaccio, A., Sciacchitano, S., Esposito, D. L. and Falasca, M. (2000). Different subcellular localization and phosphoinositides binding of insulin receptor substrate protein pleckstrin homology domains. *Mol Endocrinol* **14**, 823-36.

Ress, C., Holtmann, M., Maas, U., Sofsky, J. and Dorn, A. (2000). 20-Hydroxyecdysone-induced differentiation and apoptosis in the Drosophila cell line, l(2)mbn. *Tissue Cell* **32**, 464-77.

Rintelen, F., Stocker, H., Thomas, G. and Hafen, E. (2001). PDK1 regulates growth through Akt and S6K in Drosophila. *Proc Natl Acad Sci U S A* **98**, 15020-5.

Robinson, D. N., Cant, K. and Cooley, L. (1994). Morphogenesis of Drosophila ovarian ring canals. *Development* **120**, 2015-25.

Rorth, P. (1998). Gal4 in the Drosophila female germline. *Mech Dev* **78**, 113-8.

Roth, S., Neuman-Silberberg, F. S., Barcelo, G. and Schupbach, T. (1995). cornichon and the EGF receptor signaling process are necessary for both anterior-posterior and dorsal-ventral pattern formation in Drosophila. *Cell* **81**, 967-78.

Ruohola, H., Bremer, K. A., Baker, D., Swedlow, J. R., Jan, L. Y. and Jan, Y. N. (1991). Role of neurogenic genes in establishment of follicle cell fate and oocyte polarity during oogenesis in Drosophila. *Cell* **66**, 433-49.

Ruohola-Baker, H., Grell, E., Chou, T. B., Baker, D., Jan, L. Y. and Jan, Y. N. (1993). Spatially localized rhomboid is required for establishment of the dorsal-ventral axis in Drosophila oogenesis. *Cell* **73**, 953-65.

Sarbassov, D. D., Guertin, D. A., Ali, S. M. and Sabatini, D. M. (2005). Phosphorylation and regulation of Akt/PKB by the rictor-mTOR complex. *Science* **307**, 1098-101.

Saunders, C. and Cohen, R. S. (1999). The role of oocyte transcription, the 5'UTR, and translation repression and derepression in Drosophila gurken mRNA and protein localization. *Mol Cell* **3**, 43-54.

Scanga, S. E., Ruel, L., Binari, R. C., Snow, B., Stambolic, V., Bouchard, D., Peters, M., Calvieri, B., Mak, T. W., Woodgett, J. R. et al. (2000). The conserved PI3'K/PTEN/Akt signaling pathway regulates both cell size and survival in Drosophila. *Oncogene* **19**, 3971-7.

Schnorr, J. D. and Berg, C. A. (1996). Differential activity of Ras1 during patterning of the Drosophila dorsoventral axis. *Genetics* **144**, 1545-57.

Schulz, C., Kiger, A. A., Tazuke, S. I., Yamashita, Y. M., Pantalena-Filho, L. C., Jones, D. L., Wood, C. G. and Fuller, M. T. (2004). A misexpression screen reveals effects of bag-of-marbles and TGF beta class signaling on the Drosophila male germ-line stem cell lineage. *Genetics* **167**, 707-23.

Schupbach, T. (1987). Germ line and soma cooperate during oogenesis to establish the dorsoventral pattern of egg shell and embryo in Drosophila melanogaster. *Cell* **49**, 699-707.

Schupbach, T. and Wieschaus, E. (1991). Female sterile mutations on the second chromosome of Drosophila melanogaster. II. Mutations blocking oogenesis or altering egg morphology. *Genetics* **129**, 1119-36.

Shepherd, P. R., Withers, D. J. and Siddle, K. (1998). Phosphoinositide 3-kinase: the key switch mechanism in insulin signalling. *Biochem J* **333**, 471-90.

Soller, M., Bownes, M. and Kubli, E. (1997). Mating and sex peptide stimulate the accumulation of yolk in oocytes of Drosophila melanogaster. *Eur J Biochem* **243**, 732-8.

Soller, M., Bownes, M. and Kubli, E. (1999). Control of oocyte maturation in sexually mature Drosophila females. *Dev Biol* **208**, 337-51.

Spradling, A. C. (1986). P Element-mediated transformation. In *Drosophila: A practical approach*, (ed. D. B. Robert), pp. 175-197. Oxford, England: IRL Press.

Spradling, A. C. (1993). Developmental genetics of oogenesis. In *The Development of Drosophila melanogaster*, (ed. M. Bate and A. Martinez-Arias), pp. 1-70. New York: Cold Spring Harbor Laboratory Press.

Spradling, A. C., de Cuevas, M., Drummond-Barbosa, D., Keyes, L., Lilly, M., Pepling, M. and Xie, T. (1997). The Drosophila germarium: stem cells, germ line cysts, and oocytes. *Cold Spring Harb Symp Quant Biol* **62**, 25-34.

St Johnston, D., Beuchle, D. and Nusslein-Volhard, C. (1991). Staufen, a gene required to localize maternal RNAs in the Drosophila egg. *Cell* **66**, 51-63.

St Johnston, D., Driever, W., Berleth, T., Richstein, S. and Nusslein-Volhard, C. (1989). Multiple steps in the localization of bicoid RNA to the anterior pole of the Drosophila oocyte. *Development* **107 Suppl**, 13-9.

Stambolic, V., Mak, T. W. and Woodgett, J. R. (1999). Modulation of cellular apoptotic potential: contributions to oncogenesis. *Oncogene* **18**, 6094-103.

Stambolic, V., Suzuki, A., de la Pompa, J. L., Brothers, G. M., Mirtsos, C., Sasaki, T., Ruland, J., Penninger, J. M., Siderovski, D. P. and Mak, T. W. (1998). Negative

regulation of PKB/Akt-dependent cell survival by the tumor suppressor PTEN. *Cell* **95**, 29-39.

Staveley, B. E., Ruel, L., Jin, J., Stambolic, V., Mastronardi, F. G., Heitzler, P., Woodgett, J. R. and Manoukian, A. S. (1998). Genetic analysis of protein kinase B (AKT) in Drosophila. *Curr Biol* **8**, 599-602.

Stephens, L., Anderson, K., Stokoe, D., Erdjument-Bromage, H., Painter, G. F., Holmes, A. B., Gaffney, P. R., Reese, C. B., McCormick, F., Tempst, P. et al. (1998). Protein kinase B kinases that mediate phosphatidylinositol 3,4,5-trisphosphate-dependent activation of protein kinase B. *Science* **279**, 710-4.

Stephenson, E. C., Chao, Y. C. and Fackenthal, J. D. (1988). Molecular analysis of the swallow gene of Drosophila melanogaster. *Genes Dev* **2**, 1655-65.

Stocker, H. and Hafen, E. (2000). Genetic control of cell size. *Curr Opin Genet Dev* **10**, 529-35.

Stokoe, D., Stephens, L. R., Copeland, T., Gaffney, P. R., Reese, C. B., Painter, G. F., Holmes, A. B., McCormick, F. and Hawkins, P. T. (1997). Dual role of phosphatidylinositol-3,4,5-trisphosphate in the activation of protein kinase B. *Science* **277**, 567-70.

Sullivan, W. A., M; Hawley, R.S. (2000). *Drosophila* protocols, (ed. Cold Spring Harbor, New York: Cold Spring Harbor Laboratory Press.

Swan, A., Nguyen, T. and Suter, B. (1999). Drosophila Lissencephaly-1 functions with Bic-D and dynein in oocyte determination and nuclear positioning. *Nat Cell Biol* **1**, 444-9.

Swan, A. and Suter, B. (1996). Role of Bicaudal-D in patterning the Drosophila egg chamber in mid-oogenesis. *Development* **122**, 3577-86.

Tapon, N., Ito, N., Dickson, B. J., Treisman, J. E. and Hariharan, I. K. (2001). The Drosophila tuberous sclerosis complex gene homologs restrict cell growth and cell proliferation. *Cell* **105**, 345-55.

Tautz, D. and Pfeifle, C. (1989). A non-radioactive in situ hybridization method for the localization of specific RNAs in Drosophila embryos reveals translational control of the segmentation gene hunchback. *Chromosoma* **98**, 81-5.

Terashima, J. and Bownes, M. (2004). Translating available food into the number of eggs laid by Drosophila melanogaster. *Genetics* **167**, 1711-9.

Terashima, J. and Bownes, M. (2005). A microarray analysis of genes involved in relating egg production to nutritional intake in Drosophila melanogaster. *Cell Death Differ* **12**, 429-40.

Theurkauf, W. E. (1994). Microtubules and cytoplasm organization during Drosophila oogenesis. *Dev Biol* **165**, 352-60.

Theurkauf, W. E., Alberts, B. M., Jan, Y. N. and Jongens, T. A. (1993). A central role for microtubules in the differentiation of Drosophila oocytes. *Development* **118**, 1169-80.

Till, D. D., Linz, B., Seago, J. E., Elgar, S. J., Marujo, P. E., Elias, M. L., Arraiano, C. M., McClellan, J. A., McCarthy, J. E. and Newbury, S. F. (1998). Identification and developmental expression of a 5'-3' exoribonuclease from Drosophila melanogaster. *Mech Dev* **79**, 51-5.

Tinker, R., Silver, D. and Montell, D. J. (1998). Requirement for the vasa RNA helicase in gurken mRNA localization. *Dev Biol* **199**, 1-10.

Toker, A. and Newton, A. C. (2000). Akt/protein kinase B is regulated by autophosphorylation at the hypothetical PDK-2 site. *J Biol Chem* **275**, 8271-4.

Toker, A. and Newton, A. C. (2000). Cellular signaling: pivoting around PDK-1. *Cell* **103**, 185-8.

Torres, I. L., Lopez-Schier, H. and St Johnston, D. (2003). A Notch/Delta-dependent relay mechanism establishes anterior-posterior polarity in Drosophila. *Dev Cell* **5**, 547-58.

Twombly, V., Blackman, R. K., Jin, H., Graff, J. M., Padgett, R. W. and Gelbart, W. M. (1996). The TGF-beta signaling pathway is essential for Drosophila oogenesis. *Development* **122**, 1555-65.

Tzolovsky, G., Deng, W. M., Schlitt, T. and Bownes, M. (1999). The function of the broad-complex during Drosophila melanogaster oogenesis. *Genetics* **153**, 1371-83.

Van Buskirk, C. and Schupbach, T. (1999). Versatility in signalling: multiple responses to EGF receptor activation during Drosophila oogenesis. *Trends Cell Biol* **9**, 1-4.

Van Doren, M., Ellis, H. M. and Posakony, J. W. (1991). The Drosophila extramacrochaetae protein antagonizes sequence-specific DNA binding by daughterless/achaete-scute protein complexes. *Development* **113**, 245-55.

van Eeden, F. and St Johnston, D. (1999). The polarisation of the anterior-posterior and dorsal-ventral axes during Drosophila oogenesis. *Curr Opin Genet Dev* **9**, 396-404.

Vanhaesebroeck, B. and Alessi, D. R. (2000). The PI3K-PDK1 connection: more than just a road to PKB. *Biochem J* **346 Pt 3**, 561-76.

Vanhaesebroeck, B. and Waterfield, M. D. (1999). Signaling by distinct classes of phosphoinositide 3-kinases. *Exp Cell Res* **253**, 239-54.

Verdu, J., Buratovich, M. A., Wilder, E. L. and Birnbaum, M. J. (1999). Cell-autonomous regulation of cell and organ growth in Drosophila by Akt/PKB. *Nat Cell Biol* **1**, 500-6.

Viniegra, J. G., Martinez, N., Modirassari, P., Losa, J. H., Parada Cobo, C., Lobo, V. J., Luquero, C. I., Alvarez-Vallina, L., Ramon y Cajal, S., Rojas, J. M. et al. (2005). Full activation of PKB/Akt in response to insulin or ionizing radiation is mediated through ATM. *J Biol Chem* **280**, 4029-36.

Voronova, A. and Baltimore, D. (1990). Mutations that disrupt DNA binding and dimer formation in the E47 helix-loop-helix protein map to distinct domains. *Proc Natl Acad Sci U S A* **87**, 4722-6.

Wang, C. Y., Guttridge, D. C., Mayo, M. W. and Baldwin, A. S., Jr. (1999). NF-kappaB induces expression of the Bcl-2 homologue A1/Bfl-1 to preferentially suppress chemotherapy-induced apoptosis. *Mol Cell Biol* **19**, 5923-9.

Wang, S. and Hazelrigg, T. (1994). Implications for bcd mRNA localization from spatial distribution of exu protein in Drosophila oogenesis. *Nature* **369**, 400-03.

Ward, E. J. and Berg, C. A. (2005). Juxtaposition between two cell types is necessary for dorsal appendage tube formation. *Mech Dev* **122**, 241-55.

Wasserman, J. D. and Freeman, M. (1998). An autoregulatory cascade of EGF receptor signaling patterns the Drosophila egg. *Cell* **95**, 355-64.

Weinkove, D., Neufeld, T. P., Twardzik, T., Waterfield, M. D. and Leevers, S. J. (1999). Regulation of imaginal disc cell size, cell number and organ size by Drosophila class I(A) phosphoinositide 3-kinase and its adaptor. *Curr Biol* **9**, 1019-29.

Welsh, G. I., Miller, C. M., Loughlin, A. J., Price, N. T. and Proud, C. G. (1998). Regulation of eukaryotic initiation factor eIF2B: glycogen synthase kinase-3 phosphorylates a conserved serine which undergoes dephosphorylation in response to insulin. *FEBS Lett* **421**, 125-30.

White, K., Tahaoglu, E. and Steller, H. (1996). Cell killing by the Drosophila gene reaper. *Science* **271**, 805-7.

White-Cooper, H., Schafer, M. A., Alphey, L. S. and Fuller, M. T. (1998). Transcriptional and post-transcriptional control mechanisms coordinate the onset of spermatid differentiation with meiosis I in Drosophila. *Development* **125**, 125-34.

Williams, M. R., Arthur, J. S., Balendran, A., van der Kaay, J., Poli, V., Cohen, P. and Alessi, D. R. (2000). The role of 3-phosphoinositide-dependent protein kinase 1 in activating AGC kinases defined in embryonic stem cells. *Curr Biol* **10**, 439-48.

Wolf, B. B. and Green, D. R. (1999). Suicidal tendencies: apoptotic cell death by caspase family proteinases. *J Biol Chem* **274**, 20049-52.

Yamashita, Y. M., Jones, D. L. and Fuller, M. T. (2003). Orientation of asymmetric stem cell division by the APC tumor suppressor and centrosome. *Science* **301**, 1547-50.

Younger-Shepherd, S., Vaessin, H., Bier, E., Jan, L. Y. and Jan, Y. N. (1992). deadpan, an essential pan-neural gene encoding an HLH protein, acts as a denominator in Drosophila sex determination. *Cell* **70**, 911-22.

Yue, L. and Spradling, A. C. (1992). hu-li tai shao, a gene required for ring canal formation during Drosophila oogenesis, encodes a homolog of adducin. *Genes Dev* **6**, 2443-54.

Zhang, H., Stallock, J. P., Ng, J. C., Reinhard, C. and Neufeld, T. P. (2000). Regulation of cellular growth by the Drosophila target of rapamycin dTOR. *Genes Dev* **14**, 2712-24.

Zhao, D. and Bownes, M. (1999). Misexpression of argos, an inhibitor of EGFR signaling in oogenesis, leads to the production of bicephalic, ventralized, and lateralized Drosophila melanogaster eggs. *Dev Genet* **25**, 375-86.

Zhao, D., Clyde, D. and Bownes, M. (2000). Expression of fringe is down regulated by Gurken/Epidermal Growth Factor Receptor signalling and is required for the morphogenesis of ovarian follicle cells. *J Cell Sci* **113 Pt 21**, 3781-94.

Zhao, D., Woolner, S. and Bownes, M. (2000). The Mirror transcription factor links signalling pathways in Drosophila oogenesis. *Dev Genes Evol* **210**, 449-57.

Appendix A

ELSEVIER

Volume 122, issue 9, SEPTEMBER 2005

ISSN 0925-4773

MECHANISMS of DEVELOPMENT

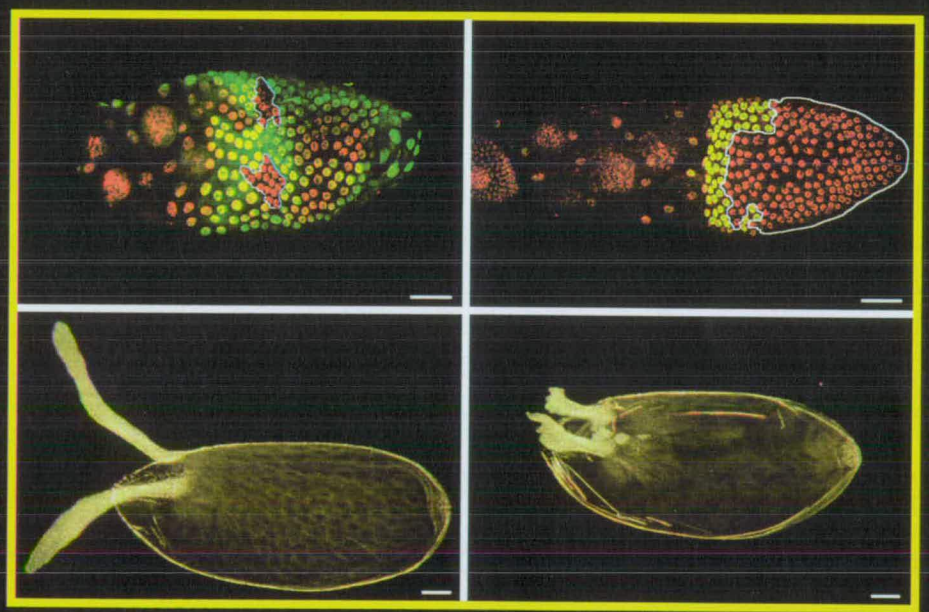

The Official Journal of the International Society of Developmental Biologists

Aims and Scope: *Mechanisms of Development* is an international journal whose purpose is to communicate contemporary studies in developmental biology with special emphasis on the characterization of molecular mechanisms underlying developmental processes in either vertebrates or invertebrates. Areas of particular interest include embryogenesis, pattern formation, cell determination and differentiation, specification of tissue type, targeted disruptions of developmental control genes, the roles of transcription factor in development, regulatory hierarchies of gene expression, cell-cell communication and signal transduction in development, as well as post-transcriptional controls of developmental processes such as regulated splicing and protein modification. Such a focus should provide a unique forum for comparing and contrasting strategies of development among a wide spectrum of organisms. The Editors are strongly committed to establishing the highest standards of quality and scientific merit, and guarantee rapid communication of important contributions. Colour illustrations will be reproduced free of charge to the authors.
Mechanisms of Development has a separate section for the publication of "cloning and expression" papers and reports of the results of molecular/gene expression screens, *Gene Expression Patterns*.

Prof. SHINICHI AIZAWA, Center for Developmental Biology, Group Dir. Lab. for Vertebrate Body Plan, 2-2-3, Minatojima, Minami, Chuou-ku, Kobe, 650-0047, Japan. Tel.: +81 78 306 3149; Fax: +81 78 306 3151; E-mail: saizawa@cdb.riken.go.jp

Prof. MARNIE E. HALPERN, Department of Embryology, Carnegie Institution of Washington, 115 West University Parkway, Baltimore, MD 21210, USA. Tel.: +1 410 554 1218; Fax: +1 410 243 6311; E-mail: halpern@ciwemb.edu

Prof. Dr. THOMAS B. KORNBERG, Department of Biochemistry, University of California, San Francisco, CA 94143, USA. Tel.: +1 415 476 8821; Fax: +1 415 514 1470; E-mail: tkornberg@biochem.ucsf.edu

Prof. MARIA LEPTIN, Institut für Genetik, Universitat zu Köln, Weyertal 121, D-50931 Köln, Germany. Tel.: +49 221 470 3401; Fax: +49 221 470 5264; E-mail: mleptin@uni-koeln.de

Prof. CLAUDIO D. STERN, Department of Anatomy and Developmental Biology, University College London, Gower Street, London WC1E 6BT, UK. Tel.: +44 20 7679 3346; Fax: +44 20 7679 2091; E-mail: c.stern@ucl.ac.uk

Dr. PATRICK TAM, Embryology Unit, Children's Medical Research Institute, Locked Bag 23, Wentworthville, NSW 2145, Australia. Tel.: +61 2 9687 2800; Fax: +61 2 9687 2120; E-mail: ptam@cmri.usyd.edu.au

---

Cover photo: *Extramachrochaete* (*emc*) is involved in dorsal appendage formation in *Drosophila* oogenesis. The upper two panels show clones of *emc* mutant follicle cells in the ovary, where nuclear GFP is green and nuclei are in red: homozygous mutant cells do not express GFP and thus appear red. The lower panels show a wild-type ovary (left) and an ovary containing *emc* follicle cell clones (right), revealing that the appendages of the mutant are shorter, abnormally shaped and fused at the base. **For further details see article by Papadia et al., pp 961–974 of this issue.**

ELSEVIER

Mechanisms of Development 122 (2005) 961–974

www.elsevier.com/locate/modo

emc has a role in dorsal appendage fate formation in *Drosophila* oogenesis

Sofia Papadia[a], George Tzolovsky[a], Debiao Zhao[b], Kevin Leaper[a], Dorothy Clyde[c], Paul Taylor[d], Eva Asscher[e], Graeme Kirk[a], Mary Bownes[a,*]

[a]*Institute of Cell and Molecular Biology, University of Edinburgh, Edinburgh EH9 3JR, UK*
[b]*Roslin Institute, Roslin, Midlothian EH25 9PS, UK*
[c]*Biosciences, University of Kent, Canterbury CT2 7NJ, UK*
[d]*MRC Human Reproductive Sciences Unit, University of Edinburgh Centre for Reproductive Biology, Edinburgh EH16 4SB, UK*
[e]*Wellcome/CR UK Gurdon Institute and Department of Anatomy, Cambridge University, Cambridge CB2 1QR, UK*

Received 23 December 2004; received in revised form 26 April 2005; accepted 5 May 2005
Available online 31 May 2005

Abstract

extramacrochaetae (*emc*) functions during many developmental processes in *Drosophila*, such as sensory organ formation, sex determination, wing vein differentiation, regulation of eye photoreceptor differentiation, cell proliferation and development of the Malpighian tubules, trachea and muscles in the embryo. It encodes a Helix-Loop-Helix transcription factor that negatively regulates bHLH proteins. We show here that *emc* mRNA and protein are present throughout oogenesis in a dynamic expression pattern and that *emc* is involved in the regulation of chorionic appendage formation during late oogenesis. Expression of sense and antisense *emc* constructs as well as *emc* follicle cell clones leads to eggs with shorter, thicker dorsal appendages that are closer together at base than in the wild type. We demonstrate that *emc* lies downstream of *fs(1)K10*, *gurken* and *EGFR* in the Grk/EGFR signalling pathway and that it participates in controlling Broad-Complex expression at late stages of oogenesis.

Keywords: Oogenesis; Extramacrochaetae; Grk/EGFR pathway; Cell fate; Dorsal appendage formation; Br-C

1. Introduction

The gene *extramacrochaetae* (*emc*) encodes a transcription factor and is involved in many diverse processes at various stages of *Drosophila* development (Campuzano, 2001 for a review). It negatively regulates the *achaete-scute* Complex (AS-C) (Botas et al., 1982) and encodes a Helix-Loop-Helix (HLH) protein (Ellis et al., 1990; Garrell and Modolell, 1990). Emc belongs to class V of HLH proteins (Massari and Murre, 2000), together with the Id proteins (Inhibitor of differentiation) in mammals (Benezra et al., 1990). Proteins of this class lack the basic region thus are unable to bind DNA (Davis et al., 1990) and are negative regulators of class I and class II HLH proteins by forming inactive heterodimers with them.

Emc regulates Sensory Organ (bristle) formation in a concentration-dependent manner by forming heterodimers with Daughterless and the AS-C proteins (Van Doren et al., 1991; Cabrera et al., 1994). It, therefore, limits the amount of Daughterless (Da) and Scute (Sc) available to form active heterodimers that promote Sensory Mother Organ (SMC, the precursor cell of SOs) formation. Thus, only cells with sufficiently high levels of Da, Ac and Sc to titrate Emc and to activate the downstream genes of the neural differentiation pathway are able to become SMCs (Campuzano, 2001). Emc function is also required in early embryogenesis for sex determination. The interaction between X-linked 'numerator' bHLH proteins (encoded by *sisterless-α*, *scute* and *sis-c*) and autosomal 'denominators' such as Emc, Daughterless and Deadpan regulates the X:A ratio which, in turn, determines whether *Sex-lethal* will be transcribed or not, thus regulating sexual fate (Younger-Shepherd et al., 1992). Only in females, with twice the concentration of Sc compared to males, are there sufficient active Sc/Da

* Corresponding author. Tel.: +44 131 650 5369; fax: +44 131 650 5371.
E-mail address: mary.bownes@ed.ac.uk (M. Bownes).

0925-4773/$ - see front matter © 2005 Elsevier Ireland Ltd. All rights reserved.
doi:10.1016/j.mod.2005.05.002

heterodimers to overcome the inhibitory effects of Emc and other putative autosomal-linked negative regulators and to activate Sxl (Campuzano, 2001). Later in embryogenesis *emc* is required for a number of processes, including Malpighian tubule formation, tracheal and muscle development and visceral mesoderm migration, by interacting with EGFR, Achaete, Breathless and Trachealess, Da and Twist (Cubas et al., 1994; Ellis, 1994). In the developing eye Emc and Hairy negatively regulate the expression of *atonal*, a bHLH gene which together with Da is necessary for the specification of R8, the first photoreceptor in an ommatidium. Downregulation of *emc* and *hairy* at specific locations by the Notch signalling pathway is essential for the initiation of eye development (Baonza and Freeman, 2001). In the wing Emc is involved in vein differentiation (de Celis, 1998, review). *emc* is expressed in the intervein cells flanking the veins where *Notch* and *E(spl)mβ* are expressed (Baonza et al., 2000). Recently Adam and Montell (2004), in a screen for genes involved in cell fate decisions in the ovary, showed that Emc has a role in follicle cell differentiation by inducing or maintaining EYA (Eyes Absent, a negative regulator of polar/stalk cell fate) in the epithelial follicle cells upon signalling from Notch, during early oogenesis.

The *Drosophila* ovary consists of about 16 ovarioles which are independent egg assembly lines. Oogenesis starts in the germarium, where a germline stem cell divides asymmetrically to give a daughter stem cell and a differentiated cystoblast, which undergoes four mitotic divisions with incomplete cytokinesis (in germarium region 1). This results in the formation of a 16-cell germline cyst within which the cystocytes (germline cells) are interconnected by cytoplasmic bridges called ring canals. The germline cyst becomes enveloped by follicle cells as it moves through germarium region 2, while within the cyst one of the two pro-oocytes (cystocytes with four ring canals) differentiates into the oocyte and the other germline cells become nurse cells (King, 1970; Spradling, 1993).

The Grk/EGFR signalling pathway establishes and regulates axis polarity (Neuman-Silberberg and Schüpbach, 1993; Queenan et al., 1997). The oocyte nucleus moves from the posterior to the anterior of the oocyte during stages 7–8 of oogenesis and as a result *gurken* (*grk*) mRNA and protein are expressed at the dorsal anterior region of the oocyte from stage 9. Gurken signals to the Epidermal Growth Factor Receptor (EGFR) on the surface of the adjacent follicle cells and through an elaborate regulation involving several genes that include *rhomboid, pointed, argos, spitz, kekkon-1, mirror* and *Broad-Complex* (Br-C), EGFR signalling results in two subsets of dorsal anterior follicle cells either side of the dorsal midline to become determined to migrate anteriorly and secrete the dorsal appendages (Ruohola-Baker et al., 1993; Morimoto et al., 1996; Deng and Bownes, 1997; Deng and Bownes, 1998; Wassermann and Freeman, 1998; Van Buskirk and Schüpbach, 1999; Zhao and Bownes, 1999; Cooperstock and Lipshitz, 2001). Downregulation of EGFR signalling results in a reduction of the number of cells exhibiting a dorsal fate leading to a reduction in the distance between the dorsal appendages whereas EGFR overexpression results in dorsalised eggs and embryos by increasing the distance between dorsal appendages (Neuman-Silberberg and Schüpbach, 1993, 1994; Queenan et al., 1997). In this paper, we show that *emc* contributes to the determination of dorsal follicle cell fate and that it acts downstream of Grk/EGFR and upstream of Br-C.

2. Results

2.1. The dynamic expression pattern of extramacrochaetae in oogenesis

A *lacZ* enhancer-trap fly line *261/31* was chosen for analysis based on its β-galactosidase expression in subsets of follicle cells during oogenesis. This line was provided from Peter Deak's collection (Deak et al., 1997). β-galactosidase expression in *261/31* was detected throughout *Drosophila* oogenesis with particularly strong expression from stages 2 to 11. Initially, staining is detected in all follicle cells (stages 2–6—Fig. $1B_1$). At stages 7–8 follicle cells over the oocyte are stained more intensely (Fig. $1B_1$) and at stage 9 *lacZ* is highly expressed in a band of follicle cells at the boundary between the oocyte and the nurse cells and in the migrating follicle cells that cover the anterior two thirds of the oocyte (results not shown), as well as in the stretched follicle cells that remain over the nurse cells. During stages 10–11 *lacZ* expression is localised to the centripetal follicle cells, the nurse cell-associated follicle cells and the dorsal anterior follicle cells; in the latter, at stage 10A expression in the columnar follicle cells becomes restricted to the region over the dorsal anterior of the oocyte. This expression pattern remains until stage 11 when two distinct subsets of stained follicle cells are defined (Fig. $1B_{1,2}$). As the dorsal–ventral axis is established during this stage, the dorsal anterior expression of this gene suggested a potential role in dorsal–ventral patterning of the egg. At stage 12 expression is localised in two discrete groups of dorsal anterior follicle cells on either side of the dorsal midline (Fig. $1B_3$), which move anteriorly over the forming dorsal appendages as the oocyte develops (stage 13) but are now connected as one band covering the dorsal midline (Fig. $1B_4$).

A fragment of genomic DNA isolated following plasmid rescue of *261/31* corresponded to the known gene *extramacrochaetae* (*emc*) (Fig. 1A). Full length cDNA was obtained from Garrell and Modolell (1990) and used in all subsequent experiments. The expression pattern of *emc* during oogenesis was determined by mRNA in situ hybridisation to whole mount ovaries (Fig. $1C_{1-6}$). Expression of *emc* is detected in all somatic follicle cells from stage 1 (in region 3 of the germarium) until stage 6

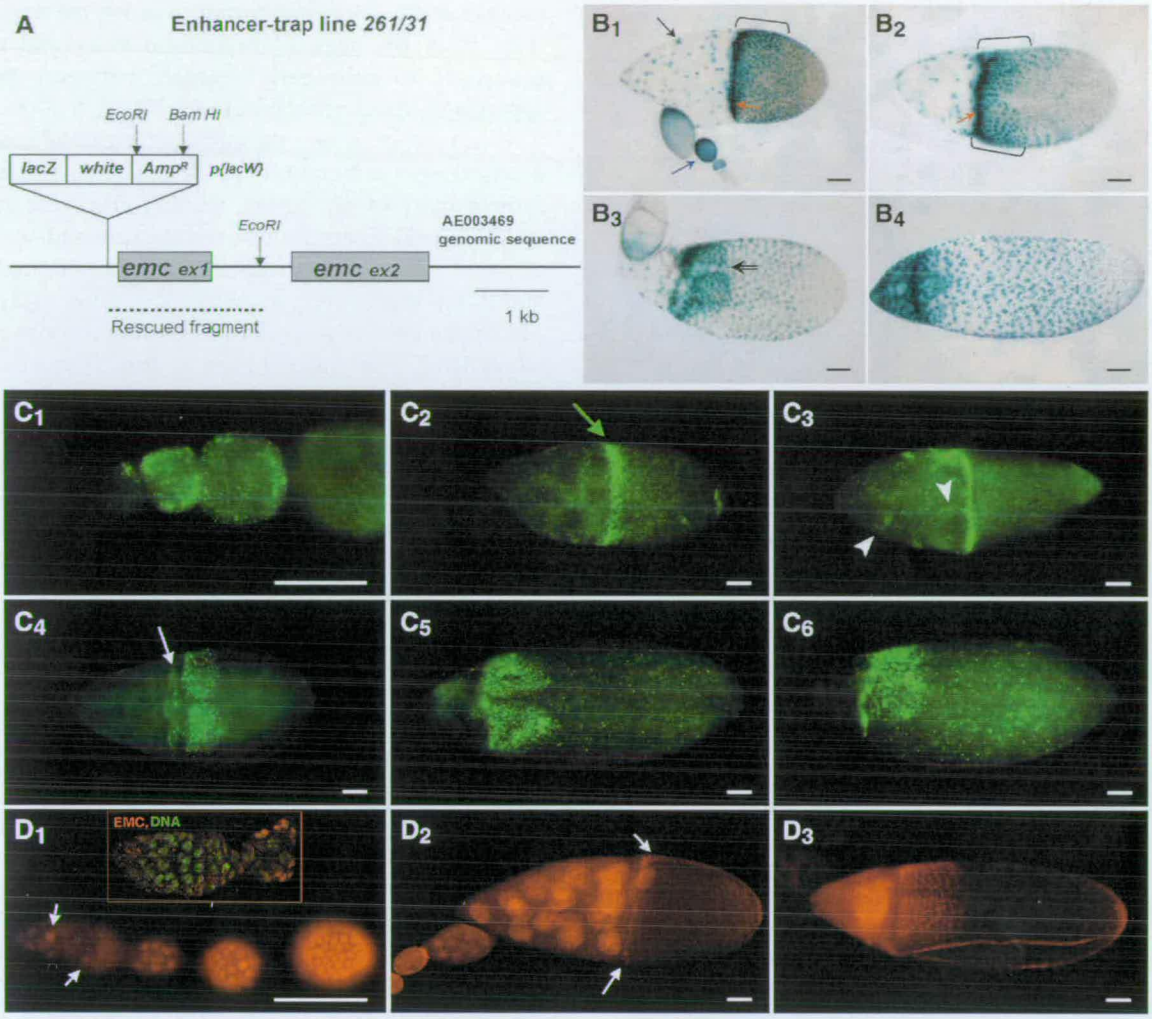

Fig. 1. (A) A genomic map of *261/31* showing the site of *P{lacW}* insertion 72 bp 5′ from exon 1 of *emc*. Exons are shaded grey and labelled ex1 and ex2 for exons 1 and 2, respectively. The solid line represents genomic DNA and the dotted line represents the rescued DNA fragment. (B_{1-4}) β-galactosidase staining pattern in egg chambers of the enhancer-trap line *261/31*. For details, see text. (B_1) An ovariole containing the germarium (not stained), egg chambers in early stages of oogenesis (stages 3, 6 and 8 are presented here) and a stage 10A egg chamber (main picture). Blue arrow, *lacZ* expression in all follicle cells covering the germline cells in the early stages of oogenesis; black arrow, expression in the stretched follicle cells covering the nurse cells; red arrow, expression in the centripetal cells and, bracket, in the area over the dorsal anterior of the oocyte. (B_2) Stage 11 egg chamber with *lacZ* expression localised in the centripetal cells (red arrow) and in two groups of lateral dorsal anterior follicle cells (brackets). (B_3) In a stage 12 egg chamber, the two groups of dorsal anterior follicle cells are separated by a gap on the dorsal midline (double black arrow). Expression is also retained in a ring of follicle cells at the border between the oocyte and nurse cells. (B_4) Strong *lacZ* expression in follicle cells over the forming dorsal appendages and in a small area over the dorsal midline (stage 13). B_1 is a lateral view while ($B_{2,4}$) are top views (dorsal is at the top) and in (B_3) dorsal is marked by the direction of the arrow. (C_{1-6}). In situ hybridisation analysis in *OrR* ovaries using a DIG labelled *emc* RNA probe and (D_{1-3}) Emc antibody staining in *OrR* ovaries. (C_1) *emc* mRNA (green) is expressed ubiquitously in stages 1 (germarium region 3)–6 of oogenesis, in the follicle cells and the nurse cell cytoplasm. Occasionally expression was also observed in region 2 of the germarium (not shown). (C_{2-3}) At stage 10A (C_2) *emc* expression is very strong in a band of follicle cells that cover the anterior of the oocyte (green arrow). There is a low level of expression in the nurse cell cytoplasm that continues in later stages. The stretched follicle cells over the nurse cells also express *emc* (arrowheads in C_3—stage 10B egg chamber). (C_4) By stage 11 *emc* is expressed in the centripetal cells (arrow) and in two discrete groups of lateral dorsal anterior follicle cells either side of the dorsal midline. (C_5) Towards stage 12 these two groups of follicle cells become restricted to dorsal anterior positions on either side of a thin gap along the dorsal midline and (C_6) later in stages 12–13 there is a continuous area of *emc* expression covering the dorsal anterior of the developing oocyte, including the dorsal midline. (D_1) Emc protein (red) is expressed in the germarium (arrows) and in the follicle cells surrounding early stage egg chambers. Inset, magnified germarium with Emc (red) and Sytox Green (green, DNA stain). Emc expression in follicle cells. (D_2) The nurse cell and oocyte nuclei strongly express Emc. In the follicle cells Emc expression is stronger in the centripetal and dorsal anterior cells (arrows). (D_3). At stage 12 Emc is expressed in two dorsal anterior patches of follicle cells and the nurse cell nuclei. (C_{4-5}) are dorsal views, (C_6) and (D_3) are dorso-lateral and (D_2) is a lateral view. Scale bar = 50 μm. Inset in (D_1) is magnified 1.2×. In all figures anterior is to the left.

(Fig. $1C_1$ and not shown). Subsequently *emc* expression becomes restricted to a tight band of follicle cells at the nurse cell-oocyte boundary and to the stretched follicle cells over the nurse cells at stage 10A and 10B (Fig. $1C_{2-3}$). During stage 11 expression is refined to two subsets of follicle cells either side of the dorsal midline (Fig. $1C_{4-5}$). Expression persists in these follicle cells as they migrate anteriorly, secreting the dorsal appendages, but *emc* is now

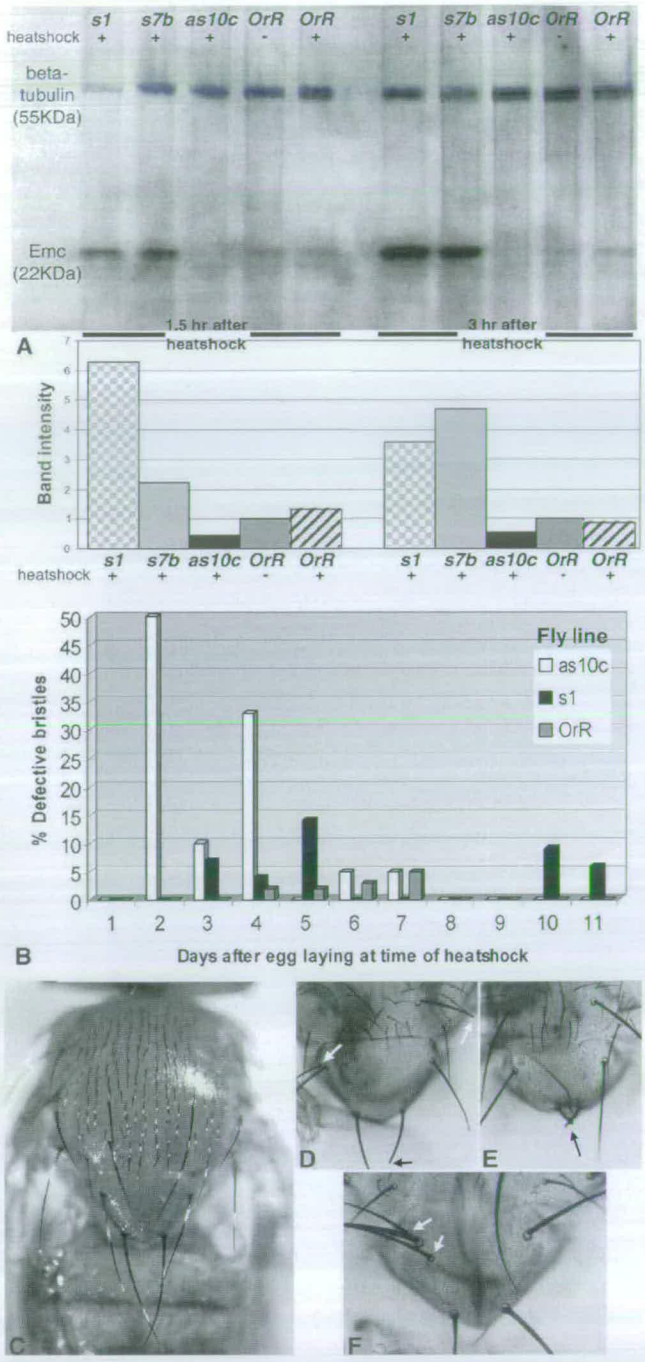

Fig. 2. (A) Western blot with Emc antibody and anti-β-Tubulin (loading control) to ovaries from wild-type, *emc* sense (*s1*, *s7b*) and antisense (*as10c*) fly lines. In lanes 1–5 the ovaries were dissected 1.5 h after heatshock and in lanes 6–10 the ovaries were dissected 3 h after heatshock. The low endogenous level of Emc in wild-type flies is not affected significantly by the heatshock treatment. Emc protein expression is significantly increased in heatshocked *s1* and *s7b* flies (lanes 1 and 2) and stays at high levels with time (lanes 6 and 7). In contrast, no Emc protein is detected in the heatshocked *emc* antisense line as10c, neither 1.5 nor 3 h after heatshock (lanes 3 and 8). The graph shows the relative intensity of bands after normalising for β-Tubulin [(Emc intensity − background)/(β-tubulin intensity − background)]. All values are expressed relative to the non-heatshocked *OrR* sample (negative control; value = 1). (B) Graph representing the phenotypic effect of the heatshock relative to the age of flies at the time of heatshock. The number of flies with defective bristles, including truncated bristles and extra bristles (but not missing bristles), which hatched following heatshock at various developmental stages is shown for one antisense (*as10c*—white), one sense (*s1*—black) and a wild type (*OrR*—grey) line. (C) Wild-type bristle pattern (*OrR*). (D) One extra scutellar bristle and truncated thickened bristles. (E) Short abnormal scutellar bristles. (F) Two additional scutellar bristles. Abnormal bristles are marked with arrows.

expressed in a single larger area covering the dorsal midline (Fig. $1C_6$). By stage 14 expression is limited to a small group of follicle cells located between the dorsal appendages (data not shown).

Emc protein follows the mRNA expression pattern and is detected by immunostaining with an *emc* antibody in follicle cells of all stages, starting from the germarium (Fig. $1D_1$ and inset). Protein is not expressed very strongly at stages 7–8. It is present in all germline cell nuclei in mid- and late oogenesis (stages 8–13) (Fig. $1D_2$), in the centripetal cells at stage 10 and in the posterior polar cells (stage 10–11). At stages 11 and 12 Emc is expressed in two dorsal anterior subsets of follicle cells either side of the dorsal midline (Fig. $1D_3$), during stage 12 these dorsal follicle cells migrate anteriorly and at stage 13 Emc is only detected in the follicle cells of the developing dorsal appendages (data not shown and Fig. 3A).

2.2. Generation of transgenic emc lines

To investigate further the role of *emc* in oogenesis we generated transgenic fly lines expressing sense and antisense RNA (Deng et al., 1999). Full-length *emc* cDNA in either the sense (s) or antisense (as) orientation was expressed under a heatshock (hs) promoter. From the eight heatshock-sense-*emc* (*hs-s-emc*) lines and 12 heatshock-antisense-*emc* (*hs-as-emc*) lines established, lines *s1*, *s7b* and *as10c* were selected for further study since they showed the highest egg abnormality rates when heatshocked (refer to Fig. 5A,B).

Western blot analysis was used to confirm the effect of the induced sense and antisense constructs on the levels of the Emc expression (Emc has a predicted molecular weight of 22 kDa). As shown in Fig. 2A, Emc protein levels are highly elevated in heatshocked sense flies (lines *s1* and *s7b*) in comparison to the low endogenous Emc expression in wild-type *OrR* flies, whereas in antisense flies (line *as10c*) Emc protein is essentially undetectable (Fig. 2A) in comparison to beta-Tubulin. Similar results were obtained with immunohistochemistry with Emc antibody (Fig. 3A–C), as described below.

2.3. Specificity of the emc constructs

In order to establish if the *emc* sense and antisense constructs were generating phenotypes corresponding to those of known *emc* mutations we investigated their effects on bristle development in the thorax. Heatshock inducible lines *s1* (sense *emc*) and *as10c* (antisense *emc*) were used.

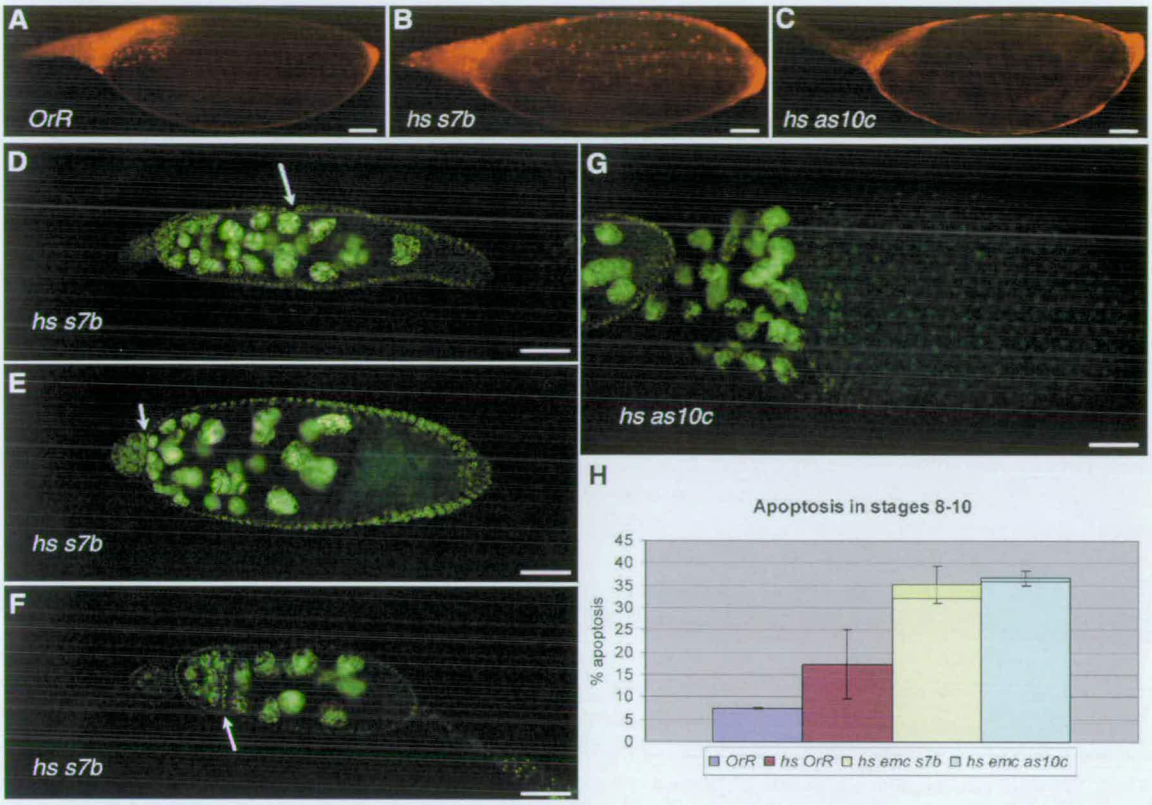

Fig. 3. (A–C) Immunohistochemistry with Emc antibody using stage 13 egg chambers. (A) Wild type Emc expression in the dorsal anterior using *OrR* ovaries. (B) Ectopic Emc in follicle cells laterally and posteriorly apart from the dorsal anterior in *hs s7b* sense *emc* flies. (C) Absence of Emc staining, even on the dorsal anterior in *emc* antisense flies *hs as 10c*. (D–G) Fused egg chambers from heatshocked sense and antisense *emc* fly ovaries. Nuclei are stained in green. (D) Arrow indicates a groove in the follicle cell layer where presumably this egg chamber should have been separated in two. (E–F) Arrows point to the irregular separation of two egg chambers. (G) A stage 11 fused egg chamber with more than fifteen nurse cells. The names of the fly lines used are written on each picture. (I) Graph showing the percentage of apoptotic egg chambers in wild-type and *emc* transgenic flies during stages 8–10.Vertical lines denote the standard deviation. Darker coloured boxes in the *s7b* and *as10c* columns represent the fraction of apoptotic egg chambers that also exhibit a fused phenotype. For heatshocked and non-heatshocked wild-type *OrR* flies this equals zero. Scale bars = 50 μm.

Females were allowed to lay eggs for 24 h, and then transferred to a new vial; this was repeated for 10 days to collect all developmental stages. The vials were then all heatshocked at once and the resulting flies were scored for bristle phenotypes.

Many flies had missing dorsocentral and scutellar bristles. However, the control wild type flies frequently had these phenotypes as well, when heatshocked. The heatshocked *emc* sense and antisense flies also showed phenotypes typical of *emc* mutations (Huang et al., 1995): extra dorsocentral and scutellar bristles, two bristles (scutellar and/or postalar) coming from one socket and short thick bristles in several locations. There were also flies with scutellar bristles facing in the wrong orientation. The frequency of occurrence of these abnormal and extra bristles is shown in Fig. 2B, and some of the phenotypes observed are shown in Fig. 2D–F, compared to the *OrR* phenotype (Fig. 2C).

Emc antibody staining in ovaries of wild type *OrR*, sense *s7b* and antisense *as10c* fly lines also confirms the specificity of the *emc* constructs and effectiveness of the heatshock regime. Emc is observed ectopically in the heatshocked sense line *s7b* (Fig. 3B—note the lateral/posterior follicle cells stained on the oocyte) compared to the wild type Emc expression pattern (Fig. 3A). At the same time there is absence of Emc staining from the heatshocked antisense line *as10c* (Fig. 3C) consistent with the 'knock-out' effect of the antisense construct.

2.4. Disruption and misexpression of emc affects egg chamber formation

In heatshocked sense and antisense *emc* ovaries we detected egg chambers fused to various extents (Fig. 3E–H). Sometimes there are 32 germline nuclei, presumably resulting from the fusion of two egg chambers, but usually there is incomplete fusion, resulting in one abnormally large egg chamber with an irregular number of nurse cell nuclei (e.g. 28 nurse cells—Fig. 3F) linked to an atrophic or underdeveloped egg chamber. These egg chambers were undergoing apoptosis but there were cases where development appeared to proceed to some extent (stage 11 egg chamber in Fig. 3H). This fused egg chamber phenotype was observed more in sense *emc* lines than in antisense *emc*

and wild-type flies never exhibited it, even when they were subjected to the same heatshock treatment as *emc* transgenic flies and the number of egg chambers undergoing apoptosis in their ovaries was increased (Fig. 3I).

2.5. Disruption and misexpression of emc affects dorsal follicle cell determination

The endogenous *emc* RNA expression analysis (Fig. $1C_{2-6}$) and the enhancer trap line *261/31* (Fig. $1B_{1-4}$) show that *emc* is expressed in the anterior follicle cells from stage 9–13. It is known that the dorsal–ventral axis is established by the EGFR signalling pathway at stage 9 and we postulated that *emc* may play a role in cell fate determination during this time. To investigate this we examined the effects of expressing both sense and antisense *emc* on eggshell patterning. Variation in expression of the *emc* sense and antisense due to position effects was expected, so an initial trial of 8 *emc* sense lines and 11 *emc* antisense lines was performed (standard heatchock, Fig. 5A,B), to establish which lines to use in a more detailed examination. The eggs were collected and examined for abnormal dorsal appendage formation, as this was likely to occur if there were defects in dorso–ventral patterning. Eggs were generally ventralised and their appendage phenotype ranged from appendages closer together or with fused bases to completely fused appendages. Occasionally they had wild-type looking appendages that were closer together at base (Fig. 4E); more frequently though they had wider dorsal appendages, usually shorter than wild-type (Fig. 4A) and irregular in shape (Fig. 4C–D,F–H), sometimes with split ends (Fig. 4G). Both sense and antisense heatshocked fly lines exhibited similar phenotypes.

We investigated the frequencies of phenotypes that arose following heatshock at different stages of oogenesis. To do this, females were heatshocked and the eggs collected at various time points after the heatshock. Fig. 5A shows variation in the frequency of abnormal phenotypes among the *emc* heatshocked sense fly lines, as expected. There are similarities between different insertion lines misexpressing the sense construct, with eggs collected 0–24 h after heatshock having the highest frequency of abnormal appendages. This shows that ectopic expression of *emc* in later stage egg chambers has the greatest effect upon dorsal patterning. The low percentages of abnormal egg chambers are to be expected, because not all egg chambers would have been at the appropriate point in dorsal–ventral axis determination to have an effect when the constructs were expressed during the short 45 min heatshock.

There is a greater variability in the frequency of eggs laid with abnormal appendages between different antisense lines disrupting *emc* (Fig. 5B), although the classes of abnormal phenotypes were similar to those of the sense lines. The heatshocked antisense *emc* lines laid abnormal eggs much later than the heatshocked sense *emc* lines, showing that disruption early in oogenesis has a greater phenotypical effect. Presumably this reflects the time needed for the already expressed *emc* RNA and protein to be turned over and disrupted by the antisense *emc* expression.

The heatshock method affects the numbers of abnormal eggs laid and the exact phenotypes observed. An alternative, more severe heatshock (see methods) led to similar phenotypes but eggs were frequently much smaller, irregular in shape and with fused appendages. Heatshock alone can cause abnormal dorsal appendage phenotypes (in *OrR*) and occasionally leads to the production of smaller eggs; however, the percentages are significantly lower than for *emc* mis-expression lines.

To investigate in detail the nature of the phenotypic changes in the appendages, eggs laid by females expressing *emc as10c* (standard heatshock regime) were collected and the spacing between the appendages was measured to see how much the appendages had moved. Since these were ventralised we compared them to wild type *OrR* eggs and to eggs laid by *gurken*^{22j} (*grk*^{22j}) females. The *grk*^{22j} flies have four copies of the wild type *grk* gene and the positioning on the appendages is influenced by *grk* via the EGFR pathway (Neuman-Silberberg and Schüpbach, 1994). Misexpression of *grk* causes a broader area of the egg to be dorsalised and the appendages are pushed further apart (Fig. 4B).

The frequency distribution (Fig. 5C) shows significant shifts in the spacing between the appendages in the eggs laid by *emc* antisense and *grk*^{22j} lines when compared to wild type eggs. The distance between appendages is bigger for the *grk*^{22j} line by approximately 17 μm. In heatshocked lines expressing *emc* antisense, the distance is smaller, i.e. the appendages are closer together, by approximately 15 μm. There is an interesting phenomenon showing that once the appendages get closer together than approximately 20 μm they fuse rather than form separately. To investigate this further and to investigate if the cells are different in number, shape or size we looked at the organisation of cells in the space between the appendages. Wild type eggs have elongated follicle cells between the dorsal appendages. The *emc* antisense mutants have a similar cellular shape, however, the cells between the *grk*^{22j} appendages are shorter and wider than in the *emc* antisense eggs and the wild type (data not shown). Thus, *emc* mutants do not change the shape of cells, but the number of cells between the appendages.

2.6. Analysis of emc homozygous mutant clones in follicle cells

Mosaic flies with *emc* homozygous clones were generated in order to investigate the effect of *emc* mutant clones in oogenesis and to confirm that the abnormal appendage phenotypes seen in the antisense analysis were due to perturbations in *emc* expression.

Follicle cell clones were observed in the ovaries of heatshocked *FLP*; *emc*^{1}, *FRT 80B/nlsGFP, FRT80B* flies as

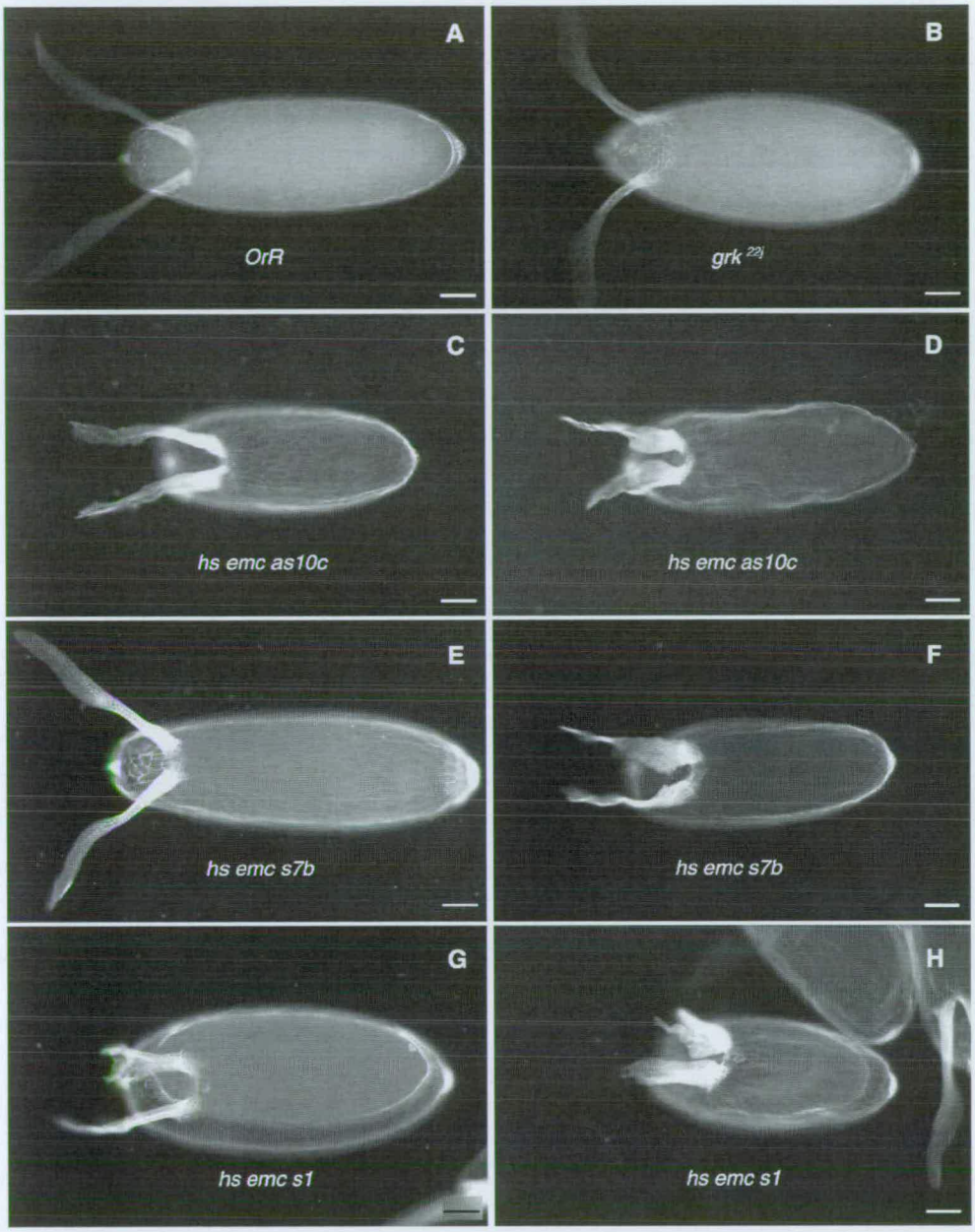

Fig. 4. The phenotypes observed in *OrR*, grk^{22j} and *emc* sense and antisense eggs. (A) *OrR*. (B) grk^{22j} with the dorsal appendages pushed further away from the dorsal midline. (C) and (D) Heatshocked *emc as10c* have appendages that are thicker and pushed closer to the dorsal midline. (E–H) are from two *emc* sense lines, *s7b* in (E) and (F) and *s1* in (G) and (H); they show the varying thickness and length of appendages and their abnormal tip morphology—these egg chambers are also ventralised. Note the wider and shorter cells between the appendages in (B). Scale bar = 50 μm. Transgenic eggs are generally smaller than wild-type.

shown in Fig. 6A,B. Occasionally the follicle cells within the clone would appear denser and smaller compared to their neighbouring follicle cells outside the clone (Fig. 6A) but the presence of *emc* mutant clones, even in quite large areas of the follicle cell monolayer (Fig. 6B) does not seem to have an immediately obvious morphological effect during oogenesis. However, the eggs laid by the heatshocked flies having *emc* clones in their ovaries have a high percentage of abnormal dorsal appendages. The most pronounced phenotype associated with the *emc* mutant clones is dorsal appendages with split ends ('antler'-type) to various degrees (Fig. 6D–H). Many other types of abnormally formed dorsal appendages were observed, ranging from complete absence of appendages with only some dorsal appendage material on the eggshell to appendages closer together or fused at base. Some of the phenotypes were also observed in eggs laid by heatshocked *OrR* flies but at a much lower percentage than the *emc* clones (Table 1); the 'antler'-type appendages though were unique to *emc* clones. Further evidence that these eggs came from egg chambers which had *emc* clones was the observation of abnormally large or misshapen cell imprints on the eggshell of the eggs with abnormal

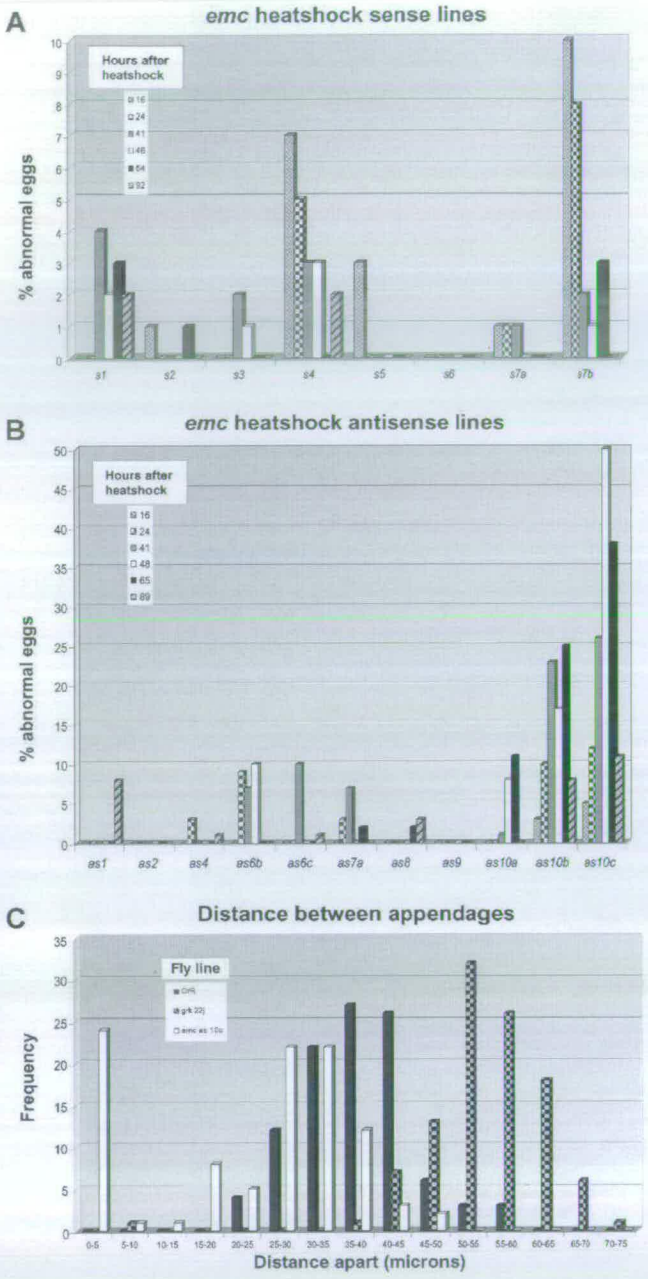

Fig. 5. (A) Graph representing the percentage of abnormal eggs laid from the 8 *emc* sense fly lines. Each line was heatshocked, separately, at 16 (spotted grey column), 24 (checked black/white), 41 (grey), 46 (white), 64 (black) and 92 (grey/black diagonal) hours before the eggs were collected for scoring and the percentage of abnormal eggs recorded. (B) Graph representing the percentage of abnormal eggs laid from the 11 *emc* antisense fly lines. Each line was heatshocked, separately, at 16 (spotted grey), 24 (checked black/white), 41 (grey), 48 (white), 65 (black) and 89 (grey/black upward diagonal column) hours before the eggs were collected for scoring and the percentage of abnormal eggs recorded. (C) Measurements of the distances between the dorsal appendages in *OrR* (black), grk^{22j} (checked grey/black) and *emc as10c* (white) (heatshocked 48 h prior to collecting for scoring) fly lines eggs. The distance between appendages is smaller in the *emc as10c* eggs compared to the wild-type as the appendages are much closer to the dorsal midline. The distance between appendages in the grk^{22j} fly line eggs is bigger compared to the wild-type as the appendages are further away from the dorsal midline. Statistical analysis of the results proved that the results are statistically significant at the 5% level.

appendages (Fig. 6I). This was never observed in heatshocked *OrR* flies, not even when they had abnormal dorsal appendages. Furthermore, the flies producing eggs with *emc* homozygous mutant clones also had extra (mostly dorsocentral) bristles in the notum (Fig. 6J–L), characteristic of *emc* mutations (Moscoso del Prado and Garcia-Bellido, 1984; Huang et al., 1995).

Antibody staining for Broad-Complex (Br-C) using *emc* mosaic flies shows that Br-C expression is not disrupted by the absence of *emc* from a clone of cells (Fig. 6M–O). This is true not only in stages 9–10 (Fig. 6M) when one could argue that Emc and Br-C do not co-localise (Fig. 7I), thus they would not be expected to be interacting, but also in stages 12 and 13 (Fig. 6N,O) where they would be expressed in the same subsets of dorsal anterior follicle cells.

2.7. *emc* and the Grk/EGFR signalling pathway

The dynamic late expression pattern of *emc* in oogenesis with the localisation in two dorsal anterior patches at stage 12 that correspond with the stage 12 expression pattern of Broad-Complex and the effect of *emc* misexpression, knock-out or clones on the egg dorsal appendage formation led us to suspect a link between *emc* and the Grk/EGFR pathway which is responsible for the establishment of the dorso–ventral (D–V) axis of the oocyte. We used in situ RNA hybridisation to investigate the position of *emc* with respect to genes that are well-known components of the Grk/EGFR (Grk/DER) signalling pathway.

As shown in Fig. 7C, in the ovaries of grk^{ED11} homozygous mutant flies *emc* ceases to be expressed in two distinct subsets of dorsal anterior follicle cells at stages 11 and 12 and is instead expressed in a broad dorsal anterior region covering the dorsal midline (compare with Fig. 7A). Mutant $gurken^{ED11}$ flies (Neuman-Silberberg and Schüpbach, 1993) lay ventralised eggs with the dorsal appendages being closer together and thinner than in the wild type (Fig. 7B); their phenotype ranges from a smaller distance between the appendages to appendages fused at the base (Fig. 7D), completely fused or a single very short appendage on the dorsal midline. *emc* mRNA is not expressed in the early stages of oogenesis and it is present in the centripetal cells at stages 9–10b (results not shown) but from stage 11 onwards its expression pattern changes to cover the dorsal midline in a single band in a manner reminiscent of the future appendage appearance of the laid egg. Therefore, we suggest that *emc* lies downstream of *gurken* in oogenesis.

Similarly, *emc* transcript expression pattern is disrupted by mutations in *fs(1)K10* and *Egfr* (*Torpedo*) genes (Fig. 7E–H′). Fs(1)K10 is required in the oocyte nucleus to restrict *grk* expression to the dorsal part of the anterior oocyte, most likely by interaction with Squid and Bruno proteins (Kelley, 1993; Norvell et al., 1999). Eggs mutant for $fs(1)K10^4$ are dorsalised, having two very wide lateral respiratory appendages (due to the—dorsal—region of *grk* expression expanding towards the ventral side) or an even

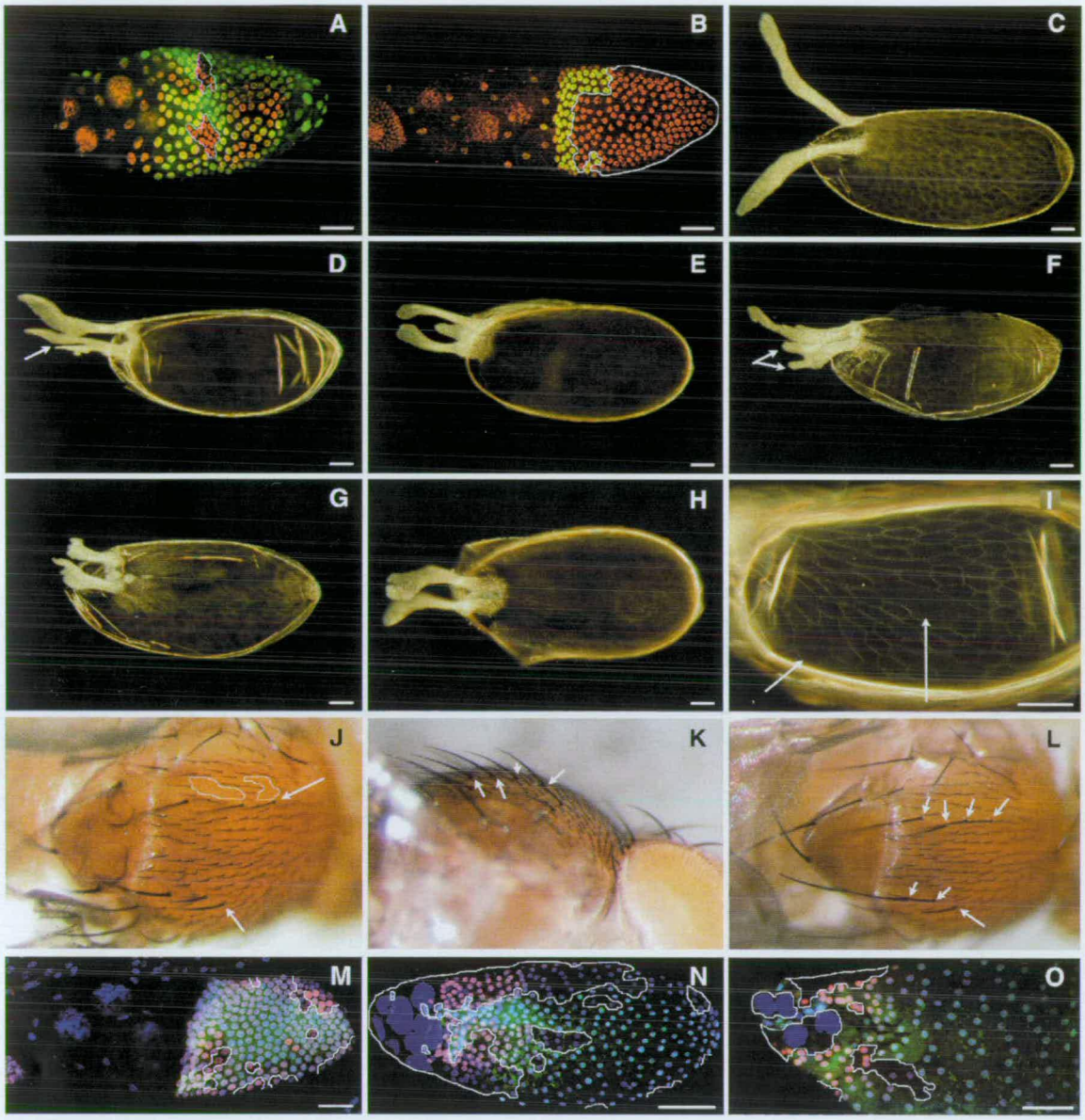

Fig. 6. Phenotypic effects of *emc* follicle cell clones. (A and B). Confocal micrographs of *emc* clones in ovaries. Nuclear GFP is green and all nuclei are in red (TO-PRO 3). Cells homozygous for emc^{1} do not express GFP and appear red rather than yellow in the overlays (clones circled with a white line). (C) Wild-type egg morphology. (D–H) Eggs from flies with *emc* follicle cell clones in ovaries. The dorsal appendages are closer together or fused at the base, have split ends (arrows), are thicker or occasionally shorter than wild type and sometimes have extra material. (I) Follicle cell imprints on the eggshell of a mosaic egg. Arrows point to the abnormally shaped large clones as opposed to the regular follicle cell pattern. (J–L) Mosaic flies have extra dorsocentral bristles (arrows) in the notum and the pattern of microchaetae can be disrupted in areas of *emc* clones (microchaetae absent from areas circled with a white line in (J)). (M–O). Confocal microscope overlays of *emc* clones (absence of green nuclear GFP staining), Broad-Complex antibody staining (red) and DNA staining (blue). The Broad-Complex expression pattern is not affected by the presence of *emc* clones; clones are circled with a white line. (M) Stage 10, (N) Stage 12 and (O) stage 13 egg chamber. Scale bars = 50 μm.

more extreme phenotype of a ring of dorsal appendage material all around the anterior of the egg (Fig. 7F,F′) because of *grk* transcripts being translated throughout the anterior of the oocyte. As shown in Fig. 7E *emc* transcripts are present in a ring all around the oocyte anterior at stage 12 instead of being restricted to two dorsal anterior follicle cell subsets, or, in milder phenotypes, *emc* is expressed in two lateral and a wide dorsal anterior follicle cell patch (Fig. 7E′). Top^{QY1} mutant flies (Schüpbach, 1987) laid ventralised eggs with a central, very thin and short dorsal appendage (Fig. 7H) or very little dorsal appendage material (Fig. 7H′). The expression of *emc* is changed accordingly, with *emc* mRNA being present in one dorsal, thinner and longer compared to the grk^{ED11} mutants, anterior group of follicle cells covering the dorsal midline at stage 12 (Fig. 7G); alternatively, *emc* is expressed in even smaller dorsal anterior spots or is absent from the follicle cells at stage 12 (Fig. 7G′), presumably reflecting the various

Table 1
Percentage of eggs with abnormal dorsal appendages from heatshocked wild-type *OrR* and mosaic *emc*[1] flies with follicle cell clones, at different times after heatshock

Collection time (h)	Eggs with abnormal dorsal appendages (%)	
	hs *OrR*	hs mosaic *emc*[1]
0–26	2.76	8.01*
26–38	9.75	13.93
38–52	0.0	2.68

Within the 0–26 h interval, the peak of eggs with abnormal DA laid from both fly lines was between 21 and 25 h after heatshock (data not shown). Statistical analysis (chi-square test) showed that the results are statistically significant at the 0.1% level for the 0–26 h after heatshock collection (chi-square = 19.41, $P < 0.001$), as indicated by the asterisk (*), but not for the 26–38 h and 38–52 h after heatshock collections (chi-square = 0.71 and 0.24, respectively; it should be ≥ 3.84 for significance at the 5% level). This means that for the last two samples the difference in the percentage of abnormality between mosaic and control flies may well be caused by the heatshock treatment but during the first 26 h after heatshock the abnormal appendage phenotypes in the mosaic flies are caused by the presence of follicle cell clones since the difference from the control flies is significant. The relatively low percentage of eggs with abnormal dorsal appendages can be explained as only a small proportion of egg chambers would be at the correct developmental stage during the heatshock. Furthermore, not all of the egg chambers would have *emc* homozygous mutant clones covering the specific subpopulations of follicle cells that affect appendage formation.

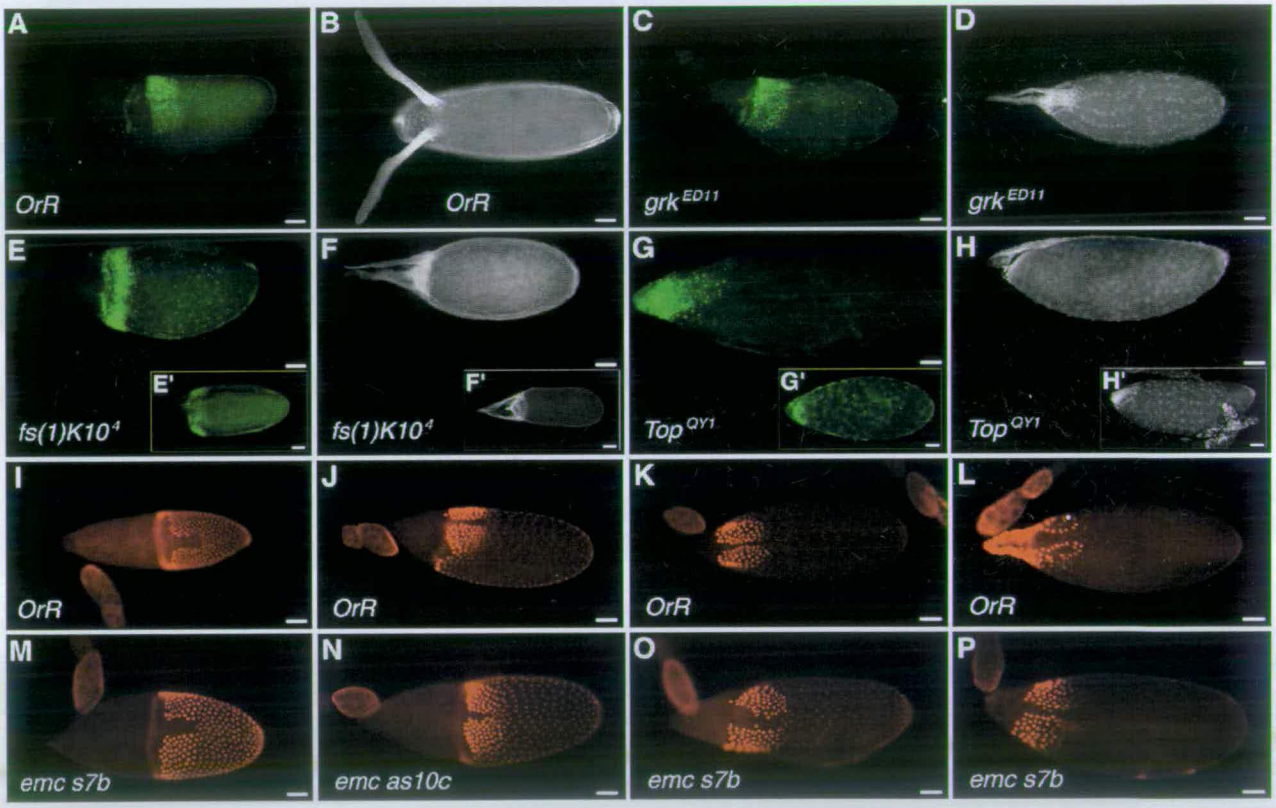

Fig. 7. (A–H′) In situ hybridisation with *emc* RNA on mutant backgrounds. (A, C, E, E′, G and G′) *emc* expression (green) in stage 12 egg chambers and (B, D, F, F′, H and H′) the corresponding dorsal appendage phenotype for each fly line. In (A) *emc* is expressed in two dorsal anterior subsets of follicle cells either side of a thin gap at the dorsal midline in wild-type *OrR* flies. *OrR* eggs have normal dorsal appendages (B). In grk^{ED11} mutant flies *emc* is expressed in a single broad dorsal anterior area covering the dorsal midline (C) and the eggs laid (D) have thin, shorter dorsal appendages fused at base (ventralised eggs) and are smaller than wild-type. *emc* is expressed in a ring of follicle cells all around the dorsal anterior (E) or in two lateral and a wide dorsal anterior patches (E′) in $fs(1)K10^4$ mutants, resulting in dorsalised eggs shorter and more round than wild-type, with four appendages all around the anterior (F) or two wide lateral appendages with appendage material connecting them (F′). In Top^{QY1} mutants *emc* is expressed in a single patch over the dorsal midline (G) or is absent from follicle cells (G′). The corresponding eggs (ventralised) have either one very short, thin dorsal appendage (H) or very little chorionic appendage material at the anteriormost region of the egg (H′). (I–P) Immunohistochemistry with a Br-C antibody. (I–L) show the expression pattern of Broad-Complex in *OrR* flies at stages 10 (I), early (J) and late (K) stage12 and stage 13 (L). (M–P) show Br-C in *emc* sense and antisense fly lines. Normal Br-C expression is not disrupted in mid-oogenesis in the sense line *s7b* (M), but later at stage 12 the shape of the patches of follicle cells expressing Br-C is affected (O and P). Disruption of normal Emc expression in the antisense line *emc as10c* does not inhibit Br-C expression and disrupts the shape of the Br-C - expressing patches only mildly (N). Scale bars = 50 μm.

degrees of ventralisation of the egg caused by the absence of EGFR signalling. These results suggest that *emc* expression is involved in the commitment to dorsal appendage fate of the follicle cells in which it is expressed, and that it is downstream of the *fs(1)K10* and *Egfr/Top* genes in the Grk/EGFR signalling pathway.

2.8. Broad-Complex expression pattern is disrupted in emc sense and, to a lower extent, antisense transgenic flies

Since the *emc* late expression pattern in oogenesis is reflected in the dorsal appendage phenotype observed, we used an antibody against the Broad-Complex (Br-C) core domain (Tzolovsky et al., 1999) on *emc hs as10c* and *s7b* fly lines. The Br-C locus is required for dorsal appendage morphogenesis and is an effector of the Grk/EGFR pathway on D–V axis formation while Dpp signalling is necessary for its correct expression along the A–P axis (Deng and Bownes, 1997). Br-C expression pattern is quite different from that of *emc* in early and mid-oogenesis (Fig. 7I) up to stage 12 where Br-C is expressed in two subsets of dorsal anterior follicle cells either side of the dorsal midline exactly like *emc*. The same pattern is followed by Br-C and Emc proteins at stage 12 and 13 (Fig. 7J–L). In the sense *emc* line *s7b* the late Br-C protein expression pattern is disrupted more often than in the antisense *emc* line *as10c* (Fig. 7O,P, compared with Fig. 7J,K), suggesting that *emc* affects *Broad-Complex* expression with respect to the dorsal appendage-producing follicle cells. Its function must be one of refining the dorsal appendage position rather than determining whether there will be dorsal appendages produced or not, since in *emc* antisense heatshocked flies BR-C was still expressed, even though Emc was knocked-out, and the BR-C expression pattern was usually normal (Fig. 7N); Br-C was also not affected in Emc null follicle cell clones (Fig. 6N,O). In the sense *emc* flies, where *emc* was ectopically expressed, Br-C was likely to be expressed in extra follicle cells, suggesting that *emc* needs to be correctly localised for the correct localisation of Br-C in the follicle cells producing the dorsal appendages, but that there must be other genes responsible for regulating the expression itself of BR-C acting on those subsets of follicle cells. Expression of Br-C during early and mid- oogenesis was not affected by *emc* misexpression (Fig. 7M compared to Fig. 7I).

3. Discussion

emc appears to have a key role in cell fate determination in somatic cells during the process where follicle cells surround the oocyte and in dorsal appendage positioning.

We have shown using β-galactosidase staining of an enhancer-trap line, in situ hybridisation to mRNA and antibody staining that *emc* has a dynamic expression pattern in oogenesis. Expression is observed both in the germ cells and in the somatic follicle cells. Maternal Emc is already known to be essential for sex determination in embryogenesis (Younger-Shepherd et al., 1992) thus the expression observed in the nurse cell nuclei was expected.

Ectopic *emc* overexpression using heatshock sense fly lines leads to a large number of fused egg chambers that eventually undergo apoptosis. Most of the abnormal egg chambers seem to be fused longitudinally, as they appear to be very long and thin. A different type of fusion is present using antisense *emc* knock-out: fusion seems to happen laterally since egg chambers that can proceed up to stage 11 of oogenesis with a normally developing oocyte and double the number of nurse cells were observed. This phenotype was not observed in heatshocked *OrR* flies. These phenotypes suggest abnormalities during enveloping of the germline cysts in germarium region 2, when egg chambers become assembled and are characteristic of mutants for *Notch*, *Delta*, *daughterless* and of ectopic *hedgehog* expression (Goode et al., 1996; Forbes et al., 1996). In this case *emc* would be implicated in enveloping the germ cell cluster, consistent with presence of the protein in the germarium and with recent findings by Adam and Montell (2004) who observe similar fused egg chambers following overexpression of *emc*. They confirm the relationship of *emc* with the Notch signalling pathway in oogenesis by identifying *emc* as an effector of Notch signalling in the differentiation of follicle cells and suggest that the fused phenotypes are caused by the failure of polar cells to differentiate (polar cells are required to induce stalks which separate developing egg chambers in the ovariole) (Adam and Montell, 2004).

Emc also functions later in development in the follicle cells, during the regulation of dorsal appendage formation, a procedure controlled by the Grk/EGFR pathway. The chorionic appendages are moved closer together and often fuse when *emc* levels are reduced by antisense expression. Similar results are seen when *emc* is removed in clones of cells, where the appendages are frequently split at their ends. We have demonstrated that *emc* mRNA expression is affected by the disruption of the normal dorso–ventral axis formation caused by mutants for *fs(1)K10*, *gurken* and *Egfr*. Specifically, the *emc* expression pattern follows the ventralisation caused by grk^{ED11} and Top^{QY1} and the dorsalisation caused by $fs(1)K10^{4}$. Therefore *emc* functions downstream of *fs(1)K10*, *gurken* and *Egfr* and upstream of the finally formed dorsal appendages.

Further support for the role of *emc* in dorsal appendage morphogenesis comes from our finding that *emc* ectopic expression affects the expression pattern of Broad-Complex, a transcription factor that regulates dorsal appendage formation (Deng and Bownes, 1997). In *emc* sense transgenic lines Br-C protein is expressed in a more irregular pattern than normal, mainly at stages 12–13. Br-C protein expression pattern coincides with that of *emc* mRNA at stage 12 of oogenesis as they are both expressed in two dorsal anterior subsets of concentrated follicle cells

either side of the dorsal midline (these 'patches' of follicle cells are discrete and visible also with nuclear markers) and in late stage 12–13 they follow the same pattern of being expressed in the migrating follicle cells that are forming the dorsal chorionic appendages. In *emc* sense flies the borders of Br-C expression are irregular and there are follicle cells in the gap between the two patches or around their borders that express Br-C. So Br-C must lie downstream of *emc* since its expression is affected by *emc* misexpression. However, *emc* is not the gene that activates Br-C since Br-C protein is expressed in the normal wild-type pattern in *emc* homozygous mutant follicle cell clones and in *emc* antisense lines where *emc* is knocked-out (or there are minor disruptions in the Br-C expression area in antisense compared with sense lines); rather, it seems that *emc* must be necessary for modulating Br-C within the areas of *emc* expression.

It would be interesting to investigate how the role of *emc* acting downstream of *Notch* (Adam and Montell, 2004) may be interlinked with its interaction with the Grk/EGFR pathway we report here. In other tissues such as the developing eye and wing *emc* is required for a number of processes and acts in parallel or is regulated by many different signals, including the EGFR and the Notch signalling pathways (de Celis, 1998; Baonza and Freeman, 2001). Further investigation of the multiple roles of *emc* in oogenesis and their specific timing should help to unravel the complexities of producing a viable, morphologically normal, egg.

4. Experimental procedures

4.1. Drosophila stocks

Wild type stocks: *Oregon R* (*OrR*) and w^k (Lüning, 1981). LacZ line, *261/31* (Deak et al., 1997). Transgenic *emc* lines were generated in our lab. Mutant alleles used: grk^{22j} (Neuman-Silberberg and Schüpbach, 1994); grk^{ED11} (Neuman-Silberberg and Schüpbach, 1993), top^{QY1} (Schüpbach, 1987). All other stocks were obtained from the Bloomington *Drosophila* Stock Center, Indiana University, USA.

4.2. In situ hybridisation in ovaries with DIG-labelled DNA probe

The protocol is based on a procedure previously described (Tautz and Pfeifle, 1989) with minor modifications.

4.3. Fluorescent in situ hybridisation in ovaries with DIG-labelled RNA probe

The protocol is based on the Tautz and Pfeifle (1989) procedure with the following modifications. Ovaries were collected and fixed in PMS, washed for 3×10 min in PBT, equilibrated for 10 min in RNA Hybrix/PBT (1:1) and then prehybridised for 1 h at 65 °C in RNA Hybrix (50% deionised formamide, 5× SSC, 100 μg/ml tRNA (RNase free), 50 μg/ml Heparin, 0.1% Tween 20). The ovaries were hybridised overnight at 65 °C in RNA Hybrix containing digoxigenin-labelled RNA probe. Templates were transcribed with either T7 or T3 polymerases (Ambion) using DIG RNA Labelling Mix (Roche, #1 277 073), to generate antisense and sense probes, the latter being used as a negative control. Detection was carried out with 1:80 dilution of anti-DIG HRP antibody (DakoCytomation, #D5101) for 1 h at room temperature (RT). For visualisation TSA-Cy3 reagent (PerkinElmer, #SAT704A) was used according to manufacturer's instructions. Ovaries were mounted in Vectashield (Vector Laboratories, #H1000) for observation.

4.4. Immunohistochemistry and western analysis

Ovaries were dissected in Ringer's and fixed for 20 min in PMS, washed with PBTW (PBS containing 0.5% Triton X-100) and incubated with 5% NGS (Normal Goat Serum) in PBTW for 1 h. To stain for Broad Complex (Br-C), a mouse anti-Core antibody (gift from G. Guild, University of Pennsylvania), which can recognise all Br-C isoforms was used in 1:60 dilution. An Emc rabbit antibody (provided by L.Y. Jan and Y.N. Jan, University of California, San Francisco) was used in 1:600 dilution. Secondary antibodies were either Alexa 488 or Alexa 568-conjugated (Molecular Probes, Invitrogen) and used in 1:400 dilution.

For the purposes of immunoblotting proteins extracted from *s1, s7b, as10c* and *OrR* ovaries were separated by SDS-PAGE electrophoresis and transferred onto reinforced nitrocellulose membrane (Schleicher and Schuell, Optitran BA-S83). To detect Emc we used the Emc antibody in 1:6000 dilution and then an anti-rabbit HRP-conjugated secondary antibody (Sigma, #A8275) in 1:4000 dilution. To visualise the immunoreactive bands the membrane was incubated for 1 min in chemiluminescent solution made up of 1.25 mM Luminol, 0.2 mM *p*-Coumaric acid and 100 mM Tris–HCl pH 8.5. Quantification of band intensity was done with ImageJ software (http://rsb.info.nih.gov/ij/).

4.5. Nuclear staining

For multicolour imaging DNA was counterstained with the appropriate nuclear stain. For blue colour DNA was stained with Hoechst 33258 (1 μg/ml) for 5 min in PBT. Nuclear yellow (Sigma, #N2137) was also used in 1 μg/ml concentration. For green colour we used Sytox Green (Molecular Probes, Invitrogen) at 150 nM concentration whereas TO-PRO-3 (Molecular Probes, Invitrogen), which can be detected in the infrared channel, was used at 250 nM concentration. No RNase digest was necessary when staining with Hoechst or Nuclear Yellow. Sytox Green

and TO-PRO-3 can stain DNA as well as RNA, therefore samples were pre-digested in 250 μg/ml RNase-A for 5–10 min. Stained samples were examined and captured digitally either on a Zeiss Axiophot fluorescent microscope or a Leica TCS SP confocal microscope.

4.6. Plasmid rescue

Genomic DNA from the *P{lacW}* enhancer-trap line *261/31* was digested with *Eco*RI and subsequently ligated overnight at 4 °C. The ligated DNA was used to transform XL1 Blue competent cells. Ampicillin selection allowed the isolation of colonies carrying the Amp^R part of *P{lacW}* plus any additional flanking genomic DNA. Plasmid DNA from two of these colonies was digested with *Eco*RI and *Bam*HI. The resulting fragment (the DNAs from both colonies were identical) was subcloned in pBluescript (SK-). M13–20 and Reverse primers were used to sequence the flanking genomic DNA and determine the P-element insertion site.

4.7. β-galactosidase staining

Female flies fed with yeast for 3 days were dissected in PBS. Ovaries were dissected and fixed for 5 min in 4% *p*-Formaldehyde in PBT, then stained overnight in 100 μl Staining Solution (10 mM Phosphate buffer, pH 7.0, 8 mM $K_3[Fe(CN)_6]$, 8 mM $K_4[Fe(CN)_6]$, 150 mM NaCl and 1 mM $MgCl_2$) to which 2.5 μl 8% X-Gal (5-Bromo-4-chloro-3-indolyl-β-D-galactoside) were added. The stained ovaries were rinsed in PBS and mounted in PBS/Glycerol (1:4).

4.8. Production of emc antisense and sense lines

To generate transgenic *emc* sense and antisense flies, a full length *emc* cDNA was used (Garrell and Modolell, 1990). *emc* cDNA was cut with a pair of restriction enzymes, *Eco*RI and *Bam*HI or *Spe*I and *Hinc*II. The resulting *Eco*RI–*Bam*HI and *Spe*I–*Hinc*II fragments of *emc* cDNA were ligated into *pCaSpeR-hs* cut with either *Stu*I and *Bgl*I or *Xba* and *Hpa*I, forming the *pHS-emc* (sense) and *pHS-as-emc* (anti-sense) constructs, respectively. Both constructs were then introduced into w^{1118} flies by P element mediated germline transformation (Spradling, 1986).

4.9. Heatshock regimes for expression of sense and antisense constructs

To investigate the bristles on the thorax batches of flies were allowed to lay eggs in vials for 24 h and then transferred to new vials. The vials were allowed to age for 0–11 days prior to heatshock at 39 °C for 45 min followed by 30 min at 25 °C and a further 45 min at 39 °C. The vials were then retained until adults hatched and the bristle patterns were observed. For most of the studies on dorsal appendage morphogenesis we used small cages, so that the eggs laid could be collected on agar plates. The heatshock regime was the same as above, except that in this case the adults were heatshocked prior to collecting eggs or observing ovaries. In an alternative, more severe, regime flies were heatshocked for 30 min in vials placed in 37 °C water bath. Heatshocked flies were transferred back to 25 °C. Eggs were subsequently collected from 0 to 48 h after heatshock.

For the mutant background experiments flies were heatshocked by transferring to vials placed in a 37 °C water bath for 1 h.

4.10. Induction of mitotic recombination by FLP/FRT system

For the generation of $emc^{1-/-}$ somatic follicle cell clones, ♂ y^1 w^{1118} $P\{ry^{+t7.2}=70FLP\}3F/Dp(1;Y)y^+$; *TM2/TM6C*, Sb^1 were crossed with ♀ w^{1118}; $P\{w^{+mC}=Ubi-GFP(S65T)nls\}3L$ $P\{ry^{+t7.2}=neoFRT\}80B/TM3$, Sb^1, female progeny of the genotype y^1 w^{1118} $P\{ry^{+t7.2}=70FLP\}3F/w^{1118}$; $P\{w^{+mC}=Ubi-GFP(S65T)nls\}3L$ $P\{ry^{+t7.2}=neoFRT\}80B/TM6C$, Sb^1 were selected and crossed with ♂ *w**; $emc^1P\{ry^{+t7.2}=neoFRT\}80B/TM6B$, Tb^1 (Xu and Rubin, 1993). Male progeny carrying the *FLP;emc*^{1}*/Ubi−GFP(S65T)nls* genes were selected and crossed with *w**; $emc^1P\{ry^{+t7.2}=neoFRT\}80B/TM6B$, Tb^1 female flies. Non-Tb 3rd instar larvae were selected and allowed to hatch. Female flies of the genotype y^1 w^{1118} $P\{ry^{+t7.2}=70FLP\}3F/w*$; emc^1 $P\{ry^{+t7.2}=neoFRT\}80B/P\{w^{+mC}=Ubi-GFP(S65T)nls\}3L$ $P\{ry^{+t7.2}=neoFRT\}80B$ were heatshocked for 1 h at 39 °C and then transferred to 25 °C in small cages. Embryos were collected in grape juice agar plates (per 400 ml: 9 g agar, 10 g sucrose, 100 ml grape juice, 1 ml 10% Nipagin (in 95% EtOH) in dH_2O) every 6–24 h and scored for abnormal appendage formation. Ovaries were dissected from heatshocked flies at 10 h intervals after heatshock. Alternatively, flies were yeasted for 3 days at 25 °C, then heatshocked for 1 h at 37 °C in a water bath, transferred to 25 °C for 4 h, heatshocked again at 37 °C for 1 h and transferred to 25 °C in yeasted vials. Ovaries were dissected 3–5 days after heatshock.

Acknowledgements

We thank L.Y. Jan and Y.N. Jan for the *emc* antibody. This project was supported by a Wellcome Trust grant (DZ and DC), a BBSRC studentship to KL, a Darwin Trust studentship to GT and SP and a Nuffield undergraduate summer studentship to EA (now studying for a PhD at Cambridge University). PT and GK were honours students; PT is now studying for a PhD at Edinburgh University. All work was undertaken at the Institute of Cell and Molecular Biology, University of Edinburgh.

References

Adam, J.C., Montell, D.J., 2004. A role for extra macrochaetae downstream of Notch in follicle cell differentiation. Development 131, 5971–5980.

Baonza, A., Freeman, M., 2001. Notch signalling and the initiation of neural development in the *Drosophila* eye. Development 128, 3889–3898.

Baonza, A., de Celis, J.F., Garcia-Bellido, A., 2000. Relationships between *extramacrochaetae* and Notch signalling in *Drosophila* wing development. Development 127, 2383–2393.

Benezra, R., Davis, R.L., Lockshon, D., Turner, D.L., Weintraub, H., 1990. The protein Id: a negative regulator of helix-loop-helix DNA binding proteins. Cell 61, 49–59.

Botas, J., Moscoso del Prado, J., Garcia-Bellido, A., 1982. Gene-dose titration analysis in the search of trans-regulatory genes in *Drosophila*. Eur. Mol. Biol. Org. J. 1, 307–310.

Cabrera, C.V., Alonso, M.C., Huikeshoven, H., 1994. Regulation of scute function by *extramacrochaete* in vitro and in vivo. Development 120, 3595–3603.

Campuzano, S., 2001. Emc, a negative HLH regulator with multiple functions in *Drosophila* development. Oncogene 20, 8299–8307.

Cooperstock, R.L., Lipshitz, H.D., 2001. RNA localization and translational regulation during axis specification in the *Drosophila* oocyte. Int. Rev. Cytol. 203, 541–566.

Cubas, P., Modolell, J., Ruiz-Gomez, M., 1994. The helix-loop-helix extramacrochaetae protein is required for proper specification of many cell types in the *Drosophila* embryo. Development 120, 2555–2566.

Davis, R.L., Cheng, P.F., Lassar, A.B., Weintraub, H., 1990. The MyoD DNA binding domain contains a recognition code for muscle-specific gene activation. Cell 60, 733–746.

Deak, P., Omar, M.M., Saunders, R.D., Pal, M., Komonyi, O., Szidonya, J., Maroy, P., Zhang, Y., Ashburner, M., Benos, P., Savakis, C., Siden-Kiamos, I., Louis, C., Bolshakov, V.N., Kafatos, F.C., Madueno, E., Modolell, J., Glover, D.M., 1997. P-element insertion alleles of essential genes on the third chromosome of *Drosophila melanogaster* : correlation of physical and cytogenetic maps in chromosomal region 86E–87F. Genetics 147, 1697–1722.

de Celis, J.F., 1998. Positioning and differentiation of veins in the *Drosophila* wing. Int. J. Dev. Biol. 42, 335–343.

Deng, W.M., Bownes, M., 1997. Two signalling pathways specify localised expression of the Broad-Complex in *Drosophila* eggshell patterning and morphogenesis. Development 124, 4639–4647.

Deng, W.M., Bownes, M., 1998. Patterning and morphogenesis of the follicle cell epithelium during *Drosophila* oogenesis. Int. J. Dev. Biol. 42, 541–552.

Deng, W., Leaper, K., Bownes, M., 1999. A targeted gene silencing technique shows that *Drosophila myosin* VI is required for egg chamber and imaginal disc morphogenesis. J. Cell. Sci. 112 (Pt 21), 3677–3690.

Ellis, H.M., 1994. Embryonic expression and function of the *Drosophila* helix-loop-helix gene, extramacrochaetae. Mech. Dev. 47, 65–72.

Ellis, H.M., Spann, D.R., Posakony, J.W., 1990. extramacrochaetae, a negative regulator of sensory organ development in *Drosophila*, defines a new class of helix-loop-helix proteins. Cell 61, 27–38.

Forbes, A.J., Lin, H., Ingham, P.W., Spradling, A.C., 1996. *hedgehog* is required for the proliferation and specification of ovarian somatic cells prior to egg chamber formation in *Drosophila*. Development 122, 1125–1135.

Garrell, J., Modolell, J., 1990. The *Drosophila extramacrochaetae* locus, an antagonist of proneural genes that, like these genes, encodes a helix-loop-helix protein. Cell 61, 39–48.

Goode, S., Melnick, M., Chou, T.B., Perrimon, N., 1996. The neurogenic genes egghead and brainiac define a novel signaling pathway essential for epithelial morphogenesis during *Drosophila* oogenesis. Development 122, 3863–3879.

Huang, F., van Helden, J., Dambly-Chaudiere, C., Ghysen, A., 1995. Contribution of the gene extramacrochaete to the precise positioning of bristles in *Drosophila*. Roux's Arch. Dev. Biol. 204, 336–343.

Kelley, R.L., 1993. Initial organization of the *Drosophila* dorsoventral axis depends on an RNA-binding protein encoded by the *squid* gene. Genes Dev. 7, 948–960.

King, R.C., 1970. Ovarian Development in *Drosophila melanogaster*. Academic Press, New York.

Lüning, K.G., 1981. Genetics of inbred *Drosophila melanogaste*. Induction of marker genes and preliminary recombination tests. Hereditas 95, 181–188.

Massari, M.E., Murre, C., 2000. Helix-loop-helix proteins: regulators of transcription in eukaryotic organisms. Mol. Cell. Biol. 20, 429–440.

Morimoto, A.M., Jordan, K.C., Tietze, K., Britton, J.S., O'Neill, E.M., Ruohola-Baker, H., 1996. *Pointed*, an ETS domain transcription factor, negatively regulates the EGF receptor pathway in *Drosophila* oogenesis. Development 122, 3745–3754.

Moscoso del Prado, J., Garcia.-Bellido, A., 1984. Genetic regulation of the achaete-scute complex of *Drosophila melanogaster*. Roux's Arch. Dev. Biol. 193, 242–245.

Neuman-Silberberg, F.S., Schupbach, T., 1993. The *Drosophila* dorsoventral patterning gene gurken produces a dorsally localized RNA and encodes a TGF alpha-like protein. Cell 75, 165–174.

Neuman-Silberberg, F.S., Schupbach, T., 1994. Dorsoventral axis formation in *Drosophila* depends on the correct dosage of the gene gurken. Development 120, 2457–2463.

Norvell, A., Kelley, R.L., Wehr, K., Schupbach, T., 1999. Specific isoforms of squid, a *Drosophila* hnRNP, perform distinct roles in Gurken localization during oogenesis. Genes Dev. 13, 864–876.

Queenan, A.M., Ghabrial, A., Schupbach, T., 1997. Ectopic activation of torpedo/Egfr, a *Drosophila* receptor tyrosine kinase, dorsalizes both the eggshell and the embryo. Development 124, 3871–3880.

Ruohola-Baker, H., Grell, E., Chou, T.B., Baker, D., Jan, L.Y., Jan, Y.N., 1993. Spatially localized *rhomboid* is required for establishment of the dorsal–ventral axis in *Drosophila* oogenesis. Cell 73, 953–965.

Schupbach, T., 1987. Germ line and soma cooperate during oogenesis to establish the dorsoventral pattern of egg shell and embryo in *Drosophila melanogaster*. Cell 49, 699–707.

Spradling, A.C., 1986. P element-mediated transformation. In: Robert, D.B. (Ed.), *Drosophila*: A Practical Approach. IRL Press, Oxford, England, pp. 175–197.

Spradling, A.C., 1993. Developmental genetics of oogenesis. In: Bate, M., Martinez-Arias, A. (Eds.), The Development of *Drosophila melanogaster*. Cold Spring Harbor Laboratory Press, New York, pp. 1–70.

Tautz, D., Pfeifle, C., 1989. A non-radioactive in situ hybridization method for the localization of specific RNAs in *Drosophila* embryos reveals translational control of the segmentation gene hunchback. Chromosoma 98, 81–85.

Tzolovsky, G., Deng, W.M., Schlitt, T., Bownes, M., 1999. The function of the broad-complex during *Drosophila melanogaster* oogenesis. Genetics 153, 1371–1383.

van Buskirk, C., Schupbach, T., 1999. Versatility in signalling: multiple responses to EGF receptor activation during *Drosophila* oogenesis. Trends. Cell. Biol. 9, 1–4.

van Doren, M., Ellis, H.M., Posakony, J.W., 1991. The *Drosophila* extramacrochaetae protein antagonizes sequence-specific DNA binding by daughterless/achaete-scute protein complexes. Development 113, 245–255.

Wasserman, J.D., Freeman, M., 1998. An autoregulatory cascade of EGF receptor signaling patterns the *Drosophila* egg. Cell 95, 355–364.

Xu, T., Rubin, G.M., 1993. Analysis of genetic mosaics in developing and adult *Drosophila* tissues. Development 117, 1223–1237.

Younger-Shepherd, S., Vaessin, H., Bier, E., Jan, L.Y., Jan, Y.N., 1992. deadpan, an essential pan-neural gene encoding an HLH protein, acts as a denominator in *Drosophila* sex determination. Cell 70, 911–922.

Zhao, D., Bownes, M., 1999. Misexpression of argos, an inhibitor of EGFR signaling in oogenesis, leads to the production of bicephalic, ventralized, and lateralized *Drosophila* melanogaster eggs. Dev Genet. 25, 375–386.